Institut für Lebensmittel- und Ressourcenökonomik (ILR)

An environmental and economic assessment of a novel Power-to-Fuel system for biogas plants

D i s s e r t a t i o n

zur

Erlangung des Grades

Doktorin der Agrarwissenschaften

(Dr.agr.)

der

Landwirtschaftlichen Fakultät
der
Rheinischen Friedrich-Wilhelms-Universität Bonn

von

Lea Jasmin Eggemann
aus
Bonn, Deutschland

2022

Referent: Prof. Dr. Thomas Heckelei

Korreferent: Prof. Dr. Ralf Peters

Tag der mündlichen Prüfung: 16.12.2021

Angefertigt mit Genehmigung der Landwirtschaftlichen Fakultät der Universität Bonn

Acknowledgement

I would like to thank my supervisors for their support in undertaking this thesis. First of all, I would like to name my late Doktorvater Peter Burauel, who has made it possible for me in the first place to do this PhD. He left this world far too soon and I will forever be grateful for his guidance and commitment towards me and my work. Secondly, I would like to thank Thomas Heckelei for his support throughout the years and him becoming my second Doktorvater without any hesitation. Thirdly, I would like to mention my gratitude towards Ralf Peters as my second supervisor, whose ideas and support has really helped me to finalise my topic and find the common thread of this thesis. It has truly been special, as it is a one of a kind in terms of interdisciplinarity. The connection of the staff unit ZukunftsCampus and the Institute of Energy and Climate Research at Forschungszentrum Jülich has enabled me to approach this thesis in the best way possible, being able to access expertise from various disciplines. Hence, I would also like to express my appreciation to the board of directors for providing funds for my PhD.

Furthermore, I would like to thank Debora, my master's student, Neus Escobar, as the co-author of my paper and the greatest help in LCA I could have wished for, Fabian, who greatly helped me with my underlying model, and my fellow PhD students Felix, Caro and Florian for their inspiration and support with crucial parts of this study. The exchange and discussions with them immensely helped to consider different aspects of the study and I would like to express my gratitude to them as well as to all the other colleagues that have guided me along the way.

Finally, I would like to thank my family and friends for supporting me throughout the course of my PhD. I am entirely grateful, and I would not have done it without them.

Kurzfassung

Power-to-Fuel (PtF)-Systeme nutzen Kohlendioxid und Wasserstoff als Ausgangsmaterialien für die Produktion von erneuerbaren Kraftstoffen und können somit zum Klimaschutz beitragen. Diese Studie versucht herauszufinden, ob ein innovatives PtF-System in Kombination mit einer güllebasierten Biogasanlage eine zukünftige Option im deutschen Energiesystem sein könnte. Bei diesem Konzept wird das Kohlendioxid aus dem Biogas genutzt, das normalerweise ungenutzt in die Atmosphäre entlassen wird. Der Wasserstoff über eine windbasierte Elektrolyse gewonnen. Die Analyse ist ein erster Versuch, die ökonomische und ökologische Leistungsfähigkeit eines solchen Systems zur synthetischen Methanolproduktion abzuschätzen. In einer techno-ökonomischen Analyse wird eine kleintechnische Methanolanlage in das analysierte System integriert. Diese Analyse gliedert sich in die Prozesssimulation, der in dieser Größenordnung noch nicht existierenden Methanolanlage, und die Entwicklung einer auf das gesamte System abgestimmten Methodik zur Kostenschätzung. Die Modulkosten werden von Herstellern erfragt und entsprechend angepasst. Hiermit können die spezifischen Herstellungskosten in Kombination mit einer bestehenden Güllekleinanlage (75 kW) auf 4,41 €/kg_{MeOH} geschätzt werden. Zusätzlich werden drei Fälle mit unterschiedlichen Mengen an CO_2 untersucht. Ein kleinerer Fall mit dem kleinsten verfügbaren Motor von MAN für das Blockheizkraftwerk (BHKW), ein etwas größerer Fall unter Einbeziehung des Biogas-Oxyfuel-Verfahrens (BOP) und ein an eine durchschnittliche deutsche Biogasanlage mit 500 kW angepasster Fall. Die Analyse zeigt, dass im Gegensatz zum Standardfall der BOP vorteilhaft ist, da er keine zusätzliche Biogasaufbereitung benötigt und die doppelte Menge CO_2 erzeugt. Daher sind die Kosten mit 3,17 €/kg_{MeOH} geringer. Generell zeigt sich, dass die Herstellungskosten pro kg Produkt mit zunehmender Anlagengröße sinken. Dies lässt sich mit den Skaleneffekten erklären. Des Weiteren zeigen Sensitivitätsanalysen, dass die H_2-Kosten und die fixen Investitionen (FCI) den größten Einfluss haben. Der Einfluss der FCI nimmt jedoch mit zunehmender Anlagengröße ab. Auch der Zinssatz und die CO_2-Kosten sind relevant, wobei die Kosten der Betriebsmittel eher unbedeutend sind. Das System wird weiter analysiert, indem Lernkurven und andere Anpassungen für die zukünftige Entwicklung berücksichtigt werden. Die Hinzunahme möglicher Erlöse aus Koppelprodukten trägt ebenfalls dazu bei, den Methanolpreis an den anderer PtF-Anlagen anzugleichen. Das System in Verbindung mit einer durchschnittlichen Biogasanlage zeigt hier mit 1,38 €/kg_{MeOH} vergleichsweise niedrige Kosten. Im zweiten Teil der Studie wird eine Lebenszyklusanalyse (LCA) von der Wiege bis zum Tor für 1 kg Methanol durchgeführt, das im integrierten System mit der Güllekleinanlage produziert wird. Angesichts der Multifunktionalität des Prozesses wird die Unsicherheit in den Ergebnissen durch verschiedene Annahmen über die Gutschriften für die Nebenprodukte Wärme und Strom des BHKW und den Gärrest aus der anaeroben Vergärung bewertet. Die meisten der insgesamt neun analysierten Szenarien zeigen deutliche Verbesserungen im Vergleich zur konventionellen Produktion aus fossilen Ressourcen. Szenario A1 erreicht eine Einsparung von 1,09 kg CO_2-Äq. gegenüber dem Referenzsystem, das 0,85 kg CO_2-Äq. emittiert. Dies entspricht einer Verbesserung von 1,95 kg CO_2-Äq.. Bei einer Jahresproduktion von 212 Tonnen Methanol können insgesamt 413 t/a CO_2-Äq. eingespart werden. Zusätzlich untersucht eine Sensitivitätsanalyse den Einfluss der Variabilität der Sachbilanzdaten auf die Ergebnisse. Diese zeigt, dass die Parameter, die den Gesamtenergiebedarf im System bestimmen, einen großen Einfluss auf die Umweltbilanz haben und daher bei der Prozessauslegung und beim Upscaling sorgfältig berücksichtigt werden sollten. Trotz der Unsicherheiten, die der Ökobilanz innewohnen, bietet das System eine interessante Option zur Herstellung von erneuerbarem Methanol, die gleichzeitig einen Beitrag zu einer Kreislaufwirtschaft leistet. Auch wenn die Wirtschaftlichkeit aktuell noch nicht gegeben ist, können zukünftige Entwicklung der Kosten und Einnahmen sowie die positiven Umweltauswirkungen dem System eine Perspektive geben.

Abstract

Power-to-Fuel (PtF) systems use carbon dioxide and hydrogen as feedstock together for renewable fuel production and can hence contribute to climate change mitigation. This study tries to evaluate whether an innovative PtF system in combination with a manure-based biogas plant could be a future option in the German energy system. Under this concept, the carbon dioxide from the biogas is used, which is normally released into the atmosphere. The hydrogen is obtained via wind-based electrolysis. The analysis is a first attempt to estimate the economic and environmental performance of such a system for synthetic methanol production. In a techno-economic analysis, a small-scale methanol plant is integrated into the analysed system. The analysis is separated into the process simulation of the methanol plant that does not yet exist at this scale and the development of a methodology for the plant's cost estimation adapted to the entire PtF concept. The module costs are determined by enquiries from manufacturers. With the prices received and some further adjustments, the specific manufacturing costs can be determined to be 4.41 €/kg_{MeOH} for methanol production combined with an existing small-manure plant (75 kW). In addition, three cases with different available amounts of CO_2 are examined. One smaller case with the smallest available engine of MAN for the combined heat and power plant, one bigger case including the biogas oxyfuel process (BOP) and one adjusted to an average German biogas plant with 500 kW. The analysis shows that, as opposed to the standard case, the BOP is advantageous as it does not require additional biogas upgrading and generates twice the amount of CO_2. Hence, the costs are lower at 3.17 €/kg_{MeOH}. In general, it is shown that the costs of manufacturing per kg product decrease with an increasing plant size. This can be explained by the economies of scale. Furthermore, sensitivity analyses shows that the H_2 costs and the fixed capital investment (FCI) have the greatest impact among the parameters. However, the impact of the FCI decreases with an increasing plant size. The interest rate and the cost of CO_2 have an impact on the costs of manufacturing as well, whereby the costs of the utilities have nearly no impact at all. The system is further analysed by considering learning curves and other adaptations for future development. The addition of possible revenues from co-products also helps to converge prices with those of other PtF plants. The system linked to an average biogas plant shows comparatively low production costs with 1.38 €/kg_{MeOH}. In the second part of the study, a life cycle assessment (LCA) is carried out, from cradle to gate, for 1 kg of methanol produced with the integrated system operated on the scale of the small-manure plant. In view of the multi-functionality of the process, the uncertainty in LCA outcomes is assessed by considering different assumptions on co-product credits for the heat and electricity from cogeneration and the digestate from the anaerobic digestion. The majority of in total nine analysed scenarios show significant improvements compared with conventional methanol production from fossil resources. Scenario A1 achieves CO_2-eq. savings of -1.09 kg, compared to the reference system which emits CO_2-eq. of 0.85 kg; an improvement of 1.95 kg CO_2-eq. is noted. At an annual production of 212 tonnes of methanol, a total of 413 t/a CO_2-eq. emissions can be saved. In addition, a sensitivity analysis examines the influence of the variability of the life cycle inventory data on the results. The sensitivity analysis shows that parameters determining the overall energy requirements in the PtF system greatly influence its environmental performance and should be carefully considered in process design and upscaling. Despite the uncertainties inherent in the life cycle assessment, the system offers an interesting option for producing renewable methanol while contributing to a circular economy. Even if the economic viability is not yet given, the future development of costs and revenues as well as the positive environmental effects can give the system a perspective.

Contents

List of tables

List of figures

Abbreviations

AACE	Association for the Advancement of Cost Engineering
ACC	Annual capital costs
AD	Anaerobic digestion
AEL	Alkaline elektrolyser
AP	Acidification potential
BASF	Badische Anilin und Sodafabrik
BGP	Biogas plant
BImSchV	Federal Immission Control Act for combustion engines (German: Bundesimmissionsschutzverordnung)
BMBF	Federal Ministry of Education and Research (German: Bundesministerium für Bildung und Forschung)
BOP	Biogas-Oxyfuel-Prozess
BtL	Biomass-to-Liquid
C	Column
CAPEX	Capital expenditures
CC	Climate Change
CCU	Carbon capture and utilisation
CEPCI	Chemical engineering plant cost index
CFC	Chlorofluorocarbon
CHP	Combined heat and power
CMS	Carbon molecular sieves
COM	Costs of manufacturing
COM_{kg}	Specific costs of manufacturing per kilogramm product
$COM_{L,GE}$	Specific costs of manufacturing related to the lower heating value of one litre gas equivalent
COND	Condensator
CP	Compressor
DAC	Direct air capture
DBFZ	Deutsches Biomasseforschungszentrum
DENA	Deutsche Energy Agentur
DM	Dry matter
EC	European Commission
EEG	Renewable Energy Sources Act (German: Erneuerbare-Energien-Gesetz)
EP	Eutrophication potential
EPD	Environmental Product Declaration
EU	European Union
FCI	Fixed capital investment
FD	Fossil depletion

FLH	Full load hours
FNR	Fachagentur Nachwachsende Rohstoffe
FU	Functional unit
GE	Gasoline equivalent
GHG	Greenhouse gases
GtL	Gas-to-Liquid
H	Heat exchanger
HT	Human toxicity
ICI	Imperical chemical industries
IMPCA	International Methanol Producers & Consumers Association
ISO	International Organization of Standardization
KTBL	Kuratorium für Technik und Bauwesen in der Landwirtschaft
LCA	Life cycle assessment
LCC	Life cycle costing
LCI	Life cycle inventory
LCIA	Life cycle impact assessment
LHV	Lower heating value
LNG	Liquid natural gas
LOHC	Liquid organic hydrogen carrier
MeOH	Methanol
MOP	Muriate of potash or potassium chloride
MSW	Municipal solid waste
MTBE	Methyl tert-butyl ether
NG	Natural gas
Nm^3	Normal cubic metre
NMVOC	Non-methane volatile organic compound
NRTL	Non-Random-Two-Liquid
ODP	Stratospheric ozone depletion
OPEX	Operational expenditures
PEM	Polymer electrolyte membrane
POF	Photochemical ozone formation
ppm	Parts Per Million
ppmv	Parts Per Million by Volume
PSA	Pressure swing adsorption
PtC	Power-to-Chemicals
PtF	Power-to-Fuel
PtH	Power-to-Heat
PtX	Power-to-X
PV	Photovoltaic
R	Reactor
REB	Reboiler

RED	Renewable Energy Directive
RWGS	Reverse Water Gas Shift
SR-POLAR	Schwarzentruber und Renon equation of state
SSP	Single superphosphate
TEA	Techno-economic analysis
TRL	Technology readiness level
V	Vessel
VOC	Volatile organic compound
vol%	Volume percent
VPSA	Vacuum Pressure Swing Adsorption
WC	Working capital
wt%	Weight percent
WTG	Wind turbine generator
WTT	Well-to-tank
WTW	Well-to-wheel

Chapter 1
Introduction

1.1 General motivation

Against the background of anthropogenic climate change, a holistic energy transition is necessary to minimise greenhouse gas (GHG) emissions and thus reduce global warming to a minimum. Currently, the energy, transport, heating and industry sectors depend on finite fossil fuels. Their use is associated with the emission of climate-damaging gases such as CO_2, thus contributing to global warming (LENTON et al., 2019). In Germany, the transition of the energy system is commonly known under the notion of the German *Energiewende.* Currently, Germany aims at a 60% GHG reduction for biofuels in their entire production and supply chain compared to fossil alternatives. As a Member State of the EU, German energy policy is also influenced by European regulations. In order to reduce emissions, the EU developed the Renewable Energy Directive (RED), which provides guidelines for the member states. According to its amendment, the RED II, a minimum share of 32% of energy consumption and 14% of fuel consumption in the EU in 2030 must be produced from renewable energy sources in order to reduce the GHG emissions in the energy and transport sector (EC, 2018). Thus far, the transition in the transport sector is particularly slow. As of 2017, it only amounted to 7.6% in the EU (EUROSTAT, 2018). In Germany, the share was 5.2% in the same year and 5.7% in 2018 (BMWI, 2019). Due to this development, Power-to-fuel (PtF) technologies are one promising way of producing renewable fuels, which are important for both the transport and the energy sector (PROGNOS, 2018).

The goal of substituting fossil-based energy carriers by renewably generated products is summarised under the term Power-to-X (PtX) in support of the German *Energiewende*. Weather-dependent regenerative energy from wind and the sun will play a major role in the future energy system and will also provide electricity for other sectors. In order to guarantee a stable supply despite fluctuating feed-in and

to avoid the curtailment of wind or photovoltaic (PV) systems, various flexibility options must be used. In addition to flexible power plants, load management, grid expansion and energy storage, flexible sector coupling with Power-to-X represents an integral part of a future supply system. It enables an accelerating expansion of fluctuating renewable energies, since they can be used in a supply-oriented manner. PtX systems do not require any security of supply. The use of energy via PtX involves the conversion of electricity into gas (Power-to-Gas, PtG), heat (Power-to-Heat, PtH) and fuel (Power-to-Fuel, PtF). Furthermore, it includes the connection to the chemical industry (Power-to-Chemicals, PtC) (ENERGIEAGENTUR.NRW, 2020).

Power-to-Fuel (PtF) (also referred to as Power-to-Liquid (PtL)) processes describe the utilisation of renewable energy for alternative fuel production, which are relevant both for the mobility as well as the energy sector (PROGNOS, 2018). These pathways make use of CO_2 captured as a waste product from industry, air, biogas or waste plants (DIETRICH et al., 2018) and combine it with renewable hydrogen (H_2) to produce synthetic fuels also referred to as electro fuels or e-fuels. The technology has high potential to be a key contributor to the German *Energiewende* and the resulting transition of the mobility sector. VARONE et al. (2015) support the aspect of PtF processes, among others, as potential storage options; PtF schemes could be a strong candidate in order to achieve the reduction target in GHG emissions and make the energy system more sustainable. The ability of synthetic fuels to convert and store excessive energy from renewable sources into chemical energy is a relevant aspect. Another advantage of the PtF concept is its compatibility with the existing system, meaning that the existing fuel and vehicle technology can be used with minor adjustments (PEARSON et al., 2014). Among PtF technologies, methanol, the simplest of the alcohols, plays an important role. This is because methanol can be used as an independent fuel or as an admixture to existing fuels. Further processing to other renewable fuels is also possible. As such, methanol already accounts for a large market share in certain countries, e.g. more than 20% in China (Yang and Jackson, 2012). On the global scale, its share grew at a compound annual growth rate of 5.5% during 2015 and 2019 (EMR, 2020).

Suitable CO_2 sources for the synthesis must have a high share of CO_2, a high punctual supply and no impurities that could damage catalysts. Aside from e.g. industrial waste gases, a source could be biogas from biogas upgrading plants, as they provide a high CO_2 concentration. German biogas plants (BGPs) are a promising carbon source for large-scale renewable CO_2 provision as pointed out by BILLIG et al. (2019). Up to the present day, the CO_2 from BGPs has simply been released into the atmosphere, although it contains great potential as a carbon source.

Therefore, its utilisation would mean a valorisation of a waste product. The capacity, as of 2016, was estimated at 10.4 million tonnes, plus an additional 1.5 million tonnes from the approximately 200 biogas upgrading plants (BILLIG et al., 2019); only the latter could substitute the CO_2 required for the entire German methanol production (VCI, 2018). Thinking that there are more than 9000 BGPs in Germany and more than 18,000 in the whole of Europe, gives a perspective of the huge potential that lies within it. There is also shown interest in upgrading small amounts of biogas into biomethane for making residues and organic waste from local and sometimes remote locations available (BIENERT et al., 2019).

Using biogenic carbon for PtF technologies can also contribute to the goal of reaching a circular economy, which aims at optimising and closing material and energy cycles wherever it is ecologically sensible. Within this goal, the EU specifically supports closing carbon cycles and making use of waste products such as CO_2 (EC, 2020). Therefore, the question about the carbon source for the PtF technology is a particularly relevant one. Concerning this, the manifold benefits of biogas plants should not be ignored, as recently summarised in a study carried out by WERN et al. (2019). BGPs do not only produce energy, heat and methane (CH_4), and, by doing so, play an important role in sector coupling; they also help to save greenhouse gas (GHG) emissions from liquid and solid manure management, convert excess nutrients into valuable fertiliser (digestate) and recycle organic waste to produce energy. Thus, they provide a relevant contribution towards the use of carbon cycles, and, when using residues and waste materials as feedstock, they even support the EU's idea of a circular economy further (EC, 2020). Besides, the production of fuels from animal manure ultimately yields "advanced biofuels" as defined by the RED II, while contributing towards a circular economy by reusing by-products and minimising waste generation (MENG et al., 2019).

Looking at livestock statistics and the growing trend of farm sizes in Germany, there is a huge potential for energetic manure utilisation in BGPs. Farmers need to find a way of processing the occurring faeces and meeting environmental regulations at the same time. From the perspective of climate protection, farm fertiliser should be used energetically in order to reduce storage emissions (FNR, 2013). Especially small-scale biogas plants, using mostly manure as a feedstock have become more prominent in Germany in recent years. Such plants are known under the term *Güllekleinanlagen*, i.e. small-manure plants and sometimes small liquid manure plant. These plants are financed under a special subsidy scheme, as they provide manure management benefits because of emission avoidance that usually occurs during manure storage. The prospect of energetically using manure

in BGPs is an interesting opportunity within a country that has many livestock farms and an issue with excess manure, also occurring from neighbouring countries such as the Netherlands. Particularly, the North and South of Germany have a high density of BGPs (DANIEL-GROMKE et al., 2017), coinciding with the location of many farms and high volumes of manure, while at the same time offering locations for wind and photovoltaics (PV). Therefore, these regions present an interesting location for PtF systems. Thus far, no small-scale upgrading plants exist on an industrial scale in Germany. The option could hence also be interesting to discover in an integrated PtF system.

1.2 **Research gap**

Conventional methanol production is mainly based on a chemical synthesis process that uses H_2 and carbon monoxide (CO). The latter is produced via steam methane reforming of the fossil resource natural gas (NG), a process which is well established on an industrial scale (Pontzen et al., 2011). As pointed out by FERRARI et al. (2014), renewable methanol could be an appropriate substitute for coal, oil, NG and products derived from them. In fact, the renewable production of methanol from H_2 and CO_2 has recently gained more attention in the scientific literature, where it has been the focus of model-based process analyses often including techno-economic analyses (TEAs) (DECKER et al., 2019, NYÁRI et al., 2020, OTTO, 2015, PETERS et al., 2020, RIVAROLO et al., 2016) as well as life cycle assessments (LCAs) (GONZÁLEZ-GARCÍA et al., 2012, MATZEN et al., 2016). In general, methanol production usually occurs in large plants on an industrial scale, although there have also been some studies about small-scale synthesis (DE JONG, 2018, RIVAROLO et al., 2016, USHIKOSHI et al., 1998). RIVAROLO et al. (2016) considered plants at a capacity of 100 kg/h methanol (553 kW_{LHV}). Apparently, manufacturers also produce such plants, such as bse engineering with a capacity of 8200 t/a (BSE ENGINEERING, 2020).

Methanol production from biomass is analysed in many different process pathways in the literature. For instance, gasification describes the thermochemical conversion of biomass at high temperatures into gaseous energy carriers. When adding a gasifying agent (e.g. air, O_2), H_2 and CO are produced, from which methanol is then synthesised (BANDI et al., 2004). Biomass gasification can also include CO_2 separation in a preceding process. Methanol is subsequently produced from CH_4. The separated CO_2 is then either released into the atmosphere or stored and sold (HUISMAN et al., 2011). It can also be used together with H_2 for additional methanol synthesis (FIRMANSYAH et al., 2018, PEDERSEN et al., 2014). Another possibility is to produce methanol by using a reformer to convert biogas

into syngas (consisting of CO and H_2), which can then be converted into methanol (BOZZANO et al., 2017, CLAUSEN et al., 2010, PREVITALI et al., 2018). Biogas can also be upgraded, and separated CO_2 is converted into CO via a reverse water-gas-shift reaction (DIMITRIOU et al., 2015). Nevertheless, the process route of CO_2 utilisation from biogas upgrading together with renewable H_2 has not played a large role in the literature yet. Overall, valorisation of biogas CO_2 has options, but developments to use it as a substitute for fossil-based CO_2 are still in their infancy stage (KAPOOR et al., 2020). The idea of using CO_2 from flue-gas of industrial processes for PtF routes is not new, on the other hand, although it has recently gained more attention (DECKER et al., 2019, MIGNARD et al., 2003, NYÁRI et al., 2020, SCHEMME et al., 2019, USHIKOSHI et al., 1998). There is literature available that considers systems similar to the one analysed in this study, meaning that they consider CO_2 from BGPs as a carbon source and combine it with renewable H_2. For instance, DECKER et al. (2019) analysed a system very similar to the one proposed here by means of a TEA, producing much higher capacities of 30 MW. Their system utilises waste CO_2 from small industrial plants and BGPs and H_2 from PEM electrolysis. Another study by RIVAROLO et al. (2016) also consider a similar process in a TEA. The authors analysed an optimised plant layout using renewable H_2 and CO_2 from biomethane production plants, however, they took electricity from the grid if renewable energy sources (RES) were not available. Cost analyses estimated methanol produced by PtF at costs between 300-1000 €$_{2015}$/kW, although they apply to commercial scale plants in the range of 5-200 MW (BRYNOLF et al., 2018).

The environmental performance of alternative technologies or production strategies is commonly analysed by means of an LCA, since it makes production options comparable (CHERUBINI et al., 2009). In the context of biogas production, LCAs have been applied, for instance, to compare the environmental impacts from manure- and crop-based BGPs to produce electricity (FUCHSZ et al., 2015); or from different agricultural substrates to produce biogas in integrated combined heat and power plants (CHP) (LANSCHE et al., 2012). PÉREZ-CAMACHO et al. (2019) analysed three utilisation scenarios for biogas production from AD, looking at biogas for electricity production, biogas upgrading as well as biomethane injection into the gas grid to provide heat and the utilisation as a fuel. Other authors use LCA to quantify impacts of classic biogas upgrading from different raw materials (BURATTI et al., 2013), as well as from more innovative production of biosynthetic CH_4 from H_2 and CO_2 (CASTELLANI et al., 2018). In the context of transport fuels, LCAs also tackle the utilisation of methanol as a fuel (AL-BREIKI et al., 2020, VERHELST et al., 2019), while other studies assess the production of

a variety of synthetic fuels from biogas through AD, e.g., compressed and liquefied biogas, methanol, or Fischer-Tropsch Diesel and dimethyl ether (DME) (MOGHADDAM et al., 2015, MOGHADDAM et al., 2016). LEE et al. (2016) evaluate the production of DME from landfill gas or manure-based biogas. However, all these systems use the CH_4 from biogas for steam reforming to syngas. Biomass gasification also plays a part in LCA literature about methanol production from syngas (AL-BREIKI et al., 2020).

1.3 **Scientific objectives**

This study aims at an evaluation of a novel PtF system using CO_2 from small-manure plants. This is done by means of both of a techno-economic analyses (TEA) and a life cycle assessment (LCA). The renewable methanol production inside such a system, in combination with CO_2 from manure-based plants, is especially interesting and, to the author's knowledge, has not been analysed before. The idea for the system, based on a concept designed by DECKER et al. (2018), is to produce synthetic fuel in the form of methanol at small-scale local sites linked with anaerobic digestion (AD) plants (i.e. biogas plants) combining biomass-based CO_2 (esp. from manure and residues) and H_2 from wind-based electrolysis. Thus, the analysis deals with a Power-to-Fuel (PtF) pathway that obtains CO_2 from biogas during the biogas upgrading process or by means of the biogas oxyfuel process (BOP) as described by SCHORN et al. (2020). A wind turbine that powers an electrolyser generates H_2. The product route will lead to methanol, which was found to be a convenient intermediate produced at a farm site (PETERS et al., 2020). Figure 1.1 shows the entire system. The novel aspect of this study is the simulation of a methanol synthesis plant in combination with a biogas plant at the local scale (40 m^3/h biogas). The system also makes use of a storage facility for renewable H_2 in order to avoid the utilisation of grid electricity. The process of direct methanol synthesis from CO_2 and H_2 has a TRL of 9, however this alternative conversion pathway for synthetic fuel production is not in use in the market yet. The whole analysis is site-specific for Germany and considers German conditions. As Lower Saxony, a federal state in the North-western part of the country, has both numerous wind and biogas locations, the area is especially interesting for such a concept.

Figure 1.1: Power-to-Fuel system as the object of study for this thesis.

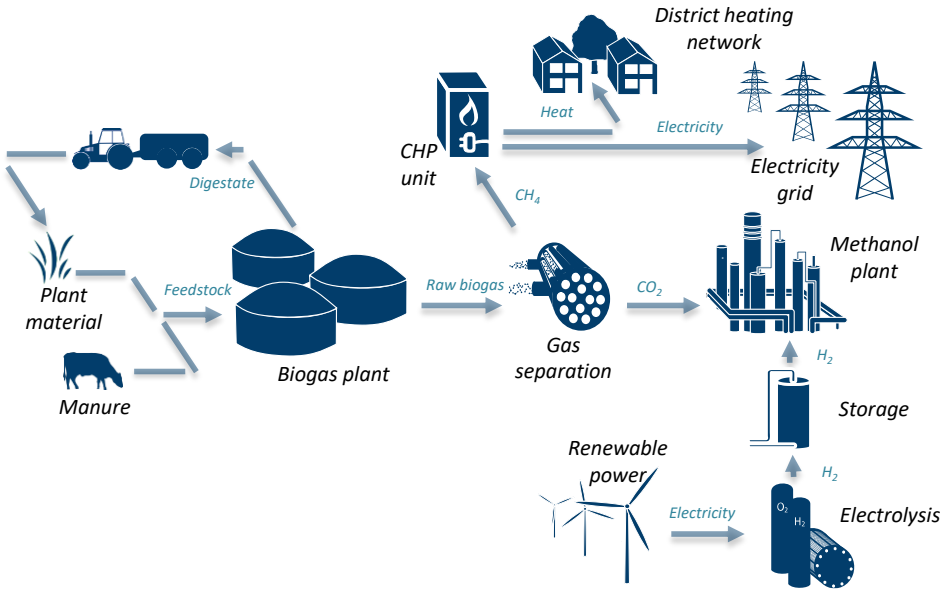

Caption: own creation; CHP = combined-heat and power.

The system analysed by this study presents a novel option to produce renewable methanol while contributing towards a circular economy, provided that its performance is also beneficial relative to the fossil alternative. In order to give an estimate on the potential of this system, we analysed it by means of a life cycle assessment (LCA) and a techno-economic analysis (TEA). If possible, the system should be viewed as a holistic system, as it affects an entire farm location and its owner. Therefore, we chose to evaluate not just the aspect of the methanol synthesis but the entire system including the BGP and biogas upgrading process in the LCA. It is important to account for the environmental impacts in its entirety and consider the system in an integrated way as presented in Figure 1.1. Due to the multi-functionality of the system, the study considers multiple scenarios in order to capture various assumptions on the credit of co-products for the digestate from the biogas plant (BGP) and electricity from the combined heat and power unit (CHP). The goal is to evaluate the system's environmental impact compared to conventional methanol production. Thus, it gives relevant insights on whether the concept is a sustainable option for future fuel production. In an additional LCA exercise, we investigate the double value of the AD system that produces energy but at the same time avoids emissions that occur from manure storage. For this, a classical biogas system is compared to an alternative system. The study therefore

also contributes to the current LCA literature of biogas plants and whether or not to include credits for avoided manure emissions. Due to the diversity of technologies for the upgrading of biogas, this study also gives an overview of them. As upgrading technologies produce different purities in CO_2 streams, some are arguably more suitable for small-scale PtF applications than others. This work focusses on a selection of three, which, on the one hand, were found to be suitable for the smaller scale, having already been subject of pilot plants and the scientific literature, and, on the other hand, were able to provide the required amounts of CO_2 in the flue gas.

The costs are analysed during a TEA, which provides the entire costs of manufacturing (COM) as well as the specific costs for the methanol. The TEA focusses on the development of a methodology for cost estimation of a small-scale methanol system, as this does not exist in the market yet. The methods used for large plants cannot be applied to small plants without further ado. Therefore, it is necessary to perform a process simulation to get the necessary data for the subsequent cost estimation. For this, the parts of the system are modelled in the Aspen Plus simulation software. The analysis considers four different plant sizes and is expanded by considering the costs and revenues of the BGP, as the farmer is the investor and would also have to pay for utilities but benefits from co-products at the same time. Hence, the profits by the entire system are also evaluated.

In order to be able to assess the PtF system, the following questions need to be answered:

- Is the introduced system preferable to conventional methanol production from an environmental point of view?
- What are the costs of small-scale methanol production and how do they compare to conventionally produced methanol?
- Could this system be an opportunity for biogas plants using manure, providing additional income and supporting the profitability of such plants?

1.4 General approach and structure

Economic and environmental analyses were carried out, investigating a novel Power-to-Fuel (PtF) system with regard to its utilisation potential. In the context of this work, a methanol plant is investigated that produces renewable methanol on the basis of CO_2 from a small-manure plant and H_2, which is produced by

electrolysis. Moreover, a cost estimation method is developed and applied to determine the production costs of the methanol plant, for which data has not been available on such a small scale. Further analyses include the calculation of costs for biogas plants and biogas upgrading. The profit for the entire system is also evaluated and several scenarios investigated.

Chapter 2 provides an overview over the current technologies that are relevant to understand for the analysis of this thesis. First, it introduces the state of the art of methanol synthesis, with a focus on the thermodynamics of the process, different possible reactor types and the process design. Additionally, current projects in research and the industry are discussed that deal with the renewable methanol synthesis, also in the context of small-scale plants. Second, the chapter describes the potential of CO_2 from biogas and biogas upgrading plants and identifies manure and agricultural residues as a relevant feedstock. Furthermore, it presents biogas upgrading technology and looks into such technology for small-scale plants, which is relatively new to the market and selects the technology most applicable to the PtF system. A focus is placed on BGPs in this chapter, as emissions are closely linked to their operation, while wind turbine and electrolyser rather contribute emissions during the construction phase, which is not considered in this study. Subsequently, relevant aspects of the PEM electrolysis are presented, which is used for the production of H_2. Chapter 3 introduces TEA and LCA methodology and further summarises relevant economic and environmental analyses of biogas and PtF systems to further place this work in the current literature. The section about the cost estimation describes, first, the component design, before the computation of the manufacturing costs is presented, which consists of the investment and operating costs. For the determination of the investment costs three possible procedures are presented, the capacity method, the surcharge factor method and enquiries from manufacturers. The methods used and the modelling performed are presented in chapter 4. At the beginning, the plant data and overall concept is presented. For this, an underlying model about the general assumptions of the system is designed, as it does not exist in real life yet. The methanol synthesis process is then modelled for the cost analysis using the simulation software Aspen Plus V10. Subsequently, the adaptation of the cost accounting methods presented in chapter 3 to the given application case are described, whereby the surcharge factor method of TURTON et al. (2009, p. 193ff) serves as a basis. In addition, the different cases investigated and the methodology used to perform sensitivity analyses is explained. Last but not least, the methodology applied for the LCA is introduced. Here, several scenarios are analysed, taking care of the multi-functionality problem using system expansion. The scenarios consider replacing

electricity from the German, a coal-based and a wind-based grid mix with the electricity generated by the CHP and account for the saved emissions. Moreover, they consider the production credit of different types of fertiliser that are replaced by the occurring digestate. The methodology for a sensitivity analysis is also explained. A complementary LCA compares two biogas systems to investigate biogas combustion in a CHP vs. a gas flare. The results from the TEA and LCA are presented and discussed in chapter 5. First, the results of the process simulation are discussed and the most important findings from this simulation are presented. Thereafter, the results of the cost calculation are presented, whereby the module sizes are calculated at first. Then, the determined module costs and the operating costs are presented before the results of the manufacturing costs are analysed. The results of three other cases with different available amounts of CO_2 are also interpreted as well as the performed sensitivity analyses. Finally, the sub-chapter discusses profits and possible development in costs for the biogas plant and the entire PtF system in order to evaluate its potential market introduction in the future. The second part of the results and discussion deals with the LCA. Results of the scenario analysis are firstly compared. Subsequently, they are compared to the reference system of conventional methanol production. Another section presents the results of the contribution analysis, analysing the contribution in impacts caused by the individual processes. The results are then discussed and those of the additional LCA are also presented. The final section ends with a summary of key findings. Chapter 6 concludes and gives an outlook on limitations and further research possibilities.

Chapter 2
Background and state of the art

This chapter provides an overview over current production technologies relevant to the analysed PtF system and explains the choices for certain technologies in the PtF system. For this purpose, methanol production, biogas production, CO_2 separation technology and electrolysis are closer investigated. First, methanol synthesis is described in 2.1, with a focus on the thermodynamics of the process, different possible reactor types and the process design. In addition, current small-scale renewable methanol production is presented, as it is particularly relevant in the context of the decentral system considered here. In section 2.2 and 2.3, the two operating utilities CO_2 and H_2 and their generation are presented. The potential of CO_2 from BGPs in Germany is investigated. The focus lies on BGPs using manure and agricultural residues, as this is the chosen pathway for the origin of biogas in this study. Gas separation technology for small-scale plants are also presented and applicable processes for the PtF system selected. PEM electrolysis is chosen for the upstream system with liquid organic hydrogen storage (LOHC) to provide decentralised H_2 for methanol synthesis. Hence, relevant aspects of it are introduced. Finally, the chapter summarises and concludes important developments and dynamics that are interesting for the general approach and modelling of this study.

2.1 Methanol production and usage

The focus of this sub-chapter is on renewable methanol production and its current standard for industry and the focus of research on the topic. Section 2.1.1 introduces the conventional and renewable options of methanol synthesis, also looking at the history. Section 2.1.2 describes the process characteristics of the methanol direct synthesis and section 2.1.3 introduces renewable concepts of it.

2.1.1 *Methanol synthesis*

Methanol is the simplest of all alcohols, with the chemical formula CH_3OH, and one of the most important basic chemical substances. Worldwide production in 2019 was 98 million t/a (METHANOL INSTITUTE, 2020), with demand rising steadily over the past years. Methanol is used both in the chemical industry as a basic material for a wide range of chemical products as well as in the fuel and energy sector. It is used for energy storage of renewable energy, as an admixture to conventional fuels and as a fuel in its own right. It is also processed into other renewable fuels. Methanol can be found in many everyday products such as resins, plastics, paints, polyesters and building materials. Moreover, it is used as a solvent in the chemical industry (OTT et al., 2012, p. 17ff). In the chemical sector, about 25% of all methanol is used for the production of formaldehydes alone. Overall, the consumption of methanol by the chemical sector accounts for just over 50% of the quantity produced, with other large shares going into the production of acetic acid (CH_3COOH) and methyl tert-butyl ether (MTBE). A further 20% of the methanol produced is used in the fuel sector either as an additive to petrol or further processed into biodiesel and dimethyl ether (DME), which can be used as an alternative to conventional diesel. Additionally, the processing of methanol into olefins accounts for another large proportion of methanol usage at just under 25% (METHANOL INSTITUTE, 2020). Methanol is characterised by a comparatively simple production process and a high PtF efficiency. Other advantages of methanol are that it is already in use as a fuel and that storage and transport are relatively simple. Disadvantages, on the other hand, are its acute toxicity, water hazard and corrosiveness to metals, which must be taken into account during production and utilisation (SCHEMME et al., 2019).

The industrial production of methanol began in the 1920s. BASF (Badische Anilin und Sodafabrik) developed a process in which methanol can be produced from synthesis gas (a mixture of H_2, carbon monoxide (CO) and CO_2) using a catalyst consisting of zinc oxide (ZnO) as the active material and chromium oxide (Cr_2O_3) as a stabiliser at high pressures (250 to 350 bar) and temperatures in the range of 320°C to 450°C. The catalyst is characterised by chlorine- and sulphur-resistance, which are contaminants of synthesis gas (OTT et al., 2012, p. 2ff). Already at this time, research on catalysts with copper (Cu) as the active material began, as these are characterised by a particularly high selectivity. Due to their low stability against sulphur, a purification process for the synthesis gas first had to be developed. Therefore, it took until the 1960s for the company ICI (Imperial Chemical Industries) to develop a methanol process with significantly milder reaction conditions for industrial usage. The process uses a Cu-based catalyst and sulphur-

free synthesis gas. This process requires temperatures of 200°C to 300°C and pressures in the range of 50 to 100 bar, which is why the process is referred to as a low-pressure process. Today's technologies are still based on the process developed in the 1960s, but on a larger scale. This was made possible by the "MegaMethanol" process developed by Lurgi in 1997, which is characterised by production quantities of up to 10,000 t/d of methanol. Since the early 1990s, research has focused on the chemical upgrading of CO_2 by hydrogenation to renewable methanol. After the general feasibility was shown and first concepts were developed, this approach was not pursued further for commercial reasons. Due to the necessary reduction of CO_2 emissions, this process route is currently once again the subject of research and industry. Up to now, mostly pilot plants using this process have been in operation. In today's large-scale industrial processes, methanol is produced exclusively by catalytic conversion of synthesis gas via the low-pressure conventional process. Compared to earlier processes with higher pressures, this one has lower investment and production costs, higher reliability and greater flexibility in the choice of plant size (OTT et al., 2012, p. 8ff). The synthesis gas is produced primarily via steam methane reforming of NG, a process with a high maturity level (PONTZEN et al., 2011).

The NG has to be produced which is mostly done abroad for Germany. The German import of NG as of 2018 is mainly coming from Russia (35-40%), although Norway and the Netherlands with 34% and 29%, respectively, also play an important part (WETTENGEL, 2019). The most prominent source of NG is the Yamal peninsula in North-Western Russia. If NG comes from there to Germany, the travelling distance is approximately 4200 km (PST PURENERGY, 2020). PETERS et al. (2019) mention that Russian NG ranked worst in several studies in terms of its CO_2 footprint, followed by Germany, Norway and the Netherlands with the lowest CO_2 emissions per kWh. Emissions occurring during NG production and transmission are mainly CO_2 emissions from energy generation via combustion and fugitive CH_4 emissions. If it is not cost efficient to utilise the NG, the gas is flared, which causes mostly CO_2 emissions. This is counted however as a contribution to the required energy, meaning that the gas is added to the gas that is required for NG production. The transmission entails fugitive CH_4 emissions due to leakages of pipelines and machines. In addition, the NG processing requires energy that leads to emissions, e.g., through acid gas processing that removes the hydrogen sulphide (KEHLER et al., 2016, p.13f).

The required NG in Germany is transported from abroad either through pipelines or using liquefied natural gas (LNG) carriers. For pipelines, which are the most

prominent transport method, it applies that the longer the transport, the higher the emissions because NG transportation entails them through leakages and energy demand for the compression. The impact was analysed and found relevant by studies in the literature (PETERS et al., 2019, PRIEUR-VERNAT et al., 2011, SIMLA et al., 2019). The LCA study by PRIEUR-VERNAT et al. (2011), investigating the European NG supply chain, discovered that non-renewable energy depletion is mainly affected by the impacts of NG production and long-distance pipeline transport. In general, the CH_4 emissions from pipeline leakages found in the literature varied from 0.7-4% according to SIMLA et al. (2019). Another option is the transport as LNG. This however entails propulsion emissions for the carrier as well as its auxiliary equipment. For instance, a vessel is equipped with a re-liquefaction installation on board in order to avoid losses, which greatly affects the ship's fuel consumption (SIMLA et al., 2019). For pipeline losses, EDWARDS et al. (2014), who carried out a well-to-tank analysis, mention losses of 0.13% of gas per 1000 km and emphasise that leakages in European networks are small due to the network being well-maintained. According to WACHSMUTH et al. (2019, p. 19), who analysed the process chain emissions from LNG, emissions from Russian pipeline NG as opposed to Algerian NG transported by vessels did not show mentionable differences. Nevertheless, pipeline losses from Norway are much lower than those coming from Russia (WACHSMUTH et al., 2019).

2.1.2 *Methanol process design*

Methanol can be synthesised by hydrogenation of CO_2 (equation 2.1) or CO (equation 2.2). The two reactions are linked via the reverse water gas shift (RWGS) reaction (equation 2.3), so that both hydrogenations can always take place, even if only CO_2 or CO is added as the reactant (OTT et al., 2012, p. 3f).

$$CO_2 + 3H_2 \rightleftharpoons CH_3OH + H_2O \qquad \Delta H_{300K} = -49.16\ kJ/mol \qquad (2.1)$$

$$CO + 2H_2 \rightleftharpoons CH_3OH \qquad \Delta H_{300K} = -90.77\ kJ/mol \qquad (2.2)$$

$$CO_2 + H_2 \rightleftharpoons CO + H_2O \qquad \Delta H_{300K} = +41.21\ kJ/mol \qquad (2.3)$$

All three reactions are equilibrium reactions and therefore no complete conversion of the educts is achieved. Since both hydrogenations are exothermic, as can be seen from the negative reaction enthalpies ΔH in equation 2.1 and equation 2.2, accompanied by a reduction of quantity of material, high pressures and low temperatures shift the equilibrium to the product side (OTT et al., 2012, p. 4). A

compromise must be found for both parameters, because low pressures are associated with lower investment and production costs and high temperatures improve the kinetics of the process. Therefore, both parameters must be adjusted to ensure the best overall conditions for the process.

The methanol synthesis is decisively influenced by the activity, selectivity and long-term stability of the catalyst. ZnO/Cr_2O_3 catalysts are used at the beginning of the industrial production of methanol. In the 1960s, these catalysts were replaced by Cu-based catalysts, as Cu is a very active metal for methanol synthesis. Aside from Cu itself, these catalyst systems consist of ZnO and aluminium oxide (Al_2O_3). The active areas lie within the Cu centres. The presence of ZnO has a stabilising effect on the Cu. The Al_2O_3 also stabilises and prevents the sintering of active particles, which would lead to catalyst deactivation. Another possibility of deactivation of this catalyst is by sulphur poisoning, therefore the synthesis gas must be sulphur-free. Today, $Cu/ZnO/Al_2O_3$ catalyst systems are almost exclusively used, although improvements are still being discussed and researched. There are big differences in the composition of these catalyst systems. ICI uses catalysts containing 61% Cu, 30% ZnO and 9% Al_2O_3. BASF's catalysts are also in similar ranges with 65% to 75% Cu, 20% to 30% ZnO and 5% to 10% Al_2O_3. However, there are also manufacturers where the Cu has a significantly lower fraction at a minimum of only 25%. (OTT et al., 2012, p. 6)

The reactor is the most important component in all chemical processes. Its design is decisive for an optimisation of methanol production with regard to kinetics, thermodynamics, selectivity and catalyst lifetime. In all cases, a compromise must be found between a sufficient reaction rate and sufficient heat removal. High temperatures have a positive effect on kinetics, but low temperatures have a positive effect on thermodynamics. Therefore, the reactors for methanol synthesis must be equipped with an effective temperature control. It is important to remove the heat generated during the exothermic hydrogenation of CO and CO_2 and hence maintain the reactor at the desired reaction temperature. To achieve this, adiabatic and quasi-isothermal reactors are primarily used (OTT et al., 2012, p. 10). In addition, research is performed on other reactor concepts, such as membrane, liquid phase and fluidised bed reactors. These are not yet in industrial use, but offer potentials for optimising methanol synthesis in the future (BOZZANO et al., 2016).

In adiabatic reactors, no active cooling of the reaction zone takes place. Instead, cooling is performed by injecting the educt mixture at various points in the reactor,

as shown in Figure 2.1, a). The injected gas is characterised by a lower temperature than the mixture already in the reactor that is the result of an exothermic hydration. This type of reactor provides a simple way of controlling the temperature. However, the temperature is not constant over the whole reactor, but shows a saw tooth-shaped pattern. The temperature is lowered with each injection, followed by a continuous increase in temperature before cooling is again caused by the next injection. Additionally, parts of the reaction mixture are injected time-delayed and therefore have a shorter retention time to react and do not pass through the entire catalyst bed. Consequently, the conversion is lower than in reactors with an active cooling system. (HANSEN et al., 2008, p. 2939f)

Figure 2.1: Possible reactor types for methanol synthesis, a) adiabatic reactor, b) quasi-isothermal reactor.

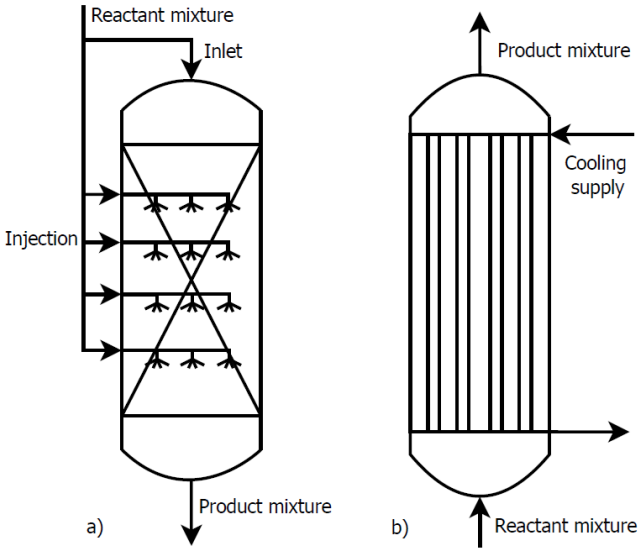

Caption: own presentation based on HANSEN et al. (2008, p. 2940).

Quasi-isothermal reactors are used to achieve better temperature control. In these reactors, the entire reaction zone is kept at an almost constant temperature. This is achieved by active cooling, usually with water vapour. The advantage of cooling with steam is that a simple temperature control by changing the steam pressure is possible. This reactor is usually designed as a standing tube bundle reactor, whereby the reaction medium flows from below through the tubes filled with the catalyst. The cooling medium is passed through the reactor in counter-current on the housing side. The steam generated in this way can be used as an energy source for a compressor or a turbine, or can be used as a heat source for distillation in the

later course of the process. The design of this reactor is shown in Figure 2.1 b). As a modification, it is also possible to pass the reaction mixture through the catalyst on the housing side and to flow the cooling medium through the tubes. In this configuration, gas is often used as cooling medium instead of steam. A further modification is to use double tubes through which the reaction mixture first flows on the inside for heating and then flows back through the outer tube filled with the catalyst, whereby steam is used on the housing side (OTT et al., 2012, p. 10f). The advantages of the isothermal reactor are optimal temperature control, the generation of a small amount of by-products, lower operating costs compared to the adiabatic reactor, and a longer catalyst service life. Disadvantages are that, compared to the adiabatic reactor, the maximum production capacity is lower due to the large total reactor volume through tubes and casings and these reactors are also more expensive to invest due to their more elaborate design (HANSEN et al., 2008, p. 2939).

2.1.3 *Projects about renewable methanol synthesis in research and industry*

In this section, current pilot and first industrial plants using the concept of renewable methanol production are described. Due to the necessary reduction of CO_2 emissions, this process route is currently a main subject of research and industry. Large CO_2 savings are possible here, as the current industrial standard for methanol synthesis is based on the fossil energy source NG. Therefore, the production of methanol currently leads to GHG emissions. However, methanol can also be produced simply by hydrogenating CO_2 with the help of H_2, as can be seen in equation 2.1. This process has recently gained more attention in the scientific literature (MATZEN et al., 2016, MILANI et al., 2015, PETERS et al., 2020). It has the advantage that instead of releasing CO_2, excess CO_2 is used for the process. Green H_2 must be used to provide this process with a climate benefit. It can be produced by electrolysis with electricity from a renewable energy source, as described in section 2.3. Otherwise, emissions would again be produced at this point. There is a large interest in both research and industry in using this CO_2-based process on an industrial scale and provide the benefits of temporal CO_2 sequestration. The idea of using CO_2 from flue-gas of industrial processes for PtF routes is a prominent option in the literature (DECKER et al., 2019, MIGNARD et al., 2003, NYÁRI et al., 2020, USHIKOSHI et al., 1998). There is the potential to produce methanol within a local PtF system, as was concluded by a study from PETERS et al. (2020).

The first pilot plant was commissioned by MCI (Mitsui Chemicals Inc.) in 2009. It produces 100 t/a of methanol with CO_2 from industrial waste gases and H_2, which is produced by photolysis of water (MITSUI CHEMICALS INC., 2008). In 2011, CRI (Carbon Recycling International) commissioned the "George Olah Renewable Methanol Plant". Here, CO_2 from a geothermal energy plant was initially used on a pilot scale to synthesise methanol. In the meantime, the production capacity has been increased to 4000 t/a, which corresponds to a recycling of 5,500 t/a of CO_2 emissions. The CO_2 comes from the waste gas of an adjacent geothermal plant, which would otherwise be released into the atmosphere. It must first be treated so that it can be used in the methanol plant. The required H_2 is produced by electrolysis. In the end, geothermal steam is used as a heat source for separation of water from methanol by distillation. The only by-products are H_2O from distillation and pure O_2 from electrolysis. The plant is modularly designed, so that an enlargement as well as an adaptation to different locations is possible. CRI claims that they were the first to produce fuels based on CO_2 on an industrial scale. Over 90% of CO_2 emissions in the entire life cycle can be saved with this process compared to the production with fossil energy sources (CARBON RECYCLING INTERNATIONAL, 2020).

The EU is also committed to producing methanol using industrial waste gases. Therefore, the EU-funded MefCO_2 project was launched in 2015. This project uses CO_2 from exhaust gases together with H_2, which is produced by electrolysis with surplus energy from, e.g., WTGs to produce methanol. The pilot-scale plant was completed in June 2019 after four and a half years and now produces 1 t/d of methanol. This means that more than 1.5 t/d of CO_2 is separated from flue gas. This pilot plant is currently one of the largest plants for production of methanol using CO_2 from exhaust gases in the EU. This plant is also modular with the aim of adapting it to different plant sizes and gas compositions of the waste gases (MEFCO_2, 2016). Meanwhile, many large companies from the energy and chemical industries have entered the research and production of renewable methanol. Companies active in the global renewable methanol market include Advanced Chemical Technologies, BASF, CRI, Enerkem, Fraunhofer, Innogy, Nordic Green, OCI N.V., Serenergy A/S and Sodra (ALLIED MARKET RESEARCH, 2020).

There is also interest in small-scale renewable methanol production plants in research and industry. As early as 1998, USHIKOSHI et al. (1998) investigated the general functionality of the process for methanol synthesis from CO_2 and H_2 in a test plant with a production capacity of 50 kg/d of methanol. Here, it can be shown that the production rate of methanol increases with an increase in pressure and that the optimum reaction temperature for this process setup is 270°C. Furthermore, a

very high selectivity can be demonstrated and a purity of 99.9% of the produced methanol is achieved. In 2016, RIVAROLO et al. (2016) published the results of a feasibility study and an economic analysis for a methanol plant with a production volume of 100 kg/h. Two different plant concepts were investigated; one separates the CO_2 by treating biogas and the other obtains the CO_2 from an external source. In both cases, the required H_2 is produced by means of an alkaline electrolyser (AEL) which obtains electricity from a renewable energy source. If this is not available, the electricity is taken from the grid. The authors showed that there is great potential for methanol production from renewable sources. In his master's thesis, DE JONG (2018) also investigated a small-scale methanol plant. The objective was to design a container-scale plant which can be operated automatically in order to be used even in remote locations. The main focus is on adapting the various components of the plant to the size of containers. The author developed a concept where the system fits into three of them. As a CO_2 source, ambient air is used. Sea water, on the other hand, is used for electrolysis. The required electricity is generated by a PV system.

There are several companies in the industry dealing with small-scale plants for renewable methanol synthesis. For example, Thyssenkrupp sells small plants with production volumes of 10 to 200 t/d methanol, which can be operated with renewable H_2 and CO_2 from industrial waste gases or biogas plants. These plants were developed together with SLF (Swiss Liquid Future) and the process is called "SLF/Uhde Methanol Process". The electricity is generated from hydropower, wind power or solar energy. The electrolysis plant was developed by Thyssenkrupp itself. This plant is known as a "Green Methanol Plant" and has a modular design. The structure of the overall concept is shown in Figure 2.2 (THYSSENKRUPP INDUSTRIAL SOLUTIONS AG, 2020). Moreover, bse engineering already produces small plants for methanol synthesis under the name "FlexMethanol". Here, only H_2 from surplus electricity together with CO_2 from exhaust gases is used for methanol production. The "FlexMethanol 10" process produces 8200 t/a methanol, whereby it is stated that the process is scalable according to the needs of the buyer. In this process an AEL cell is used to produce the H_2. For methanol synthesis, a tube bundle reactor is used, which is operated at 240°C and 40 bar. Investment costs of less than 3000 €/kW are given (BSE ENGINEERING, 2020). Founded in 2014, Ineratec manufactures modular chemical plants for PtX and gas-to-liquid (GtL) applications using innovative reactor concepts, including reactors for methanol synthesis. These are compact reactors with microstructure technology, which can be used in container-scale modular designs (INERATEC, 2017).

Figure 2.2: Process design of the "Green Methanol Plant" developed by the Thyssenkrupp Industrial Solutions AG.

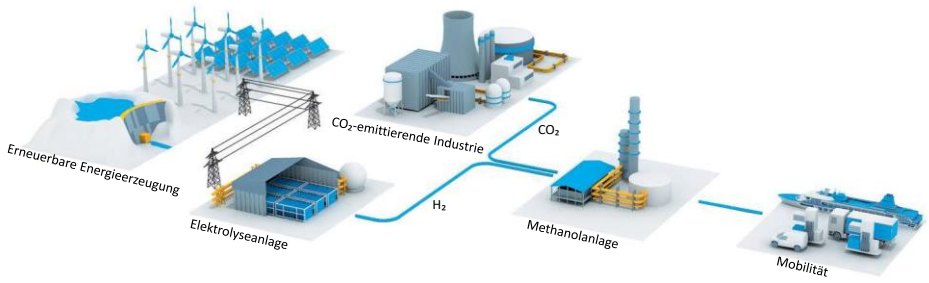

Caption: THYSSENKRUPP INDUSTRIAL SOLUTIONS AG (2020).

There is already a general interest in producing methanol from renewable sources and thus ensure a reduction in CO_2 emissions. However, the current focus of research is rather on large plants, which can be operated in combination with CO_2 from industrial waste gases. So far, there are no investigations corresponding to the plant concept of the methanol synthesis in combination with small-manure plants. The research concentrating on the connection with biogas plants, is primarily based on the production of synthesis gas from which methanol or other liquids are produced (BOZZANO et al., 2017, CLAUSEN et al., 2010, HUISMAN et al., 2011, SWANSON et al., 2010). This process is called Biomass-to-Liquid (BtL). There are also a few studies on methanol synthesis, where the CO_2 is captured from larger biogas plants and used as an educt (DECKER et al., 2019, RIVAROLO et al., 2016, SCHORN et al., 2020).

2.2 Biogas production and carbon dioxide separation

First, section 2.2.1 offers the potential of biogas production and CO_2 generation in Germany. The potential and the location of plants as well as their co-products and subsidisation are of interest for the evaluation of costs and the potential location of the analysed system. Section 2.2.2 also gives an introduction about the processes of biogas production which will later be important to understand the environmental impacts. It then goes into more detail about the plants' technology and operational stages. Section 2.2.3 talks about manure as a feedstock and introduces small-manure plants in more detail. In section 2.2.4, the different processes are presented, which can be used to separate the CO_2 from the raw biogas. Finally, section 2.2.5

looks at available small-scale applications for biogas upgrading, as there have not been many of these in Germany yet.

2.2.1 *Carbon dioxide potential from biogas plants in Germany*

There are currently approximately 9500 biogas plants (BGPs) in Germany, summing up to a capacity of 5 GW_{el} (as of 2019) (FACHVERBAND BIOGAS, 2020). The average plant size of a German BGP was 468 kW as of 2018. Plant capacities are the largest in the North and East with >500 kW. In fact, one fourth of the German capacity of biogas occurs in the federal state of Lower Saxony with 1.36 GW_{el} installed as of 2018 (AGENTUR FÜR ERNEUERBARE ENERGIEN, 2019). In the South and South-West the capacities are small to medium with an average of <370 kW. The development of new BGPs has decreased since 2012 and new plants have mostly been designed for manure utilisation (DANIEL-GROMKE et al., 2017). The fact that plant numbers have not increased as much as power increase, suggests an increase in plant size capacity during recent years (HEMMERLING et al., 2018), as can also be seen in Figure 2.3. This is mostly caused by the recent developments in the German Renewable Energy Sources Act (EEG; German: Erneuerbare Energien Gesetz), which only continues to financially support flexible BGPs, meaning an extension of another combined-heat and power plant (CHP) that can provide more flexible electricity production. The amended EEG 2014, e.g., eliminated feedstock-related bonuses as well as the technology bonus. Thus, incentives to build new plants or develop and expand old ones were cut off. Recently, the EEG started to specifically promote a plant category using mainly manure and agricultural residues, which has resulted in an increased construction of the so-called small-manure plants (DENA, 2017). In the long term, it is expected that only such BGPs will develop that use biogenic waste products (DENA, 2017). In the whole of Europe, there are about 18200 biogas installations with an installed electric capacity of 11.1 GW as of 2019 (EBA, 2020).

According to BILLIG et al. (2019), CO_2 from renewable sources presents a convenient source of carbon. In fact, BGPs prove to be very interesting in this respect, as biogas contains a significant share of CO_2. There is the possibility to utilise it in the form of collected flue gas from biogas upgrading and apply it in PtF concepts, as the flue gas provides a high CO_2 concentration with few trace gases (VIEBAHN et al., 2018). KAPOOR et al. (2020) who reviewed valorisation opportunities for biogas mention CO_2 from BGPs as a relevant option, as it can be used to replace fossil-based CO_2. However, the authors state that developments are

still in the early stages. Employing CO_2 from BGPs as a feedstock also proves to be a challenge since it is often available at the local level only; hence, transport and logistics are difficult, especially in rural areas with only few plants. Given that central processing plants are only profitable if there is enough CO_2 in close distance (VIEBAHN et al., 2018), a possible solution can be to implement a farm-site, small-scale gas separation plant (LEE et al., 2016).

Figure 2.3: Number and installed electric capacity including flexibilisation (Überbauung) of biogas plants in Germany.

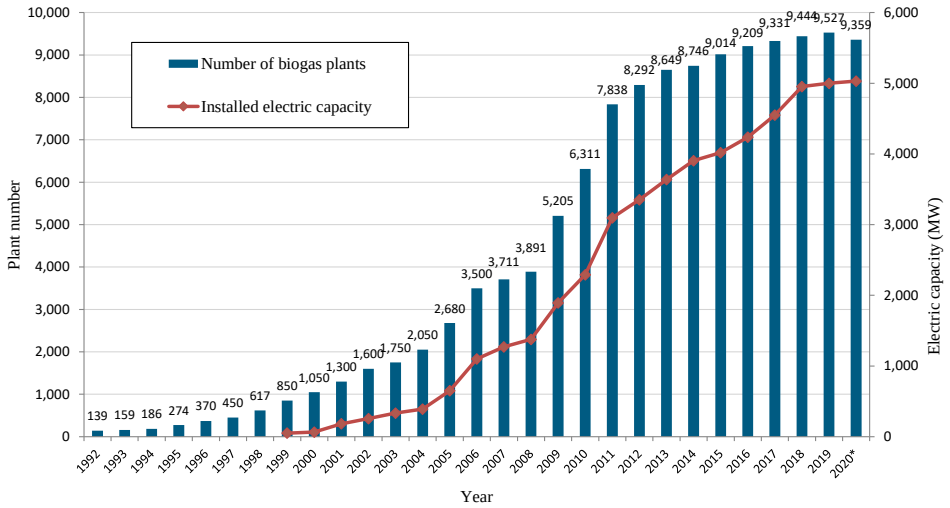

Caption: FACHVERBAND BIOGAS (2020).

Biogas upgrading is common practice in Germany (p.111, FNR, 2016). So-called biogas upgrading plants utilise the technology of gas separation to produce biomethane, which is a CH_4-rich gas that has NG quality and can thus be fed into the gas grid. Biomethane is a renewable and flexible energy carrier that can easily be transported to consumers. There are also concepts for biogas filling stations for utilisation in NG-dedicated vehicles or local solutions of using it in central or decentral CHP units (DENA, 2017). As of 2020, there are about 232 German upgrading plants (EBA et al., 2020). These types of plants recorded increasing numbers in recent years. In 2019, there were a number of 214 plants at 203 locations with an estimated upgrading capacity of almost 133,000 Nm³/h (DENA, 2019c). Biogas upgrading plants reached a total of 610 in Europe as of 2018 (EBA, 2020). The technology is mostly used in combination with large biogas plants because of the high capital costs. As of March 2019, biogas upgrading plants inject biomethane into the NG grid at a capacity starting from >100 Nm³/h. The majority of plants

injects 350 Nm³/h and more (DENA, 2019a). Especially among the smaller plants, there are also concepts where biomethane is not fed into the grid and instead used energetically as a fuel (ERNEUERBARE ENERGIEN, 2011). Another concept, introduced by BEYRICH et al. (2019, p. 126), is the flexible upgrading through implementation of an upgrading unit and a CHP. During times when the NG grid has a low intake capacity, upgrading is interrupted and biogas can be burnt instead in a CHP. BRAUTSCH et al. (2013) analysed the additional construction of a biomethane CHP unit at a residential building, already provided with a CHP using NG mainly for heat provision. The biomethane CHP proved to increase the heat provision, while at the same time showing advantages in the CO_2 balance compared to a regular CHP (p.136ff).

The latter concept could be relevant in the PtF-concept introduced in this study. Usually, the biomethane is injected into the gas grid but there is not necessarily a connection to the grid next to a small-manure plant. Therefore, the energetic utilisation of the biomethane at local scale is applicable. According to BILLIG et al. (2019), there is a large CO_2 potential from biogas plants and biogas upgrading plants in Germany. They estimated a capacity of 10.4 million tonnes of biogas plants and 1.5 million tonnes of biogas upgrading plants as of 2016. The potential of CO_2 captured by German biogas upgrading plants roughly corresponds to the overall methanol production of 1 million tonnes in Germany in 2016 (VCI, 2018), which means that the German CO_2 demand for methanol production could be satisfied if all the CO_2 from biogas upgrading plants could be made available.

2.2.2 *Biogas production*

The general biogas production process

The function of a biogas plant (BGP) is to produce a biogas from organic biomass under anaerobic conditions, meaning in an oxygen-free environment. During this process, also referred to as anaerobic digestion (AD), microorganisms transform plant and animal feedstock into biogas and fermented, residual biomass (called digestate). The classical biogas system produces electricity and process heat in combined heat and power (CHP) units, where the biogas is burnt after some sort of pre-treatment. On the other hand, biogas can also be upgraded and used as a substitute for NG. The process steps of a BGP with options of biogas upgrading are summarised in Figure 2.4. For reasons of comprehension, we divide the biogas

Figure 2.4: Presentation of a biogas plant and the process steps included in each stage.

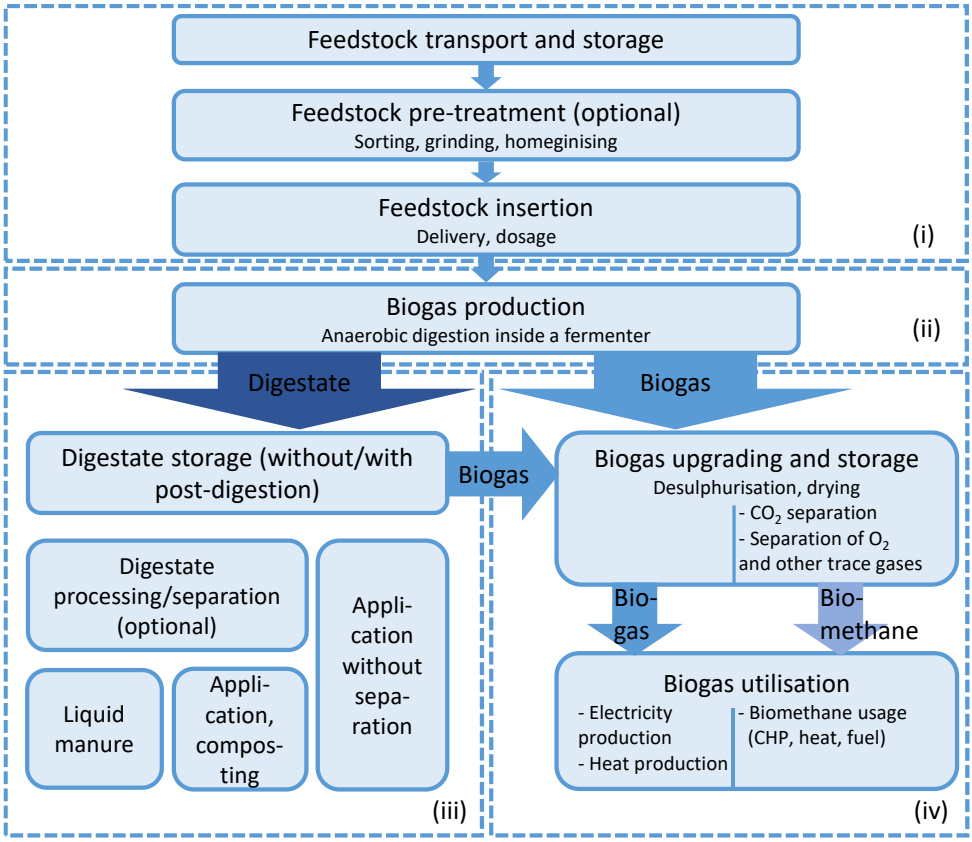

Caption: own creation based on the FNR (2016, p.23).

system into four stages, i.e. (i) feedstock management, (ii) biogas production, (iii) digestate storage and utilisation and (iv) biogas utilisation according to the FNR (2016). Table 2.1 shortly presents the stages' characteristics. In the remainder of this chapter, the stages are explained in more detail. (i) Feedstock management

Feedstock transport, pre-storage, pre-treatment and insertion techniques can vary among plants. Normally, the feedstock is inserted either manually using a tractor, a pump (for liquid feedstock) or machinery such as a conveying screw or a push floor. Pre-storage of manure occurs either in mostly gas-tight tanks or sometimes open pits, while plant feedstock is stored in open or closed silos (FNR, 2016, p. 24ff). Especially animal faeces from indoor housing can be directly discharged from the stables through a slatted floor into a naturally sloped pipe system that leads into the fermenter. Thus, it offers the advantage of continuously adding small amounts of organic material without causing shock loads or temperature

fluctuations in the fermenter. Another possibility is to lead the manure into a pre-storage tank where it can be mixed with co-substrate such as feed or straw residues. It is important to keep the dry matter (DM) content below 12-16% to maintain pumpability (BAYLFU, 2007).

Possible plant feedstocks that are used in BGPs are maize, grass silage, whole-plant cereal silage, grain cereals and others. Their share amounts to 48.9% of the total feedstock input in BGPs as of 2017 (FNR, 2019a). Maize occupies with 72% by far the largest cultivation area in Germany as of 2020 (FACHVERBAND BIOGAS, 2020). As of animal waste, which occupies a share of 44.5% as of 2017, mainly cattle manure is used (72%), followed by pig manure (10%), cattle dung, i.e. solid manure (9%) and an insignificant share of poultry manure (FNR, 2019a). Concerning the feedstock, we focus on manure and agricultural waste/residues such as straw and feed residues, as normally used in small-manure plants. Moreover, such residues provide a high potential for energetic utilisation and are promoted under the German Energy Law (EEG). Usually, their production requires resources, but as they occur as residues from livestock farming, they can be perceived as waste materials. Nevertheless, in general, plant feedstocks have much higher emissions due to their cultivation (O'KEEFFE et al., 2019).

Table 2.1: Four stages of biogas systems.

Stage	Short description
i) Feedstock management	Feedstock is grown and/or collected to produce the substrate for the biogas production. Several types of feedstock can be used such as animal waste, agricultural residues, industrial or municipal solid waste, energy crops or renewable raw materials.
(ii) Biogas production	Biogas and a digested residue, the so-called digestate, are produced during this step inside digester tanks. These tanks are fed either directly with feedstock or with feedstock from a collection tank. Anaerobic digestion (AD) occurs inside the fermenters (also called digesters) by different microorganisms such as bacteria and methanogenic archaea.
(iii) Digestate storage and utilisation	Digestate is used as organic fertilizer to produce crops and is, thereby, redirected to stage (i); this presents a convenient way to close carbon cycles.
(iv) Biogas utilisation	The produced biogas can be used for combined heat and power generation or as a biofuel. It can also be upgraded to natural gas quality (biomethane).

The installed power of BGPs is dependent on the type of feedstock used. Small biogas plants with a range of capacity up to 150 kW_{el} are mainly fed with animal faeces. The mass-related share of renewable raw materials increases with an increasing plant capacity, meaning the more renewable raw material is used, the higher the plant performance. The share of animal faeces usually decreases in this context. According to an evaluation among plant owners in 2015 and 2016, an average feedstock mix of 22% renewable raw materials and 78% animal faeces is used in the performance range of up to 150 kW_{el}. In the range over 500 kW_{el}, about 70% are renewable materials while animal faeces are only about 30% (DANIEL-GROMKE et al., 2017).

(ii) Biogas production

The AD process consists of four steps that occur simultaneously inside the reactor (also called the fermenter). During the hydrolysis, carbohydrates, proteins and fat are split into simpler organic compounds such as amino and fatty acids and sugar. Cellulosis and hemicellulosis can also be converted, but have to be converted to carbohydrates first. Lignin cannot be converted under anaerobic conditions but requires aerobic processes that do not produce CH_4 (p. 64, EDWARDS et al., 2014). The acidification phase (acidogenesis) includes the reduction of intermediate products to lower fatty acids, as well as CO_2 and H_2 by fermentative (acid generating) bacteria. During the acetogenesis, acetogenic bacteria transfer the products from the acidogenesis into acetic acid, while CO_2 and H_2 remain. The last step, called methanogenesis, describes the conversion into CH_4 by anaerobic methanogenic archaea. Biogas, which is the final product, contains mainly CH_4 (50-75%) and CO_2 (25-50%), while it also contains small traces of O_2, nitrogen (N_2), hydrogen sulphide (H_2S), H_2 and others (see Table 2.2). The composition varies depending on several factors, such as the feedstock mix, the used fermentation procedure and technical parameters such as retention time and temperature. Also, the insertion of the feedstock plays a part, which can be differentiated between batch and continuous processes. The type of fermentation differs between wet and dry fermentation, while the first mainly applies for processes with a dry matter content of up to 12% (FNR, 2016). The CO_2 formation is highly dependent on the pH value (p. 9, WEINRICH et al., 2020). Both the biogas and CH_4 yield are primarily linked with the share of organic dry matter in feedstock; hence, solid manure yields a biogas quantity that can be twice as high as that of pure liquid manure or slurry. Solid manure usually contains straw and other waste products in the feedstock. If manure is diluted, the biogas yield is in general lower (FNR, 2013).

Table 2.2: Composition of biogas according to the FNR (2016).

Component	Concentration
Methane (CH_4)	50–75 vol.-%
Carbon dioxide (CO_2)	25–45 vol.-%
Water (H_2O)	2–7 vol.-%
Hydrogen sulphide (H_2S)	20–20000 ppm
Nitrogen (N_2)	< 2 vol.-%
Oxygen (O_2)	< 2 vol.-%
Hydrogen (H_2)	< 1 vol.-%

Biogas yields depend mainly on the DM content and the energy content in the feedstock, as well as the retention time inside the fermenter and the type of fermentation. Yields are generally much higher for plant feedstock compared to animal manure. Out of animal manure, poultry faeces achieve the highest yield with 30-100 m^3/t (usually Nm^3), while pig and cattle slurry only achieve 15-25 m^3 biogas per tonne. Plant material, such as wheat grain for instance, can yield 610 m^3/t (BIOGAS INFO, 2020). The CH_4 yield is also linked with the feedstock and higher for plant material compared to animal faeces. Scenarios with manure as the single feedstock lack behind in energy content and, thus, in CHP engine power, meaning the degree of electrical and thermal efficiency (LANSCHE et al., 2012). Biogas from cattle manure has a slightly lower biogas yield and average CH_4 content than gas from pig manure. Pig manure has more proteins, which cause higher CH_4 yields, while cattle manure is mainly composed of carbohydrates.

(iii) Digestate storage and utilisation

The digestate of a BGP refers to the remaining inorganic components of the feedstock. Its composition is heterogeneous and depends on several parameters, same as the composition of the biogas. Digestate storage occurs either in open or gas-tight storage tanks after the fermenter. Open storage can cause emissions in case of residual gas potential. Longer retention times of the feedstock inside the fermenter can decrease the potential of the residual gas (Restgaspotenzial) (ZORN et al., 2014, p. 126). The much reduced methane formation caused by the AD process is notable compared to untreated manure. Inside the fermenter, part of the organic substance is metabolised so that there is much less easily degradable carbon in the digestate. The mitigation of CH_4 emissions is therefore connected with the degree of degradation of the feedstock and also with the retention time inside the

fermenter. Especially, N_2O and CH_4 emissions from digestate can be reduced by implying longer retention times (FNR, 2016, p. 187).

Digestate can be separated into solid and liquid parts. Solid parts, e.g., can be further used for burning (energy production) or, as the liquid parts as well for fertilisation (POESCHL et al., 2010). Digestate can be used as a substitute for mineral fertiliser (WENDLAND et al., 2012). Almost all of the small-manure plants in Germany apply most of their digestate to their own fields. Approximately one third also applies digestate to other fields. However, exchange markets for biogas manure (Güllebörsen) and spreading of digestate on the fields of individual feedstock suppliers only play a subordinate role. This is simply because small-manure plants rarely purchase additional feedstock, as they can cover their demand themselves. As digestate quantity increases with increasing plant size and substrate throughput (Substratdurchsatz), the spreading of the digestate on fields of larger farms becomes increasingly difficult. Therefore, plants with >75 kW (about 41%) frequently apply digestate on the fields of external feedstock suppliers to discharge of their digestate (SCHOLWIN et al., 2019). For safety, there need to be collecting devices around the BGPs, such as an earth wall made of cohesive material, to avoid digestate spillage in case of accidents (FNR, 2016, p. 100).

(iv) Biogas utilisation

The first step after the fermenter is usually the cleaning of the biogas. It comprises the removal of unwanted components such as H_2S, moisture, siloxanes, ammonia and volatile organic compounds (VOCs). It is inevitable for most of the biogas applications like CHPs or boilers to avoid damage (KAPOOR et al., 2020). To take care of the cleaning process, biogas is normally dehydrated and desulphurised before it can be burnt in a CHP (see Figure 2.4). When biogas is burnt inside a CHP, electricity and heat are generated. The main part of the electricity production is used for direct local electricity production, which is fed into the electricity grid; on average, about 8% are used for the plant itself. It mainly requires electricity for the rotating machinery inside the fermenter. The heat is used partly by the fermenter and partly for injection into a local district heating network, which heats adjacent stables, as well as residential and municipal buildings in close distance to the plant. CHP emissions are regulated by the *Bundesimmissionsschutzverordnung* (BImSchV[1]). Especially CH_4 is regulated to a maximum when coming from CHPs and biogas upgrading. If it exceeds certain values, a catalyst or post-combustion

[1] 44th Federal Immission Control Act for combustion engines (§ 16)

unit are required, respectively, in order to comply with the permitted quantities. (FNR, 2016)

Gas storage is necessary during CHP downtimes in case of maintenance or hazardous incidents. It should be preferably the size of the daily biogas production up to twice its size (FNR, 2016, p.56). Biogas storage options are low, medium and high pressure storage tanks, while low-pressure storages are by far the cheapest option. They consist of foil with a pressure of 0.5-30mbar and are the ones most commonly used. The method is possible as a gas hood on the fermenter (integrated storage) or as an external storage. The gas hood is applied gas-tight to the upper edge of the fermenter. Depending on the filling level of the gas storage tank, the film expands. This offers a flexible storage option. In the event that the gas storages can no longer hold additional biogas and/or the gas cannot be used inside the CHP, e.g. due to maintenance work or extremely poor quality, the unusable part must be disposed of without damage. The requirements for the operating permit are handled differently from state to state, whereby the installation of an alternative to the CHP is mandatory for gas flows of 20 m³/h and above. According to the technical requirements of the EEG 2012 (§ 6 par. 4 No. 2), all biogas plants must be equipped with additional gas consumption devices from 2014 onwards. This can be a stationary emergency gas flare, a gas burner or also a reserve CHP. (FNR, 2016)

Alternative biogas production and utilisation in a gas flare

An alternative to the utilisation of biogas in a CHP unit (compare Figure 2.5) as a standard plant has recently been discussed in Germany. The idea is that the biogas plant would only be equipped with a flare instead of a CHP, which saves costs and effort. Such exclusive biogas burning via a gas flare would also be possible as presented in Figure 2.6 while potentially offering emission savings. OSTERBURG (2019) introduced this alternative biogas system at a symposium about manure management options for BGPs. He talked about the importance of existing BGPs at livestock farms and mentioned the option of simply having a fermenter and gas flare on site to avoid direct manure emissions from storage. The CHP unit would not be a necessity. The idea was to avoid the typically occurring manure emissions and to reduce the gas building potential during fertiliser/manure application at the same time. The question here is whether it could also be beneficial in the plant's environmental performance, as there are no scientific studies comparing the two options with one another yet.

Figure 2.5: General biogas plant including burning of raw biogas in a combined-heat and power (CHP) unit to produce heat and electricity. Digestate is used as a fertiliser on fields and thus closes carbon cycles.

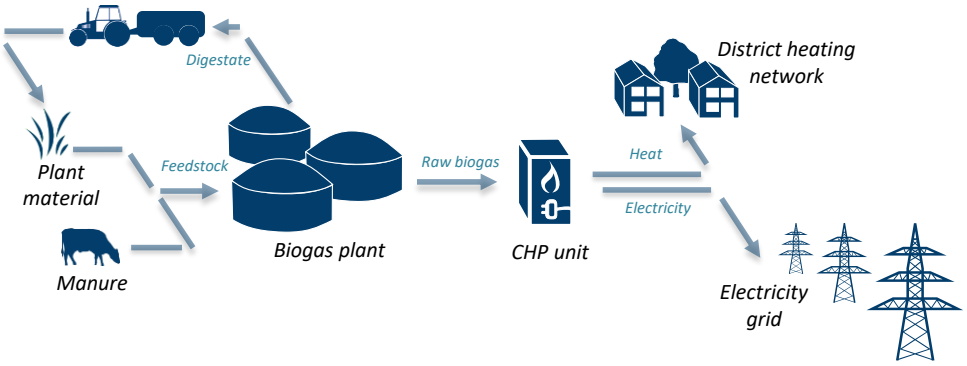

Caption: own creation.

Generally, when burning biogas, CH_4 is oxidised with O_2 to CO_2 and H_2O, as follows

$$CH_4 + 2\ O_2 \rightarrow CO_2 + 2\ H_2O.$$

Figure 2.6: Alternative process of biogas utilisation in a gas flare.

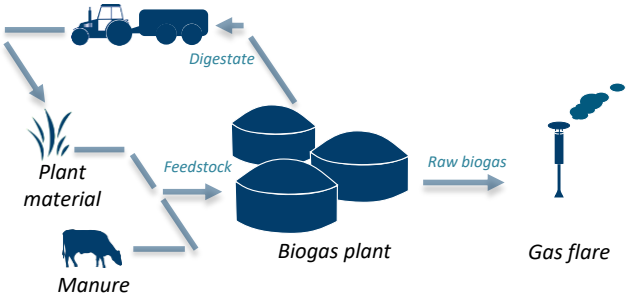

Caption: own creation.

During the burning of biogas in a gas flare, the same reaction occurs. The trigger for this combustion reaction is heat, i.e. energy supply by an ignition spark or pilot flame. When the ignition temperature of CH_4 of approximately 600 °C is reached, the reaction takes place as long as sufficient fuel and O_2 are available. Aside from O_2 and CH_4, several other gases occur such as N_2, H_2S, ammonia and halogenated hydrocarbons. Other undesirable products in the flue gas can be CO, NO_x and dioxins or furans among others, depending on the combustion temperature, the reaction time and O_2 supply. Optimal combustion conditions have been found to be at a temperature of 850 to 1200°C and a reaction time of <0.3 s (RUSSOW, 2013).

2.2.3 *Manure as a feedstock in small-manure plants*

The definition of manure used in this study is the one given by WEINFURTNER (2011), who refers to it as a mixture of faeces, urine and water with a DM content of ≤10%. It can also be called slurry or (semi) liquid manure. The german term *Gülle* is equivalent to it. It is distinguished from solid manure, which contains litter, such as straw residues, and thus a higher DM content.

Aside from manure and residues, there are other possible feedstocks for BGPs, which, however, are not part of this study. We decided to focus on BGPs using primarily agricultural residues because they do not require cultivation that is connected to additional GHG emission and they are an important part of a circular economy. Furthermore, energy crops are still an issue of debate due to them occupying land that could be used as farm land for producing food. Their extensive utilisation is therefore questionable in a sustainable energy system with sector coupling. Finally, this means that the plant sizes we look at are smaller than those of plants that feed renewable raw materials. Especially, waste products are subsidised such as manure. A special focus is therefore on those plants running with manure, such as small-manure plants.

Small-manure plants are a specific category of BGPs, characterised by mainly using manure as a feedstock (≥80%) beside other residual biomass, usually taken from livestock farming (SCHOLWIN et al., 2019). Since 2012, the EEG includes a special remuneration class for the fermentation of liquid manure. The most current EEG continues to explicitly support this class in the future. Therefore, only small manure plants developed and slowly expanded their potential, amounting to approximately 800 plants in 2019 (FNR, 2020a). They are spread across Germany, but accumulate in regions with high manure disposal (see Figure 2.7). They currently receive 23.14 cent per kWh under the EEG because profitability is highly dependent on the operational conditions on site and sometimes not given (FNR, 2020a).

Especially, liquid manure from pigs and cattle is a convenient feedstock and has been increasingly used in German BGPs. It can easily be pumped, transported and stored, since it has a low dry matter content (FNR, 2013). Small-manure plants run on average mostly with manure. However, the manure does not have as high of an energy content as renewable raw materials such as maize. Plant material generates higher CH_4 yields than animal faeces (FNR, 2016). Thus, even though on average

only 3% of renewable raw materials are added as feedstock, their energy impact is 14.7% (SCHOLWIN et al., 2019). In total, 160 million tonnes of manure (liquid and solid) were accrued in Germany as of 2016. So far, only 30% of the amount of manure is used in BGPs, generating 4 TWh_{el}/a, suggesting that a huge potential could be developed. The remaining amount is stored without processing and spread on the fields (SCHOLWIN et al., 2019). The highest amounts of manure occur in the north-eastern part of the federal state of Lower Saxony and the south-east of Bavaria, where there are many livestock farms (THRÄN et al., 2011). THRÄN et al. (2011) calculated a fuel potential of manure-based biogas of 90 PJ/a for 139 million tonnes per year of liquid manure, suggesting the large potential of manure in biogas production.

Figure 2.7: Location and number of small-manure plants in Germany.

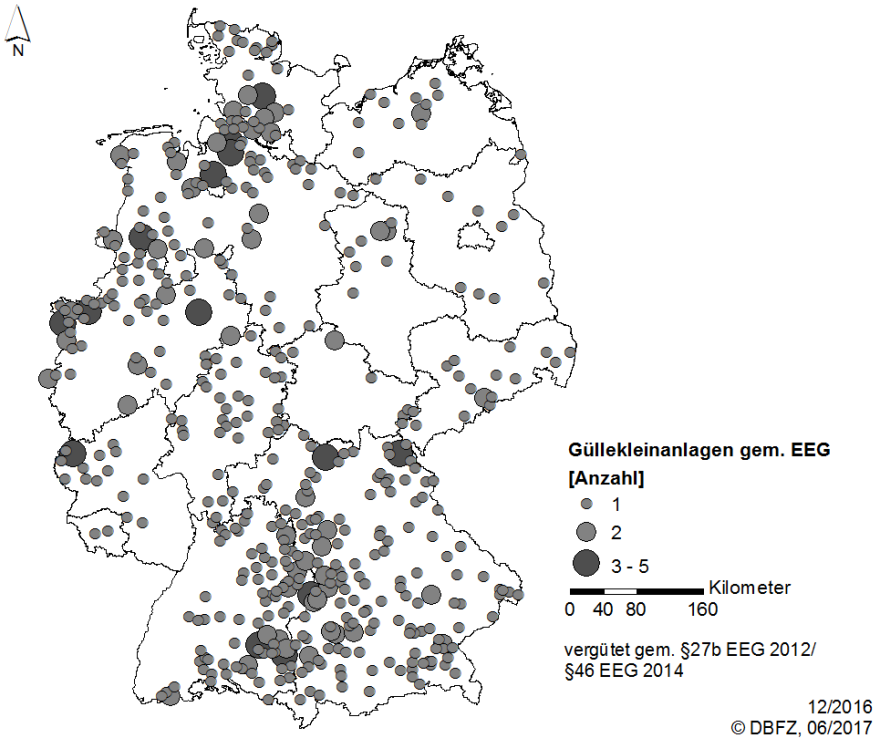

Caption: DANIEL-GROMKE et al. (2017).

The EEG supports the class of BGPs up to a capacity of 75 kW, and there have been discussions about extending the threshold. New small-manure plants have the capacity of 150 kW and shall receive financing in future energy policy. However, from a technical point of view, they are not favourable, as plants need a second flexible CHP plant if greater than 100 kW. Optimal would be the capacity of

100 kW because the CHP plant can be run at 80 kW while the reserve power can be used to make up for lost feed-in times in the event of disturbances (BAYERISCHES LANDWIRTSCHAFTLICHES WOCHENBLATT, 2019). A problem concerning this is that, according to the FNR, only about 10% of cattle farms have more than 200 dairy cows; with the liquid manure produced by 200 animals, however, only a 30 kW system can be operated. Until now, especially farms in Western Germany have too few animals for a manure plant. The FNR introduced a new project that will develop small-manure plants, starting from 150 animals. The project evaluates the possibilities in terms of profitability in a feasibility study (FNR, 2020a).

2.2.4 *Carbon dioxide separation technology*

The raw biogas mainly consists of methane (CH_4) and CO_2. If there is no option to use the heat of a CHP locally in an efficient way, it is favourable to upgrade the biogas and, e.g., transport the biomethane through the NG grid (FNR, 2012). The processes presented in the following are already used commercially in large BGPs for the production of biomethane. However, no gas separation processes have been used in German small-manure plants up to now, because a connection to the gas network is often not worthwhile and alternative concepts are not yet commercial. Most biomethane is in fact used for cogeneration of heat and power (88%), while 5% are each used for fuel and heat generation and the remaining 2% are exported (as of 2017) (DANIEL-GROMKE et al., 2020). Upgraded biogas, i.e. biomethane, has to fulfil certain requirements when injected into the gas grid. It is generally differentiated between H-gas (high caloric gas; ≥95 mol-% CH4 and ≤5 mol-% CO2) and L-gas (low caloric gas; ≥90 mol-% CH_4 and ≤10 mol-% CO_2). The captured CO_2 in the weak gas stream is a waste product and released into the atmosphere after treatment. There are threshold values in biomethane for components that occur in raw biogas that must be complied with. Regulations also include requirements for the heating value of the biomethane and the allowed leakage of CH_4 into the air via flue gas, which is why post-treatment of the gas is considered. (GRAF et al., 2013). For the plant concept used in this thesis the gas separation of the raw biogas occurs by a biogas upgrading plant, whereby the CH_4 is used in the CHP to produce electricity and heat, as shown in Figure 1.1. The CO_2-rich flue gas is then fed into the methanol plant.

The entire upgrading process is divided into the steps of pre-treatment, CO_2 separation and the post treatment of weak gas (Schwachgasnachbehandlung) (FNR,

2016). The pre-treatment processes are also used in small-manure plants to prepare the biogas for the usage in CHPs. They are divided into the two steps of desulphurisation and drying. Desulphurisation removes the harmful hydrogen sulphide (H_2S), which leads to corrosion of the plant components and damages the catalyst. In terms of H_2S removal, various processes such as biological desulphurisation (inside and outside the fermenter), desulphurisation using activated carbon (eligible for fine desulphurisation achieving less than 1 ppm) or bio-scrubbers are possible (FNR, 2014). A very common technique is to blow air into the fermenter. However, this is not favourable in case of biogas upgrading, as strip air enters the fermenter (FNR, 2016, p.108). The process using activated carbon is particularly useful for fine desulphurisation. It is economically feasible with a charge with 500 ppmv; at the end, a level of purity below 1 ppmv can be reached. Another possibility, mainly suitable for rough desulphurisation (Grob-Entschwefelung), is the direct precipitation with iron salts inside the fermenter such as iron(III)-hydroxide or others (FNR, 2014, p.15ff). Afterwards a drying process is carried out to remove the water vapour, which also leads to corrosion. It usually occurs immediately after the fermenter via condensation, adsorption or absorption drying (FNR, 2016, p.110f). Ammonia traces in biogas are also largely removed during that stage as part of the water condensate. The content of H_2 in biomethane does not have any restrictions and is noncritical for values in a single-digit percent range. During the second step of biogas upgrading, the CO_2 can be separated from the pre-treated biogas. However, biogas upgrading technologies face the problem of CH_4 slip into the CO_2-rich flue gas stream, making it difficult to obtain pure streams of CH_4 and CO_2, although certain processes perform better than others. The technology is usually chosen according to the desired product gas quality, the CH_4 losses and ultimately the upgrading costs, which can vary depending on local conditions (GRAF et al., 2013).

For BGPs, there are a number of technologies that separate CO_2 and other components from the biogas in order to obtain biomethane. Possible technologies for biogas upgrading are classic membrane processes, cryogenic membranes, pressure swing adsorption (PSA), pressurised water scrubbing, and other physical and chemical scrubs. PSA is, together with amine and water scrubbing, the most commonly used technique in Germany. Figure 2.8 shows the distribution of the different technologies as of 2017. Table 2.3 presents the main upgrading technologies used in Germany and their characteristics. In summary, many technologies achieve purities of CH_4 up to 99%. The mode of operation is evaluated by (COLLET et al., 2017), who classify membrane processes as easy, PSA as intermediate and amine and water scrubbing as complex processes. However, not all of the processes available on the market are suitable for the plant concept

investigated in this thesis. This is because a high concentration of CO_2 is required in the weak gas stream, which is not the case with all processes. Therefore, pressurised water scrubbing and physical absorption, such as organic solvent scrubbing (Lösemittelwäsche), are not suitable as processes, as they have a high N content in the flue gas, but only little CO_2 (ADLER et al., 2014b). From the commercial processes, PSA, amine washing and membrane processes are still suitable. In addition, the biogas oxyfuel process (BOP) developed by SCHORN et al. (2020) is considered, in which no separation of the CO_2 takes place, but the CH_4 is also converted into CO_2 in the CHP. The three upgrading processes considered, as well as the BOP, are described in more detail in the remainder of this chapter.

Figure 2.8: Distribution of different upgrading technologies in Germany as of 2017.

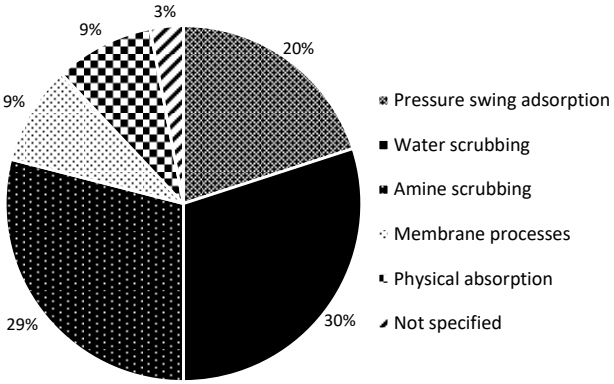

Caption: own creation according to FNR (2018).

In absorptive processes, the biogas is brought into contact with a liquid, in which its components dissolve. The processes are based on the different solubility of the various gas components in the liquid. In the physical processes, only this effect is used, whereas in the chemical processes, a subsequent chemical reaction between the detergent and gas components takes place. Since the physical processes are not suitable for the further use of CO_2, they are not dealt with here. On the other hand, the chemical process using an amine solution, known as amine scrubbing, is extremely selective towards CO_2. In this process, concentrations of 99.99% by volume of CO_2 are achieved in the weak gas stream. In this process, the strong bond between the amine solution and CO_2 is exploited by means of a reversible chemical reaction, whereby a significantly higher loading of the scrubbing liquid can be achieved than in physical processes. The disadvantage of the strong bond is that more energy is needed to regenerate the detergent, which must be boiled out at temperatures of 120 to 140°C. Before the cleaned solution can be reused, it must

be cooled down to the absorber's operating temperature of approx. 40°C. Pre-treatment is also important in this process in order to achieve the longest possible life of the washing solution. In the absorption column, the biogas is fed in counter current to the washing solution. The loaded amine solution leaves the absorption column and is led to a regeneration stage before being fed back into the absorption column. Although the selectivity of the amine scrubbing is high and advantageous for PtF technology, it also has some disadvantages such as the usage of chemicals that are water-polluting, harmful to health and corrosive and require trained personnel and safety precautions, as well as the high energy demand. The latter could be solved by implementing a locally intelligent heat supply and utilisation concept (ADLER et al., 2014b, p. 34f). Nevertheless, the plant layout requires much space which is another disadvantage (BEYRICH et al., 2019).

Table 2.3: Biogas upgrading technologies and their characteristics.

	Pressure swing adsorption	(Pressure) Water scrubbing	Chemical absorption (amine)	Physical absorption	Membrane processes
Concept[a]	Alternating physical adsoprtion and desorption using changes in pressure	Physical absorption using water as solvent; regeneration by pressure reduction	Chemical absorption using suds (amine); regeneration through H_2O-steam	Similar to physical absorption using organic solvents (Gensorb® or Seloxol®)	Pore membranes use drop of pressure; others the diffusion rate of gases
Ease of operation[b]	Intermediate	Complex	Complex	-	Easy
Applicable for small-scale PtF systems[c]	Yes	No	Yes	No	Not specified, but found applicable[f]
Methane slip (%)[d]	1-5	0.5-2	1-4	0.1	2-8
Methane content (%)[e]	>97	>98	>99	?	>96
Process pressure (bar)[d]	4-7	5-10	4-7	0.1-4	5-10

[a] FNR (2016), [b] COLLET et al. (2017), [c] LOHSE (2019), [d] FNR (2020b), [e] VIEBAHN et al. (2018), [f] OESTER et al. (2018).

The PSA is suitable for the further use of CO_2 with proportions of 87vol% to 99vol% of CO_2 in the weak gas stream. This process exploits the different adsorption behaviour of the gas components of the raw biogas. An adsorbent is used for this purpose, which can consist of activated carbon, molecular sieve zeolites or carbon molecular sieves. On this adsorbent, the CO_2 binds more easily than the CH_4 so that the materials can be separated from each other. High pressures and low temperatures promote CO_2 adsorption. Therefore, the raw biogas is first cooled and brought to a working pressure of 4 to 7 bar before it is fed into the adsorber. There, the CO_2 is bound and the CH_4-rich gas is removed. Shortly before saturation of the adsorber occurs, the raw biogas stream is diverted to a fresh adsorber and the loaded adsorber is regenerated in order to be able to reuse it later. For this purpose, the adsorber is expanded and the adsorptive, which consists mainly of CO_2, is extracted by a vacuum pump at a pressure of approximately 100 mbar. To ensure a continuous separation with this process, several adsorbers are operated in parallel. The name of the process stems from the fact that the adsorbers are exposed to a constant pressure change between adsorption and regeneration phase. Theoretically, the adsorber has a virtually unlimited service life, so that no exchange is necessary, provided that no harmful substances, such as sulphur compounds, are contained in the supplied biogas. Therefore, the pre-cleaning of the raw biogas for this process is important to remove these impurities (ADLER et al., 2014b, p. 34f). Compared to amine scrubbing, PSA has a higher electricity demand due to the constant pressure changes. However, it does not need, either heat, or process chemicals (FNR, 2016). Additionally, it has advantages with regard to flue gas post-combustion. The flue gas is not contaminated with strip air and can, thus, be led into a combustion system with heat utilisation (GRAF et al., 2013). A disadvantage of PSA is the comparatively high CH_4 slip (1-5%) (FNR, 2016) and the very high need for space by the plant layout (BEYRICH et al., 2019).

Another possible method for gas separation is the membrane process. This is a relatively new method of biogas treatment. In general, both wet and dry membrane processes are used, although only the dry process has been used in biogas plants to date. The driving force for the separation is the partial pressure difference of the CO_2 between the two sides of the membrane. Diffusion membranes are used in the field of BGPs, where the separation takes place due to different solubility and diffusion speed of the gas components in the membrane. Since CO_2 has a higher permeability than CH_4, it diffuses faster through the membrane than CH_4. Desulphurisation is also necessary in this process in order to protect the membrane. The membrane itself is mostly used in the form of hollow fibres or tubes, whereby several membranes are usually operated in series and/or parallel connection. The

necessary partial pressure difference can be achieved both by pressure on the feed side and by vacuum on the weak gas side, whereby the former is usually used. Membrane separation plants can be designed in various configurations, however, usually two- or three-stage cascades are used. Advantages of this process are the simple technical design, the uncomplicated handling and the high operational reliability (ADLER et al., 2014b, p. 34f). On the other hand, there is the high compression effort and the resulting high costs involved. Due to the low investment costs, this method is suitable especially for small volume flows of biogas (ADLER et al., 2014b, p. 34f). Multistage processes for membranes can also provide high purities of CO_2 of 95-99% in the flue gas (BAENA-MORENO et al., 2020).

In addition to the standard procedures for biogas upgrading, this work considers another possibility for providing the CO_2. The BOP, which was developed by SCHORN et al. (2020), does not require a separate plant for biogas treatment, but the existing CHP is retrofitted. With the addition of pure oxygen (O_2) and recycled CO_2, the CH_4 contained in the biogas is converted into CO_2. The CO_2 present at the end of this process can then be used to produce methanol. In this process, approximately twice the amount of CO_2 is available compared to the other processes with the same amount of raw biogas. The structure of this process is presented in Figure 2.9. As shown, the co-product O_2 from the electrolysis is used for the BOP. Otherwise, it would be released into the atmosphere without further usage. In order to control the temperature in the CHP, a part of the CO_2 stream is recycled and mixed with the O_2 and the raw biogas. In the CHP unit, the mixture is burned to produce electricity and heat, with a mixture of CO_2 and H_2O emerging from the CHP as exhaust gas. The H_2O can be separated from the CO_2 by a heat exchanger. A partial flow of the CO_2 is recycled, and the amount of CO_2 added can be used to regulate the combustion temperature. The remaining CO_2 is fed into the methanol plant together with the H_2. (SCHORN et al., 2020)

Figure 2.9: Mode of operation of the biogas oxyfuel process.

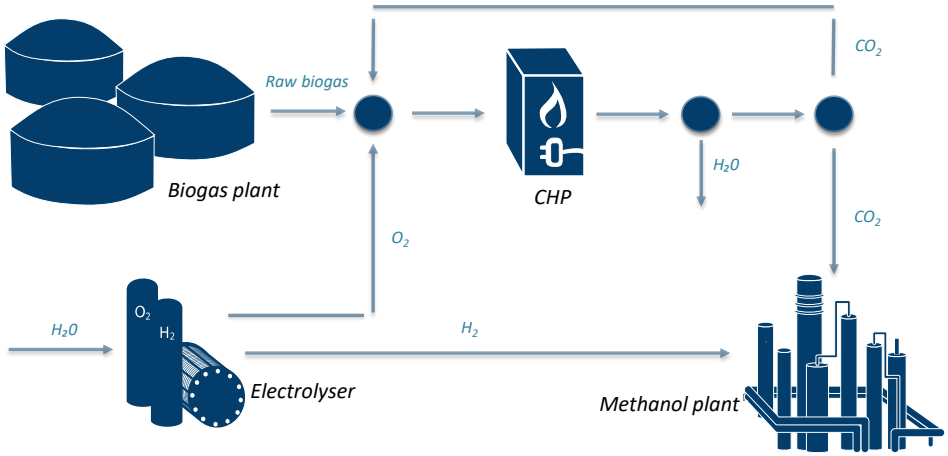

Caption: own presentation according to SCHORN et al. (2020); CHP = Combined heat and power plant.

The last step of the upgrading process is the post treatment or the post-combustion of weak gas, which is necessary for the PSA and the membrane process to achieve the desired purity of the CO_2 for the methanol plant. In the case of amine scrubbing and BOP, post-treatment is not necessary, since high concentrations of CO_2 are already present which are sufficient for the methanol synthesis (BEYRICH et al., 2019, SCHORN et al., 2020). There are various possible post-treatment processes that could be applicable to the PtF system, the choice of process being mainly dependent on the CH_4 content. Three processes are in commercial use: catalytic afterburning, regenerative-thermal oxidation and the weak gas burner (katalytische Nachverbrennung, regenerativ-thermische Oxidation und Schwachgasbrenner). In catalytic afterburning, residual amounts of CH_4 are oxidised into CO_2 and H_2O at temperatures of 300°C. An autothermal operation is possible above a CH_4 content of 0.5vol%. This means that no additional supply of combustibles or external heating are necessary; only for starting up the process an auxiliary firing system (Stützfeuerung) or an electrical preheating is required. The regenerative-thermal oxidation only requires CH_4 contents of 0.3vol% in order to be able to operate autothermally. An auxiliary firing system is also necessary to heat the ceramic storage masses to the operating temperature of approximately 800°C. When flowing through the storage mass, the CH_4 oxidises to CO_2 and H_2O. Frequent changes in direction of flow ensure optimal utilisation of the released energy. The weak gas burner, also known as FLOX burner, requires CH_4 contents of 4vol% for

stable CH_4 combustion, otherwise a supporting gas must be added. It is therefore particularly suitable for separation processes with high CH_4 contents, such as the membrane process. The process requires preheating to 450 to 500°C (ADLER et al., 2014b).

2.2.5 *Small-scale applications for biogas upgrading*

Biogas upgrading linked with a small-manure plant requires low upgrading capacities. The German biogas plants with upgrading technology, which are in operation as of March 2019, have an average injection capacity of 620 Nm^3/h (DENA, 2019a). Small-scale applications are currently scarce in Germany, as economic disadvantages below 200 m^3/h of biogas make it difficult to scale down upgrading technologies and remain their profitability. Nevertheless, BIENERT et al. (2019) point out the importance of promoting these in order to make use of the decentralised distribution of residues and organic wastes. Only then, can these potentials be utilised. In recent years, there has been more and more research concerning small-scale biogas upgrading (BEYRICH et al., 2019, BIENERT et al., 2019, CANEVESI et al., 2019, KHAN et al., 2017). For instance, there is a number of mostly Scandinavian manufacturers who offer small-scale biogas upgrading as summarised in a review paper by HOYER et al. (2016). BIENERT et al. (2019) analysed different upgrading technologies with technology readiness levels (TRLs) of 3 to 7 with respect to their technical, economic and environmental performance. They collected data via questionnaires from manufacturers and made a comparison between these innovative technologies and existing large-scale technologies used in the market. According to them, there are at least eight technologies that are currently developed, enabling capacities under 40 Nm^3/h. An FNR project by BEYRICH et al. (2019) also considered small-scale biogas upgrading and their specific costs. Furthermore, they estimated biomethane feed-in potentials and biomass potentials of these plants and found that there are large differences at the regional scale. Biomethane potentials happen to exceed feed-in potentials in some regions, which means that plants would have to consider a different transport network than the NG grid. This in turn requires a higher energy input, as higher pressure levels are needed. They found potentials of conversion to biomethane for 16-24% and 30-44% of the plants in Germany with a capacity $\geq$400 kW_{el}, depending on the scope of the heat utilisation (25% or 50%, respectively).

In general, the literature and web pages of manufacturers show mostly small-scale options for PSA and membrane processes. Although there are a few examples of small plants using water scrubbing in Sweden, Hungary and Iceland (BIOSLING, 2012, LEMS et al., 2010, ÞORBJÖRNSSON, 2016), the technology is more

frequently used for large-scale systems. Simple and cheap systems are preferred for the smaller scale, according to LEMS et al. (2010), who claim that membrane processes would be suitable. Cryogenic membranes, on the other hand, are still not widely used. One manufacturer was found who provides upgrading with pure CO_2 as a product that can even be used in the food industry. Nevertheless, the smallest scale offered so far is 350 Nm³/h. The technology is also rather energy intensive with a demand of 0.41 kWh/Nm³ (DEN HEIJER, 2019, FNR, 2016). This process is interesting because of its high quality CO_2 stream, but was not considered further due to lack of data. Amine scrubbing is also another technology to be considered for PtF systems, especially, because a master's thesis at the Forschungszentrum Jülich analysed upgrading technologies and found that amine scrubbing and PSA are both possible technologies for CO_2 recovery of such a PtF system as the one presented. The thesis considered the available upgrading technologies and decided which one was the most convenient based on the market share and data availability, as well as the composition of the flue gas (LOHSE, 2019). While small-scale PSA concepts are analysed, small-scale amine scrubbing was not found in the literature.

In general, PSA is mainly used at plants with a raw biogas production of 400-2800 m³/h (DENA, 2019b, VIEBAHN et al., 2018). Although it may be possible to use it in smaller plants, there are no commercial small-scale applications in Germany just yet. The smallest PSA application in Germany, according to DENA (2019a), is the plant in Allendorf, Eder (Federal state of Hessen) which processes 110 Nm³/h biogas. KHAN et al. (2017) claim that several manufacturers provide PSA at a small scale (10-10,000 m³/h). On most of the manufacturers' websites, however, there are no indications on such small capacities. There are studies looking at the development of PSA technology on a smaller scale (<100 Nm³/h), such as CANEVESI et al. (2019), who showed that PSA is feasible below <100 Nm³/h and estimated costs for this case. Furthermore, they validated upgrading with carbon molecular sieves (CMS) in experiments as a commercially available, selective material. Purities can be up to 99%. An American company tests PSA at a very low capacity of 100 cc/min or 0.006 kg/h (or 0.005 m³/h with biogas density of 1.23 kg/m³ [60:40]) (L&C SCIENCE TECHNOLOGY, 2020). There are also developments in vacuum PSA for the smaller scale (BIENERT et al., 2019). Different PSA technologies using vacuum by the company SYSADVANCE (2019) can provide the separation of several unwanted components. Biomethane production occurs, here, at capacities as small as 50 Nm³/h with zero CH_4 losses. CO_2 purification is also available using Vacuum Pressure Swing Adsorption (VPSA) from 100 Nm³/h CO_2-rich gas. AUGELLETTI et al. (2017) analysed a PSA process for a capacity of 100 Nm³/h biogas and

whether it is feasible. The process uses zeolite 5A as an adsorbent, and consists of two PSA units. The biomethane stream acquired NG quality with <3% CO_2 and a flue gas stream of almost pure CO_2 content >99% is achieved. During the first unit, the biomethane is produced. The flue gas is then send into the second unit where CO_2 is recovered and the residual gas stream is recycled to the first unit. As the flue gas is extracted periodically from the first unit, the process incorporates storage systems, one between the two units and another one for mixing the recycled gas with the raw gas before the first unit.

According to KHAN et al. (2017), membrane separation is available for low capacities of biogas. It also has the advantage that it requires a small space compared to the other technologies. Even though, the membrane separation is possibly applicable for small-scale plants, there still seems no market for it in Germany (KHAN et al., 2017). A Swiss manufacturer offers small-scale options of membrane processes that appear to be suitable for industrial production. In fact, its compact design inside one container safes investment costs and makes the small-scale upgrading profitable (BFE, 2019). They provide hybrid small-scale membrane upgrading plants with capacities of 50 and 100 Nm³/h and even smaller (up to 3 Nm³/h) (APEX AG, n.a.). The biomethane can either be produced at NG quality or it can be compressed to 300 bar and used as a fuel. Before the membrane stage, the biogas is dried, desulphurised and compressed. The membrane process uses a hollow fibre membrane that lets CO_2 and H_2O pass through. A CH_4-enriched retentate and a CO_2-enriched permeate are obtained. CH_4 slip is ≥1%, but can be adjusted, depending on the membrane steps and the required quality. The flue gas can be used in a micro gas turbine, generating energy for the biogas plant. Heat production can then be adjusted to the operation of the biogas plant depending on the season, obtaining an energy self-sufficient operation (OESTER et al., 2018). There is also another pilot plant in Czech Republic that runs a membrane process at a capacity of 12 Nm³/h (MARŠÁLEK et al.), showing that there are some available processes outside of Germany.

2.3 **Renewable hydrogen production via electrolysis**

In addition to CO_2, H_2 is needed for the synthesis of methanol. This must be generated using a renewable process, as otherwise unwanted greenhouse gases would be produced. Various options are available for this purpose, such as biomass reforming and water electrolysis. However, only electrolysis is considered in this paper, as this technology enables H_2 generation at a stand-alone wind turbine at the farm site. Currently, 20 billion Nm³ of H_2 are annually produced in Germany, of which only 5% is green H_2. To this day, most H_2 is produced from fossil sources

such as natural gas (NG) (HERBERT SMITH FREEHILLS, 2020). On a global scale, 70 million tonnes of H_2 per year are produced annually as of 2020 which corresponds to roughly 780 billion Nm^3 (IEA, 2020). When looking at the national scale, the German hydrogen strategy (NWS) acts on the assumption of having an import quota of H_2 of 80-90% in 2030, as it cannot produce the required H_2 from renewables by itself. In fact, various studies expect import quotas between 80 and 100% (MATSCHOSS et al., 2020). In a global H_2 infrastructure, it may hence be possible to consider the production of H_2 in different parts of the world and import it (HEUSER et al., 2020). However, the PtF system presented in this study rather aims for a local-scale solution where there is renewable H_2 production from a small-scale wind-powered electrolysis system. The idea is to provide a farm-site with a local WTG that produces electricity for H_2 generation. In the end, the availability of H_2 plays a crucial role for the concept. DECKER et al. (2019) identify excellent locations in North-western Germany for such a plant concept. Wind conditions are sufficient and a local WTG can provide the required power. As the North-western part of Germany also supplies sufficient manure resources, the geographical conditions shape this region as an ideal position for a PtF system setup. Other regions of Germany could also be considered, given that they can produce renewable H_2 and supply manure. For instance, the South of Germany has many BGPs and has some good locations for solar power that could provide renewable H_2 (BUNDESNETZAGENTUR AND BUNDESKARTELLAMT, 2020). The location of the BGP, providing data for this study, also shows potential for wind installations. It is located in Eastern Germany in the federal state of Saxony. A few WTG of 5 MW in total are installed on the land adjacent to the plant (AG BERGLAND CLAUSNITZ, 2019).

In electrolysis, water is split into its two components H_2 and O_2 with the help of electrical energy, whereby two partial reactions take place. At the cathode, H_2 is produced by a reduction reaction and O_2 is produced at the anode by oxidation, whereby the two partial reactions are separated by an ion-conducting electrolyte. Three different types of electrolysers can be distinguished, using different electrolytes: the alkaline electrolysis (AEL) with a liquid, basic electrolyte, the PEM electrolysis (polymer electrolyte membrane) with a proton-conducting, polymeric solid electrolyte and high temperature electrolysis with a solid oxide as electrolyte (MERGEL et al., 2012). In the plant concept introduced, PEM electrolysis is used because it is characterised by good part-load behaviour and fast dynamics, which is particularly important in combination with a renewable energy source with fluctuating electricity production (SMOLINKA et al., 2018). In PEM electrolysis, hydrogen ions (H^+) diffuse from the anode through a proton-

conducting polymeric solid electrolyte and a membrane to the cathode, as shown in Figure 2.10. As mentioned above, the required electricity comes from a WTG, in order to avoid greenhouse gas emissions, which would occur if grid electricity were used due to the sometimes high proportions of conventional energy sources in the electricity mix (BHANDARI et al., 2014). The WTG is installed on site and always produces H_2 when electricity from the WTG is available, which is why fast dynamics are particularly important for the electrolyser. The good partial load behaviour is also important in connection with a WTG, because then H_2 can be produced even at low wind speeds, when the WTG does not produce full power.

Figure 2.10: Functional principle of polymer electrolyte membrane (PEM) electrolysis.

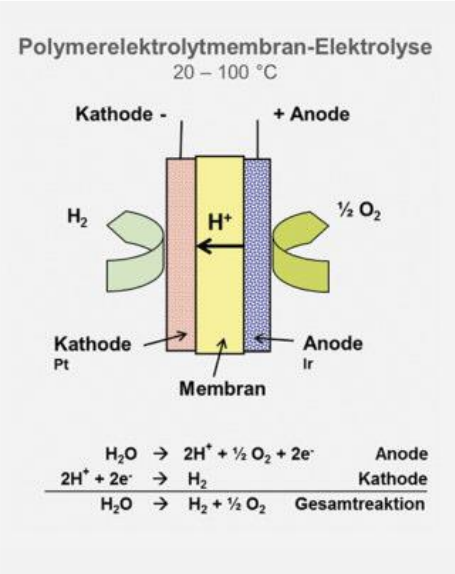

Caption: MERGEL et al. (2012).

A liquid organic hydrogen carrier (LOHC) provides a possible storage system for the produced H_2 with the aid of an organic substance. The H_2 is stored in liquid form in a tank under standard conditions. For storage, the organic substance is hydrogenated, whereby heat is released. Withdrawal of H_2 using dehydration occurs under the supply of heat. The advantage is that the storage medium is liquid and therefore easy to store. A disadvantage is the energy requirement for dehydration (MODISHA et al., 2019).

2.4 Concluding remarks

This chapter introduced the state of the art of the various sub-systems of the overall plant concept which are required for understanding it. For conventional methanol synthesis, natural gas is converted to synthesis gas via steam reforming. The gas is mostly imported to Germany via pipelines. However, there are several studies and projects focussing more and more on renewable methanol using bio-based carbon sources. For the methanol synthesis, the production of the raw materials is of particular interest. It has a relevant impact on costs and often entails environmental emissions. Hence, renewable H_2 production via wind-based electrolysis is explained. The PEM technology is selected here, as it serves the requirements for a PtF system in the best way. Moreover, the current state of the art of the anaerobic digestion process as well as the biogas upgrading were described. BGPs offer a high potential as a sustainable carbon source. Their main locations are in the North-West and South of Germany. Numbers of the small-manure plants, a category of BGPs that uses mostly manure and agricultural residues as feedstock, have significantly increased in recent years. Hence, this study focusses especially on such plants utilising waste materials. Generally, locations with both excellent wind locations for H_2 production and many BGPs based on manure and residues are ideal for the PtF system investigated in this study. For instance, this applies to the North-West of Germany. For methanol production, pure CO_2 must be obtained from gas separation. Biogas upgrading technologies were presented as well as an alternative, the biogas oxyfuel process (BOP), which provides pure CO_2 while avoiding biogas upgrading entirely. In order to gain pure CO_2 from the other processes subsequent flue gas cleaning (normally legally required anyways) must be considered. Finally, this chapter presented existing small-scale applications of the upgrading technologies. To the author's knowledge, there are no commercial small-scale upgrading plants in Germany as of today. Nevertheless, there appear to be a couple of small-scale upgrading options by foreign manufacturers, some also providing CO_2 purification. However, these are often at higher capacities than required for the small-manure plant. In summary, the membrane process is found to be the most suitable for small-scale applications. Compared to the others, it is a relatively simple process with small space requirements and it has already available manufacturing options in the market. There is also increasing research about small-scale PSA, therefore, it may become of interest in the long term.

Chapter 3
Economic and environmental analyses of biogas and Power-to-Fuel systems

The chapter introduces the types of analyses that are utilised for the evaluation of the PtF system. For this purpose, the fundamentals of techno-economic analysis and life cycle assessment are presented. These are followed by a literature review of relevant studies, namely existing cost analyses as well as environmental analyses of biogas and PtF systems, which helps to place this thesis in the current scientific literature. The chapter ends with some concluding remarks.

3.1 Fundamentals of techno-economic analysis

This sub-chapter introduces the cost estimation for chemical installations and processes. In general, the costs of manufacturing (COM) are of particular interest for chemical plants. Figure 3.1 gives an overview of the cost structure as described by TURTON et al. (2009, p. 193ff). The COM are divided into annual capital costs (ACC) and operational expenditures (OPEX). The ACC reflect how much it costs to build a plant, whereby the total capital expenditures (CAPEX) are allocated to the operating lifetime of the plant. The OPEX, on the other hand, show how much it costs to operate the plant and include direct, fixed and general costs. The total CAPEX is the sum of the financial resources required to build the plant. These in turn are made up of the working capital (WC) and the fixed capital investment (FCI), the latter being divided into direct costs, indirect costs, contingencies and fees and auxiliary devices. In the following sections, a more detailed presentation of the cost items in Figure 3.1 is given. Section 0 first describes the design of various components, as this is required for cost accounting. In the following sections, the calculation of the total capital requirements, i.e. the CAPEX (3.1.2) and the OPEX (3.1.3) are presented. Finally, the calculation of the COM is described in section 3.1.4.

Figure 3.1: Cost structure for determining the manufacturing costs according to TURTON et al. (2009, p. 193ff).

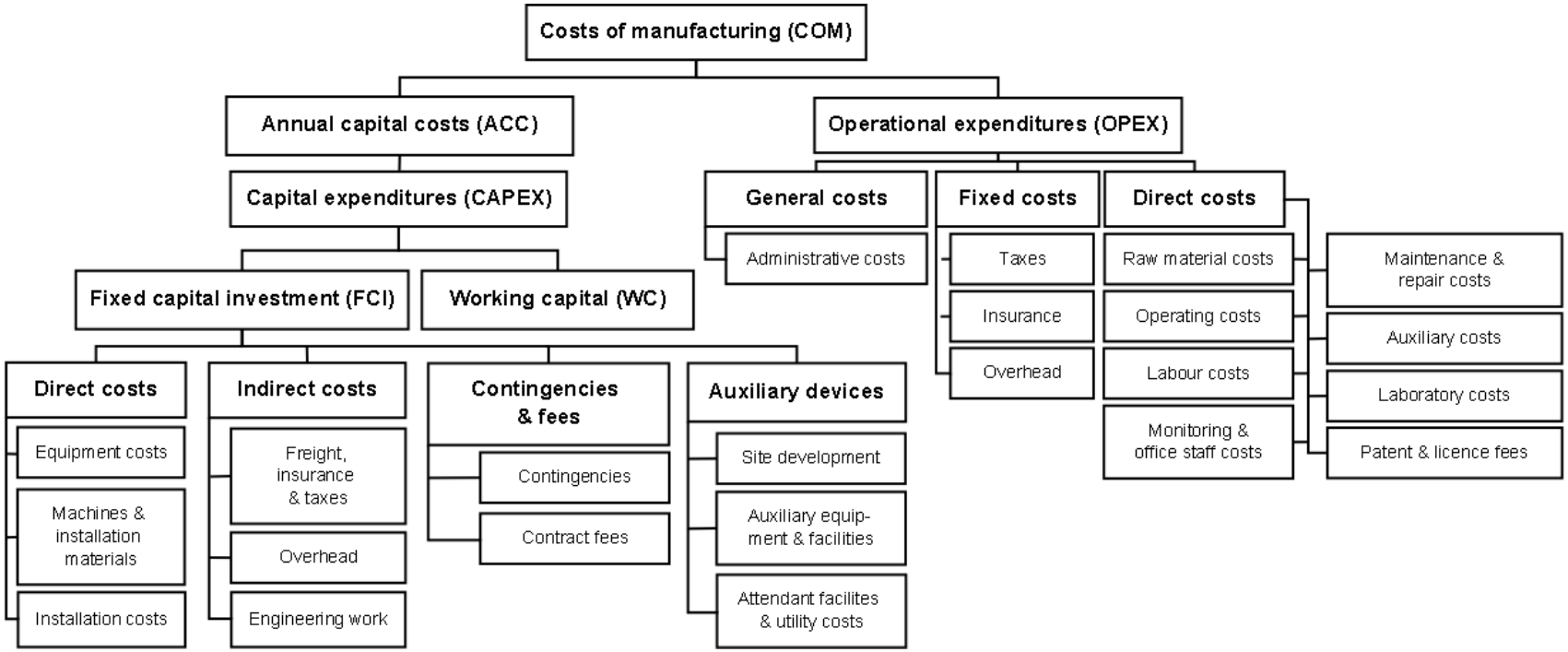

3.1.1 *Module design*

In order to determine the costs of the various components, they must first be designed. For this purpose, this section presents the various equations for calculating the component sizes for the methanol plant. The design is based on the equations and assumptions of BIEGLER et al. (1997, p. 111ff), since these allow a fast and solid determination of the required capacity or size parameters. For the calculation, various process variables must be known, which can be taken from the results of the process simulation in Aspen Plus. In the following sections, the equations for the calculation of the heat exchangers, the reactors and the separation vessels are presented.

Heat exchangers

Counter-current shell-and-tube heat exchangers are assumed, since they are used as a standard in the chemical industry (PETERS et al., 2003, p. 642). An important parameter for these heat exchangers is the heat transfer surface A, which can be calculated using equation 3.1 (BIEGLER et al., 1997, p. 113).

$$A = \frac{\dot{Q}}{k \cdot \Delta T_{\ln}} \tag{3.1}$$

Here, $\dot{Q}$ is the heat flow and can be taken from the results of the process simulation. k is the heat transfer coefficient, which is a proportionality factor for the heat transfer at an interface. It varies according to the transfer conditions, whereby liquid states provide particularly good conditions, which is expressed by high k values. The values for different transmission conditions are shown in Table 3.1 and are taken from the VDI heat atlas (KIND et al., 2013, p. Cc 1). The upper k values of the respective category are chosen, since particularly suitable transmission conditions within the pipes are assumed. $\Delta T_{\ln}$ is the mean logarithmic temperature difference and is calculated using equation 3.2 (BIEGLER et al., 1997, p. 113).

$$\Delta T_{\ln} = \frac{(T_{1,\text{in}} - T_{2,\text{out}}) - (T_{2,\text{in}} - T_{1,\text{out}})}{ln\left(\frac{T_{1,\text{in}} - T_{2,\text{out}}}{T_{2,\text{in}} - T_{1,\text{out}}}\right)} \tag{3.2}$$

Table 3.1: Typical heat transfer coefficients for shell-and-tube heat exchangers, condensers and evaporators depending on the type of transfer according to VDI heat atlas (KIND et al., 2013, p. Cc 1).

Construction design	Transmission condition	Estimated k-value (W/m²K)
Shell-and-tube heat exchanger	Gas-gas	5 to 35
	Gas-liquid	15 to 70
	Liquid-liquid	150 to 1200
Shell-and-tube condenser	Cooling water-organic vapours	300 to 1200
Shell-and-tube evaporator	Heating steam-thin liquids	600 to 1700

Here, T_{in} are the inlet temperatures and T_{out} the outlet temperatures of the two flows. The temperature differences of the two media on both sides of the heat exchanger are put in proportion to each other. To illustrate this, the currents are shown in Figure 3.2 on a schematic diagram of a heat exchanger. The heat exchanger itself is displayed as a black box. The temperatures required for the calculation of the mean logarithmic temperature difference occur each at the inlet and outlet of both flows. Thereby, the two flows are not mixed in the heat exchanger, but indirect transfer takes place. One medium passes through the tubes in the heat exchanger, the other is fed into the casing through the heat exchanger, with the two media flowing in counter current. The heat is transferred via the lateral surface (Mantelfläche) of the pipes. The hot medium is cooled and the cold medium is heated. In this case, a minimum temperature difference of 10 K is applied to both sides of the heat exchanger (PETERS et al., 2003, p. 970).

Figure 3.2: Schematic diagram of a heat exchanger as black box with the two media 1 and 2.

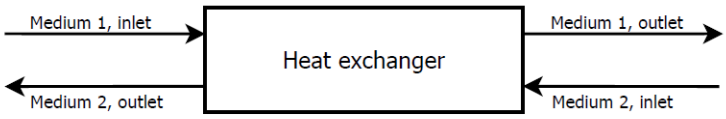

Caption: own creation.

Using the results of the process simulation and the VDI heat atlas (KIND et al., 2013, p. Cc 1), the heat transfer surface A of the shell-and-tube heat exchangers can be calculated. Furthermore, this calculation can be used to calculate the condenser and reboiler of a column, since these are also heat exchangers. The usual heat transfer coefficients for these heat exchangers can also be found in Table 3.1. In addition, the calculation of the heat transfer surface is required for the calculation

of the volume of a tube bundle reactor, since the principle of a heat exchanger is also effective there [46], which is described in more detail in the following section.

Reactor

For the calculation of the reactor, a standing tube bundle reactor is assumed analogous to the standard design of methanol reactors. This reactor is similar in its design to a shell-and-tube heat exchanger. It also consists of tubes which are placed in a casing and the heat transfer takes place between the fluids in the tubes and the housing. The difference to the shell-and-tube heat exchanger is that there are catalyst pellets inside the tubes, where the reaction takes place. The lateral surface is filled by a cooling medium that regulates the reaction temperature. In contrast to a normal tube bundle heat exchanger, the tubes have a larger diameter so that sufficient space for the catalyst pellets is available. In addition, the reactor is designed vertically and flows from bottom to top to prevent the catalyst pellets from being washed out. (OTT et al., 2012, p. 10f)

For the design of the reactor, the reactor volume must be determined. For a tube bundle reactor, the volume of the vessel $V_{Reactor,vessel}$, which is determined via the space velocity, and the volume of the tubes V_{Tubes} must also be determined, as described by OTTO (2015). Thus, the required total volume of the reactor $V_{Reactor,total}$ can be determined via equation 3.3.

$$V_{\text{Reactor,total}} = V_{\text{Tubes}} + V_{\text{Reactor,vessel}} \tag{3.3}$$

To calculate the pipe volume, the heat transfer surface A of the tubes is first determined using equation 3.1. This corresponds to the outer surface of the tubes. Then, the volume of the tubes V_{Tubes} can be determined by means of the outside pipe diameter D_a using equation 3.4.

$$V_{\text{Tubes}} = \frac{A \cdot D_{\text{a}}}{4} \tag{3.4}$$

The volume of the vessel $V_{Reactor,vessel}$ is determined by means of the catalyst volume V_{Cat} and the space velocity, which is the reciprocal of the retention time. The catalyst porosity ϵ is assumed to be 0.5, which gives equation 3.5 (BIEGLER et al., 1997, p. 118).

$$V_{\text{Reactor,vessel}} = \frac{V_{\text{Cat}}}{1-\epsilon} = \frac{2 \cdot \dot{n}}{s \cdot \rho} \tag{3.5}$$

Here, $\dot{n}$ is the material flow and ρ the molar density under standard conditions. The values of material flow and density can be determined by means of the process simulation.

Separator vessels

For the design of the vertical vessels, their volumes V_B are calculated using (BIEGLER et al., 1997, p. 112)

$$V_B = 2 \cdot \frac{\dot{m}_L \cdot \tau}{\rho_L}, \tag{3.6}$$

where $\dot{m}_L$ is the liquid mass flow at the container outlet, τ the retention time and ρ_L the liquid density. The values for the mass flow and its density can be taken from the results of the process simulation.

3.1.2 *Capital expenditures*

As described above, investment costs (FCI) and current assets (WC) are needed to determine the total capital requirement (CAPEX). The WC is required for necessary cash reserves and takes into account investments for raw materials and supplies that must be kept in stock, as well as receivables from customers, payables to suppliers, expenses for labour and raw material costs for commissioning and taxes. It must be available during commissioning and throughout operation. It will be available again after shutdown of the plant. According to PETERS et al. (2003, p. 233), the share of the WC for most chemical plants is between 10% and 20% of the CAPEX. This value varies depending on the complexity of the process, the number of products and the storage period of the products (TOWLER et al., 2008, p. 317). In this paper, an average of 15% of the total capital requirement is assumed, which leads to equation 3.7 that includes the percentage chosen for working capital and the investment costs.

$$\text{CAPEX} = \text{FCI} + \text{WC} = \frac{\text{FCI}}{0.85} \tag{3.7}$$

Depending on the progress of the project, there are different methods for calculating the FCI, which are divided into five classes by the AACE International (Association

for the Advancement of Cost Engineering) (CHRISTENSEN et al., 2011). The classes with the corresponding project progress and methods are listed in Table 3.2.

Table 3.2: Cost estimate classification matrix of the fixed capital investment according to CHRISTENSEN et al. (2011).

Class	Maturity level	Purpose of estimate	Methodology	Expected accuracy range
5	0-2%	Concept screening	Capacity method/ order-of-magnitude estimate	L: -20 to -50% H: +30 to +100%
4	1-15%	Study or feasibility	Surcharge factor method/ study estimate	L: -15 to -30% H: +20 to +50%
3	10-40%	Budget authorisation or control	Semi detailed structural method/ preliminary estimate	L: -10 to -20% H: +10 to +30%
2	30-75%	Control or bid/tender	Detailed estimation of unit cost based on quotations/ definitive estimate	L: -5 to -15% H: +5 to +20%
1	65-100%	Check estimate or bid/tender	Detailed cost calculation with final plan and component costs/ detailed estimate	L: -3 to -10% H: +3 to +15%

H = High, L = Low.

As can be seen in the table, the methods to determine costs can only be used at certain stages of the project progress, which leads to varying degrees of accuracy in estimating the results. A wider range of estimation accuracy in the early stages of the project results from the fact that less data is available and therefore less accurate methods must be applied. The further the project progresses the more data is available, the more elaborate methods can be applied and thus more accurate results can be achieved. The values given in the table reflect typical ranges of variation of the calculated results from the real costs. For example, in the case of class 5, the costs can be in the range of -20% to -50% below and -30% to +100% above the calculated costs. Therefore, the maximum range of results for class 5 is -50% to +100% of the calculated values. The exact range of deviation for each application depends on the complexity of the process, available reference information and other risks.

In the following sections, the cost estimation methods relevant for this work are explained in more detail. First, the class 5 capacity method is presented. This is

followed by an introduction to the surcharge factor method of TURTON et al. (2009, p. 193ff), which is assigned to class 4 and represents a feasibility study. Finally, the cost estimation based on manufacturer enquiries is carried out, which typically only becomes apparent when the project progresses rapidly in the accuracy range of class 2.

Capacity method

The capacity method is the simplest but also the most imprecise method for calculating investment costs of a plant. Its accuracy of estimation is in class 5 according to the AACE International (CHRISTENSEN et al., 2011). The maximum deviation of real costs from the calculated costs is from -50% to +100%. In this method, capacity and costs of a reference plant are used to calculate the costs for another plant capacity. The method can be applied both to a complete system and to individual components. A degression coefficient d is required to enable comparisons between the two capacities. It indicates how the costs develop when the plant is resized, as the correlation is usually not linear. The costs for the desired capacity can be calculated using equation 3.8 according to TURTON et al. (2009, p. 186),

$$C = C_0 \cdot \left(\frac{S}{S_0}\right)^d, \tag{3.8}$$

where C is the cost of the desired size, C_0 the cost of the reference case, S the desired capacity, S_0 the capacity of the reference case and d the degression coefficient. The last factor is usually smaller than 1 due to economies of scale, which means that the costs of a plant or component do not increase proportionally with capacity, but usually more slowly. This means that larger plants or components have lower unit costs than smaller ones. This is due to the fact that capacity scales with volume and thus with the third power of length, whereas costs depend on material consumption and thus on the surface area, which scales with the second power of length. It results in a frequently used value for the degression coefficient of 0.6, whereby the use of this value is known as the "six-tenth factor" rule. This is because the different scaling of capacity and costs results in a proportional relationship between costs and capacity with a power of 2/3. This degression coefficient can be used for individual components as well as for an entire plant, whereby more precise results can be achieved for an entire plant than for individual components if this value is used. Since the various degression coefficients of the individual components are sometimes greater and sometimes smaller than the used value, they balance each other out overall. Furthermore, there are literature sources

that provide values for individual components in order to increase the accuracy of the estimation. However, this also results in a higher effort in contrast to the application of this method to a complete plant. (PETERS et al., 2003, p. 242ff)

According to PETERS et al. (2003, p. 242), the coefficient of degression can generally range from less than 0.3 to greater than 1 for various components, with a value of 1 indicating a linear relationship. If the value is greater than 1, the costs increase disproportionately with an increase in capacity, which is why in this case several components with smaller capacities could be used in parallel as an alternative to reduce costs.

The capacity method can better be adapted to a plant if the costs of a plant or a component are known for at least two capacities. Then a plant- or component-specific degression coefficient can be determined using equation 3.9.

$$d = \frac{ln\left(\frac{C_0}{C}\right)}{ln\left(\frac{S_0}{S}\right)} \tag{3.9}$$

Here, C and C_0 are the capital costs for the two different capacities and S and S_0 are the two capacities. With the help of degression coefficients calculated in this way, the FCI for further plant or component capacities of the same type can be determined more accurately than with general coefficients.

Surcharge factor method

For a project progress of 1% to 15%, surcharge factor methods can be applied to achieve a higher estimation accuracy compared to the capacity method. These methods reach results with an estimation accuracy in the range of -30% to +50%. There are various methods, which differ in their effort and accuracy. The simple methods use general surcharge factors (Zuschlagfaktoren), whereas more precise methods use component-specific factors. In the following, the surcharge factor method according to TURTON et al. (2009, p. 193ff) is presented, which is based on a method developed by GUTHRIE (1969). This allows the plant costs to be calculated as accurately as possible despite the early project phase. In this phase, the total costs are determined by summing up the module costs of the individual apparatuses and machines. Costs from other categories listed in Table 3.3 are also considered. Here, the expenses are subdivided into four categories: direct costs,

indirect costs, contingencies and fees and costs for auxiliary devices. Direct costs include the costs of the equipment itself, additional connecting materials and machinery for installation as well as installation work. Indirect costs include costs for freight, insurance and taxes, overhead costs for construction and engineering hours. Contingencies and fees include costs for unforeseen events, such as accidents, and contract fees. The auxiliary facilities comprise costs for site development, auxiliary and additional facilities, auxiliary installations and equipment. The costs for contingencies and fees as well as for auxiliary facilities are included into the FCI using standard factors. The direct and indirect costs, on the other hand, are included in the total module costs C_{TM}.

Table 3.3: Factors for the investment costs according to TURTON et al. (2009, p. 194).

Direct costs	
Equipment costs	Acquisition costs of equipment
Connecting materials and machinery for installation	Piping, isolation, fireproofing, foundations and structural support, building technique, measuring equipment, electrical installations, painting associated with equipment
Installation work	Work required for the installation of equipment and materials
Indirect costs	
Freight, insurance and taxes	Transport costs for equipment and machines to the plant location
Construction overhead	Ancillary labour costs (Lohnnebenkosten), staff overhead, ancillary labour costs and staff overhead for supervisory staff
Contractor engineering expenses	Wages and overhead for planning and layout, project management, design-engineering work
Contingencies and fees	
Contingencies	Costs for covering contingencies, e.g. accidents
Contractor fees	Fees vary according to plant type
Auxiliary facilities	
Site development	Purchase of land, excavation, electrical installations, water and wastewater drains, roadworks, footpaths, parking
Auxiliary buildings	Office buildings, maintenance bay, control rooms, storehouse, service building (cafeteria, changing rooms, ward)
Off-sites and utilities	Storage, loading and unloading equipment for raw materials and products, necessary apparatuses for the supply of utilities (e.g. cooling water, steam generation), environmental protection facilities (e.g. wastewater treatment), fire protection systems

Taking all four categories into account, equation 3.10 is used to calculate the investment costs for a new plant. It is assumed that a new site must be developed. (TURTON et al., 2009, p. 213f)

$$\mathrm{FCI_{GR}} = 1.18 \sum_{i=1}^{n} C_{\mathrm{TM}} + 0.5 \sum_{i=1}^{n} C_{\mathrm{BM}}^{0} \tag{3.10}$$

These costs are known as $\mathrm{FCI_{GR}}$, where GR stands for *grass root*. The $\mathrm{FCI_{GR}}$ assumes that contingencies account for 15% of module costs and that charges account for 3%, resulting in a factor of 1.18 for module costs. The costs for auxiliary equipment are calculated with a share of 50% of the bare module costs C_{BM}^{0}. (TURTON et al., 2009, p. 213f)

If, however, the extension of the plant is affected, the costs for auxiliary equipment are omitted and the equation is simplified to equation 3.11. (TURTON et al., 2009, p. 213)

$$\mathrm{FCI_{BF}} = 1.18 \sum_{i=1}^{n} C_{\mathrm{TM}} \tag{3.11}$$

These investment costs are called $\mathrm{FCI_{BF}}$. Here, BF stands for *brown field*, which means that no new site has to be developed, but that the plant is an extension of an existing site. Hence, in order to determine the FCI, the total module costs $\mathrm{C_{TM}}$ and, in the case of a new site development, also the bare module costs C_{BM}^{0} are required. The total module costs are calculated using the bare module factor $\mathrm{F_{BM}}$ via equation 3.12 from the bare module costs. (TURTON et al., 2009, p. 198)

$$C_{\mathrm{TM}} = C_{\mathrm{BM}}^{0} \cdot F_{\mathrm{BM}} \tag{3.12}$$

The bare module factor is made up of various factors. These are the pressure factor Fp, which considers the system pressure, and the material factor $\mathrm{F_M}$, which considers the material used. In addition, the direct and indirect cost factors from Table 3.3 are considered in the bare module factor. The factors for pressure and material are required, since the costs of the bare modules are based on the assumption that the material carbon steel is used and ambient pressure affects the module. The direct and indirect cost factors are general factors, which take into account various cost items associated with the plant construction. With the help of the bare module factor, better adjustment results to special applications can be achieved. Therefore, in the following the calculation of the bare module cost is

presented and then the determination of the bare module factor. To calculate the bare module costs equation 3.13 is used (TURTON et al., 2009, p. 850).

$$C_{\mathrm{BM}}^{0} = 10^{K_1 + K_2 \cdot log_{10}(Z) + K_3 \cdot [log_{10}(Z)]^2} \tag{3.13}$$

$K_{1\text{-}3}$ are coefficients for the bare module costs, which are based on manufacturer prices from 2001. Their values for some components can be taken from Table 3.4. Z is a capacity or size parameter whose calculation has already been presented in section 0. It corresponds to a different parameter for each module. For example, for compressors, Z is the capacity of the compressor, for heat exchangers it is the transfer surface A. There are ranges for each module within which the size parameter should lie in the best case. These can be taken from Table 3.4, as well as the parameter used for the respective module. If the upper limit of the capacity range is exceeded, several modules of the same type must be used, since further scaling for this component is not possible or not reasonable. If, on the other hand, the lower limit is undershot, the value of the lower limit is used, as no further cost degression is assumed.

Table 3.4: Factors for the bare module costs and capacity range according to TURTON et al. (2009, p. 851f).

Module	K_1	K_2	K_3	Size	Min.	Max.
Radial compressor	2.2897	1.3604	-0.1027	Capacity (kW)	450	3000
Shell-and-tube heat exchanger	4.3247	-0.3030	0.1634	Area (m²)	10	1000
Column	3.4974	0.4485	0.1074	Volume (m³)	0.3	520
Vessel, vertical	34.9740	0.4485	0.1074	Volume (m³)	0.3	520

The bare module costs calculated with equation 3.13 refer to the year 2001 and must hence be converted to the year in which the data are collected. The CEPCI cost index (chemical engineering plant cost index) is used for this purpose as an adaptation factor for module costs. To convert the calculated costs, the CEPCI values both from the reference year as well as the year in which the data is collected must be known. Then, using equation 3.14, the bare module costs for the year of the study can be calculated (TURTON et al., 2009, p. 190). The CEPCI for the 2001 reference year is 394 and for 2019, it is 607.5 which is used as the year of the study (ECONOMIC INDICATORS, 2019).

$$C_{\mathrm{BM,base}}^{0} = C_{\mathrm{BM,ref}}^{0} \cdot \left(\frac{\mathrm{CEPCI}_{base}}{\mathrm{CEPCI}_{\mathrm{ref}}}\right) \tag{3.14}$$

where $C^0_{\mathrm{BM,base}}$ is the bare module cost in the year of study, i.e. 2019, $C^0_{\mathrm{BM,ref}}$ is the bare module cost in the reference year 2001, CEPCI_{base} is the cost index in the year of the survey 2019 and $\mathrm{CEPCI}_{\mathrm{ref}}$ is the cost index in the reference year 2001.

Subsequently, a currency adjustment to the Euro (€) has to be carried out, since the bare module costs are in US dollars (US-$). The average exchange rate for the year 2019 of 1.12 US-$/€ is used for the conversion to Euro (STATISTA, 2019). This results in the bare module cost for the year of the study in Euro $C^0_{\mathrm{BM,€,base}}$ via equation 3.15.

$$C^0_{\mathrm{BM,€,base}} = \left(\frac{C^0_{\mathrm{BM,base}}}{1.12}\right) \tag{3.15}$$

In order to calculate the total module costs, the bare module factor F_{BM} is still missing. As described above, it is composed of the pressure factor Fp, the material factor F_M and the direct and indirect cost factors.

For some components, such as compressors and columns, values for the total bare module factor are available for different materials, so that these can simply be taken from TURTON et al. (2009, p. 872) and used in equation 3.12 together with the bare module costs. For heat exchangers and vessels, however, a single determination of the pressure factor Fp and the material factor F_M is necessary. The additional constants $B_{1\text{-}2}$ consider this in the calculation of the module costs. These constants represent the direct and indirect module costs. This results in equation 3.16 for the calculation of the module costs for heat exchangers and vessels (TURTON et al., 2009, p. 866).

$$C_{\mathrm{BM}} = C^0_{\mathrm{BM,€,base}} \cdot (B_1 + B_2 \cdot F_{\mathrm{M}} \cdot F_{\mathrm{P}}) \tag{3.16}$$

The values for $B_{1\text{-}2}$ and F_M are given in Table 3.5. The pressure factors for heat exchangers and vessels must be calculated. The pressure factor for shell-and-tube heat exchangers with a system pressure of 5 bar to 140 bar is calculated using equation 3.17 (TURTON et al., 2009, p. 205).

$$F_{\mathrm{P}} = 10^{C_1 + C_2 \cdot log_{10}(p) + C_3 \cdot [log_{10}(p)]^2} \tag{3.17}$$

where $C_{1\text{-}3}$ are coefficients for the pressure factor, where C_1=0.03881, C_2=0.11272 and C_3=0.08183 (TURTON et al., 2009, p. 866). p is the system pressure, whereby the existing pressure is increased by a safety margin of 50% (BIEGLER et al., 1997, p. 112). If the pressure is below 5 bar, Fp = 1 is assumed. The pressure factor for horizontal and vertical tanks can be calculated using equation 3.18 (TURTON et al., 2009, p. 204).

$$F_{\mathrm{P}} = \frac{\frac{p \cdot D}{2 \cdot p_{\max} \cdot E - 1.2 \cdot p} + CA}{t_{\min}} \tag{3.18}$$

D is the diameter, p_{max} the maximum operating pressure, E the weld efficiency (Schweißnahteffizienz), CA the corrosion allowance and t_{min} the minimum allowable vessel thickness. A safety margin of 50% on the system pressure p is also taken into account here.

This means that all variables are known in order to be able to calculate the FCI using this method.

Table 3.5: Constants $B_{1\text{-}2}$ and the material factor F_M for the calculation of module costs from TURTON et al. (2009, p. 867f).

Module	B_1	B_2	F_M, stainless steel
Shell-and-tube heat exchanger	1.63	1.66	2.75
Vessel, vertical	2.25	1.82	3.10

Cost estimation based on quotations

The cost estimate based on quotations is normally only made after the project has progressed to 30%. The results are then within an accuracy range of -15% to +20%, which corresponds to class 2 in the AACE International classification (CHRISTENSEN et al., 2011). However, budget offers can also be obtained in earlier project phases. These serve as an aid to decision-making, whether a planned project can be implemented. Manufacturer enquiries can help, in order to obtain more accurate results than with the capacity method, when the surcharge factor method cannot be used, e.g. due to too small capacities of modules. For very small capacities, the method of TURTON et al. (2009, p. 193ff) leads to a clear overestimation of the module costs, because even at relatively large capacities cost degression is no longer expected and applicable.

For the enquiries, it is necessary that the data for the individual module are available from a process simulation. These include the media and their composition, mass or volume flows, temperatures and pressures. Furthermore, the module sizes must be obtained, which can be calculated as described in section 0. Additionally, the building materials for the modules are determined. If all of this information is known, suitable manufacturers can be contacted for the individual modules to obtain price quotations for them. In order to integrate the prices received into the surcharge factor method, the prices must first be calculated back from 2020 to 2019 using the CEPCI, as this is the year of the study. Then, a factor for transport costs and direct and indirect component cost factors are added to obtain the total module cost C_{TM}. These can be used in equation 3.11 to determine the FCI of the plant.

If the cost estimate based on quotations for the main modules is applied in an early project phase, it cannot be assumed that the results will be within the accuracy range of class 2. This is because estimates of this class usually contain much more information beyond the determination of the main module costs. Since the received producer prices are included in the class 4 surcharge factor method, it can be assumed that the results are at least as accurate as this class achieves. Due to the explicit prices received for the modules, the results are expected to be more in the inner accuracy range of class 4 than if general module prices were assumed.

3.1.3 *Operating expenditures*

The operating costs are the costs that arise during the daily operation of a plant. These costs are calculated in costs per time, in contrast to the CAPEX, which give a total cost indication for the plant. For this purpose, the various cost items are divided into the three categories direct, fixed and general costs, which are listed in Table 3.6 with their respective sub-items. The direct costs include the raw material costs C_{RM}, operating utilities costs C_{UT}, operating labour costs C_{OL}, costs for direct supervisory and clerical labour C_{DS}, costs for maintenance and repairs C_{MR}, costs for operating supplies C_{OS}, laboratory charges C_{L}, and costs for patents and royalties C_{PR}. These costs represent operating costs that vary with the production rate. They increase with an increased production rate and decrease with a decreased production rate, but this relationship does not have to be proportional. Fixed costs, on the other hand, are independent of the production rate because they are charged in constant rates even when the plant is not in operation. These include tax and insurance expenditure C_{TI} and overheads C_{O}. General costs are higher-level expenses that are necessary for the business functions. They rarely vary with the

production rate and include the administrative costs C_A. To calculate operating costs, all the components described above must be added together. For many components, there are general factors which are listed in Table 3.6. If the standard values from TURTON et al. (2009, p. 225) are inserted, equation 3.19 is used to calculate the OPEX.

$$\text{OPEX} = \frac{C_{\text{RM}} + C_{\text{UT}} + 2.215 \cdot C_{\text{OL}} + 0.146 \cdot \text{FCI}}{0.97} \tag{3.19}$$

Table 3.6: Cost parameters of the operating expenditures according to TURTON et al. (2009, p. 225).

Parameter	Variables and multiplying factors
Direct manufacturing costs	
Raw material cost	C_{RM}
Utilities cost	C_{UT}
Operating labour	C_{OL}
Direct supervisory and clerical labour	$C_{\text{DS}} = 0.18 \cdot C_{\text{OL}}$
Maintenance and repairs	$C_{\text{MR}} = 0.06 \cdot \text{FCI}$
Operating supplies	$C_{\text{OS}} = 0.009 \cdot \text{FCI}$
Laboratory charges	$C_{\text{L}} = 0.15 \cdot C_{\text{OL}}$
Patents and royalties	$C_{\text{PR}} = 0.03 \cdot \text{OPEX}$
Fixed manufacturing costs	
Local taxes and insurances	$C_{\text{TI}} = 0.032 \cdot \text{FCI}$
Plant overhead costs	$C_{\text{O}} = 0.6 \cdot (C_{\text{OL}} + C_{\text{DS}} + C_{\text{MR}})$
General manufacturing expenses	
Administration costs	$C_{\text{A}} = 0.15 \cdot (C_{\text{OL}} + C_{\text{DS}} + C_{\text{MR}})$

To determine the operating costs, therefore, only the raw material costs C_R, operating material costs C_{UT} and operating labour costs C_{OL} need to be determined as well as the investment cost. To calculate the raw material and operating material costs, the specific costs $C_{RM,i}$ and $C_{UT,i}$ must be multiplied by the respective mass flows $\dot{m}_i$ or operating resource flows P_i and the operating time T_O. For this purpose, the specific costs $C_{RM,i}$ and $C_{UT,i}$ are taken from the literature. The mass and operating material flows can be determined by means of the process simulation. This results in equations 3.20 and 3.21 for calculating the raw material costs C_R and the cost of operating utilities C_{UT}.

$$C_{\text{RM}} = \left(\sum_{i=1}^{n} \dot{m}_i \cdot C_{\text{RM},i}\right) \cdot T_{\text{O}} \tag{3.20}$$

$$C_{\text{UT}} = \left(\sum_{i=1}^{n} P_i \cdot C_{\text{UT},i}\right) \cdot T_{\text{O}} \tag{3.21}$$

For large plants, it is possible to calculate the operating labour costs using the method of ALKHAYAT et al. (1984). However, this is not transferred to small plants. It can be assumed that small plants are operated automatically and no separate personnel has to be hired for them; instead, a full maintenance contract is concluded for the plant.

3.1.4 *Costs of manufacturing*

As described at the beginning of the chapter, production costs are composed of the annual capital costs and operating costs and can be calculated using equation 3.22.

$$\mathrm{COM} = \mathrm{OPEX} + \mathrm{ACC} \tag{3.22}$$

The calculation of the OPEX is already described in the previous section. The ACCs are determined by applying the annuity method to the FCI together with a return on current assets, also called the working capital. It is assumed that only the chemical plant will lose value, but not the working capital. Therefore, the annuity method is only applied to the FCI. This ensures that the investment sum is spread evenly over the lifetime n of the investment and takes into account the annual interest rate i. As the working capital does not decrease in value, only the interest has to be paid for it. To calculate the ACC, the annuity method and the interest rate are summarised in equation 3.23. The first summand in the brackets represents the annuity (imputed depreciation of the production plant and interest) and the second the interest payment for the working capital. (SCHEMME et al., 2019)

$$\mathrm{ACC} = \mathrm{FCI} \cdot \left(\frac{i \cdot (1+i)^n}{(1+i)^n - 1} + \left(\frac{1}{0{,}85} - 1 \right) \cdot i \right) \tag{3.23}$$

By applying this combined method, the total capital requirement is distributed evenly over the lifetime of the plant. In addition to the annual COM, specific production costs are of interest as they ensure comparability with other plant sizes and other fuels. On the one hand, the specific manufacturing costs per kilogram of product ($\mathrm{COM_{kg}}$) are relevant which can be calculated using equation 3.24 (SCHEMME et al., 2019).

$$\mathrm{COM_{kg}} = \frac{\mathrm{OPEX+ACC}}{\dot{m}_{Product}} \tag{3.24}$$

Here, $\dot{m}_{\text{product}}$ is the product mass flow of methanol. On the other hand, the production costs can be related to the lower heating value (LHV) of one litre gasoline equivalent (GE) in order to ensure energy comparability between different fuels. To calculate the specific manufacturing costs related to the lower heating value of one litre of gasoline equivalent ($COM_{L,GE}$), the LHV of methanol is required, as shown in equation 3.25 (SCHEMME et al., 2019).

$$COM_{L,GE} = \frac{OPEX+ACC}{\dot{m}_{Product} \cdot \frac{LHV_{MeOH}}{LHV_{GE}}} \tag{3.25}$$

3.2 **Fundamentals of life cycle assessment**

A life cycle assessment (LCA) analyses the environmental impacts linked with all stages of a product's life usually from cradle-to-grave and sometimes for limited production steps. A formal approach is defined by the International Organization of Standardization (ISO, 2006a, ISO, 2006b). The approach covers four steps, as also shown in Figure 6 (blue boxes). They are explained in more detail in this sub-chapter and if not provided with another reference, they are in accordance with the ISO standards.

3.2.1 *Goal and scope*

The goal and scope definition talks about aims and intention of a study, as well as its functional unit and system boundaries. The functional unit is a measure for the product's quantified functions, i.e. the inputs and outputs related to it. It makes a system comparable to a reference system, e.g. if there are two different systems that produce biogas in different ways. Hence, the functional unit for each system could then be the kilowatt-hours of produced heat or electricity or the cubic meters of obtained biogas. The system boundary defines the boundaries within which the product's manufacturing, usage and disposal are analysed. It makes assumptions

Figure 3.3: Steps of a formal life cycle assessment.

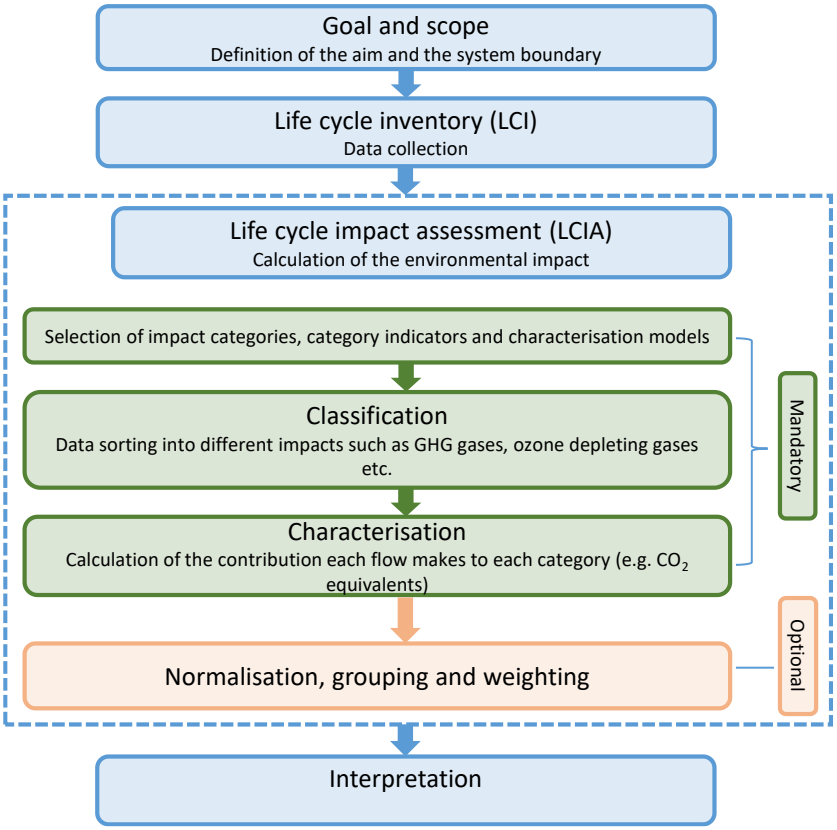

Caption: own creation in accordance with the ISO standards (ISO, 2006a, MCMANUS, 2012, p.15).

about constraints due to data and cut-off criteria. The latter describes the level of precision and completeness within an LCA. As it is impossible to know and account for all impacts of a product, it is inevitable to cut-off, i.e., leave out, certain processes. LCA systems are often represented in a flow diagram which considers all unit processes within the boundaries. Normally, boundaries are defined for either the production of a product (cradle-to-gate), the utilisation and end-of-life phase (gate-to-grave or sometimes gate-to-gate) or both (cradle-to-grave) (ISO, 2006a, ISO, 2006b). The terminology for LCAs of transportation fuels often differentiates between well-to-pump (WTP) and well-to-wheels (WTW) analyses. The first describes the exploitation and transportation of feedstock and the production, the transport and the distribution of a fuel. The second also includes the operation of the vehicle (LEE et al., 2016).

In general, it can be differentiated between attributional and consequential LCAs, which pursue different objectives. An attributional LCA quantifies the material and energy flows, as well as the environmental impacts, that are ideally directly linked with a product's life cycle. The consequential approach stretches the boundaries and also includes indirectly linked environmental burdens as a consequence of the production decision. Hence, the systems contain only processes that are affected by the decision and thus change or modify their output (SONNEMANN et al., 2011, p. 47f). In principle, the attributional approach is also suitable for analyses that expand their system boundaries. However, the consequential approach is generally more elaborate than the attributional one, as it contains assumptions about processes and market mechanisms that occur far away from the actual product (BECK et al., 2019).

3.2.2 *Life cycle inventory*

The LCI comprises all inputs and outputs within the product system that occur for the production of the functional unit. For each unit process, data must be collected, as well as input and output flows defined; i.e., energy and raw materials used, other products produced and emissions emitted to air, soil and water (ISO, 2006a, ISO, 2006b). There are often constraints during data collection, which is why background data of elementary flows within the system are often taken from life cycle inventory databases. Foreground data of the main unit processes that are evaluated can also be gathered from literature or own measurements. LCA software can help to process inventory data (MCMANUS, 2012).

If the system produces valuable products aside from the main one, there are different opportunities to account for so-called co-products. This problem is called multi-functionality problem and often applies to integrated fuel production systems with cogeneration (ESCOBAR et al., 2015). It needs to be considered whether to allocate impacts to all products produced or use system expansion. According to the ISO (ISO, 2006a, ISO, 2006b), this can be solved by either partitioning (often referred to as 'allocation') or system expansion. The ISO 14044 (ISO, 2006b) recommends system expansion over allocation for attributional LCAs when the system delivers more than one product or function. This entails assuming that co-products replace other products in the market, generating co-product credits under system expansion approaches. The need for assumptions produces uncertainty due to modelling choices, in addition to parameter and model uncertainty (HUIJBREGTS et al., 2001). The products to be replaced normally depend on the relative prices, amongst other market factors, which in turn depend on the geographical and temporal scope of the LCA. In attributional LCA, co-product

credits are normally estimated by considering those co-products to be most likely replaced in the market, i.e. from average suppliers (FINNVEDEN et al., 2009). On the contrary, consequential LCA considers suppliers of marginal technologies by incorporating economic reasoning (EKVALL et al., 2004). Thus, the influence of such assumptions on results from both attributional and consequential LCA can be critical, especially when comparing systems against each other, and must be conveniently assessed through scenario analysis (ESCOBAR et al., 2014).

3.2.3 *Life cycle impact assessment*

The life cycle impact assessment (LCIA) evaluates the LCI results to determine significant environmental impacts. For this, the inventory data is associated with environmental categories and impact category indicators (also category indicator) in an attempt to better understand the impacts. This means that LCI results are assigned to impact categories, which in turn each have a quantifiable category indicator. However, the choice of impact categories introduces subjectivity. Furthermore, the LCIA phase can also include iterative processes, which require the re-evaluation of the goal and scope if they are impossible to achieve. The steps in an LCIA are summarised in the dashed blue box in Figure 6. Three of four presented steps are mandatory, beginning with the selection of impact categories, category indicators and a characterisation model. During the classification step, input and output flows are sorted into different impact types such as GHG gases, ozone depleting gases and others. In the characterisation step, their relative contribution to each impact category is quantified using characterisation factors (e.g. kg CO_2-eq. as presented in Table 3.7). Last but not least, it is optional if normalisation, grouping or weighting are applied. The first describes the calculation of the indicator results relative to a reference factor in order to better understand the magnitude of each indicator. Grouping combines impact categories into sets and sometimes sorts and ranks them based on value-choices. The categories either are sorted on a nominal basis or ranked according to a given hierarchy (ISO, 2006a, ISO, 2006b). Weighting converts indicator results using selected weighting factors or aggregates results across impact categories. Weighting helps with the identification of the most important impact categories and provides an aggregated score for the results (SALA et al., 2018).

For the characterisation step, there is a number of characterisation models available in LCA software to simplify the process. Although there are several models that can be used for this stage, such as CML 2001, TRACI 2.1, Environmental Footprint

2.0 and 3.0, we decided to introduce the ReCiPe 2016 in this study. The model is commonly used and also relevant for this LCA. It differentiates between the individualist, hierarchist and egalitarian perspective. This choice category determines the time horizon, which in turn affects both midpoint and endpoint modelling of climate change. Midpoint analyses consider impact categories such as global warming, i.e., climate change, marine and freshwater eutrophication and particulate matter among others. Endpoint analyses, on the other hand, use characterisation factors to summarise the impact categories in three main areas of protection, namely human health, (terrestrial and aquatic) ecosystems and resource availability (HUIJBREGTS et al., 2016). Weighting factors of environmental indicators are also included in the model, providing relative global warming impacts for a 100-year period for CO_2, CH_4 and N_2O as presented in Table 3.7. Commonly, the hierarchist view is taken, where the global warming potential of CH_4 and N_2O is 34 and 298 times higher compared to CO_2, respectively.

Table 3.7: ReCiPe 2016 value choices of the modelling of the effect of GHGs and global warming potential for the three perspectives according to HUIJBREGTS et al. (2016, p. 24f).

Choice category		Individualist	Hierarchist	Egalitarian
Time horizon		20 years	100 years	1000 years
Name	Formula			
Carbon dioxide	CO_2	1	1	1
Methane	CH_4	84	34	4.8
Nitrous oxide	N_2O	264	298	78.8

In the following, several environmental indicators are described that are calculated under the ReCiPe 2016 model and relevant to this analysis:

- Climate change or global warming potential (CC or GWP); excluding or including biogenic carbon, accounts for all GHG emissions in kg CO_2-equivalents (kg CO_2-eq. = category indicator) (CREMIATO et al., 2017).
- Freshwater and marine eutrophication potential (EP) have kg P-eq. and kg N-eq. as category indicators. It refers to an accumulation of nutrients in water or soil, i.e. the nutrient concentration rises above the specific water or soil volume. An augmentation in nutrients can lead to an overproduction of aquatic plants and algae, which then cover the water surface and reduce oxygen and sunlight penetration through the water's top layer. In soil,

nitrogen can leach into water streams and cause eutrophication (MEZZULLO et al., 2013).

- The acidification potential (AP) accounts for NO_x, SO_x and ammonia emissions and summarises them under the category indicator of kg SO_2-eq. According to MEZZULLO et al. (2013), acidification is the effect of increasing pH acidity in waters and soils. Acid rain, as a form of acidification, can also be caused by air emission. It has a harmful effect especially on vegetation and is then summarised under the term terrestrial acidification.
- Human toxicity refers to several toxic substances that can be cancerous and non-cancerous and pose a risk to human health (kg 1,4-DB-eq.).
- The photochemical ozone formation (POF) cover the substances that are responsible for the production of photochemical ozone in the troposphere (kg NO_x-eq.) (CREMIATO et al., 2017).
- Fossil depletion (FD) refers to abiotic resource consumption (kg oil-eq.).
- Stratospheric ozone depletion (ODP) refers to ozone-depleting gases that damage the ozone layer (kg CFC-11-eq.) (KUCKSHINRICHS et al., 2012).

There are certain levels of uncertainty and variability that occur due to the subjective choices, e.g., in impact categories and allocation or system expansion approaches. The level of completeness and precision (cut-off criteria) that is achieved is judged based on the LCIA results. Therefore, a sensitivity analysis should be carried out that shows how LCIA results are affected by methodological choices and data changes. It identifies the main elementary flows that contribute to the environmental impacts and those that are negligible. This makes it possible to check and validate the LCIA with reference to the goal and scope setup (EC et al., 2010).

3.2.4 *Interpretation*

The last phase in an LCA is the interpretation phase, which presents the results and compares them with the defined goal and scope. The phase should explain limitations, draw conclusions and ideally provide recommendations enabling future improvement of the system. It should also contain a sufficient evaluation of completeness, consistency and sensitivity. Further, it is important to point out that

LCIA results only represent the environmental potential and do not include risks or safety margins (ISO, 2006a, ISO, 2006b).

3.3 **Relevant cost analyses**

This sub-chapter reviews the literature regarding relevant cost analyses of BGPs and biogas upgrading technologies. Then, it collects relevant analyses of PtF systems and looks at the combination with wind electricity. The prices for methanol, CO_2 and H_2 are compared.

3.3.1 *Costs of biogas plants and biogas upgrading technologies*

There has been extensive literature on cost estimation of biogas and upgrading technologies and the costs of CO_2 capture (KHAN et al., 2017, SUN et al., 2015). Generally, costs are determined by the scale, the technology and the grid injection (BEYRICH et al., 2019). Costs for BGPs vary widely and depend on different factors such as feedstock used and AD technology (BIENERT et al., 2019). Co-products are frequently counted to revenues such as sales of fertiliser and heat (COLLET et al., 2017, ZHANG et al., 2013). However, there have not been many studies considering the valorisation of the CO_2 from BGPs. Apart from methanation of CO_2 in biogas, which has lately gained more interest, a recent study by DANIEL-GROMKE et al. (2020) considered among others potential revenue options from selling CO_2 from biogas upgrading as a by-product in the future. They examined plants with 250 and 500 m³/h. Essential for such sales would be a market demand and realistically achievable revenues. Specific revenues from 25 €/t to 250 €/t CO_2 were considered. The results show that sales of CO_2 can reduce electricity generation costs by about 1-11 ct/kWh_{el} related to the main product electricity from biomethane cogeneration. In general, it is difficult to lower the levelised cost of electricity (LCOE) for small-manure plants, as the CO_2 price would have to be very high. COLLET et al. (2017) assume biogas production costs of 0.36 €/m³ for the AD of sewage sludge. Other literature found values between 0.24-0.30 €/m³. The sales of co-products generated by the system is often considered as revenues (COLLET et al., 2017). ZHANG et al. (2013) also consider the possibility of selling co-products such as fertiliser and a “carbon credit sale” by means of an LCC (p. 492). They discover that the results are highly dependent on the price of nutrients for fertiliser credits.

SUN et al. (2015), who looked at investment and operating costs of upgrading technologies, conclude that the technology’s selection depends highly on individual

case- and site-specific conditions. Nevertheless, biogas upgrading technologies compared with each other show similar costs. Interestingly, there is a wide variety in costs to be found in the literature, depending on the size of plants. An LCC study by LOMBARDI et al. (2020) emphasise that larger upgrading plants perform better in economic analyses as their payback time decreases. In VIEBAHN et al. (2018), for example, large-scale costs of 95 €/t_{CO2} by means of a membrane process are given. The costs for amine scrubbing are even lower at 71 €/t_{CO2} and the PSA also has costs in the range of 101 €/t_{CO2}. These costs of the three processes refer to raw biogas flows of 700 m^3/h at 8400 FLH and a CO_2 content of 48vol.-% in the raw biogas. Another study by ADLER et al. (2014b) even finds upgrading costs lower than those. The average specific costs for biomethane from renewable raw materials are estimated at 7 €-ct/kWh_{LHV} and from manure at 7.4 €-ct/kWh_{LHV} (DENA, 2020). COLLET et al. (2017) calculate, e.g., production costs for rather small plant with a production capacity of 230 m³/h biogas from sewage sludge. Costs reach 0.104 €/kWh_{LHV} for membrane separation and are only slightly lower with 0.101 €/kWh_{LHV} for amine scrubbing, which translates into costs as high as around 600 €/t_{CO2}, when assuming a share of 46vol.-% CO_2 in biogas. For a plant of 50 m³/h (208 kW), GÖKGÖZ et al. (2020) assume specific costs of 5.7 €-ct/kWh_{LHV} which is about half of the costs calculated by COLLET et al. (2017). The authors also consider an off-grid approach where biomethane is sold as a fuel. With this, the costs could be decreased to 2.9 €-ct/kWh_{LHV}. DANIEL-GROMKE et al. (2020) estimated specific costs for biomethane at 9-13.5 €-ct/kWh_{LHV} for a manure plant (70% manure, 30% energy crops) with 250 kW.

Under current conditions, biogas upgrading is not profitable for German small-manure plants due to low biogas streams and high specific investment costs (BEYRICH et al., 2019, KHAN et al., 2017). However, small-scale upgrading is claimed to be financially possible at several pilot plants in countries such as Switzerland (OESTER et al., 2018), Iceland (ÞORBJÖRNSSON, 2016) and Hungary (LEMS et al., 2010). BIENERT et al. (2019) analysed innovative small-scale upgrading technologies that are not available in the German market yet. According to them, some can even achieve costs which are close to large-scale plants (around 90 €/t_{CO2}). An important point will be the demand for such small-scale applications in the future which can determine the costs of upgrading. Manufacturers announced relatively competitive price information given that they receive a sufficient amount of orders (GÖKGÖZ et al., 2020).

3.3.2 *Costs of Power-to-Fuel systems and renewable methanol*

As mentioned above, several studies have tackled the idea to use CO_2 from flue gas of industrial processes for PtF routes in cost analyses. Their number has increased especially in recent years. DECKER et al. (2019), who analysed a system similar to the one proposed by this study though at a larger scale, calculated the price of methanol in the range of 1.32-1.73 €/l_{GE} (gasoline equivalent). SCHEMME et al. (2019) also looked at synthesis pathways in a TEA following the cost calculation method by TURTON et al. (2009), considering CO_2 from flue gas and H_2 from PEMEL. For a methanol plant with 300 MW, they calculated a price of 1.89 €/l_{DE}. Cost analyses estimated methanol produced by PtF at costs between 120-680 $€_{2015}$/MWh (0.66-3.76 €/kg), although they applied to commercial-scale plants in the range of 5-200 MW. Methanol from other technologies, such as gasification of lignocellulose, reached lower production prices of 30-120 $€_{2015}$/MWh (0.17-0.66 €/kg) and of 60-100 $€_{2015}$/MWh (0.33-0.55 €/kg) from hydrogenation of biogas (BRYNOLF et al., 2018).

Overall, the H_2 costs have the highest share in total costs in methanol from PtF in most studies (DECKER et al., 2019, PÉREZ-FORTES et al., 2016, SCHEMME et al., 2019). Decker et al. (2019) also point out the importance of the price of electricity, which is connected to the H_2 price, for the economic performance of the system. NYÁRI et al. (2020) confirmed this issue, although they found that their methanol plant is not profitable under current market conditions, mainly because of the high costs of H_2 production. However, the scientific community assumes a sharp decrease in costs due to a decline in investment costs. A future value with an expansion of the wind energy and lower investment costs of the electrolyser is often assumed as a prerequisite, resulting in costs of 4.6 €/kg_{H2} (ROBINIUS et al., 2018a). DECKER et al. (2019) calculate costs of 3.27 to 6.24 €/kg_{H2}, for larger H_2 production plants in combination with a wind farm. The price differences are due to the varying locations with different FLHs of the wind turbines. BRYNOLF et al. (2018) expect investment costs for PEM electrolysers of 800 €/kW for 2030 and SMOLINKA et al. (2018) estimate them at approximately 500 €/kW for 2050. Thus, it can be expected that CAPEX and therefore total costs for the electrolyser will decrease significantly.

A doctoral thesis by OTTO (2015) compared CO_2-utilisation options, among them methanol synthesis with H_2 from alkaline electrolysis (AEL) and CO_2 from chemical scrubbing of flue gas from fossil plants. The profitability analysis includes the estimation of the investment cost, specific production costs, influence of CO_2 certificate prices on the production costs and the CO_2 avoidance costs. The results

show that, at a capacity of 1.69 million t/a (934 MW_{LHV}), the production costs in the CO_2-based process (1.108 €/kg_{MeOH}) are 3.3 times higher than in conventional production. H_2 costs again dominate the costs of manufacturing. A study by PÉREZ-FORTES et al. (2016) investigated the methanol direct synthesis in a TEA which focussed primarily on the synthesis process as an option for carbon capture and utilisation (CCU), taking values for the upstream production of H_2 and CO_2 separation from the literature. The most expensive components of a plant, whose size is comparable to conventional methanol plant (440 kt_{MeOH}/a), were the compressor system followed by the heat exchanger network. The results showed that the plant could be profitable if the methanol price increased by a factor two, the H_2 costs decreased by a factor of 2.5 or the CO_2 price decreased to 222 €/t (PÉREZ-FORTES et al., 2016). In fact, CO_2 from flue gas can be obtained at costs for capture from the iron and steel industry between 50-70 €/t_{CO2} and in the cement industry between 70-150 €/t_{CO2} (BRYNOLF et al., 2018). VIEBAHN et al. (2018), e.g., give costs for direct air capture (DAC) of 480 €/t_{CO2}. In other sources, however, both significantly higher and significantly lower costs can be found (SCHEMME, 2020).

3.4 Environmental assessments of biogas and Power-to-Fuel systems

This study considers a life cycle assessment (LCA) about a PtF system, including several sub-processes and systems which each entail emissions and follow different assumptions concerning emissions. First, this sub-chapter focusses on BGP, as their analysis in LCA studies varies greatly and considers different cut-off criteria. Second, it summarises LCAs about biogas upgrading and CO_2 utilisation and, finally, emissions from PtF systems including H_2 from electrolysis are analysed.

3.4.1 *Life cycle emissions from biogas systems*

Environmental emissions

During biogas and biomethane production numerous sources of emissions occur, such as from the biomass used as a feedstock, the transport and storage of feedstock, the digestate storage, the biogas utilisation and more. The processes can have negative effects on ecosystems, among others harming human health and the balance of species. Thus, emissions from AD should be avoided. The most

important ones are CO_2, CH_4, nitrous oxide (N_2O) and fluorinated compounds such as chlorofluorocarbons (CFCs). Most emissions stem from the provision of biomass, which can positively be influenced when residues and waste products are chosen. Agriculture in Germany is the source of numerous emissions caused by, e.g., the emissions from cultivation of land (CO_2 and N_2O) and the digestion of ruminants. However, plants also sequester CO_2 during photosynthesis and contribute to CO_2 emission reductions. Therefore, biogas and biomethane can present a valuable substitution option for fossil resources. Especially, the co-generation of heat and electricity offers a reduction in GHG emissions, as heat is used as a co-product. (FNR, 2012)

As an accounting example for agricultural emissions linked to BGPs, there is the German agricultural emission inventory by the KTBL[1] (WULF et al., 2019). The important emissions that are credited to BGPs are shown in Figure 3.4. CH_4 can be emitted during the phase of AD from the fermenter either by unintended leakages in the cover or the controlled overpressure security valve and from the open storage of digestate. N_2O and NH_3 emissions from open storage and digestate application are also included in the inventory. CH_4 and CO_2 emissions by the CHP unit are usually assigned to the energy sector under the inventory. In addition, CO_2 emissions from the conversion of plant biomass are usually not included, unless energy crops are part of the feedstock. However, these emissions cannot be specifically shown from the calculations, as the inventory does not distinguish between different utilisation paths of the harvested products. Emissions from crop cultivation are calculated primarily from the type of fertilisers used (mineral or organic) and their application technology.

The LCA literature proves to be inconsistent in their consideration of biogas system emissions, which is due to individual system boundaries based on different international and regional backgrounds and inventories as well as variations in the design of such systems. Therefore, it is difficult to compare the results of LCA studies with each other. System boundaries or functional units often vary as well as assumptions concerning feedstock and technical and agricultural aspects (BURATTI et al., 2013, HIJAZI et al., 2016). As stated by POESCHL et al. (2012b), emissions of BGPs are connected to feedstock production, plant operation and construction, digestate handling and processing as well as application. The system boundaries around these emissions are set differently, meaning that restrictions to systems are common, cutting off certain production steps.

[1] Kuratorium für Technik und Bauwesen in der Landwirtschaft

Furthermore, the environmental performance is based on many different choices such as the choice of the FU, various cultivation and feedstocks as well as location, the final utilisation of the generated energy and the treatment of digestate (PÉREZ-CAMACHO et al., 2019).

Figure 3.4: Emissions for biogas production.

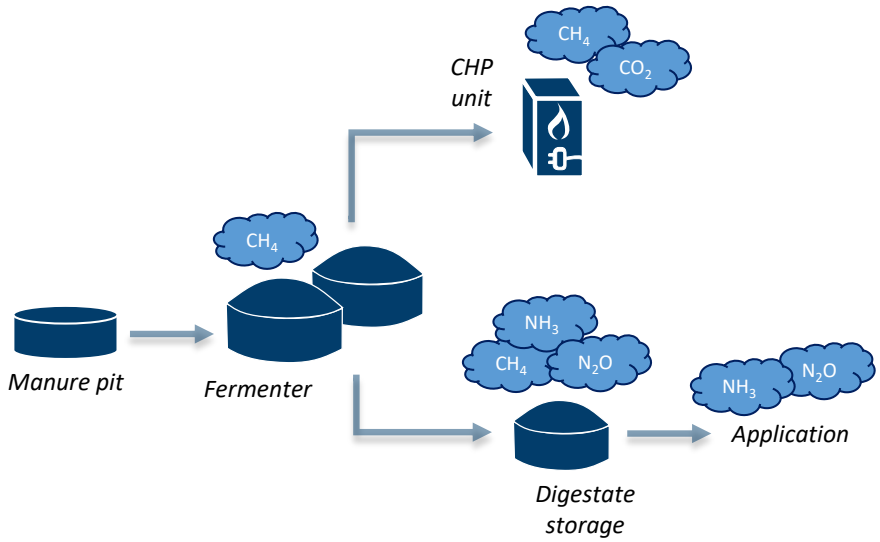

Caption: WULF et al. (2019); CHP = Combined heat and power plant.

From the construction side, BGPs differ in their pre-storage of manure and storage of digestate, distinguishing between open and closed storage systems. This largely determines the emissions from the plant, as open storage has significantly higher emissions. There is unanimous agreement in LCAs of BGPs that open digestate storage negatively affects the GHG balance of a plant (ESTEVES et al., 2019, LANSCHE et al., 2012, PAOLINI et al., 2018). MEZZULLO et al. (2013) discovered that digestate storage tanks need to be covered in order to make the AD plant beneficial and avoid additional CH_4, CO_2 and NH_3 emissions. HIJAZI et al. (2016) also find that the GHG balance of a biogas plant can be improved by the collection of biogas during digestate storage or by using a gas flare during downtimes of the CHP. The German-wide survey for biogas plant operators in 2010 showed that two thirds of the German biogas plants have a gas-tight digestate storage. Besides, for newly-built plants it is mandatory to have such a storage (ZORN et al., 2014). As law requires a closed storage in recently-built BGPs, CH_4 emissions from AD are close to zero (FNR, 2016).

Environmental burdens for biogas plants with plant material are mainly due to the cultivation which can be omitted for manure. Emissions influencing eutrophication and acidification potential are lower for plants which are run exclusively with manure, as crops cause emissions during their production phase (LANSCHE et al., 2012). This is confirmed by an LCA from O'KEEFFE et al. (2019) who find that smaller scaled manure plants show GHG mitigation potential by negative kg CO_2-eq. emissions as opposed to larger crop-based plants whose emissions are positive. The feedstock origin was also found to have an influence on the impact categories of eutrophication (freshwater and marine) and metal depletion by POESCHL et al. (2012a, p. 189). As long as straw and cattle manure are assumed to be waste, upstream processes such as cultivation processes and animal husbandry can be excluded from the analysis, as also done by POESCHL et al. (2012b). While some studies include e.g. animal husbandry, many omit this part, as well as the collection, transport and handling of the manure. It depends on the system boundaries again and can sometimes be due to lack of data or expected low impacts (ESTEVES et al., 2019). For instance, ZHANG et al. (2013), who looked at manure-treatment options in a cradle-to-gate LCA, assumed that the collection is already done by the livestock farm anyways. Therefore, they would not add this stage to the analysed system. A similar reasoning is followed by OEHMICHEN et al. (2017), who assume that manure emissions are ascribed to livestock production and hence inexistent until the BGP production stage, when the manure as feedstock is ready to be inserted into the fermenter. Emissions from pre-storage are thus non-existent. Therefore, CH_4 and NH_3 emissions occur only during the stages of AD and digestate storage (OEHMICHEN et al., 2017). ZHANG et al. (2013), on the other hand, included N and P emissions from pre-storage of manure, but did not specify the type of storage further. Direct emissions from raw manure storage were also considered by FUCHSZ et al. (2015), considering Western-European emission factors for numerous substances per animal and year. If storage or pre-treatment of manure together with other feedstock occurs at the BGP, it should be accounted for according to (LIEBETRAU et al., 2017). A review by PAOLINI et al. (2018) summarises the significant decrease in emissions when feedstock is stored in closed tanks.

Studies have also found that transport can contribute significantly to the climate change category in biogas systems (BURATTI et al., 2013, RAU, in press). However, the inclusion of transport in studies varies as well, also depending on regional settings (ESTEVES et al., 2019). As this study neglects the application of digestate due to the system boundaries set, we do not go further into detail about them. While other studies have also decided to leave this step out (ESCOBAR et al., 2015, MEZZULLO et al., 2013), it is important to bear in mind that it causes

emissions dependent on the chosen technique (SOTERIADES et al., 2018). However, its application is less polluting compared to raw manure application as digestate replaces mineral fertiliser and reduces NH_3 and N emissions into the ground water to a minimum (SCHNEIDER-GÖTZ et al., 2007). The construction of the plant can also be included, but many sources found the relatively small contribution in the overall impact (ESTEVES et al., 2019, LANSCHE et al., 2012, MEZZULLO et al., 2013, RAU, in press). For the most part, emissions coming from plant manufacture are negligible for the whole life cycle impacts, as they only occur once in the lifetime of the plant whereas the emissions due to plant operation are reoccurring.

Credits and avoided emissions through manure credits

In general, the literature shows the importance of biogas systems in terms of credits which often make a difference in their environmental balance. As mentioned in section 3.2.1, environmental credits are linked to the avoided emissions from substituting the use of certain products for valuable co-products of an evaluated system (e.g., through a substitution or system expansion approach). Often considered are fertiliser credits from digestate as well as heat and electricity credits (ESTEVES et al., 2019). The replacement of mineral fertiliser by digestate as an organic product is found to decrease the overall environmental impacts of biogas systems (VAN STAPPEN et al., 2016). Moreover, digestate as opposed to raw manure has much lower odour emissions when applied in the fields (FACHVERBAND BIOGAS E.V., 2018). An LCA of manure-based biogas production by LANSCHE et al. (2012) found a relatively insignificant contribution by heat credits compared to electricity. However, the credit is dependent on the thermal efficiency of the CHP and also the chosen reference system, according to OEHMICHEN et al. (2017). They assumed to replace heat from the German heat mix which comprises a mix of NG and boilers run with fuel oil. Their calculated credits were also insignificant compared to the credits achieved by improved manure management which were almost six times as high.

A matter of debate are the avoided CH_4 emissions from conventional manure storage that are often credited to BGPs. Also referred to as improved manure management or manure credit, the avoided emissions have been included in various LCA studies during the past years, some also carrying out system expansion over allocation (BÖRJESSON et al., 2010, EDWARDS et al., 2014, FNR, 2013, HIJAZI et al., 2016, LANSCHE et al., 2012, O'KEEFFE et al., 2019, OEHMICHEN et al.,

2017). In fact, it is possible to consider negative CH_4 emissions of biogas systems for keeping the manure within a closed system and avoiding open manure storage. These saved emissions are then considered within the biogas system as opposed to the conventional, open-air storage of raw manure that emits CH_4 directly into the air (LIEBETRAU et al., 2017). However, environmental credits for using a more efficient process within a biogas system involves a double counting effect, as the substitution of renewable electricity already accounts for avoided emissions. This should be avoided by LCA standards (EC et al., 2010). Seemingly, the LCA literature does not concern itself too much with the double counting problem. Only few studies were found to include emissions from pre-storage of manure without considering the manure credit at all (FUCHSZ et al., 2015, ZHANG et al., 2013). The eligibility of the method of counting avoided emissions could be confirmed after a phone call with an expert from DBFZ[2] (OEHMICHEN, 2020), such that a double purpose of a BGP is indeed existent. O'KEEFFE et al. (2019) even point out that there is more research required in replacing general statistics for manure credits with actual farm data, especially against the background of the RED II.

3.4.2 *Emissions from biomethane production*

The upgrading of biogas to biomethane generates additional climate-relevant emissions, mainly due to the efficiency of the upgrading plant in terms of CH_4 slip and the own energy demand of the upgrading and feed-in plants (FNR, 2012). CH_4 slip is not so much of importance for emissions from upgrading, as a closed system is assumed in this study, where the CH_4 in the flue gas is post-treated and converted into CO_2. It has been shown in the scientific literature that larger treatment capacities can lead to reduced GHG emissions due to their lower specific energy demand. The injection of biomethane into gas networks with lower pressure levels in turn reduces the energy needed to increase the pressure at the entry point (FNR, 2012). If biomethane that is not needed in the CHP is fed into the NG grid, it can be seen as a replacement of NG production (KHAN et al., 2017). Nevertheless, this is not an option in this study as small-manure plants are assumed to usually be in remote locations and lack a connection to the grid (WERN et al., 2019). Therefore, the requirements are not as rigid as for biomethane that is injected. Instead the biomethane is burnt in a CHP, which also shows advantages over NG. COLLET et al. (2017) found that the burning of biomethane including membrane upgrading for the production of 1 MJ showed fewer emissions than burning of NG in a boiler.

[2] Deutsches Biomasseforschungszentrum

Most emissions stem from the fossil CO_2 from the gas combustion, while remaining emissions come from transport and resource extraction.

There has been extensive literature covering emissions from biomethane production in recent years (AWE et al., 2017, KHAN et al., 2017). Concerning the process assumptions, the studies also vary widely. While some studies consider the upgrading stage only, such as KOHLHEB et al. (2020) who focusses on the PSA technology, many others include the whole biogas system within their boundaries (BURATTI et al., 2013, COLLET et al., 2017, GROSSO et al., 2012, LOMBARDI et al., 2020). LOMBARDI et al. (2020), e.g., compared five different upgrading technologies in LCA and LCC analyses, while also including biogas production from organic fraction and municipal solid waste (MSW). They found that amine scrubbing performed particularly well due to their low demand in electricity and the low amount of CH_4 slip. PSA also performed well especially in human toxicity. Some technologies need additional material such as solvents for amine scrubbing and high-pressure water scrubbing. This also influences the environmental performance in terms of amine and potassium. Membrane permeation shows good performances with only 3% higher GWP than amine scrubbing. They also confirmed that environmental performance is mainly linked with the electricity consumption of the different technologies (LOMBARDI et al., 2020). Emissions are furthermore linked to the installation of post-combustion treatment which is required for amine scrubbing and recommended for membrane processes (FNR, 2012). It is linked with the CH_4 slip in the flue gas which has to remain below a threshold value according to the BImSchV. The energy consumption by the different technologies, applicable for the PtF system, the requirement for chemicals and the fine desulphurisation and required water are shown in Table 3.8.

Table 3.8: Energy demand, as well as required chemicals and processes for the chosen upgrading technologies.

	Pressure swing adsorption	Amine scrubbing	Membrane processes
Electricity demand (kWh/Nm³)[a]	0.20-0.25	0.06-0.15	0.18-0.33; 0.3-0.4 (BlueFEED)[b]
Heat demand (kWh/Nm³)[a]	-	0.5-0.8	-
Necessary flue gas treatment (EEG&GasNZV)[a]	Yes	No [c]	Yes
Required chemicals[a]	No	Yes	No
Necessary fine desulphurisation[a]	Yes	No	Recommended
Required water[a]	No	No	No

[a] FNR (2020b), [b] OESTER (2019), [c] COLLET et al. (2017).

3.4.3 *Life cycle assessments of Power-to-Fuel systems and methanol production*

There are various LCAs in the literature about synthetic fuel production (AHLGREN et al., 2015, DEUTZ et al., 2018, LEE et al., 2016, MOGHADDAM et al., 2015, MOGHADDAM et al., 2016). PÉREZ-FORTES et al. (2016) analysed the CO_2 emissions of a renewable methanol plant and compared them to those of a conventional methanol plant. They used H_2 and CO_2 without including their original source in the boundaries and found avoided CO_2 emissions for the renewable plant. Setting a similar boundary, OTTO (2015) concluded that CO_2-based methanol synthesis, as opposed to conventional production, leads to a net CO_2 reduction of between 747 and 918 g CO_2/kg_{MeOH}, depending on the operating parameters. Renewable methanol production from biomass that is not treated by AD has also been a subject of LCAs, such as from sugarcane bagasse as in RENÓ et al. (2011) or from CO_2 as a by-product from biomass fermentation of sugars into ethanol by MATZEN et al. (2016), but these pathways are not of further interest here.

MILLINGER et al. (2020) conclude in a WTW study that it is possible for several e-fuels including methanol to achieve significant improvements in GHG emissions replacing fossil fuels. They also consider using CO_2 from different biomass sources. The potential for GHG reductions by using surplus electricity for fuel generation,

such as methanol among others, is also investigated by UUSITALO et al. (2017). Here, CO_2 is taken from flue gases though neither specified further nor included in the model. The authors emphasise the large potentials for GHG mitigation as well. RIVAROLO et al. (2016) analysed the environmental impacts of methanol produced by a PtF system similar to the one investigated in this thesis, using AEL for H_2 production. However, they took electricity from the grid if renewable energy sources (RES) were not available. Their capacity with 100 kg/h methanol (553 kW_{LHV}) is also much higher than the one considered here. Furthermore, they state that if CO_2 was obtained from biogas upgrading, the cycles' impact is equal to zero. The reasoning behind it is that the CO_2 emitted by the fuel combustion has before been sequestered by the biomass entering the AD plant. In general, renewable electricity generated by windfarms or PV emits less pollutants and GHG emissions than fossil fuels (COLLET et al., 2017). Thus, it is preferable to utilise it for the generation of H_2. Emissions of e-fuels produced from the electricity mix would break even with fossil fuels in 2038, as only then will the electricity mix be clean enough (MILLINGER et al., 2020).

The idea of using excess renewable energy for H_2 production already exists, although for a different product route, producing additional CH_4 from CO_2 after biogas upgrading in a PtG approach (BIENERT et al., 2019). A similar product system is considered by COLLET et al. (2017) in an LCA comparison of direct methanation from biogas with biogas upgrading without methanation. CASTELLANI et al. (2018) also analysed the energy and carbon footprint of biosynthetic CH_4 production, combining renewable H_2 with CO_2 coming from an innovative biogas upgrading process. MILLINGER et al. (2020) consider using CO_2 from biogas upgrading for methanation. Nevertheless, alternative production of CH_4, such as methanation does not play a role in this study, as it exceeds its scope. The alternative utilisation options of biomethane in PtG applications or as a fuel are also not further investigated. This study focusses exclusively on CO_2 utilisation from biogas upgrading and its usage in a PtF system. Similar amounts of CO_2 as from biogas upgrading also arise from alcoholic (biomass) fermentation i.e. the production of bioethanol (DOTZAUER et al., 2018). The required carbon for methanol production could also be supplied by biomass gasification (LI et al., 2017). However, this study does not cover either of these. At least to the author's knowledge, there have been no other LCA studies about the PtF system investigated in this study.

3.5 Concluding remarks

An extensive literature search shows that there are no general methods for determining the costs of small-scale plants. This chapter describes the procedure for calculating the cost of production based on the method of TURTON et al. (2009, p. 193ff) and how it can be adapted using quotations from manufacturers. The LCA steps under the ISO standards are also described, as this study follows them closely. After introducing the fundamentals of TEA and LCA, this chapter focusses on relevant analyses in the literature. In general, it can be said that small-scale biogas upgrading is mostly not profitable, although there appears to be much research in the field and recent studies have found technologies that are more competitive. Studies about PtF systems, similar to the one investigated in this study, have found large-scale applications for methanol production to be competitive to other renewable production options, though not compared to conventional fuel production. From an environmental point of view, however, these applications appear to be more promising because saved CO_2 emissions as opposed to their conventional pathways were estimated. Furthermore, the limitations and assumptions in different inventories make it difficult to compare LCA studies about biogas systems. While almost all individual sub-processes are covered in environmental analyses, an analysis of an integrated system such as in this study is lacking. Although there are studies utilising CO_2 from flue gas, none have particularly considered the built-up of small-scale biogas upgrading of manure-based biogas in combination with methanol production.

Chapter 4
Methods

In this chapter, the methodology is presented, focussing on the system design and underlying model as well as the techno-economic analysis and the development of a cost estimation method for this. Furthermore, it introduces the methodology of the life cycle assessment.

4.1 System design and underlying model

This sub-chapter introduces the system elements and boundaries as well as the dedicated calculations. First, the system and the approach to the model are explained (section 4.1.1). Second, the calculation of the amount of available CO_2 is presented (section 4.1.2). Third, the amount of methanol can be determined with it, and the corresponding parameters for H_2 production can be adjusted (section 4.1.3). Section 4.1.4 shows the stepwise calculation approach for this case study based on the given data. Finally, data of the biogas plants as a pre-condition for the subsequent analyses is explained in more detail in section 4.1.5.

4.1.1 *System description and general modelling approach*

The PtF system under study is a site-specific integrated system as shown in Figure 4.1. It was specifically developed at the Research Centre 'Forschungszentrum Jülich' (North-Rhine Westphalia, Germany) in accordance with DECKER et al. (2018), although adjusted for smaller scales in this study. It includes the following components: a) a biogas production plant using anaerobic digestion (AD), corresponding to a small-manure plant; b) a CO_2 recovery unit, upgrading biogas to biomethane with a post-combustion unit for the flue gas; c) a CHP in which the biomethane is burnt; d) a wind turbine generator (WTG) and polymer electrolyte membrane (PEM) electrolyser for H_2 supply, including a liquid organic hydrogen carrier (LOHC) storage facility for buffering; and e) a methanol synthesis plant.

Figure 4.1: Detailed Power-to-Fuel system under study showing the combination of a biogas plant (a) with gas separation (b) and combined heat and power plant (CHP) (c) and a wind turbine and electrolyser with storage facility (d), as well as a methanol plant (e).

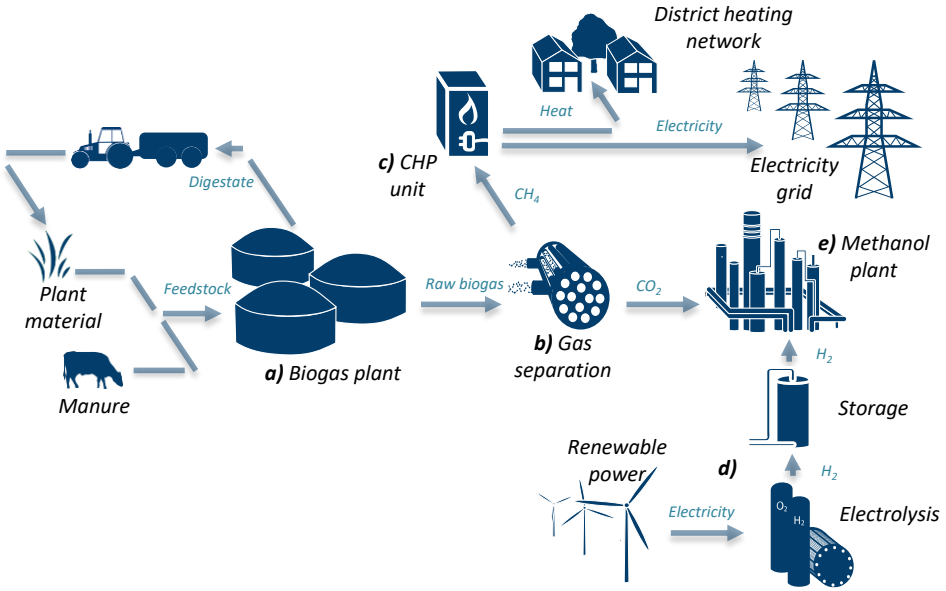

Caption: own creation.

The overall concept is decentralised, so that the five subsystems at the location of an BGP can be integrated. Most components of the system meet the technology readiness level (TRL) of 9 and are readily available to be used in an operational environment. However, methanol production is not yet available on such a small scale. The membrane upgrading technology is applied with data from OESTER et al. (2018), a Suisse manufacturer. They merchandise plants on a similar scale as here, although they are not used on a commercial scale by small-manure plants in Germany yet. The TRL of the PEM electrolyser is assumed to be 8 as defined by SABA et al. (2018). PEM systems can be purchased from several manufacturers, although their current market penetration is limited in Germany. The main processes within the system of the standard case are described below, while major technical characteristics and associated process parameters are included in Table 4.1:

a) The biogas plant (BGP) represents a classic small-manure plant (75 kW). Inside its fermenter, a mix of manure and straw residues obtained from livestock farming is converted through AD into raw biogas and digestate. Both types of feedstock are considered residues; hence, their respective upstream production processes up to

the PtF facility gate are not of interest. The manure is directly transported from the stable to the facility through an automatic manure scraper into the preliminary storage tank, which is located underground and covered with concrete. The manure is pre-stored for a short period until it is pumped into the fermenter. The digestate obtained as a co-product from AD is then openly stored onsite and re-used as a fertiliser.

Table 4.1: Main process parameters characterising the innovative Power-to-Fuel system for the standard case (case 1) and associated data sources.

Parameter	Value
Electricity CHP (kW)	75[a]
Heat CHP (kW)	98[a]
Engine output CHP (kW)	205[a]
Plant electricity demand (%)	8[a]
Plant heat demand (%)	35[a]
Volume flow of raw biogas (m³/h)	39.39[b]
Number of cows (providing manure for the 75 kW biogas plant)	126[c]
CH_4 losses during AD (%)	1.40[a]
Methane slip during PSA (%)	1.50[d]
Share of CO_2 gain from post-combustion (%)	1.83[b]
Electrolyser capacity (kW)	950[b]
Wind turbine capacity (kW)	1040[b]
FLH wind turbine	2000[b]
Capacity of methanol plant ($kW_{th,LHV}$)	138.38[b]
FLH methanol plant	8500[a]

[a] Rau (2019), [b] own calculation; approach shown in the remainder of this chapter, [c] calculated according to Rutzmoser et al. (2014), [d] Lohse (2019); WTG = wind turbine generator, PEM = Polymer electrolyte membrane, CHP = combined heat and power plant, LHV = Lower heating value.

b) An additional sub-system of gas separation is assumed that processes the biogas and provides CO_2, as it is required for the methanol synthesis in this concept. Due to the already existing application of the membrane process at small-manure plants and its comparatively small space requirement, which would be preferable, this separation process is assumed in the following. A flue gas stream with 98.25% of CO_2 and 1.75% CH_4 is considered, assuming that biomethane from upgrading has a purity of 95% (LOHSE, 2019). Flue gas treatment through recuperative post-

combustion could possibly be carried out to achieve a pure stream of CO_2. This process requires a minimum CH_4 of 0.3vol% in the flue gas which is provided in this case.

c) The concentrated CH_4, i.e. the biomethane, is subsequently burnt in the CHP unit. In industrial scale installations, the biomethane is injected into the gas grid in Germany. Nevertheless, feeding into the grid is not profitable for small-manure plants and there is not always a connection to the grid next to small-manure plants, which are often located in remote areas. This is why it was assumed that biomethane is used on site. Therefore, the biomethane is assumed to be used as a combustible in a CHP, which generates energy in the form of heat and electricity. According to SCHOLWIN et al. (2014, p. 12), every CHP can be fired with both NG and biogas from a technical point of view. This is an advantage for the system proposed, as it can be an expansion to already existing BGPs. The separated CO_2 presents itself as a basic material for the added methanol synthesis. The available CO_2 thus determines the capacity of the methanol plant.

d) A WTG is also implemented in the system to produce H_2 by means of a PEM electrolyser. Its mode of operation was already described in 2.3. The required power for the electrolysis is supplied it. Since the WTG does not supply electricity for the entire operating time of the methanol plant, an LHOC storage facility is considered. A tank provides a buffer facility whereby H_2 can be stored after production. The capacities for the electrolyser and the WTG must be selected in such a way that continuous operation of the methanol plant is guaranteed. It is estimated that the wind turbine has a capacity of around 1 MW, producing electricity for water separation with a 950 kW electrolyser. It is also assumed that the H_2 is produced in close proximity to the farm, hence no transport is involved.

e) Methanol is finally produced on a pilot scale in a plant with a nameplate capacity of 212 tonnes of methanol per year, assuming 8500 full load hours (FLH), corresponding to 138 $kW_{th,LHV}$. It should be noted that the methanol synthesis runs at 80 bar and 250°C.

The developed model describes the PtF system underlining the assumption for the LCA and the cost analysis. The results and assumption have an impact on the LCA calculations and on the cost analysis, since calculated values act as operating conditions for the process design model of the system. In general, the goal of the simplified model is to quantify the amount of methanol that can be produced with a certain amount of biogas under certain environmental and economic conditions.

As the amount of biogas is unknown in this specific case, and varies slightly depending on digestion conditions, the known capacity of the CHP and the measured percentage composition of the biogas are used for the calculation. The model is based on primary data from measurements and simulations of a biogas plant in the East of Germany, as well as secondary data from the Ecoinvent 3.5 database and the literature. The model setup assures full load drive of the CHP. Hence, if the capacity of the CHP is, e.g., 75 kW_{el}, the PtF system runs such that the full capacity is utilised. As there are losses of CH_4 through the biogas upgrading process, the initial CH_4 stream and ultimately the initial biogas stream have to be greater. This can easily be achieved by using more feedstock, as long as the fermenter capacity allows it. As exact amounts of produced biogas were unknown, a model was developed to estimate the relevant gas flow and materials, whereby constant temperatures were assumed for simplification that are typical for these kind of BGPs as the logbook of the mentioned BGP indicates.

4.1.2 *Available carbon dioxide*

First, the calculation of the available CO_2-volume for methanol production is presented. Figure 4.2 shows the relevant processes considered for this. The raw biogas from the fermenter is sent into the gas separation stage. Biogas upgrading technology divides the biogas into a CH_4-rich stream and a CO_2-rich stream. The first continues into the CHP unit (see Figure 4.2, V_I), while the second is treated by post-combustion in order to obtain pure CO_2 gas that can be used for methanol production (see Figure 4.2, V_{II}).

The volume of the biogas produced by the fermenter can be calculated as follows

$$\boldsymbol{V_{Biogas} = V_{Biogas,CH4} + V_{Biogas,CO2} + V_{Biogas,O2}}, \quad (4.1)$$

where $V_{Biogas,CH4}$ is the volume of CH_4, $V_{Biogas,CO2}$ the volume of CO_2 and $V_{Biogas,O2}$ the volume of O_2 in the biogas. For simplification, the O_2 volume is neglected at the stage of gas separation due to its insufficient quantity. Hence, the volume of biogas produced by the fermenter minus the O_2 is the same volume that enters the gas separation stage, which means

$$V_{Gas\ separation} = V_{Biogas,CH4} + V_{Biogas,CO2}. \quad (4.2)$$

Figure 4.2: Model showing the process steps to estimate the available CO_2 from biogas upgrading.

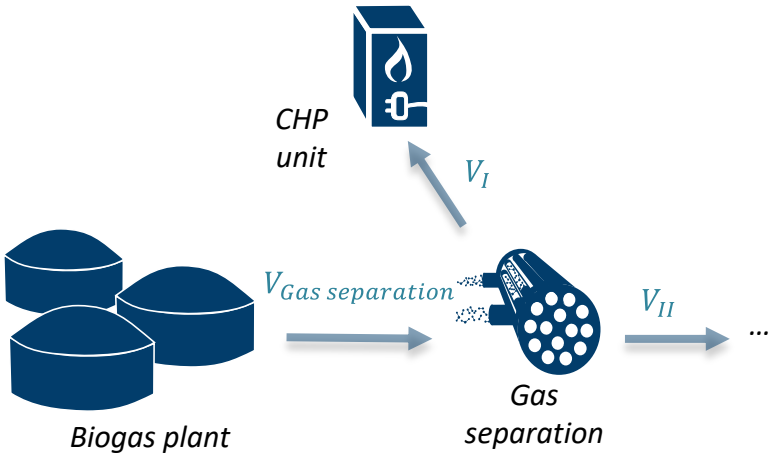

Caption: own creation; $V_{Gas\ separation}$ = volume flow of biogas that goes into the stage of gas separation; V_I = volume flow of biomethane; V_{II} = volume flow of flue gas, which provides the CO_2 utilised for methanol production.

The volume of $V_{Gas\ separation}$ is also described by

$$V_{Gas\ separation} = V_I + V_{II}. \tag{4.3}$$

The V_I, as in Figure 4.2, calculates the amount of the biomethane. It is a theoretical calculation of the used CH_4 volume, which is necessary to run the CHP at 100%. The volume of CH_4 available in the biomethane is equal to

$$\boldsymbol{V_{CHP,CH4} = \frac{P_{CHP}}{LHV_{CH4}} * p_{plant},} \tag{4.4}$$

with P_{CHP}, the engine output (Brennstoffleistung) of the CHP unit, LHV_{CH4}, the lower heating value of CH_4 of 9.97 kWh/m³ and p_{plant}, the utilised capacity of the CHP unit that can be adjusted if required. Assuming p_{plant} at 100% and P_{CHP} at 205 kW, a volume of 20.56 m³/h is calculated.

Usually, in biogas upgrading, the percentage of the biomethane is known as well as the CH_4 slip going into the flue gas. Depending on the technology, the CH_4 slip in the flue gas is variable. The percentage of CH_4 going into both streams determines

the composition of both product streams later on. The volume of CO_2 remaining in the biomethane can be described as

$$V_{CHP,CO2} = V_{CHP,CH4} * \frac{a_{CHP,CO2}}{a_{CHP,CH4}}, \quad (4.5)$$

where the variable $a_{CHP,CO2}$ describes the percentage of CO_2 and $a_{CHP,CH4}$ the percentage of CH_4 in the biomethane. As mentioned above, the percentage distributions can be determined according to the upgrading technology.

The V_{II} in Figure 4.2 refers to the calculation of the composition of the flue gas. The volume of CH_4 in the flue gas is equal to

$$V_{MeOH,CH4} = V_{Biogas,CH4} * a_{MeOH,CH4} \quad (4.6)$$

where $a_{MeOH,CH4}$ is the percentage CH_4 slip.

Knowing the volume of CO_2 that continues into the biomethane from equation 4.5, we can calculate the remaining CO_2 in the flue gas stream, which is

$$V_{MeOH,CO2} = V_{Biogas,CO2} - V_{CHP,CO2} \quad (4.7)$$

Now, taking equations 4.5, 4.6 and 4.7 into account, the entire volume entering the gas separation can be summarised as

$$V_{Gas\ separation} = V_I + V_{II} = (V_{CHP,CH4} + V_{CHP,CO2}) + (V_{MeOH,CH4} + V_{MeOH,CO2}). \quad (4.8)$$

For methanol production, biogas upgrading should produce flue gas which contains CO_2 that is as pure as possible. In order to achieve this, most technologies require post-combustion. If burnt with pure O_2, the process will avoid the intrusion of unwanted gases such as N through the ambient air. In this way, the CH_4 in the flue gas can be converted into CO_2 and the production of CO_2 can thus be increased. The total mass of CO_2 available after post-combustion is summarised as

$$m_{Total,CO2} = m_{MeOH,CO2} + m_{Post,CO2}\,, \tag{4.9}$$

where the first summand, using equation (4.7), is equal to

$$m_{MeOH,CO2} = V_{MeOH,CO2} * \delta_{CO2}. \tag{4.10}$$

The second summand, i.e. the CO_2 mass that is obtained through the conversion is equal to

$$m_{Post,CO2} = V_{MeOH,CH4} * \delta_{CO2} * \left(\frac{M_{CO2}}{M_{CH4}}\right), \tag{4.11}$$

where δ_{CO2} is the density of CO_2 and M_{CO2} and M_{CH4} are the molar masses of CO_2 and CH_4, respectively. Table 4.2 shows the relevant values.

Table 4.2: Relevant parameters for the calculation of the available CO_2 after post-combustion according to WIEGLEB (2016).

Parameter	Variable	Value	Unit
Density of CO_2	δ_{CO2}	1.98	kg/m³
Molar mass of CO_2	M_{CO2}	44.01	g/mol
Molar mass of CH_4	M_{CH4}	16.04	g/mol

4.1.3 *Methanol and hydrogen production*

Once the amount of CO_2 obtained from the biogas plant is known, we can calculate the amount of methanol to be produced. Figure 4.3 summarises the steps that calculate the corresponding amounts of H_2 and methanol. For the production of methanol, CO_2 and H_2 are brought into a chemical reaction. The methanol process considered in this study, as described by OTTO (2015), occurs inside an autothermal reactor at 250°C and 80 bar. It directly transforms CO_2 and H_2, requiring 1.37 kg CO_2 and 0.19 kg H_2 for the production of 1 kg of methanol. The equation parameters are summarised as

$$CO_2 + 3H_2 \rightleftharpoons CH_3OH + H_2O, \tag{4.12}$$

Beside methanol, 0.56 kg of water arise by the reaction.

In this model, all parameters are adjusted to the CO_2 that occurs in the flue gas of the biogas plant. This means that the electrolyser and WTG are also adjusted to the CO_2 potential. The total amount of CO_2 is equal to the amount of CO_2 in the flue gas from equation 4.10 and the converted CH_4 from equation 4.11, which is equal to

$$m_{Total,CO2} = m_{MeOH,CO2} + m_{Post,CO2} \quad (4.13)$$

Using $m_{Total,CO2}$, the total amount of methanol, is then

$$m_{Total,MeOH} = \frac{m_{Total,CO2}}{1.37}. \quad (4.14)$$

After the full production is calculated, the amount of H_2 required for methanol production is calculated as

$$m_{H2} = m_{Total,MeOH} * 0.19. \quad (4.15)$$

Figure 4.3: Calculation steps relevant for methanol production and hydrogen production.

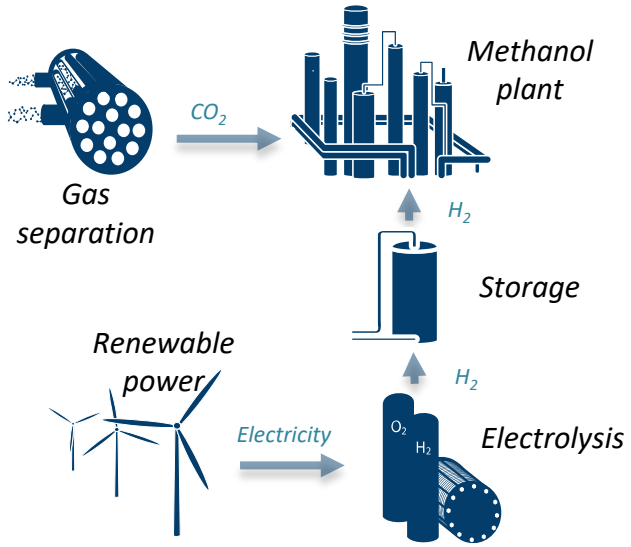

Caption: own creation.

The capacity of the electrolyser is calculated as follows,

$$P_{Electrolyser} = \frac{m_{annual,H2} * LHV_{H2}}{FLH * \eta} \quad (4.16)$$

Where $m_{annual,H2}$ is the required annual amount of H_2 and LHV_{H2} the lower heating value of H_2, i.e. 120 MJ/kg. The efficiency of the electrolyser η is assumed at 0.7 (BUTTLER et al., 2018). The FLH indicate the full load hours of the electrolyser, whereby a value of 2000 h/a is assumed here for good wind locations (DECKER et al., 2019). This value is derived from the FLH of the WTG, since the electrolyser can only be operated if there is power available. Subsequently, the calculated capacity of the electrolyser is then used to determine the capacity of the WTG. For this purpose, an additional 10% is added to the required capacity of the electrolyser. This factor considers the electricity losses, the technical availability and a safety margin. With 2000 FLH of the WTG and the required amount of H_2 of 4.67 kg/h, obtained from equation 4.15, the capacities of the electrolyser and the WTG can be determined. This results in a required capacity of the electrolyser of 950 kW and the WTG of 1040 kW.

4.1.4 *Model calculation considering the given data*

Since the amount of biogas is not known from measurements, the calculation has to be carried out, starting from the calculation of required CH_4 that needs to be produced for the CHP unit in order to guarantee its full-load drive, considering CH_4 slip through the upgrading process. The calculations start with the given parameters in Table 4.3. Note that the composition of biogas was measured at two different plants, i.e. small (75 kW) and large (500 kW). More detail about them is given in the next section. The CH_4 volume going into the biomethane is firstly calculated using equation 4.4. After that, the CH_4 losses through upgrading are added in order to determine the initial CH_4 production by the fermenter. Subsequently, this value can be used to calculate the CO_2 streams at each process step (biogas production, upgrading, after post-combustion) and, finally, show how much CO_2 is available for the methanol production. The workload of the CHP unit can be varied in the model. If the workload is lower, it means that less CH_4 enters the CHP and less biogas is produced. In reality, however, the fermenter produces biogas independently from the CHP unit. The calculation of the CH_4 and CO_2 streams and the calculation of the digestate with the adjusted feedstock are presented in the following.

Table 4.3: Relevant parameters for the two plant sizes for which data is available from RAU (2019).

Parameter	Variable	Value		Unit
		75 kW plant	500 kW plant	
Engine output	P_{CHP}	205[a]	1317.5[b]	kW
CH_4 in biogas[c]	a_{CH4}	53	59	%
CO_2 in biogas[c]	a_{CO2}	46	40.4	%
O_2 in biogas[c]	a_{O2}	1	0.6	%

[a] Manufacturer information, [b] own calculations, [c] own measurements at biogas plant in Rechenberg-Bienenmühle on Nov 8th 2018; CHP = Combined-heat and power unit.

Calculation of the methane and carbon dioxide streams

The amount of CH_4 that goes into the flue gas together with the CH_4 in the biomethane make up the total volume of CH_4 in the biogas (see Figure 4.2), which can be calculated as

$$V_{Biogas,CH4} = V_{CHP,CH4} + V_{MeOH,CH4} \quad (4.17)$$

The volume of CH_4 slipping into the flue gas stream, $V_{MeOH,CH4}$, is equal to the percentage CH_4 slip ($a_{MeOH,CH4}$) multiplied by the volume of CH_4 in biogas. Note that we cannot calculate the volume of CH_4 in biogas by using equation 4.6, as we do not know the total amount of biogas. However, we can use the volume of CH_4 at the CHP unit (calculated using equation 4.4), dividing it by the consequential share of CH_4 entering the CHP unit ($a_{CHP,input,CH4}$) and multiplying it by the CH_4 slip $a_{MeOH,CH4}$. This determines the volume of CH_4 in biogas and rewrites equation 4.17 as

$$V_{Biogas,CH4} = V_{CHP,CH4} * \left(1 + \frac{a_{MeOH,CH4}}{a_{CHP,input,CH4}}\right). \quad (4.18)$$

For modelling the upgrading process, a composition of the biomethane is chosen with 95% of CH_4 and 5% of CO_2. Most technologies achieve higher purities, but the share appeared to be reasonable as a conventional assumption according to LOHSE (2019). The composition can, however, be adjusted in the model. The

assumption for the CH_4 slip was 1.5%, although it is also adjustable. Utilised parameters are summarised in Table 4.4. In general, it can be said that if the share of CH_4 in the biomethane is increased, i.e. the CH_4 slip decreased, it would leave more CO_2 available for methanol production and ultimately increase production. 1% more CO_2 means a 1.3% increase in methanol. As the provision of CO_2 is also linked to the biogas plant and its share in biogas is known, it can be calculated taking the volume of CH_4 in the biogas from equation 4.18 and inserting it into

$$V_{Biogas,CO2} = V_{Biogas,CH4} * \frac{a_{Biogas,CO2}}{a_{Biogas,CH4}} \quad (4.19)$$

In this equation, $a_{Biogas,CO2}$ and $a_{Biogas,CH4}$ are the shares of CO_2 and CH_4 in biogas, respectively.

Table 4.4: Utilised parameters for the biogas and biogas upgrading from the literature and own assumptions.

Parameter	Variable	Value	Unit
Lower heating value CH_4	LHV_{CH4}	9.97[a]	kWh/m³
Share of CH_4 in biomethane	$a_{CHP,CH4}$	95[b]	%
Share of CO_2 in biomethane	$a_{CHP,CO2}$	5[b]	%
CH_4 slip	$a_{MeOH,CH4}$	1.5[b]	%
Share of CH_4 entering the CHP unit	$a_{CHP,input,CH4}$	98.5 [b]	%

[a] WIEGLEB (2016), [b] own assumptions based on the literature.

The percentage composition of the flue gas is equal to the share of CO_2, calculated as

$$a_{Flue\ gas,CO2} = \frac{V_{MeOH,CO2}}{V_{MeOH}}, \quad (4.20)$$

where V_{MeOH} is the total volume of the flue gas, as

$$V_{MeOH} = V_{MeOH,CO2} + V_{MeOH,CH4}, \quad (4.21)$$

and the share of CH_4 calculated as

$$a_{Flue\ gas,CH4} = \frac{V_{MeOH,CH4}}{V_{MeOH}}. \quad (4.22)$$

Adjustment of feedstock and calculation of the digestate

The biogas stream and its composition are calculated, knowing the capacity of the CHP. This means that the calculated stream corresponds to the CHP's full-load drive. If we assume a CH_4 slip of 1.5% from the remaining gas that goes into the flue gas, we should note that the biogas stream must initially be larger than what was calculated. It would be necessary to produce 1.5% more biogas to further guarantee the full-load drive of the CHP. This requires an increase in feedstock of 1.5%. However, such a small increase is insignificant and compensated for by the daily fluctuations and is not pursued further. As biogas production is variable due to external conditions, such as weather events, it is also normal that fluctuations in biogas yield occur. Therefore, the system can be easily attached to any BGP without any changes.

The adjusted biogas production to meet the model conditions is given in equation (4.1), where $V_{Biogas,CH4}$ and $V_{Biogas,CO2}$ are known from equations 4.18 and 4.19 and $V_{Biogas,O2}$ is equal to

$$V_{O2,base} = V_{Biogas,CH4} * \frac{a_{O2}}{a_{CH4}}, \quad (4.23)$$

so that the total biogas production, when adjusted, is equal to

$$V_{Biogas} = \left(V_{CHP,CH4} * \left(1 + \frac{a_{MeOH,CH4}}{a_{CHP,CH4}}\right)\right) * \left(1 + \frac{a_{CO2}}{a_{CH4}} + \frac{a_{O2}}{a_{CH4}}\right). \quad (4.24)$$

The digestate output can be calculated via the mass balance, knowing how much input is fed into the plant and how much biogas is produced from the AD process (STINNER, 2018). The produced biogas is subtracted from the total digestate input to calculate the mass of digestate as

$$m_{digestate} = m_{feedstock} - m_{biogas}. \quad (4.25)$$

4.1.5 *Biogas plant data*

Primary data, taken from a biogas plant in eastern Germany, was compiled from a personal communication at the TU Bergakademie Freiberg (RAU, 2019). General data about both plants can also be found online (SÄCHSISCHES NETZWERK BIOMASSE E.V., 2020a, SÄCHSISCHES NETZWERK BIOMASSE E.V., 2020b). However, the nominal capacity of the large plant is 500 kW instead of 700 kW (RAU, 2019). The adjacent dairy cow farm with 1400 animals has its own feed production in the form of grain from wheat cultivation. Liquid manure and feed residues as well as straw residues from dairy cow farming on-site provide feedstock for a large plant with two CHPs (344 kW and 180 kW) connected with two fermenters, a second-step digester with recirculation of the digestate and two biogas storages to be prepared for upcoming operation modes like partial load or the deactivation of the CHPs. A small-manure plant with a CHP of 75 kW and one fermenter uses almost 90% of dairy cow manure and 10% of straw residues, coming from the same farm, as feedstock. The fermenter and CHP unit of the small-manure plant are located approximately two kilometres away from the farm. The feedstock is frequently transported there. However, this was not considered in this work, assuming close proximity of the sites. The workload of the 75 kW-CHP unit is assumed at 100% in this study, as the CHP engines are able to compensate down times. The plant runs with a total engine output of 205 kW. It has a gas Otto engine by MAN that was installed in 2013 and an electrical efficiency of 36.6%. The electricity demand makes up 8% and the heat demand 35% of the own production. Heat is used for the local heating network, heating two residential buildings with a total of nine apartments. Relevant plant data is summarised in Table 4.5.

Using two different CHPs, one with 180 kW by Schnell and one with 344 kW by MTU, the large plant actually has a total capacity of 524 kW. It runs nominally at 500 kW, so we adjusted the utilised capacity in equation 4.4 to 95.4%. The MTU CHP's thermal energy provision is 396 kWh_{th} (RAU, 2019), but for the 180 kW CHP unit, the energy efficiency as well as the thermal capacity was not communicated and taken from ZÄH (2006). According to the thermal energy efficiency of 45%, the capacity is equal to 192.9 kW_{th}. Heat is, on the one hand, released to the ambient air, especially in the summer, and, on the other hand, it is used for work on the farm such as the drying of wood and grain, the milking carousel or the laundry. The large plant uses dairy cow manure (81.8%) and plant material (approximately 18%). Aside from that, the fermenter is fed with enzymes

Table 4.5: Data of the small-manure plant (75 kW) as provided by RAU (2019).

Parameter	Value	Unit
Electrical capacity of CHP	75	kW_{el}
Thermal capacity of CHP	98	kW_{th}
Engine output CHP	205	kW
Full load hours	8500-8600	h
Electrical efficiency	36.6	%
Engine type and year of installation	Gas Otto engine by MAN, 2013	-
Plant electricity demand	8 | 6	% | kW_{el}
Plant heat demand	35 | 34.3	% | kW_{th}

CHP = combined heat and power plant.

and iron (II) chloride for desulphurisation. The plant uses about 11.2% silo (grass and triticale) and 6.7% of plant residues from feed processing. The latter contains wheat residues, namely husk (the leafy outer covering of a grain – (Spelz)), stalks and other residues of the plant. It also contains beet pulp/slices that are feed residues. Apart from that, an additional amount of 3900 kg/h of the digestate is recirculated. The detailed composition of feedstock input can be found in Table A 1 in appendix A. Measurements for the digestate composition only exist for the larger plant, but are comparable for the small-manure plant, as manure from the same stable enters the fermenter. The detailed composition of digestate can be found in Table A 2 in appendix A**.** The injection of all fermenters also for the small-manure plant occurs continuously with a retention time of 150 days which is restricted by law (EC, 2018). Emissions for the CHP plants with 344 kW and 75 kW were measured in Clausnitz and Rechenberg-Bienenmühle in November of 2018. All technical data of the entire system can be found in Table 4.6. While the small-manure plant still stores the digestate in four open tanks, the large plant has a gas-tight storage facility.

Table 4.6: CHP-related data of the large biogas plant (500 kW).

	Dual-fuel engine (Zündstrahlmotor)	Gas Otto engine	Unit
Electrical capacity of CHP	180	344	kW_{el}
Thermal capacity of CHP	396	192.9	kW_{th}
Engine output CHP*	428.6	888.9	kW
Electrical efficiency	38.7	42	%
Heat efficiency	44.5	45	%
Year of installation	2004	2008	-
Manufacturer	Schnell (Scania)	MTU	-
Used capacity of CHP	95.4		%
Full load hours	8500-8600		h
Plant electricity demand	8 | 40		% | kW_{el}
Plant heat demand	50 | 294.4		% | kW_{th}

*together 1317.5 kW; CHP = combined heat and power plant.

From measurements at the plants, the biogas composition is known and the calculated mass flows are shown in Table 4.7. The small-manure plant has a biogas stream of approximately 40 m³/h and a CH_4 content of 53vol-%. With a CO_2-share in biogas of 46vol-%, it provides a mass flow of 34.29 kg/h of CO_2 after the gas separation stage and post-combustion. All CHP engines are assumed to run at 8500 full load hours (FLH). There is air induced into the fermenter to capture some of the hydrogen sulphide (H_2S) and H_2S was measured up to 200 ppm in raw biogas at the small-manure plant. The large plant also uses activated carbon for fine desulphurisation, as slightly higher H_2S values were measured. After this, the gas contains only 0-5 ppm. For reasons of simplification, small components of biogas were neglected in the calculations, such as H_2, H_2O and other trace gases. Yet, it should be pointed out that they must be removed due to corrosion of the equipment. Biogas upgrading usually removes most unwanted components during pre-stages of desulphurisation and drying.

Finally, when calculating the annual or hourly CH_4 emissions from manure per animal, it is necessary to know the number of animals on the farm. The numbers can be found in Table 4.8. In general, young heifers up to 27 months produce less than half of the amount of manure compared to a fully grown dairy cow. Suckler cows also produce 20-25% less manure than dairy cows. Due to this, the heifers were calculated as half a fully-grown cow, thus 200 heifers are equivalent to 100

Table 4.7: Composition and amount of biogas.

	75 kW plant		500 kW plant	
	Share (Vol-%)	Mass flow (kg/h)	Share (Vol-%)	Mass flow (kg/h)
CH_4	53[a]	14.76[b]	59[a]	94.88[b]
CO_2	46 [a]	35.28[b]	40.4[a]	178.89[b]
O_2	1[a]	0.55[b]	0.6[a]	1.92[b]
Biogas	100	50.6	100	275.7

[a] own measurements at biogas plant in Rechenberg-Bienenmühle on Nov 8th 2018, [b] own calculations.

dairy cows or cows. Heifers from suckler cow husbandry are negligible due to them being kept outside year-round. Suckler cows are calculated as half a cow as well because of their seasonal grazing (RUTZMOSER et al., 2014). As mentioned above, the entire farm has three CHP engines of 75 kW, 180 kW and 344 kW. We calculated the share of animals relating to each CHP. The results are presented in Table 4.9. The 75 kW CHP obtains manure from 126 animals.

Table 4.8: Dairy cow numbers and their breed at the farm in Clausnitz.

	Number of animals[a]	Dairy cow equivalents[b]
Dairy farming		
Dairy cows [1]	680	680
Heifers up to 1 year [2]	200	100
Heifers 1 to 2 years [1]	200	100
Suckler cow husbandry		
Suckler cows [3]	260	130
Heifers up to 1 year [3]	30	-
Heifers 1 to 2 years [3]	30	-
Total	1400	1000

[a] RAU (2019), [b]own calculations; [1] kept on slatted floor; [2] kept on straw; [3] manure is used from all animals but suckler cows and their heifers due to them being in the fields six month of the year, meaning there are only 180 days of manure accumulation inside.

Table 4.9: Dairy cow numbers and their CH_4 emissions from manure storage relating to the capacity of the CHP units supplied at the farm in Clausnitz based on own calculations.

Capacity (kW)	Number of animals	CH_4 emissions from manure storage (kg/h)
75	125.2	0.34
180	300.5	0.83
344	574.3	1.57

4.2 Techno-economic analysis

This study carries out a techno-economic analysis aimed at the methanol synthesis, which has not been analysed on such a small scale before. The previously calculated parameters that are relevant for the cost estimation of the standard case can be taken from Table 4.1. The cost analysis aims at the standard case (75 kW) as well as three other cases, referring to different methanol plants adapted to BGP sizes. This sub-chapter describes the applied method in detail.

4.2.1 *Process simulation with Aspen*

From the plant concept described above (Figure 4.1), the methanol synthesis (e)) is simulated in the process simulation software Aspen Plus (Version V 10) (ASPEN TECHNOLOGY, 2017). On a graphical interface, the user can display their process model and simulate it, whereby a model library and several libraries for material values are available. In this section, a description of the process structure as well as the performed modelling is given, which forms the basis for the subsequent cost analysis. The structure of the methanol synthesis process, which is shown in Figure 4.4, is based on a process developed by SCHEMME (2020). This process has been developed for plants with a capacity of 300 MW. In this thesis, the methanol synthesis has a capacity of only 138.38 kW, therefore the given process has to be adapted to the new conditions of such a small plant.

First, some general assumptions for the simulation must be made. The process simulation is performed in Aspen Plus as a static simulation, as this is sufficient to obtain the desired information for cost accounting. In order to calculate the different components, suitable thermodynamic models must be selected and implemented, which have already been developed in Aspen Plus. For components with a pressure below 10 bar, the NRTL model (Non-Random-Two-Liquid) (RENON et al., 1968) and for higher pressures the SR-POLAR model (Schwarzentruber and Renon equation of state) (SCHWARTZENTRUBER et al., 1989) are used.

Figure 4.4: Process flow chart of the simulated methanol synthesis process with educt and product flows for the standard case.

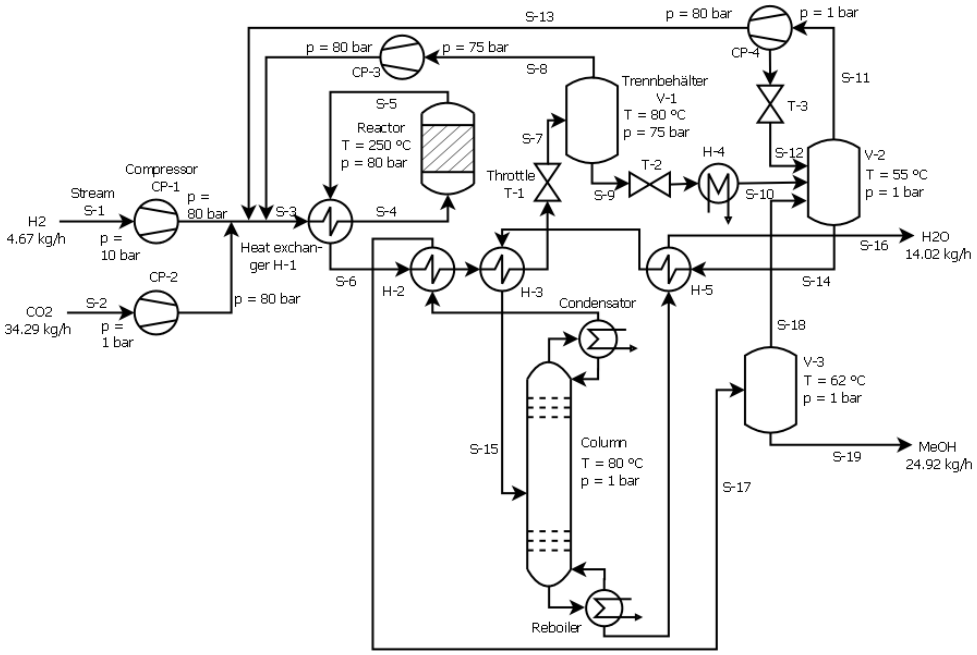

Caption: own presentation based on SCHEMME (2020).

With these general assumptions, the template can be adapted to the conditions of the small plant. For this purpose, the process is rebuilt in Aspen Plus with the help of the template. As reactants, H_2 and CO_2 are fed into the process, whereby the mass flow of CO_2 is 34.29 kg/h in the standard case. Besides this, assumptions for the inlet pressure and the inlet temperature have to be made. Here, it is assumed that the CO_2 has ambient pressure and a temperature of 25°C. The required mass flow of H_2 is determined by the desired molar ratio of H_2 to CO_2 before the reactor. A ratio of 4:1 is chosen, which leads to a required H_2 mass flow of 4.67 kg/h. An inlet temperature of 25°C by the H_2 is assumed, while the pressure is assumed to be 10 bar, as it corresponds to the outlet pressure of the PEM electrolyser used. Thus, the inlet conditions differ from those of Schemme (SCHEMME, 2020). Schemme assumes that both reactants are supplied via a pipeline at a pressure of 30 bar. These assumptions do not apply to the plant simulated in this study, since both reactants are produced on site. The lower inlet pressures cause differences to Schemme's template for the two compressors (CP) of the inlet flows, which are designated CP-1 and CP-2 in Figure 4.4. In both processes, the educts are compressed to a pressure of 80 bar, which is optimal for the reaction. These

differences in the compression ratio must be taken into account when selecting the compressors later. For the process simulation, multi-stage radial compressors with intercooling are assumed and adjusted so that the pressure ratio per stage is below three, which is an appropriate value according to WOODS (2007, p. 46). The adjustments incorporate intercooling at the outlet of the compressors after each stage so that temperatures are not too high for the material. After compression, the two inlet flows are mixed with each other and two return flows. They are heated to a temperature of 230°C via the process heat exchanger H-1. This sets the desired inlet conditions for pressure, temperature and molar ratio of H_2 to CO_2 for the reactor. The RGibbs model (CHAVES et al., 2016, p. 201), which is implemented in Aspen Plus, is used to simulate the reactor. It allows a simple calculation of the reactor without considering the kinetics. This is done because the kinetics play a subordinate role in the reactions for methanol synthesis (WOODS, 2007, p. 195) and the effort for integration is considered too high in relation to the benefit. Aspen Plus also specifies that the reaction temperature should be maintained at 250°C and the remaining heat generated by the exothermic reactions is purged. The heat is reused in the reboiler of the column during a later stage of the process. However, this reuse is not simulated in Aspen Plus for simplification.

The reactor produces the desired product methanol (CH_3OH) and H_2O as a by-product. In addition, parts of the reactants H_2 and CO_2 as well as CO also escape, as the reactions are equilibrium reactions. Therefore, further process steps are necessary to obtain methanol that is as pure as possible at the end of the process. The aim is to first separate the unreacted educts from the methanol-water mixture in order to feed them back into the reactor. For this purpose, it is necessary to cool the mixture so that only the educts are gaseous and the methanol-water mixture remains in liquid form. Then a separation by means of a separation vessel (V) is possible. The mixture of gaseous educts is fed back to the process heat exchanger H-1. Here, the product mixture is cooled down for the first time and the educt mixture is heated up at the same time. The two flows are not mixed, but the heat is transferred indirectly via the walls of the heat exchanger. In order to reach the desired temperature for separation of liquid and gaseous components in the separation vessel V-1, the mixture is further cooled by means of two further heat exchangers H-2 and H-3 until it reaches the desired separation temperature of 80°C.

The throttle T-1 expands the mixture to 75 bar. Subsequently, it is fed into the first separation tank, where most of the methanol and H_2O exist in liquid form. In the vertical separation tank, the gaseous components CO_2, H_2 and CO rise as gases and are discharged at the top of the tank. As the stream S-8 contains a large proportion of unreacted components, it is recompressed to 80 bar in the compressor CP-3 and

mixed with the reactant streams heading back to the reactor. At the bottom of the tank, the liquid mixture leaves the vessel as flow S-9. To further separate reactants from it, the mixture is expanded to ambient pressure and cooled down to 55°C via an air heat exchanger. The cooling occurs with the help of ambient air. The mixture is fed into a second separation tank V-2, in which the gaseous components are again extracted at the top. These are compressed back to reactor pressure in the multi-stage compressor CP-4. By suitable cooling, the resulting condensate, which is rich in methanol, can be branched off after each stage. The entire condensate is expanded to ambient pressure by means of throttle T-3 and fed back to vessel V-2. The remaining flow from CP-4, which is named S-13, is mixed with the educts and fed back into the reactor. The mixture, which leaves tank V-2 at the bottom, now consists almost exclusively of methanol and H_2O. It only contains a residual amount of CO_2. A distillation column is used to separate the water-methanol mixture. Before the mixture is fed into the column, it is heated to the desired distillation temperature of 80°C via the two heat exchangers H-5 and H-3. The column (K) is first calculated in Aspen Plus using the DSTWU model implemented there (CHAVES et al., 2016, p. 244), and then it is replaced by a RadFrac column (CHAVES et al., 2016, p. 249) for a more precise configuration. The column consists of the actual vessel in which the separation takes place with the aid of filling materials, a condenser (COND) at the top of the column and a reboiler (REB) at the bottom. The condenser serves to condense a part of the mixture and feed it back into the column so that the liquid passes through the column again. The condenser is cooled with cooling water. In the reboiler, on the other hand, part of the mixture is boiled up and fed back into the column in gaseous form so that it rises and also passes through the column again. Steam generated in the reactor heats the reboiler, though not depicted in the template. High purities can be achieved by letting the mixtures pass through the column multiple times. The methanol and CO_2 residues leave the column at the top and the water exits at the bottom. The water still has a high temperature, which is transferred to heat exchanger H-5. The methanol leaving the column at the head is first led to heat exchanger H-2, where it is heated up again. After heating, the distillate is transferred to a third separation vessel V-3 to separate the remaining CO_2. The CO_2 is then returned to container V-2 in order to be fed back into the reactor after compression via compressor CP-4.

The methanol leaves container V-3 at the bottom and can either be used directly or processed into other products. The aim is to ensure that the methanol produced has a purity of at least 99.85%, which is the lower limit according to IMPCA (International Methanol Producers & Consumers Association) (IMPCA, 2015). For this purpose, the column is adjusted by testing so that the desired purity is achieved

and, at the same time, the amount of heat required in the reboiler is lower than the amount of heat generated in the reactor. This ensures that the overall process requires no external heat. All heat sinks can be covered, using the five heat exchangers and the waste heat from the reactor. The utilities required for the process are cooling water for the condenser, cooling air for heat exchanger H-4, steam for the reactor and the reboiler and electricity to drive the compressors. In addition to the raw material flows, these utility flows must be considered in cost accounting.

4.2.2 *Development of a cost estimation method*

After the process modelling is completed, the cost estimation can be carried out. A goal of this is to determine the costs of manufacturing (COM) and the specific costs of manufacturing (COM_{kg} and $COM_{L,GE}$). The specific costs of manufacturing are suitable to compare the costs of the developed process with other processes. For the computation of the COM, the capital costs as well as the operating cost must be determined. For the calculation of the capital costs, the modules must be designed at first. With the help of the units' sizes, the component prices are then determined by means of quotations. Subsequently, the resulting calculation of the capital costs is presented. Finally, the last section deals with the operating costs.

Module design

During the phase of the component or module design of the methanol synthesis process, the main modules are dimensioned from the process simulation. They comprise four compressors, seven heat exchangers, including condenser and reboiler of the column, one reactor, three separation vessels and the column itself.

The required capacity is relevant for the compressors. This can be taken from the results of the process simulation performed in Aspen Plus, and, therefore, no further calculation is necessary. For the reactor, the decisive parameter is the volume. The reactor volume is calculated according to the procedure of Otto (OTTO, 2015). Equation 3.3, 3.4 and 3.5 are used for this. The values required for the calculation, namely the temperatures at the inlet and outlet, the heat flow, the mass flow and the density can be taken from the results of the simulation. For the space velocity, a conservative value of 6000 /h is assumed from the literature (CHOI et al., 2018, HIRANO et al., 1995). The value of 1700 W/m²K from Table 3.1 is used for the heat transfer coefficient, which is the upper value for a shell-and-tube evaporator, since the reactor is cooled by steam (KIND et al., 2013, p. Cc 1) [45, p. Cc 1]. An

outer diameter of 1.9 cm is assumed for the tubes, which is a typical value for seamless tubes that are installed in shell-and-tube heat exchangers (PETERS et al., 2003, p. 703).

The heat exchangers are assumed to be shell-and-tube heat exchangers. For these, Aspen Plus displays a heat transfer surface, which is their most important characteristic. For verification purposes, the areas are also calculated using equation 3.1. This requires the inlet and outlet temperatures of the two media and the heat flow from Aspen Plus. In addition, the respective heat transfer coefficients depending on the transfer conditions must be known. The values used for the seven heat exchangers can be found in Table 4.10. The calculated heat transfer surfaces are compared with those from Aspen Plus and the larger value is used to achieve a higher safety of the calculated area.

Equation 3.6 is used to calculate the volumes of the separation tanks, for which the liquid mass flow and the liquid density at the bottom of the respective tank are needed. This can again be taken from the simulation. Furthermore, an assumption for the retention time has to be made. According to BIEGLER et al. (1997, p. 112) a common retention time is five minutes.

Table 4.10: Heat transfer coefficient used for the shell-and-tube heat exchangers according to KIND et al. (2013, p. Cc 1).

Module	Utilised k-value (W/m²K)
H-1	35
H-2	70
H-3	70
H-4	70
H-5	1200
COND	1200
REB	1700

The column consists of a vessel as well as a condenser and a reboiler. In Aspen Plus, the vessel has a large height on a small diameter, which is technically not possible. Therefore, it is simply requested with the process conditions of the inlet and outlet flows without any size specification regarding volume, height or diameter. Condenser and reboiler are assumed to be shell-and-tube heat exchangers. Their calculation has already been described for the heat exchangers.

Manufacturer enquiries

The calculated component sizes help to determine the component costs and, thus, subsequently, the investment costs of the entire plant. As the plant under consideration is a small-scale plant, the standard methods for determining the module costs, such as the surcharge factor method by TURTON et al. (2009, p. 197ff), cannot be applied. They are adapted to certain capacity ranges of the components that are higher than the capacities used here. The components of this plant are much smaller than the lower capacity limit, which is why the use of Turton's method would lead to an overestimation of costs. Thus far, no cost accounting methods for such small methanol plants can be found in the literature. Hence, the costs of the main components are determined by means of manufacturer enquiries. For this purpose, different data is needed. In addition to the manufacturing materials, various operating parameters, such as the operating pressure and temperature, the composition of the mixtures and the mass or volume flows are required. Moreover, some parts require their previously determined size parameters from the simulation.

For the compressors, the enquiries include the existing volume flows, the inlet and outlet pressures, the inlet temperatures, the capacity as well as the existing fluid. The enquiries for the compressors CP-3 and CP-4 additionally include the composition of the volume flows. Concerning the reactor, the desired design is a vertically installed shell-and-tube reactor with cooling by means of steam. The enquiry also contains the reaction at hand, as well as the calculated volume, the mass flow, the temperature and the pressure. Stainless steel is specified as material. The heat exchangers are requested as shell-and-tube heat exchangers. The calculated heat transfer surfaces are not given, because the manufacturers calculate these themselves. For this, they need different specifications for the fluids in the tubes and in the shell space. These include composition, density, viscosity, specific heat capacity and thermal conductivity. In addition, the inlet and outlet temperatures, the mass flows, the pressure, the material and the heat output are given. For the vessels, the calculated volume, pressure, mixture and the desired material are required. The enquiry for the column needs only the inlet temperature, the inlet mass flow, the composition at the inlet as well as the desired purities of methanol and water.

In order to get offers from manufacturers, the procedure is the following. First, a search for suitable manufacturers for the different components is undertaken. Since the plant size is in a range between laboratory and industrial scale, many manufacturers are already eliminated. The manufacturers, who offer one or more

of the components in the desired size, are contacted with the information described above. The texts used for the different components can be found in German in appendix B. The search for manufacturers regarding the compressors shows that they are not available as radial compressors, as these come either with higher volume flows or lower pressures. Therefore, diaphragm and piston compressors are requested instead, which can operate in the ranges required for the small plant. The disadvantages compared to the radial compressors are a higher space requirement and high weight.

Investment costs and annual capital costs

The component prices of the manufacturers must be converted for the determination of the investment costs so that they can be used in equation 3.11 for the total module costs C_{TM}. This is because the manufacturers' quotations are normally ex-factory. It must also be noted that the cost calculation is carried out for the year 2019, but the offer prices correspond to the costs at the time of the enquiry, which is between June and August 2020. Therefore, the received prices are converted from 2020 to 2019 using the CEPCI. This is done with equation 3.14, where the received module prices are used for $C^0_{BM,ref}$. The most recent CEPCI is available for March 2020 with a value of 586.2 and is used for the $CEPCI_{ref}$. The $CEPCI_{act}$ for the year 2019 has a value of 607.5 (ECONOMIC INDICATORS, 2019). These costs will then be subject to transport costs. PETERS et al. (2003, p. 244) give a general factor for transport costs of 10% on the purchase price. However, this factor clearly overestimates the delivery allowance of the small plant. One manufacturer states transport costs that correspond to a value of 1%, which is why this value is used instead of the general factor. On top of the freight, the direct and indirect component cost factors have to be added. Since TURTON et al. (2009, p. 201ff) applies the bare module costs C^0_{BM}, the factors B_1 and B_2, which are listed in Table 3.5, cannot be used. This is because B_1 and B_2, together with the pressure and material factor, deal with the bare module costs, which are not available. The costs of the manufacturers already take into account the material and the system pressure, which is not the case for C^0_{BM}. PETERS et al. (2003, p. 244ff) list the direct and indirect component cost factors independently from material and pressure, thus, the factors are taken from them. The factors given refer to the entire plant and can be adapted to our specific case. On the one hand, there is a distinction between three types of plants: solid, solid-fluid and fluid plants. On the other hand, different factors are taken into account depending on whether a new site development or a plant extension is involved. The plant investigated in this study refers to both a fluid plant and a plant extension, as it is built at an already existing

farm-site. The resulting factors are listed in Table 4.11. The total module costs C_{TM} result after applying the accumulated factor of 3.3. These can now be used to calculate the investment costs using equation 3.11. Here, the formula for the "Brown Field" costs is used, as it is assumed that the farm-site is simply extended. Besides, costs for building extensions are already considered in the direct component cost factors by PETERS et al. (2003, p. 244ff). Equation 3.7 determines the total capital expenditures from the investment costs. Subsequently, the annual capital costs (ACC) can be calculated using equation 3.23, which are required for the calculation of the costs of manufacturing. The ACC is calculated using the annuity method. For this method, an interest rate of 8% and an investment period of 20 years is assumed in accordance with SCHEMME (2020).

Table 4.11: Factors for the direct and indirect component costs according to PETERS et al. (2003, p. 244ff).

Factor type	Description	Factor
Direct	Component cost	1.00
	Installation	0.47
	Instrumentation and controls	0.36
	Piping	0.68
	Electrical systems	0.11
	Buildings	0.05
	Service facilities	0.30
Indirect	Engineering and supervision	0.33
	Sum	3.30

Operating expenditures

In contrast to the module costs, there are no size restrictions when calculating operating expenditures (OPEX), which is why the method of TURTON et al. (2009, p.197ff) can be applied. Most of the matters of expense of the OPEX correspond to general factors, which are listed in Table 3.6. Only the raw material, utilities and labour costs must be calculated for each plant size that is analysed. It is assumed that no additional personnel need to be hired for the present case with a small-size plant and a plant extension. The plant can be operated largely automatically and the work can be carried out by the personnel of the biogas plant. Due to the unessential labour costs, the OPEX include neither the corresponding cost component C_{OL} nor all other cost components related to it. These are the costs for direct supervisory and clerical labour C_{DS}, the laboratory charges C_L, a share of overheads C_O and the administration costs C_A. This simplifies equation 3.19 for the calculation of the operating costs to

$$OPEX_{new} = \frac{C_{RM}+C_{UT}+0.146 \cdot FCI}{0.97}. \quad (4.26)$$

The calculation of the OPEX requires the raw material costs C_R and operating costs C_B as well as the FCI, whereby the calculation of the latter has already been described above. To determine the raw material and utility costs, equation 3.20 and equation 3.21 are used. For the process, the quantities of the two raw materials CO_2 and H_2 and the three operating media (electricity, cooling water and steam) are required. The amount of air needed to cool H-4 is neglected, because there are no costs for this. The required quantities of raw materials and utilities can be taken from the results of the process simulation.

In addition, the operating hours of the methanol plant are required, which are set at 8500 h/a, as described above. This means that the plant is in continuous operation. Only short downtimes are planned, which are needed for maintenance. For the calculation, the determination of appropriate prices for the missing unit costs for the five utilities CO_2, H_2, electricity, cooling water and steam are required. For the utilities, the costs are taken from the literature and, if necessary, adjusted to the current year. The values used can be found in Table 13. For the electricity price, the industry value for the year 2019 is used. The purchase at this price is only possible with a power consumption in the range of 160,000 kWh to $20 \cdot 10^6$ kWh (BDEW, 2020). The price is exclusively used for the electricity that is required for the operation of the compressors inside the methanol plant.

Table 4.12: Utility costs for the calculation of the operating expenditures.

Utilities	Costs	Reference
Electricity	0.1690 €/kWh	BDEW (2020)
Cooling water	0.0597 €/t	PETERS et al. (2003, p. 898) (updated to 2019)
Steam	22.5378 €/t	PETERS et al. (2003, p. 898) (updated to 2019)

For the raw materials, price differences depending on the size of the plant must be taken into account. For large industrial plants, many values for the two raw materials CO_2 and H_2 are available in the literature. However, since both raw materials are produced locally in plants adapted to the methanol plant, values for these plant sizes are needed, since the economies of scale are also effective here. Prices for the membrane process are available in the report by BEYRICH et al. (2019) and from the company Apex AG (OESTER, 2019). The costs refer only to the biogas upgrading plant including post-treatment of flue gas. It is assumed, that the biogas plant already exists and that no further costs are incurred. For standard

biogas plants, fine desulphurisation with activated carbon is common practice. There is usually no fine desulphurisation in small-manure plants, which is why the cost for the activated carbon that occurs at the large BGP is added. The activated carbon costs 3 €/kg and is changed every ½ year according to RAU (2019). An amount of 720 kg/a for the small-manure plant and 1440 kg/a for the large plant are required (BIOBG, 2012, p. 2). The technical equipment of the filter reactor is not taken into account due to lack of data. The membrane costs given in the two references, BEYRICH et al. (2019) and OESTER (2019) are based on the lower heating value of the biogas. For the use in this thesis, a conversion to cost per kilogram of CO_2 is necessary, using

$$C_{CO_2} = \frac{C_{\text{Biomethane}} \cdot \text{LHV}_{\text{Biogas}}}{x_{CO_2} \cdot \rho_{CO_2}}, \tag{4.27}$$

where C_{CO_2} is the cost of CO_2, $C_{\text{Biomethane}}$ is the cost of biomethane, which is taken from the corresponding reference and listed in Table A 1 in appendix A. The $\text{LHV}_{\text{biogas}}$ is the lower calorific value of the biogas in the existing composition, which results in 5.28 kWh/m³ for this plant. The x_{CO_2} describes the volume share of CO_2 in the biogas, which is assumed to be 46%, and ρ_{CO_2} is the density of CO_2. The cost of activated carbon is only known per year and is converted to the cost per kWh_{LHV} of biogas. Equation 4.27 is used to calculate the cost of desulphurisation per kg CO_2 which can be added to the cost of CO_2 by biogas upgrading and post-combustion. It should be mentioned that no firm statement can be made here about the purity of the CO_2. It must be checked whether the CO_2 is present in a sufficiently pure form.

For the H_2 production costs, we require the costs of the three components WTG, electrolyser and storage. The calculation of the storage is only possible as a rough estimate, as the exact local storage size can only be determined based on actual wind data. Nevertheless, this exceeds the scope of this thesis. Therefore, the costs for a larger LOHC storage calculated by SCHORN (2018) are reduced to this application by comparing the plant size of the two methanol plants. For the WTGs, the CAPEX and OPEX are taken from a report of the German WindGuard (WALLASCH et al., 2019). This report states the main investment costs as well as auxiliary investment costs for different plants and the operating costs per decade respectively. For the calculation, the stated values are adapted to the present application. The values used for CAPEX and OPEX are listed in Table 4.13. The study IndWEDe (SMOLINKA et al., 2018) determines the costs of the electrolyser. There, the costs are also shown separately for CAPEX and OPEX, depending on the type of electrolyser. The used values for the PEM electrolyser are also shown

in Table 4.13 and reflect the costs, which were estimated by means of an industry survey for the year 2017. In the future, the study expects around 500 €/kW in the year 2050, namely costs of one third of the current cost. Specific costs for onshore wind are expected at 920 €/kW for the CAPEX and 23 €/kW for the OPEX. For the calculation of the COM, the capacities of the wind turbine and the electrolyser are also needed. Their calculation can be found in chapter 4.1.3, where the capacity is calculated using equation 4.16.

Table 4.13: Assumptions for the calculation of hydrogen costs.

Component	CAPEX per kW (€/kW)	OPEX per kW and year (€/kW)	Year	Reference
Wind turbine generator (WTG)	988	28	2018	WALLASCH et al. (2019)
	920* [1]	23** [2]	2050	[1] KREIDELMEYER et al. (2020), [2] BRÄNDLE et al. (2020)
Electrolyser	1470	13	2017	SMOLINKA et al. (2018)
	500		2050	SMOLINKA et al. (2018)

* without grid connection cost (70-90 €/kW), ** 2.5% of CAPEX.

In order to calculate the total H_2 costs, the capacities of the WTG and the electrolyser have to be combined with the corresponding CAPEX and OPEX. The production costs can then be determined as described in 3.1. The OPEX of the electrolyser also include the costs for the H_2O required for the electrolysis. A price for the water of 2 €/m³ is assumed (DECKER et al., 2019). The required amount of H_2O can be determined from the amount of H_2, which is known from the process simulation via the reaction equation of the process. The result is that this amount has to be multiplied by a factor of nine to obtain the amount of H_2O. The production costs per kilogram of H_2 correspond to the raw material costs of H_2 required for the calculation of the methanol plant. This allows the raw material costs to be determined first and then the operating costs. Using these and the ACC, the COM can then be calculated using equation 3.22. In addition, the specific COM per kilogram of methanol can be determined using equation 3.24 and per litre of gasoline equivalent using equation 3.25. For this purpose, the product mass flow of methanol is also required, which can be taken from the process simulation. Furthermore, the LHV of methanol and that of one litre of gasoline equivalent are

needed. The lower heating value of methanol is 19.9 MJ/kg and that of one litre gasoline equivalent is 32.18 MJ/L (EDWARDS et al., 2014).

4.2.3 *Case studies*

Within the scope of the cost analysis, this work analyses four different cases. In general, the cases differ in their CHP and methanol plant capacities as well as their gas separation technology. As explained above, the data for the biogas plants were obtained for two plant sizes, namely 75 kW and 500 kW. The specifications for the cases and associated assumptions are explained below, while Table 4.14 summarises the different cases with values calculated from chapter 4.1.

Table 4.14: Capacity of the combined-heat and power plant and methanol plant as well as biogas upgrading technology for the four cases based on own calculations.

Variable	Unit	Case 1 Standard case / small-manure plant	Case 2 Smallest MAN CHP-engine	Case 3 Biogas Oxyfuel Process	Case 4 Average biogas plant
Capacity of the CHP	kW	75	37	64	500
Capacity of the methanol plant	kW	138.38	75.68	305.86	693.3
Volume stream of raw biogas	m^3/h	39.39	21.54	39.39	227.38
Share of CO_2	Vol.-%	46	46	46	40.4
Gas separation		Membrane	Membrane	BOP	Membrane
Mass stream of CO_2	kg/h	34.29	18.76	75.79	171.83

CHP = Combined-heat and power plant, BOP = Biogas oxyfuel process.

Case 2 is associated with the smallest CHP engine available from MAN, namely 37 kW. It presents another possibility of small-scale plants as an opportunity for local manure utilisation and avoidance of emissions (BIENERT et al., 2019). The engine's capacity corresponds approximately to half of the capacity of the 75 kW plant; thus, about half of the CO_2 is available for the methanol plant. The energy efficiency of the CHP is 33% according to MAN (2020). Other plant data, such as

the composition of the biogas, is the same as for case 1. Case 3 is adapted to the biogas oxyfuel process (BOP), which was already presented in 2.2.4 and is embedded in the overall structure shown in Figure 4.5. Initially, the BGP of the BOP has the same capacity as the standard case. The use of the BOP reduces its efficiency of the CHP, resulting in a power of 64kW (SCHORN et al., 2020). Due to the BOP, about twice as much CO_2 is available from the same amount of raw biogas as in the standard case. The CH_4 contained in the biogas is converted into CO_2, which results in the greater amount of CO_2 available for the methanol plant. The step of gas separation is omitted in this design and the raw biogas is fed directly into the CHP and used there for the production of electricity and heat by adding pure O_2 from the electrolysis. Hence, the process has a comparatively lower separation effort than the other cases, which include biogas upgrading and potentially post-combustion. This process only has the combustion process that would happen in the CHP anyways. In addition to the CHP, a fan and a heat exchanger are required for the drying of the flue gas (SCHORN et al., 2020). In case 4, the plant size is adapted to an average German biogas plant with a capacity of the CHP of 500 kW. For this plant, the composition of the substrate for the biogas plant is different, which results in a changed composition of the raw biogas. Therefore, a slightly lower CO_2 content of 40.4vol-%, compared to the small-manure plant with 46vol-%, is assumed for this application. For case 2 and case 3, the assumptions of the standard case are used, because the system uses the small-manure plant.

Figure 4.5. Adapted concept including the biogas oxyfuel process (BOP) as described by SCHORN et al. (2020).

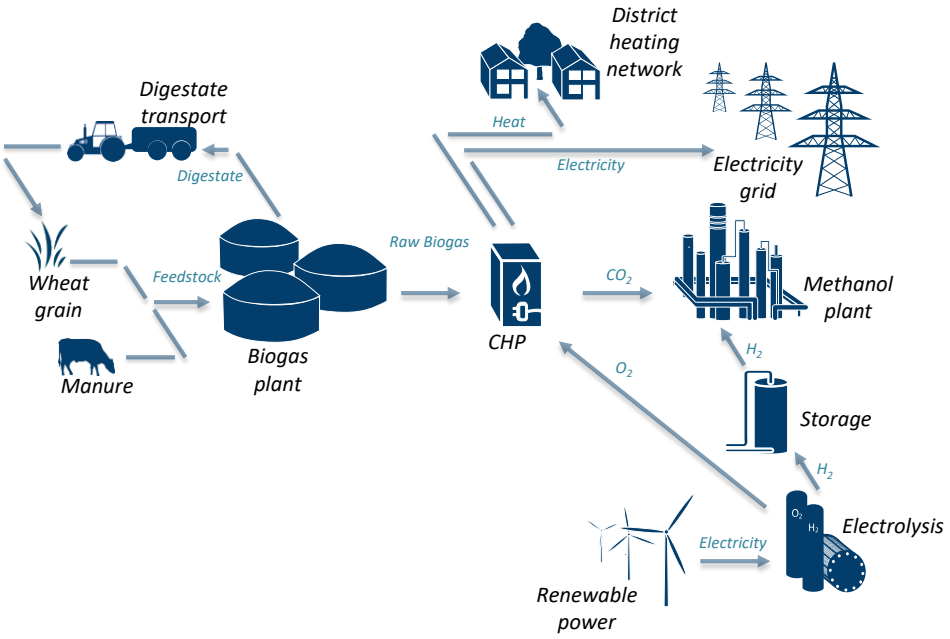

Caption: own creation; CHP = Combined-heat and power plant.

Another difference between the cases is the gas separation. The gas separation is omitted in case 3 and is replaced by a conversion in the CHP. For case 1, 2 and 4, membranes are assumed as the separation process. The costs for the provision of CO_2 will be adjusted to the respective case, since they differ depending on the size of the membrane plant and for the BOP. The costs for case 1, 2 and 4 are available for the biomethane and must be converted using equation 4.27. The costs used for the calculation are between 220 €/t and 270 €/t and are shown in Table A 6 in appendix A. The table also shows the basic costs for PSA and amine scrubbing for case 4, which are very close to the membrane prices. Therefore, it can be assumed that for the other two separation processes hardly any change in the COM of methanol would occur. All other operating costs are assumed to be constant and are calculated with the same values as in the standard case, whereby the required quantities are adapted to the case.

The capacity method, as described in section 3.1.2, is used for the modelling of the cases because the component costs cannot be determined via manufacturer enquiries for all plant sizes. This method delivers results in the accuracy range of

class 5 according to CHRISTENSEN et al. (2011). This means that the determined component prices can differ from -50% to +100% from the actual costs. However, results can be obtained that are more accurate depending on the application of the method. In its simplest application, only the total capital requirements of two plant capacities are compared by means of a general degression coefficient. By applying special degression coefficients adapted to the individual components, the accuracy of the results can be increased. The most accurate results of this method could be achieved if component prices were available for two investigated cases from which the degression coefficients are calculated using equation 3.9. Therefore, the components for case 3 are requested from manufacturers in order to determine the total module costs C_{TM} for case 2 and 4. As it was not possible to achieve prices for all components, additional degression coefficients for the components are calculated using the module costs of the standard case as well as those of WALMAN (2018) for the smallest case of 30 MW. This is possible because Walman's plant is almost identical in its design to the design used in this thesis. For the calculation, the prices and component sizes are taken from her and compared with the calculated ones received for the standard case. It should be noted that the calculated prices in her thesis were calculated for the year 2017. Therefore, the prices must be converted to 2019 using the CEPCI via equation 3.14. For this purpose, the CEPCI of 562 is used as a basis (WALMAN, 2018). Furthermore, it should be noted that WALMAN (2018) already includes direct and indirect module costs, which is why the components must also be added to the prices in case 1 before comparison of the components is possible. The determined degression coefficients can then be used to calculate each component cost for the different cases using equation 3.8. For this, the size of the component must be known for the respective case. The equation is also used for the other three cases as described for the standard case in section 4.2.2.

With the component costs, the FCI can then be determined. Subsequently, the COM can be calculated using the FCI and operating costs for the respective case. The raw material and utility flows required for the operating costs can be taken from the results of the process simulation. For the costs of operating utilities and H_2, the same values are assumed as for the standard case described above. Only the CO_2 costs are adjusted to the case.

4.2.4 *Sensitivity analysis*

In order to investigate the sensitivity of manufacturing costs to various parameters, sensitivity analyses are carried out for the cases investigated. For this purpose, one input parameter is varied for each case and the associated change in specific manufacturing costs is investigated (TOWLER et al., 2008, p. 308). In this way, it can be shown which parameters have the greatest influence on the specific COM. The five raw material and resource flows, the interest rate and the FCI are varied in the course of this work. The parameters are each varied by ±50% around the initial value if more precise values for the limits cannot be found. For the CO_2 costs, the calculated value from the report by BEYRICH et al. (2019) is used as the upper limit for case 1 (+89%) and case 2 (+65%), as it clearly exceeds the +50% limit. For the other cases, the standard variation is used, as the costs from the report by BEYRICH et al. (2019) are not applicable for these two applications. This is because case 3 is the BOP, which does not use separation technology by means of a membrane process, and case 4 is an average German biogas plant with a higher capacity. Furthermore, the lower limit for H_2 costs is 4.6 €/kg, which is expected to be achievable due to an expansion of wind energy and decreasing costs for the electrolyser in the future (ROBINIUS et al., 2018b). For the FCI, the accuracy class 4 is used as the limit representing the maximum range, which means a reduction of the lower limit to -30%. The upper limit remains unchanged as it corresponds to the standard +50%. In addition to the individual variation of the parameters, a "best subcase" and a "worst subcase" is also examined, in which all parameters are assumed to have the best and the worst values respectively. This shows to what extent a variation of the manufacturing costs is possible for the examined cases.

4.2.5 *Cost calculation of the biogas and biogas upgrading plant*

A general cost estimation of the BGP and biogas upgrading plant is also carried out with the goal to evaluate additional costs and revenues that could be relevant for the farmer and determine the annual revenues by the entire concept. The goal is to see whether it could affect the investment decision. For this, the profit of the BGP and biogas upgrading plant is calculated from the total costs and revenues. The levelised cost of electricity generation (LCOE) (€/kWh). Cost data is mostly considered from the BGPs in Clausnitz (75 kW) and Rechenberg-Bienenmühle (500 kW) and some values from the literature. This means that only case 1, 3 and 4 are considered. The livestock farm is not part of this analysis, due to lack of data, but would potentially also yield costs and revenues.

The CAPEX of the BGPs are calculated using equation 3.7. An amortisation period of 20 years is assumed as well as an interest rate of 4% according to the FNR (2016). The FCI of 425,000 € is known for the small-manure plant and comprises the cost of the fermenter, the digestate storage facility and the district local heating network (RAU, 2019). The FCI is comparatively low compared to the investment cost of almost 695,000 € provided by the FNR (2016). This was due to a high own capital contribution and the discount for purchasing another plant of the same size for a different location and thus reduced planning effort. The 500 kW plant's investment cost could not be summed up due to deferred investments and incomplete data. Investment costs were available for another plant located in Raitzen, Saxony, whose CHP size is comparable to the 500 kW plant. It also includes a biogas upgrading unit using physical absorption. Although the technology is different, the 2.5 million € of investment costs are taken to consider a plant combined with an upgrading unit. It is comparable to the investment costs of 2.2 million € for the same plant size without upgrading by the FNR (2016). ACC are calculated using equation 3.23. The costs of the upgrading plants are calculated via the annual amount of CO_2 produced. The price calculated in section 4.2.2 contains investment cost as well as costs for services and maintenance and the cost of electricity.

The OPEX are comprised of the operating and utility costs which are added. Data must partly be taken from the literature, as not all cost data is known. Some average values are taken from the FNR (2016), while others for the small-manure plant are collected from an article by BAYERISCHES LANDWIRTSCHAFTLICHES WOCHENBLATT (2019) which has more recent numbers concerning this type of plant. For the direct operating costs, the BGP abides by site-specific assumptions. As heat is produced on-site and taken from the CHP, there are no expenditures for the required heat. The demand is subtracted from the total heat production and the cost of energy can be seen as the foregone profit from not selling the energy. Other utilities such as labour costs are considered. Network charges for electricity usually also have to be paid, but they can be retrieved/recovered via the tax. Furthermore, it is assumed that the costs of raw materials are equal to zero, as all of the feedstock are residues from livestock farming. Therefore, they have no prices assigned to them. An exception is made for the enzymes used in the 500 kW plant, as well as the iron (II) chloride that must be purchased. In contrast, it is possible to assign a (negative) price to the manure which is discussed below. The assumptions relevant for the calculation of the utilities costs are summarised in Table A 8 and Table A 9 in appendix A. Costs for electricity generation, purchase of activated carbon two times per year as utility costs and maintenance costs are assumed here.

Revenues calculated comprise heat and electricity sales as well as saved expenditures from digestate which can substitute mineral fertiliser. A negative manure price can also be applicable, depending on the region. Due to the excess manure problem and restricted N loads in soils, livestock farmers have to discharge of the accumulated manure at their farms. A price of 10 €/m³ was found for manure from the Netherlands, where there is a particular problem of excess manure (AGRARHEUTE.COM, 2016). Furthermore, small-manure plants usually do not need more manure than already accumulated on-farm. A revenue from CO_2 sales is also considered.

4.3 **Life cycle assessment**

An LCA of the PtF-system introduced in this study is carried out under German conditions. This study focusses on a main LCA about the standard case, i.e. the small-manure plant with 75 kW, described in section 4.1.5. The LCA is in accordance with the ISO standards (ISO, 2006a, ISO, 2006b) in order to guarantee the strict following of the methodology. This sub-chapter follows the methodology, having section 4.3.1, 4.3.2 and 4.3.3 describe the procedure. In section 4.3.4, the approach for the sensitivity analysis is presented. As the accounting for manure credits is questionable by LCA standards, we considered additional LCA exercises of simple BGPs, i) with a classic biogas CHP and ii) with only a gas flare. These LCAs were conducted to show the impact of saved CH_4 emissions in AD systems. It means that the CH_4 emissions accounted for from pre-storage in the standard case were deducted, i.e. assumed as a manure credit. Table 4.15 shows an overview over the LCAs in this study. The main LCA could also be representable for a larger plant, as the impacts are shown per kg of methanol produced, the BGP used waste feedstock as well and because we did not include capital goods. However, the large plant in our case study has a closed digestate storage, which would improve the carbon footprint of the BGP.

Table 4.15: Main assumptions about the life cycle assessments that are carried out in this study.

	Main LCA	Additional LCAs	
		i) Biogas plant with CHP	ii) Biogas plant with gas flare
Goal and scope	Integrated PtF-system including renewable methanol synthesis at a biogas site	Classic biogas system	Potential biogas system
Functional unit	1 kg of methanol	1 m³ of biogas	1 m³ of biogas
Co-products	Electricity and heat from CHP, fertiliser from digestate	Electricity and heat from CHP, fertiliser from digestate	Fertiliser from digestate
System boundary	PtF system according to Figure 4.1; manure credits not considered	Smaller than main LCA, only including the fermenter and a subsequent burning of biogas within a CHP unit	Smaller than main LCA, only including the fermenter and a subsequent burning of biogas within a gas flare
Reference system	Conventional methanol production via methane steam reforming	System ii)	System i)

The main LCA has already been described in detail in EGGEMANN et al. (2020). Therefore, the LCI and other assumptions concerning the system boundaries and scenarios are mainly taken from this paper. However, some improvements and adaptations are made that had not been considered before. This is primarily due to a detailed modelling of the methanol synthesis in the simulation software Aspen Plus as well as adaptations concerning data of the AD as well as the addition of the production of activated carbon for fine desulphurisation and the waste water treatment of the water obtained at the end of the methanol synthesis. The electricity demand for methanol synthesis is obtained from the process simulation which is adjusted to the small-scale case and deviates from the value used before. Furthermore, emissions from pre-storage of manure were eliminated due to the local conditions. The precise changes are pointed out in the LCI in section 4.3.2. The additional LCAs are carried out, using the same BGP data as for the standard case. Its approach is described in section 4.3.5.

4.3.1 *Goal and scope*

The main LCA aims at quantifying the environmental impacts from a novel PtF system, from cradle to gate. This implies that the system boundaries include processes up to the stage at which the main product, i.e., methanol, is delivered at the plant gate, hence excluding further processing, use and disposal. The functional unit (FU) is defined as 1 kg of methanol produced by a PtF plant with a capacity of approximately 212 tonnes of methanol per year (138.38 kW_{LHV}). It means that only case 1, i.e. the standard case, is considered in the LCA. The production of capital goods for the respective units has been neglected from the present assessment as primary data is not available.

Several co-products are generated across the life cycle such as fertiliser, heat and electricity. In order to subtract additional functions delivered by the co-products, the 'system expansion' approach is applied according to ISO 14044 (ISO, 2006b). It is assumed that co-products generate environmental credits by substituting for average products available in the market. The system boundaries are shown in Figure 4.6, including the so-called avoided processes that generate those co-product credits. An important point is that the manure does not get transported from the stables, but flows directly (transported by an automatic manure scraper) into the preliminary storage tank. As the retention time in the pre-storage tank is very short and the tank is under the ground below concrete, we argue that the CH_4 emissions from manure pre-storage are negligible. In support of this, a personal communication with the TU Freiberg (RAU, 2019) about the local conditions of the BGP arrived at the conclusion that emissions from the concrete pre-storage tank should indeed be insignificant to the environment. Control shafts of the pit are very small and the liquid manure is stored in the ground at a low temperature, for which reason, no reactions should take place or if so, only very slowly. We argue that the pre-storage emissions of raw manure below concrete are indeed negligible in this LCA application.

Figure 4.6: Flow diagram of the Power-to-Fuel system proposed, from cradle to gate, by applying system expansion to subtract impacts from co-product generation.

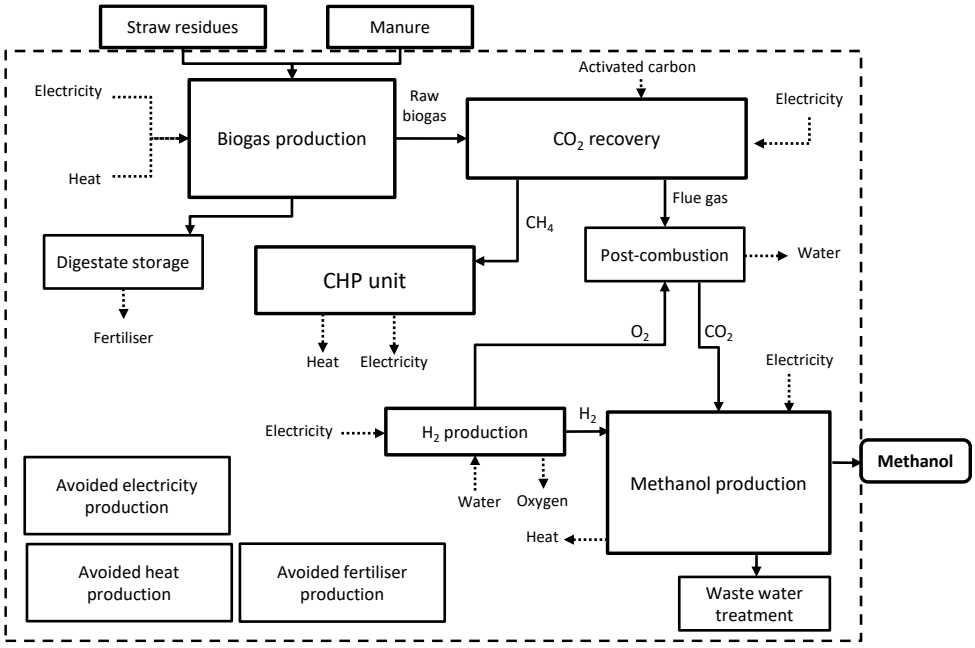

Caption: own creation.

Several scenario formulations were defined to tackle uncertainty in LCA results due to assumptions on avoided processes, as shown in Table 4.16. It is firstly assumed that the digestate can be used as a fertiliser since its DM content (7.34%) contains 3.4wt% elemental nitrogen (N), as well as 5.3wt% potassium (as K_2O) and 2.4wt% phosphorus (as P_2O_5) (Table A 2 in appendix A). Hence, in the first scenario formulation, i.e. A1, the substitution is based on the N content, assuming that digestate replaces urea as a major organic fertiliser in the market, with an average N content of 46%. In scenario A2, we assume that K_2O in digestate replaces potassium chloride – also known as muriate of potash (MOP) – with a K_2O content of 60% (EC, 2019). In scenario A3, using the digestate as fertiliser based on its P_2O_5 content avoids producing single superphosphate (SSP) with a P_2O_5 content of 20% (IPNI, 2019). Overall, these fertilisers were chosen due to their relevance as the main commercial fertilisers in the EU (EC, 2019). The data for the composition of the digestate was measured from the digestate storage facility at the large plant and is shown in Table A 2. In addition to the digestate, the assessed PtF system generates electricity as a co-product from the CHP, which can be fed into the grid. In order to capture uncertainty in the source of electricity that is most likely to be replaced, we assumed that it substitutes for electricity from the average German

electricity mix (A). As alternative scenario formulations, electricity from the CHP replaces average off-shore wind electricity (B) or electricity from coal (C), as best-case and worst-case scenarios in the context of Germany, respectively, from the environmental point of view. Finally, excess heat from the CHP replaces heat from NG at industrial boilers in the EU which represents a major NG-fired heat source in Germany. In order to calculate environmental benefits brought about by the proposed system, fossil-based methanol production was considered as the reference process, which does not deliver additional co-products according to the Ecoinvent 3.5 database (WERNET et al., 2016). The process is based on conventional methanol production via steam methane reforming that requires heat, electricity and NG as resources.

Table 4.16: Scenario formulations of the PtF system assessed with choices on avoided processes under the system expansion approach.

	N content in digestate replaces urea production (as N)	K_2O content in digestate replaces potassium chloride (MOP) production (as K_2O)	P_2O_5 replaces single superphosphate (SSP) production (as P_2O_5)
CHP-electricity replaces average electricity from the German mix	A1	A2	A3
CHP-electricity replaces wind-based electricity produced in Germany	B1	B2	B3
CHP-electricity replaces from a coal-based electricity produced in Germany	C1	C2	C3

4.3.2 *Life cycle inventory*

LCI data for the main processes at the foreground level was collected from own measurements and combined with technical process parameters for the biogas and methanol plants. The energy efficiency was calculated at 35.58% based on the individual energy efficiency rates shown in Table 4.17. The process of methanol production is the most intensive in the use of electricity, followed by the electricity

demand of the BGP and the CO_2 separation by membrane. Yet, only 25% of the electricity production of the CHP and 35% of the produced heat is used within the system, given that H_2 production is wind-based. The methanol synthesis data was obtained from a process design application for small plants in Aspen Plus as described in chapter 4.2.1. Primary data was combined with secondary data for the energy demand of the biogas upgrading, as well as certain emission factors of the BGP. It must be noted that the production of capital goods for the main processes considered in the foreground system are not included within the system boundaries due to data limitations at this stage. Manure application and transport are also not included since it is assumed that the integrated system is located on-farm. The main assumptions made and data sources employed through the LCI, are described as follows, while the LCI is shown in Table 4.18:

Table 4.17: Energy efficiency of the main sub-processes included in the system boundaries to produce 1 kg of methanol by means of the Power-to-Fuel system proposed.

	Biogas production plant (incl. CHP)	Polymer electrolyte membrane electrolysis	CO_2 recovery plant	Methanol synthesis plant
$\eta_{sub-system}$	0.65[a]	0.70[b]	0.92[c]	0.85[d]

[a] RAU (2019), [b] SCHIEBAHN et al. (2015), [c] Sun et al. (2015), [d] Schemme et al. (2020).

a) Biogas production: The LCI data was taken from a BGP located in Eastern Germany, via personal communication with the Technical University Bergakademie Freiberg (RAU, 2019). The plant's characteristics and assumptions have already been described in section 4.3.1 and also in more detail in chapter 4.1. Its feedstock is considered waste from livestock farming and entails zero emissions according to the RED II. As the raw manure is only shortly stored in a covered tank below a concrete floor, the emissions of pre-storage are thus expected to be inexistent. Therefore, CH_4 and ammonia (NH_3) emissions occur only during the stages of AD and digestate storage. N_2O emissions from AD are neglected according to IPCC (2006b) as data is scarce, while the process releases negligible quantities of H_2, H_2S, H_2O and other trace gases. We further considered CH_4 losses in the form of both rest gas potential arising from the open storage of digestate and leakages as well as overpressure security valves from the fermenter. These are estimated at 1 kg/MWh equivalent to 1.4%, mainly coming from the digestate storage facility (FNR, 2016, RAU, 2019). The leakage of NH_3 from the fermenter is lower than 0.05% of the N content in the digestate and hence excluded (EMEP/EEA, 2016, WULF et al., 2019). NH_3 emissions of 2.66% of the N in the

digestate, occurring during storage, were included in the inventory based on a Tier 2 approach from EMEP/EEA (2016). The values for the N content as well as other components in digestate arise from on-site measurements from the digestate storage tank of the larger plant, which is fed with the same manure, though slightly different additives, and have the same retention time of 150 days.

b) CO_2 recovery: The energy demand for the membrane technology of the standard case capacity is provided for a capacity of 40 m^3/h raw gas by the Apex AG (OESTER, 2019). It is stated in kWh/Nm^3 raw gas. Since the exact amount of raw gas per hour is known within the system, this can be converted to MJ/h. The electricity demand is in fact higher than that used in EGGEMANN et al. (2020) because that paper used data for more industrial, large-scale upgrading processes. Here, a closed upgrading system and thus no emissions are assumed. As biogas upgrading includes upstream desulphurisation and dehydration, it should guarantee that the biogas no longer contains sulphur when entering this stage (ADLER et al., 2014a). The membrane technology by OESTER et al. (2018) also includes fine desulphurisation via activated carbon. As desulphurisation is part of the upgrading technology described by VIEBAHN et al. (2018), we assumed that the LCI includes the demand of electricity for desulphurisation as part of the CO_2 separation process. The required activated carbon of 0.085 kg/h is also considered, which was not considered in EGGEMANN et al. (2020). In addition, the process of obtaining pure CO_2 would require some sort of post-combustion. If the combustion process is run with pure O_2, the formation of harmful NO_x emissions can be avoided. The O_2 from the H_2 production is sufficient, as the process only requires 2.4% of it. The amount is subtracted from the O_2 occurring in the modelled process, assuming it has already been transmitted to the post-combustion process.

c) CHP: Emissions were measured for the 75 kW CHP. When calculating the CH_4 losses due to biogas production and upgrading, we assumed that an additional 1.5% of biogas is required to guarantee a full-load drive of the CHP. This translates into additional feedstock requirements in input that can be easily operated with the existing fermenter, as presented in chapter 4.1.4. Emissions data for the CHP gas engine without a catalyst was measured at the plant in Eastern Germany in November of 2018. As the CO_2 in the flue gas is biogenic, it is excluded from the inventory. If it was included it would have an impact of 0.26 kg per kg methanol. The NO_x emissions by the CHP were adjusted as compared to those used in EGGEMANN et al. (2020), as there was a mistake and they were actually lower. They were corrected by one decimal.

Table 4.18: Life cycle inventory of all inputs and outputs associated with the production of 1 kg of methanol by means of the Power-to-Fuel system proposed.

INPUTS		**OUTPUTS**	
Methanol synthesis		**Methanol synthesis**	
CO_2 (kg)	1.37	Methanol (kg)	1.00
H_2 (kg)	0.19	Water (kg)	0.56
Electricity (MJ)	1.79	Process heat (MJ)	2.99
CO_2 recovery		**CO_2 recovery**	
Biogas (m^3)	1.58	CO_2 in flue gas (kg)	1.37
Electricity (MJ)	0.15	H_2O (m^3)	1.96E-05
Activated carbon (kg)	0.0033	Biomethane 95vol.% (kg)	0.66
Biogas production		**Biogas production**	
Electricity (MJ)	0.85	Biogas (m^3)	1.56
Heat (MJ)	4.86	Urea as N (kg)	0.69
		Potassium chloride as K_2O (kg)	1.09
		Single superphosphate as P_2O_5 (kg)	0.49
		NH_3 emissions from digestate storage (kg)	7.87E-04
		CH_4 losses from AD and digestate storage (kg)	8.07E-03
CHP		**CHP**	
CH_4 (kg)	0.66	Electricity (MJ)	10.63
		Heat (MJ)	13.89
		Emissions	
		SO_2 (kg)	2.20E-03
		NO_x (kg)	1.31E-02
		CO (kg)	6.97E-03
		NMVOC (kg)	1.50E-04
		CH_4 (kg)	2.10E-02
H_2 production (PEM)		**H_2 Production (PEM)**	
Electricity (MJ)	32.27	Oxygen (kg)	1.33
Water (kg)	1.69E-03	H_2 (kg)	0.19

CHP = Combined heat and power plant.

d) H_2 production: Production data for the wind turbine and H_2 electrolysis as well as the methanol production were obtained from own simulations performed by the Institute of Electrochemical Process Engineering within the Institute of Energy and Climate Research at the Forschungszentrum Jülich. Assuming 2000 FLH of the wind turbine, a factor of 4.25 was considered for 8500 FLH for methanol synthesis and the AD process.

e) Methanol production: The methanol production process was carried out under 250°C at 80 bar inside an isothermal reactor that uses 1.37 kg of CO_2 per kg of methanol, as also described by BILLIG et al. (2019). The 138.38 $kW_{th,LHV}$ methanol synthesis plant uses 34.29 kg of CO_2 per hour, and 4.7 kg of H_2. The treatment of the discharged water from the process is also considered in a waste water treatment process, an additional process that is introduced to the analysis in EGGEMANN et al. (2020). Another difference compared to that study is that the excess heat from the methanol process is not accounted for. The process simulation showed that it is only about 10 kW and temperatures lie far below low pressure steam level. It would also not be profitable from an economic point of view, considering the additional infrastructure that would have to be built. Furthermore, the electricity demand was adjusted compared to the LCA in EGGEMANN et al. (2020) by a factor of 3.2 higher than the one used before.

For the reference process, we consider that conventional methanol production in Germany is carried out via the steam reforming of NG, importing NG from Russia as one of the main import partners. According to KEHLER et al. (2016), the CH_4 emissions for transport in and from Russia vary between 0.32-0.97% of the gas produced. Hence, losses of 0.65% are assumed. This fits with the optimist values stated by SIMLA et al. (2019, p. 54). Associated LCI data for the local NG extraction is taken from the process in Ecoinvent 3.5 (Wernet et al., 2016) by considering energy consumption only and neglecting capital goods, same as in the proposed system. The LCI data related to NG and energy demand for the methanol synthesis is also taken from Ecoinvent and presented in Table 4.19.

Table 4.19: Utilities required for conventional methanol production according to WERNET et al. (2016).

Utility	Value	Unit
Electricity	0.266	MJ/kg MeOH
Heat	6.930	MJ/kg MeOH
Natural gas	0.652	m^3/kg MeOH

4.3.3 *Life cycle impact assessment*

The characterisation method ‘ReCiPe 2016’ (HUIJBREGTS et al., 2016) was chosen for the calculation of environmental impacts at the midpoint level, as implemented in GaBi Life Cycle Engineering Suite (KUPFER et al., 2019). This proves to be a comprehensive method for comparative impact assessments of energy systems and transport fuels (CAVALETT et al., 2013, TREYER et al., 2014). The “hierarchist perspective” was taken, as a neutral scenario for the analysis of future socio-economic developments (HUIJBREGTS et al., 2016). Moreover, it estimates the climate change potential from GHG emissions over a 100-year horizon, in line with the temporal scope for developing low-carbon economies, according to the RED II. We considered the following impact categories due to their importance in the environmental performance of alternative fuels (MORALES et al., 2015, ROCHA et al., 2014): climate change (excluding biogenic carbon) (CC) (CO_2-eq.); freshwater and marine eutrophication potential (EP) (kg P-eq.); terrestrial acidification potential (AP) (kg SO_2-eq.); fossil depletion (FD) (kg oil-eq.); photochemical ozone formation (POF) (kg NO_x-eq.); human toxicity (HT) (kg 1,4-DB-eq.); and stratospheric ozone depletion (ODP) (kg CFC-11-eq.).

4.3.4 *Sensitivity analysis*

In addition to the scenario analysis described above in section 4.3.1, a sensitivity analysis is also carried out in order to assess the influence of parameter uncertainty on the results. In particular, it considers a range of variability for those parameters that is highest in the PtF implementation on a pilot scale, namely: i) the CH_4 emission intensity of the BGP associated with the fermenter and the digestate storage; ii) the energy efficiency of the PEM electrolysis; iii) the electricity input for methanol production; iv) the energy input to the BGP; and v) the heat input to the BGP. The sensitivity analysis was carried out by means of the GaBi Analyst Tool. We assumed lower and upper bounds for each of the aforementioned parameters based on the literature, as is shown in Table 4.20.

Table 4.20: Parameters considered for the sensitivity analysis and associated range of variability relative to the base values incorporated into the life cycle inventory.

Parameter	Base value	Range of variability (±CCP-1)	Reference
i) CH_4 losses from anaerobic digestion and digestate storage (kg/h)	0.21	±75%	GRAF et al. (2013), SCHEUTZ et al. (2019)
ii) Electricity demand of electrolysis (MJ/kg H_2)	171.63	±17%	BUTTLER et al. (2018), BRYNOLF et al. (2018)
iii) Electricity demand for methanol synthesis (MJ/kg methanol)	1.79	±30%	WEISKE (2020/unpublished, p. 95)
iv) Electricity demand of the biogas plant (MJ/h)	21.60	±25%	STINNER et al. (2015), SCHOLWIN et al. (2019)
v) Heat demand of the biogas plant (MJ/h)	123.48	±30%	ZIELBAUER et al. (2007), DANIEL-GROMKE et al. (2017)

CV = coefficient of variation relative to the base value.

As the scientific literature is uncertain about the accounting of manure credits, results for different assumptions about emissions from pre-storage are also shown. This is done to visualise the effects they can have on the entire system and the differences in results, as they are expected to be important. One study ($LCA_{Storage}$) considers the pre-storage emissions accounted to the system. For this, CH_4 emissions from open pre-storage of manure are calculated by following the IPCC (2006a) guidelines, and employing reference values for Germany (Haenel et al., 2020). Specifically, we considered manure generated by 126 cows, which is the number of cows on-site corresponding to 75 kW as calculated in chapter 4.1.5. According to HAENEL et al. (2020), NH_3 emissions from pre-storage of manure are zero, when the facility has a roof made out of concrete, as is the case. Moreover, manure is only kept inside the pre-storage tank temporarily; hence the short retention time avoids the formation of floating covers that enable nitrification (Wulf et al., 2019). A second study (LCA_{Credit}) looks at the possibility of manure credits, which are the same CH_4 emissions which are previously accounted for as pre-storage emissions. Yet, now they are credited to the system for avoiding open-manure storage. Table 4.21 shows the different CH_4 emissions by the system for the LCI. LCA_{Base} refers to the CH4 emissions as assumed by the main LCA.

Table 4.21: Evaluated life cycle assessments (LCAs) considering different CH_4 emissions; LCA_{Base} refers to the accounting of anaerobic digestion (AD) emissions, while $LCA_{Storage}$ accounts for both AD emissions and emissions from pre-storage of manure and LCA_{Credit} neglects pre-storage emissions but instead considers the avoided pre-storage emissions as manure credits.

	LCA_{Base}	$LCA_{Storage}$	LCA_{Credit}
Pre-storage emissions (kg/h)	-	0.34	-
Manure credit (kg/h)	-	-	-0.34
AD emissions (kg/h)	0.21	0.21	0.21

4.3.5 *Additional life cycle assessments concerning the methane emissions in biogas systems*

Aside from the analysis of the standard system and the visualisation of the different assumptions about manure credits, we undertook another small LCA exercise to shed light on the debate about the avoided CH_4 emissions. While the double use is clearly promoted by renowned institutions, the LCA community is still critical about the approach. In order to make the existence of the dual purpose of BGPs clear, we compare i) a classic BGP with a CHP unit to another case ii) introduced by OSTERBURG (2019). This case includes burning of biogas through a gas flare, as described in chapter 2.2.2 (Figure 2.6). Due to burning the biogas without further usage, this case misses to generate energy. Therefore, it misses out on the electricity and heat credits generated in case i), while still offering an emission reduction from open manure storage, which clearly presents its benefit. Moreover, it offers reduced CH_4 emissions in the flue gas, as all CH_4 is converted during the combustion. The analysis also follows the ISO standards (ISO, 2006a, ISO, 2006b). For both cases, the functional unit is 1 m^3 of biogas produced. The system boundary is comparable with the one of the main LCA, as it does not consider emissions from the stables. It begins with manure pre-storage below the ground where the feedstock is ready to be fed into the fermenter. Emissions from avoided raw manure storage are ascribed to the system as the manure credits that are discussed in chapter 3.4.1 and covered in the LCA_{Credit} described in section 4.3.4. The system boundaries for both cases are shown in Figure 4.7. The scenario variations introduced in the main LCA were mostly kept for both cases to take care of the multi-functionality of the system. However, the avoided fertiliser production is not considered, as it exactly the same for both systems.

Figure 4.7: System boundaries of the biogas systems analysed in the additional LCA showing the boundary for case i) with a combined-heat and power unit (left) and case ii) with a gas flare (right).

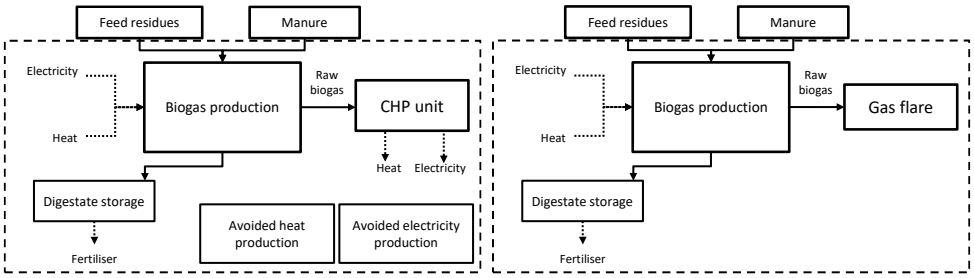

Caption: own creation.

The additional LCA uses the data and assumptions for the biogas plant in section a) of chapter 4.3.1. Case i) also includes the assumptions for the CHP in section c) in the same chapter. Subsequently, the same LCI data is applied as well. In contrast to the CHP, the combustion of biogas using a gas flare yields zero CH_4 emissions. The entire CH_4 is converted during combustion, as also analysed in a simulation in Aspen Plus. The LCIA was adapted to the assumptions for the main LCA, using the characterisation method ‘ReCiPe 2016’ for the calculation of impacts at the midpoint level. The “hierarchist perspective” is taken as well and the same impact categories are considered as stated in chapter 4.3.3.

Chapter 5
Results and discussion

In this chapter, the results of both the techno-economic analysis and the life cycle assessment are presented and discussed. The chapter also summarises key findings.

5.1 Results and discussion of the techno-economic analysis

This sub-chapter presents the results of the cost analysis. Section 5.1.1 first deals with the results of the process simulation. This is followed in section 5.1.2 by the presentation of the results of the cost estimation for the standard case and in section 5.1.3 for the other cases investigated. In section 5.1.4, the results of the sensitivity analyses for all investigated cases are presented. Finally, section 5.1.5 presents and discusses profits and possible development in costs for the biogas plant and the entire PtF system.

5.1.1 *Results of the process simulation*

Using the results of the simulation in Aspen Plus, various process parameters can be determined. Important general parameters, which do not or only minimally differ for the cases investigated, are the turnover of CO_2 inside the reactor, the achieved purity of methanol at the end of the process and the power and heat requirements for the overall process. These are listed in Table 5.1. The turnover of CO_2 indicates the proportion which is achieved during one process run. The low value shows why the two recycling streams of unreacted educts are necessary. If there was no recirculation, almost 2/3 of the added CO_2 would not be converted and still be emitted into the atmosphere. In addition, the methanol yield would also decrease significantly. Therefore, it follows that the increased electricity demand by the two compressors CP-3 and CP-4 for the recirculation is justified in order to achieve a complete conversion by several runs of the CO_2 through the reactor.

Table 5.1: Results of the process simulation for general parameters such as turnover of CO_2, purity of methanol, electricity and heat demand.

Parameter	Value
Conversion of CO_2	36.7%
Purity of methanol	99.898%
Electricity demand	1.79 MJ/kg_{MeOH}
Heat demand	-5.58 MJ/kg_{MeOH}

The low turnover is due to the equilibrium reactions for methanol synthesis (equation 2.1, 2.2 and 2.3), so that an equilibrium between educts and products is established in the reactor and never the entire educts react to products. The equilibrium could be shifted further to the side of the products by higher pressures and lower temperatures, which would increase the turnover per circulation. However, the increase in pressure would be at the expense of the electricity required for the compressors, which would have to compress the educts to higher pressures. Lower temperatures lead to a reduced activity of the catalyst as well as deteriorated kinetics, which is why the temperature cannot be lowered arbitrarily. Therefore, as a compromise, a pressure of 80 bar and a temperature of 250°C are used in the reactor, which reach the conversion of 36.7% of CO_2.

The purity of the methanol produced is achieved by adjusting the column settings. The aim is to at least fulfil the requirements of the IMPCA specification (IMPCA, 2015) and at the same time only require as much heat for the column reboiler as is provided by the reactor. The result value of 99.898% fulfils the IMPCA specifications of a minimum purity of 99.85%. Furthermore, a maximum water content of less than 0.1% is specified in the requirements. With a water content of 0.005%, this value can also be met. The product flow contains a residual CO_2 content of 0.097%. During the synthesis of methanol, other by-products may be formed in small quantities, for which the IMPCA (2015) also specifies maximum values. Since these by-products are not considered in the process simulation, no statement can be made about their content. Due to the high selectivity of the catalyst (OTT et al., 2012, p. 6), generally, very small quantities of by-products occur, which is why they are neglected and it is assumed that they are within the permissible range. In addition, any impurities which could be contained in the supplied CO_2 stream from the biogas upgrading plant, are not considered. Due to the fact that the proportion of methanol is significantly above the minimum limit, it can be assumed that the purity of methanol will be within the permissible range despite by-products and impurities. Therefore, the renewable methanol produced in

this plant can be utilised for all standard applications for which conventional methanol is otherwise used.

Moreover, electricity and heat requirements are of particular interest for the process. The electricity demand is made up of the demand of the four compressors and is shown in Table 5.1 converted to the amount of methanol produced. It is important to note that the calculated value is adapted to the simulated multi-stage radial compressors. In the actual application case they cannot be used because compressors with these small volume flows but high pressures are not offered. Therefore, there may be deviations from reality. The power consumption of the process is significantly higher than the value of 0.556 MJ/kg_{MeOH} calculated by SCHEMME (2020). This is due to the lower inlet pressures of the reactants, which means that the compressors CP-1 and CP-2 have a higher power requirement. The heat demand, which is also shown in Table 5.1, converted to the quantity of methanol produced, is the result of the calculation of all heat sources and sinks of the process. All main components except for compressor CP-3 and the column vessel are included in the consideration, as these two have neither heat emission nor absorption. The heat exchangers are interconnected as far as possible in the process layout, as shown in Figure 4.4. Only heat exchanger H-4 cannot be connected internally and is cooled by external supply of air. In addition, the steam generated by the reactor is used to heat the reboiler. The excess heat from the compressors, the separation vessels and the condenser cannot be used internally within the process. This results in the excess heat of the individual components as shown in Table 5.2. The excess heat is due to the exothermic reactions in the reactor. Due to the suitable interconnection of the heat exchangers and the heating of the reboiler by means of steam from the reactor, it is possible to supply all heat sinks of the process with heat sources from the process and no external heat needs to be supplied to the synthesis. This is possible because the purity of the methanol is adapted to the heat demand of the reboiler, so that the demand in the reboiler is below the available quantity of the reactor, and sufficient heat sources at a high temperature level are available to serve all sinks. The excess heat is available at low temperature levels and therefore most of it cannot be used further. A part of it, especially heat from the compressors at the highest temperature level, could be coupled in the overall plant concept, as heat is required, e.g., for the fermenter, drying of feed or cereals and other processes. However, the use of waste heat from the methanol process is not worthwhile, as a heat output of around 10 kW is not economically viable in terms of the infrastructure to be installed. Accordingly, only the waste heat from the CHP could be used in the entire concept.

Table 5.2: Results of the heat integration of several modules.

Module	Heat demand (MJ/kg_{MeOH})
CP-1	-0.61
CP-2	-0.65
CP-4	-0.07
R-1	-1.65
H-4	-0.10
V-1	-0.11
V-2	-0.09
V-3	-0.50
REB	1.62
COND	-3.41

The product streams of methanol and H_2O can be taken from the process simulation, as well as the required amount of H_2. This can be determined from the desired molar ratio of H_2 to CO_2 in front of the reactor, whereby the molar ratio is specified in Aspen Plus and the programme calculates the required mass flow at the inlet from this. This results in the mass flows listed in Table 5.3 for the four calculated applications with their respective available CO_2 quantities. The mass flows of CO_2 are derived from the respective raw biogas flows listed in Table 4.14, together with the proportion of CO_2 in these. For case 2, slightly more than half of the available quantity of CO_2 is available compared to the standard case. For case 3, the amount of CO_2 is made up of the amount contained in the raw biogas and the amount converted from CH_4, resulting in slightly more than twice the amount compared to the standard case. The mass flows can then be used to calculate the required raw material flows and the quantity of H_2O produced in relation to the amount of methanol produced. The results are shown in Table 5.4. This shows that 1.376 kg of CO_2 are needed to produce 1 kg of methanol and 0.563 kg of water is produced with each kg of methanol produced. In addition, 0.187 kg of H_2 are required for each kilogram of methanol produced. These values correspond well with the values calculated by SCHEMME (2020) for the large-scale plant. Therefore, there are no differences due to the plant size with regard to this.

Table 5.3: Required raw material and product flows according to the process simulation carried out in this thesis.

Mass flow (kg/h)	Case 1	Case 2	Case 3	Case 4
CO_2	34.29	18.76	75.79	171.83
H_2	4.67	2.55	10.32	23.41
MeOH	24.92	13.63	55.08	124.86
H_2O	14.02	7.67	31.00	70.27

Table 5.4: Raw material and product mass flows in relation to the methanol produced.

	Raw material and product flows			
Unit	H_2	CO_2	MeOH	H_2O
kg/kg_{MeOH}	0.187	1.376	1	0.563

Furthermore, the flows of operating utilities relevant for the cost estimation can be determined for the four cases investigated. These include the electricity required for operating the compressors, the cooling water for the condenser and the steam required for the reactor and reboiler. To calculate the total electricity demand, the demand of the individual compressors can be added together. Aspen Plus provides the compressors' demand. This results in the quantities listed in Table 5.5 for the four cases. To determine the cooling water and steam requirements, Aspen Plus defines corresponding "utilities" which give an output for the respective operating flows. The results are also shown in Table 5.5. It is apparent that only small quantities of all operating materials are required for a small plant. The quantities scale proportionally to the existing plant size. In the standard case, the required annual electricity quantity of 105,230 kWh is below the minimum limit of 160,000 kWh which is required to achieve the price of electricity for industrial users. Nevertheless, this price is assumed, since the total purchase quantity together with other plant components and other devices is presumably higher so that the limit is reached.

Table 5.5: Required utility flows according to the process simulation performed in this thesis.

Utility flows	Unit	Case 1	Case 2	Case 3	Case 4
Electricity	kW	12.38	6.77	27.36	62.03
Cooling water	t/h	4.07	2.23	9.00	20.41
Steam	t/h	0.023	0.013	0.052	0.11

In addition to the process conditions relevant for the operating costs, relevant process parameters for the individual modules can also be taken from the simulation. These are required for module design and for manufacturer enquiries. Process parameters include the temperatures, pressures, the composition of the mixture and the mass flows at different stages of the process. The results obtained for the mass flows, temperatures and pressures for the standard case can be found in Table 5.6, whereby the positions of the individual flows correspond to the process flow diagram that is shown in Figure 4.4.

Table 5.6: Important parameters of the process flows for the standard case (case 1) according to the process simulation performed in this thesis.

Flow	Mass flow (kg/h)	Temperature (°C)	Pressure
S-1	4.67	25	10 bar
S-2	34.29	25	1 bar
S-3	119.01	89	80 bar
S-4	119.01	230	80 bar
S-5	119.01	250	80 bar
S-6	119.01	149	80 bar
S-7	119.01	84	75 bar
S-8	78.69	80	75 bar
S-9	40.32	80	75 bar
S-10	40.32	55	1 bar
S-11	2.20	55	1 bar
S-12	0.87	42.35	1 bar
S-13	1.33	158.28	80 bar
S-14	41.47	55	1 bar
S-15	41.47	80	1 bar
S-16	14.02	28.67	1 bar
S-17	27.42	64.07	1 bar
S-18	2.48	62	1 bar
S-19	24.92	62	1 bar

The flows S-1 and S-2 represent the reactant flows of H_2 and CO_2. These are mixed with the two recycled flows S-8 and S-13 to form flow S-3. This results in the mass flow of 119.01 kg/h that is fed to the reactor. The large quantity is due to the low conversion in the reactor. Thus, a share of about 2/3 of the total mass flow must be recirculated. Only 40.32 kg/h leave vessel B1 at the pit and are processed further. This finally results in the two product streams S-16 and S-19, where S-16 is the by-product H_2O and S-19 the desired methanol. Table 5.7 shows the composition of flows consisting of the five components CO_2, H_2, CO, H_2O and MeOH in wt%. The two raw material flows CO_2 and H_2 are assumed to be 100% pure. After the reactor, the mixture has a weight proportion of methanol of only about 1/4. Due to the numerous separation steps, a methanol purity of 99.898 wt% and a water purity of 99.81 wt% can finally be achieved. For the three other cases, the temperatures, pressures and compositions are those of the standard case, as these are the determined settings by the process modelling. Only the mass flows differ between the cases, which is why the results of these are shown in Table A 3 in appendix A. With the parameters described in this section, all the variables required for the cost estimation are known.

Table 5.7: Composition of the process flows according to the process simulation performed in this thesis.

Flow	Composition (wt%)				
	CO_2	H_2	CO	H_2O	MeOH
S-1	0	100	0	0	0
S-2	100	0	0	0	0
S-3	78.39	14.36	2.89	0.59	3.77
S-4	78.39	14.36	2.89	0.59	3.77
S-5	49.6	10.41	2.89	12.38	24.72
S-6	49.6	10.41	2.89	12.38	24.72
S-7	49.6	10.41	2.89	12.38	24.72
S-8	73.35	15.73	4.38	0.89	5.65
S-9	3.25	0.01	0	34.78	61.96
S-10	3.25	0.01	0	34.78	61.96
S-11	59.8	0.2	0.06	4.5	35.44
S-12	3.24	0	0	11.38	85.38
S-13	96.52	0.34	0.1	0.03	3.01
S-14	0.82	0	0	33.82	65.36
S-15	0.82	0	0	33.82	65.36
S-16	0	0	0	99.81	0.19
S-17	1.245	0	0	0.005	98.75
S-18	12.77	0	0	0	87.23
S-19	0.097	0	0	0.005	99.898

5.1.2 *Cost estimation of the standard case*

Results of the module design

The module design is the basis for the cost estimation and is carried out for all main modules except for the column, as no data for calculation is available. The procedure described in section 3.1.1 and section 4.2.2 is applied for the respective modules. For this purpose, the required values from the process simulation are used, which can be found in Table 5.6 and Table A 4 in appendix A. The respective calculated size parameters are listed in Table A 5, with the value for the column given for case 1 coming from subsequent manufacturer enquiries. When the calculated size parameters for case 1 are compared to the lower capacity limits given in Table 3.4, they are much lower. The calculated capacities of the compressors for case 1, e.g., lie in the range between 0.26 kW and 6.24 kW, whereas the lower capacity limit has a value of 450 kW. As the surcharge factor method assumes the value of the lower limit if the size parameter falls below it, it

can be assumed that the costs calculated with this method will exceed the actual costs. The other components also fall below the capacity limit, except H-1 which is with 10.99 m² above the limit value of 10 m². Due to the large gap of all components to the lower capacity limit (except H-1), the module costs are determined by means of manufacturer enquiries. H-1 is also part of these enquiries, as this would involve only a small amount of additional work and more accurate results can be achieved by this method.

Module prices resulting from manufacturer enquiries

For the requests of module costs, suitable manufacturers are investigated, who produce one or more of the required modules in the desired size. A total of about 30 manufacturers were contacted and feedback was received from about two thirds of them. These also included negative feedback and follow-up queries that did not result in offers. In the end, module prices could be obtained from ten manufacturers, with at least one price for each module. Table 5.8 lists the manufacturers from whom component prices were received. In addition, an abbreviation is given for each manufacturer, which is used instead of the company name in the following. In the bibliography, the websites of the respective manufacturers are also listed.

Table 5.8: Manufacturers who supplied module prices.

Manufacturer	Abbreviation
B.Beger GmbH	Beger
ENVIMAC Engineering GmbH	Envimac
fluitec mixing + reaction solutions AG	Fluitec
Haug Sauer Kompressoren AG	Haug
Andreas Hofer Hochdrucktechnik GmbH	Hofer
Howden Thomassen Compressors B.V.	Howden
MAXIMATOR GmbH	Maximator
Julius Montz GmbH	Montz
Schwarz Systems GmbH	Schwarz
Viesel Apparatebau GmbH	Viesel

Table 5.9 shows the module prices obtained in the course of this work and with the corresponding manufacturer. It is noticeable that the module prices differ greatly from each other in some cases. For instance, four prices were obtained for compressor CP-1, with the highest price corresponding to about 3.5 times the lowest price. The biggest differences are found in compressor CP-4, where the most expensive offer exceeds the cheapest by a factor of 10. It should be noted that some manufacturers have only given indicative prices, while others made precise offers,

which can result in certain differences. In addition, different types of compressors were requested, which may give another explanation. The manufacturers HAUG and MAXIMATOR offer piston compressors (Kolbenverdichter), while the offers from HOFER and HOWDEN are for diaphragm compressors (Membranverdichter). The highest prices for the compressors come from HOWDEN in each case and the prices from HOFER are also significantly higher than the prices for the cheapest piston compressors. Therefore, it can be assumed that diaphragm compressors are more expensive than piston compressors. The prices used for further calculation are listed in Table 5.10 with the respective module type, whereby the lowest prices were used in each case. For comparison, the manufacturing costs are also calculated with the maximum prices for all modules, which is described as case 1B. The prices listed in Table 5.10 are adjusted to the year of calculation, i.e. 2019, with the adjustment being made using the CEPCI via equation 3.14.

Table 5.9: Module prices without value-added tax received from enquiries; prices marked with * are indicative prices. M = manufacturer.

Module	Offer 1		Offer 2		Offer 3		Offer 4	
	Price (€)	M	Price (€)	M	Price (€)	M	Price (€)	M
CP-1	102,700	Haug	174,790	Hofer	200,000*	Maximator	359,500	Howden
CP-2	121,200	Haug	293,980	Hofer	365,500	Howden		
CP-3	25,000*	Maximator						
CP-4	30,000*	Maximator	73,100	Haug	351,750	Howden		
R-1	60,000*	Fluitec						
H-1	4,820	Viesel	10,755	Beger				
H-2	4,500	Beger						
H-3	8,640	Beger						
H-4	3,780	Beger						
H-5	4,010	Beger						
V-1	2,575	Beger	4,250	Schwarz				
V-2	790	Beger	2,950	Schwarz				
V-3	780	Beger	2,850	Schwarz				
C-1	53,450*	Envimac	56,000	Montz				
COND	6,800	Beger						
REB	4,100	Beger						

Also included are the transport costs and the direct and indirect cost factors. A value of 1% on the purchase price is calculated for the transport costs, since HAUG offered precise transport costs for the three compressors, which lie in this range. As it can be assumed that the transport costs of the compressors are higher than the transport costs for most of the other components, these are taken as a general value. This is because the compressors are large and heavy components. The heat exchangers, tanks and the reactor, on the other hand, are much smaller and lighter and thus easier to transport. Only the column could incur higher transport costs, but this is offset by the lower transport costs of the other components. The values from Table 4.11 are used for the direct and indirect component cost factors. It shows that for all four compressors the piston compressors are the cheapest, which is why these are used. This means that the compressors differ from the design in the process simulations, in which centrifugal compressors were assumed. The used piston compressor CP-1 from HAUG has a length of 2.1 m, a width of 1.3 m and a height of 1.2 m with a weight of 850 kg. Compressor CP-2 has the same length and height with a width of 1.4 m and a weight of 1100 kg. The prices quoted for both compressors include an electric control. All parts that come into contact with the process gas are made of stainless steel. The remaining parts, the plant and compressor frames are made of steel. For the CP-3 and CP-4 compressors, indicative price quotations from MAXIMATOR are used. Therefore, no exact data is available for these. It can be assumed that these compressors are smaller and lighter than CP-1 and CP-2 due to their lower capacities. For all other modules, the module types are used that were also assumed for the size calculation. The reactor from the company FLUITEC has a length of 1.5 m to 2.5 m and a diameter of 250 mm. The volume of at least 0.375 m³ is thus significantly higher than the volume calculated in this study. It contains 52 tubes and the material used is 1.4571 stainless steel. The heat exchangers, which also include the condenser and reboiler, are also made of either 1.4571 or 1.4404 stainless steel. No size information is available from the manufacturer BEGER . The tanks are made of material 1.4301 and have the calculated size. The column is designed as a packed column. From the information provided by the manufacturer ENVIMAC , it can be inferred that a column height of about 7 m and a diameter of 200 mm is expected. This results in a volume of 1.4 m³.

The costs listed in Table 5.10 correspond to the total module costs C_{TM} from the method of TURTON et al. (2009, p. 213) and can be used in equation 3.11 to determine the investment costs of the plant. The total costs of all components added together as well as the investment costs can be found in Table 5.12. There, the total costs are also given when using the highest component prices in each case.

Table 5.10: Module costs converted to 2019 incl. transport costs as well as indirect and direct module cost factors of the standard case.

Module	Size parameter	Price (€)	Manufacturer	Module type
CP-1	6.24 kW	354,736.78	Haug	Piston compressor
CP-2	5.32 kW	418,637.76	Haug	Piston compressor
CP-3	0.62 kW	86,352.67	Maximator	Piston compressor
CP-4	0.26 kW	103,623.21	Maximator	Piston compressor
R-1	0.085 m³	207,246.42	Fluitec	Shell-and-tube, vertical
H-1	10.99 m²	16,648.80	Viesel	Shell-and-tube
H-2	0.74 m²	15,543.48	Beger	Shell-and-tube
H-3	5.44 m²	29,843.48	Beger	Shell-and-tube
H-4	0.45 m²	13,056.52	Beger	Shell-and-tube
H-5	0.04 m²	13,850.97	Beger	Shell-and-tube
V-1	0.0108 m³	8,894.33	Beger	Vertical
V-2	0.0085 m³	2,728.74	Beger	Vertical
V-3	0.0056 m³	2,694.20	Beger	Vertical
C-1	1.4 m³	184,622.02	Envimac	Filling material
COND	1.26 m²	23,487.93	Beger	Shell-and-tube
REB	0.15 m²	14,161.84	Beger	Shell-and-tube

Results of the operating expenditures

In addition to the investment costs, the operating costs are needed to determine the total costs of manufacturing. The methodology described in section 4.2.2 is used for this purpose. The OPEX are calculated via equation 4.26. For this, the raw material costs C_{RM} must be determined via equation 3.20 and the utility costs C_{UT} via equation 3.21. The required quantities of the different raw materials and inputs are taken from the process simulation and are listed in Table 5.3 and Table 5.5. For the calculation, the costs per unit of the raw materials and utilities are also necessary. The operating utilities are taken from the literature and can be found in Table 4.12. For the raw materials, the costs are calculated or converted.

The CO_2 costs for the biogas upgrading are usually given in relation to the biomethane in €/kWh, since the separated CO_2 in current plants is the unwanted gas component that is separated. Therefore, the costs have to be converted to the CO_2. For the standard case, the costs come from the commercially operated plant type "BlueFEED" from the company APEX AG (n.a.). The costs for gas separation by means of membrane processes for a gas flow of approximately 40 m³/h are given at 0.032 €/$kWh_{biomethane}$ (OESTER, 2019). However, it does not take into account

the post-combustion of the flue-gas that is necessary for the application. This is because in the case of the conventional upgrading plant, the CO_2-rich flue gas stream is released into the atmosphere, as it is not needed. Therefore, the costs for post combustion of 0.0071 €/kWh$_{LHV}$ from BEYRICH et al. (2019) are added to the price, since they specify the costs individually. The costs of fine desulphurisation, i.e. of activated carbon, is also added to the costs of the raw material CO_2. For the small-manure plant, a cost of 1.22 €-ct/kWh and for the large plant, a cost of 2.19 €-ct/kWh are required. Converting and adding this to the cost for CO_2 gives a CO_2 price of 234.29 €/t, according to a calculation using equation 4.27. Compared to CO_2 costs from the literature for biogas upgrading which can fall below 100 €/t$_{CO2}$, these costs are significantly higher. From this, it can be seen that the costs per tonne of CO_2 are lower for larger biogas upgrading plants. The CO_2 costs from industrial waste gases are also lower than the costs for this application. Only the costs for CO_2 capture from ambient air are currently higher than in the case under investigation.

In order to determine the H_2 costs, the costs of the individual components needed for this application are calculated. The procedure is already explained in section 4.2.2 and the basic prices used for the WTG and the electrolyser are given in Table 4.13. The capacities result in the production costs per kg of H_2 listed in Table 5.11, divided for the three components WTG, electrolyser and storage, as well as the total costs of H_2, which are needed for the calculation of the methanol plant. The calculated costs of 8.93 €/kg$_{H2}$ are much higher than the H_2 costs for larger plants in the literature, which are about half of it. The difference between the calculated costs in this study and the costs from the literature is largely due to the higher investment costs of the electrolyser. Current investment costs of 1470 €/kW are assumed, while literature assumes 500 €/kW for 2030 to 2050. Using these costs, it would be possible to reduce H_2 costs to 6.57 €/kg$_{H2}$. Since the investigation in this study is carried out for 2019, the higher investment costs are used. For the future, however, it can be assumed that these costs will decrease. The calculated raw material and input costs can then be used in equation 4.26 to calculate the operating costs. In addition, the previously calculated FCI are needed. Together with these, the operating expenditures result, which can be found in Table 5.12.

Table 5.11: Results of the hydrogen costs from the three components wind turbine generator (WTG), electrolyser and storage.

	Unit	Components			Total
		WTG	Electrolyser	Storage	
Capacitiy	kW	1040	950	-	
COM_{kg}	€/kg$_{H_2}$	3.37	3.91	1.65	8.93

Results of the costs of manufacturing

The costs of manufacturing (COM) can be calculated from the investment and operating costs. For this, the investment costs must first be converted into annual capital costs (ACC) using equation 3.23. These can then be used together with the OPEX in equation 3.22 to determine the COM. The results of the module costs as well as the total COM and the specific costs can be found in Table 5.12 for the standard case (Case 1) and under the assumption of maximum module costs (Case 1B). It is evident that the specific manufacturing costs per kilogram of methanol of 4.41 €/kg are much higher than the market price of methanol in September 2020, with a value of 0.275 €/kg (METHANEX, 2020). They are also higher than that of larger methanol plants based on a similar process design. SCHEMME (2020) calculated costs of 1.049 €/kg for a 300 MW methanol plant and costs of 1.119 €/kg for a 20 MW plant. Compared to the large-scale plant, the COM have more than quadrupled.

Table 5.12: Results of the calculation of the cost components and the manufacturing costs for the standard case and the case with maximum module costs.

Cost component	Unit	Standard case (case 1)	Maximum module costs (Fall 1B)
Module costs*	€	1,496,129.16	4,388,045.67
FCI	€	1,776,653.38	5,210,804.23
CAPEX	€	2,090,180.44	6,130,357.92
ACC	€/a	206,038.24	604,296.22
OPEX	€/a	728,476.76	1,245,501.20
COM	€/a	934,515.00	1,849,797.42
COM_{kg}	€/kg	4.41	8.73
COM_L	€/L_{GE}	7.14	14.12

*incl. transport costs as well as indirect and direct factors

For the calculation of the COM using the maximum component prices, the manufacturing costs are doubled. For better illustration, Figure 5.1 shows the calculated manufacturing costs per kilogram of product for the standard case and for the case with maximum module cost. The total costs are divided into the six cost components H_2 costs, CO_2 costs, utility costs, annual capital costs, remaining direct operating costs, and fixed and general operating costs.

Figure 5.1: Specific costs of manufacturing (COM) for the standard case and the maximum module costs, divided into six cost components.

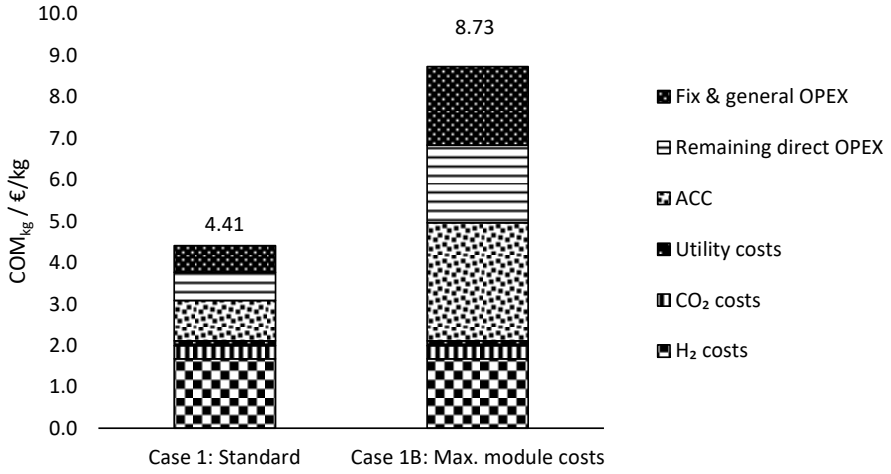

Caption: OPEX = Operational expenditures, ACC = Annual capital costs.

In the standard case, the H_2 costs account for the largest share of the COM, followed by the ACC, which account for a larger share in contrast to large-scale plants. The ACC account for a share of 22.0%, whereas they account for only 2.6% in the large-scale plant examined by SCHEMME (2020). The author's calculation is based on the year 2030, which is why lower H_2 costs are assumed among other things. Nevertheless, it can be seen that the share of ACC is significantly lower than in this study, as the share of ACC would be even lower if the higher H_2 costs assumed in this study were used. In the calculation with the maximum module costs, the ACC represent the largest share. The remaining direct OPEX, which include costs for maintenance and repairs, costs for operating supplies and costs for patents and royalties as well as the fixed and general operating costs also increase. This is due to them being calculated using general factors that are linked to the FCI as can be seen in Table 3.6. The H_2, CO_2 and utility costs remain constant, as no changes are made to the plant and therefore the same quantities are required.

5.1.3 *Cost estimation of the other cases*

Carbon dioxide costs for the biogas oxyfuel process adapted with manufacturer prices

This section adapts the CO_2 price for case 3 (biogas oxyfuel process). The COM for the CO_2 in this case can decrease significantly if actual quotation prices from

manufacturers are taken. According to LOHSE (2019) and SCHORN et al. (2020), the CAPEX are calculated for 2018 using the method by TURTON et al. (2009), although the permissible limit values for the calculation are not reached. Therefore, the costs for the fan and heat exchanger are likely to be overestimated. That is why the quotation price received from manufacturers for the heat exchanger H-1 is used and adjusted to the size of case 3. As the heat exchanger is responsible for the majority of the cost and its price would decrease by a factor of 7, the FCI can thus be decreased significantly. They are shown in Table 5.13 as a comparison. Since the fan is calculated without manufacturer prices, the cost estimated is possibly still too high, but no additional data is available.

Table 5.13: Module costs and fixed capital investment (FCI) of the biogas oxyfuel process for a small-manure plant (75 kW) from LOHSE (2019) and this study.

Source	Heat exchanger (€)	Fan (€)	FCI (€)
LOHSE (2019)	118,068.26*	15,439.70*	144,375.00*
This study	16,648.80	15,439.70*	32,088.49

*adjusted to 2019, exchange rate of 2019 (1.12 $/€).

The OPEX in this study are higher compared to SCHORN et al. (2020). On the one hand, the OPEX are adapted from 8000 to 8500 FLH, and, on the other hand, the loss in revenue (LIR) considers a higher electricity price of 22.14 €-ct/kWh compared to 15 €-ct/kWh. This price is normally achieved by small-manure plants. The electricity demand of the fan is calculated for 0.275 kW, using an electricity price of 0.169 €/kWh, which sums up to costs of 395.04 €/a. Compared to SCHORN et al., a higher amount of CO_2 is generated, as they only assumed a composition of CO_2 in biogas of 40% and due to the higher FLH. Thus, instead of 500 t/a, the plant generates 644.2 t/a.

In total, it can result in CO_2 costs of 38.87 €/t compared to 88 €/t, causing COM_{kgMeOH} of 3.17 €. If the OPEX are simply based on the cost of the electricity demand of the fan, as the loss in revenue (LIR) can be considered in the OPEX of the BGP, it results in an even lower CO_2 price of 5.93 €/t. As the CO_2 price does not contribute significantly to the system, the COM_{kgMeOH} could only be reduced to 3.13 €. The cost estimates and the effect on the manufacturing price of methanol are shown in Table 5.14.

Table 5.14: Cost estimates of the annual capital cost (ACC), the capital expenditures (CAPEX) and the annual operational expenditures (OPEX) for the COM of CO_2 and methanol of case 3 (Biogas Oxyfuel Process*).

	FCI (€)	ACC (€)	OPEX (€)	Produced CO_2 (t/a)	COM_{kgCO2} (€/kg)	COM_{kgMeOH} (€/kg)
With LIR	32,088.49	3,425.31*	21,613.46**	644.22	38.87	3.17
Without LIR	32,088.49	3,425.31*	395.04***	644.22	5.93	3.13

* Interest rate of 7% and 20-year investment period according to SCHORN et al. (2020), ** including the loss in revenue (LIR) from the decreased efficiency of the combined heat and power plant, *** not including the LIR.

Cost of manufacturing

This section presents the results of the cost estimation for the cases 2, 3 and 4 introduced in section 4.2.3. The procedure is largely analogous to the standard case. First, the cases are simulated in Aspen Plus, whereby the results have already been presented in section 5.1.1. For the calculation of the manufacturing costs, the components are first designed according to the procedure described in the section module design in chapter 4.2.2. The results for the size parameters can be found in Table A 5 in appendix A. Since the effort to determine the module costs for all four cases from manufacturer inquiries exceeded the scope of this work, it is not possible to determine the component costs for all cases in this way. The manufacturers who submitted quotations for the standard case were randomly asked for further quotations for the modules used for case 3 (Biogas Oxyfuel Process) in order to determine the costs for cases 2 and 4, using the capacity method. However, only the module prices for the heat exchangers and the vessels can be obtained from the manufacturer Beger, which are listed in Table 5.15. As compared to the case 1 prices from Beger in Table 5.9, the prices for the two cases are very close to each other with no change in prices at all for H-1 and H-2. In fact, this depicts the problem with the capacity method. It only works with the support of manufacturers and their fair offers. If they do not want to or cannot give more detailed or more specific offers, the method will partly fail.

Since prices for case 3 are not available for all modules, it is not possible to calculate the module costs for case 2 and case 4 alone with own cost data. For this reason, degression coefficients are calculated by comparing the results for the

standard case with those of WALMAN (2018) for a 30 MW plant. Where cost data is available for case 3, degression coefficients are determined from these and the standard case. This promises more accurate results than the comparison with WALMAN (2018), as exactly the same components as well as more accurate prices from offers are available here.

Table 5.15: Component prices obtained for case 3 and calculated degression coefficients using the results of the standard case in relation to WALMAN (2018) or, if available, to case 3.

Module	Module cost (case 3) (€)	Coefficient of degression A	Coefficient of degression B
		Case 1 & Walman	Case 1 & case 3
CP-1	-	0.312	-
CP-2	-	0.313	-
CP-3	-	0.452	-
CP-4	-	0.452	-
R-1	-	0.267	-
H-1	10755	0.881	0
H-2	4500	0.907	0
H-3	8740	0.637	0.015
H-4	4165	0.559	0.123
H-5	4440	0.331	0.126
V-1	2700	0.709	0.068
V-2	880	0.515	0.156
V-3	825	-	0.081
C	-	0.180	-
COND	7580	0.246	0.137
REB	4630	0.424	0.154

The calculation is carried out according to the procedure described in section 4.2.3. The required size parameters of the modules of case 1 can be found in Table A 5 in appendix A. These are used as capacity S in equation 3.9. Furthermore, the module costs for the standard case including all factors are required, which can be found in Table 5.10 and are used as C. In addition, the sizes and costs of the modules from WALMAN (2018) are required, which are used for S_0 and C_0. These can be found in Table A 7 in appendix A. The designations of the modules have been adapted to the application in this study. For comparison, the designations from the source are also given.

To calculate the degression coefficients via the module prices of case 3, the calculated size parameters from Table A 5 are used for S_0 and the prices given in Table 5.15 are used for C_0. For S and C, the values for the standard case are used as before. This results in the degression coefficients for the modules listed in Table 5.15, whereby the degression coefficients between case 1 and WALMAN (2018) are denoted by A and those in the comparison between case 1 and case 3 by B. It should be noted that the components CP-3 and V-3 are not present in WALMAN (2018). Therefore, the degression coefficient of compressor CP-4 is used for CP-3, as it is a similar module. No calculation is necessary for vessel V-3, since a degression coefficient from the obtained prices is available here. For the reactor and the column, a calculation based on the size parameter is not possible. The size was not calculated for the column and, for the reactor, costs in WALMAN (2018) are given separately for vessels and pipes based on volume and heat transfer area. However, no separate costs for these parts can be taken from the manufacturer's price. Therefore, the plant capacities are used as size parameters for both of these modules. WALMAN (2018) has a plant capacity of 30 MW. The capacities of the methanol plant for the four cases can be taken from Table 4.14. A comparison of the degression coefficients shows large differences. The degression coefficients for A are significantly larger than for B. Values in the range of 0.6 (A), reflect the scaling of large-scale plants. In case of B, the economies of scale are very small, as the scope is in the range of prototype construction and the degression effect is more relevant when producing higher unit numbers. If available, the degression coefficients of B are used in the following, as these are better adapted to the present application. For the heat exchangers H-1 and H-2, however, degression coefficients of zero result, since the two module prices obtained are the same. This would mean no change in costs for all four cases for these components, which is considered unrealistic. One reason for the same prices is that they are estimated by the manufacturers based on effort, which presents a problem of requests for quotations in early project phases. Therefore, the degression coefficient of H-4 is used for these two modules, as it has a more realistic value. The degression coefficients from WALMAN (2018) are particularly high for these modules. This is due to the fact that they are based on higher numbers of units and for plants with a high readiness for marketing. Thus, the effect is only transferable for certain plant sizes, while prices of prototypes, as used in this case, are expected to have higher uncertainties. Therefore, the degression coefficients for the heat exchangers by WALMAN (2018) are not used. Equation 3.8 is used to calculate the total module costs C_{TM} for the different cases. In addition to the degression coefficient d, the size parameters for each module for the standard case are required, which are used for S_0, as well as the size parameters for the calculated case for S. The calculated size parameters can be found in Table A 5. In addition, the costs of the components for the standard case are required, which can be found in Table 5.10. They are used for C_0. This

results in the component costs for the cases which can be found in Table 5.16. The costs given there are already converted to the year 2019 and include transport and direct and indirect module cost factors. Cost drivers are the compressors CP-1 and CP-2 as well as the reactor and the column.

Table 5.16: Module costs converted to 2019 incl. transport costs as well as indirect and direct module cost factors for case 2 to case 4.

Module	Total module costs C_{TM} (€)			Degression coefficient
	Case 2	Case 3	Case 4	
CP-1	293,939.00	454,190.73	586,128.94	0.312
CP-2	346,605.73	536,540.76	693,098.64	0.313
CP-3	65,795.64	123,575.98	178,816.84	0.452
CP-4	78,856.81	148,171.84	214,479.06	0.452
R-1	176,370.12	256,175.77	318,837.29	0.267
H-1	15,476.34	18,376.23	20,322.44	0.123
H-2	14,454.44	15,543.48	18,940.34	0.123
H-3	29,583.63	30,188.89	30,550.12	0.015
H-4	12,145.77	14,386.36	15,906.46	0.123
H-5	12,689.85	15,336.23	16,749.00	0.126
V-1	8,534.97	9,326.09	9,930.94	0.068
V-2	2,484.58	3,039.61	3,506.72	0.156
V-3	2,566.80	2,849.64	3,070.12	0.081
C-1	165,593.96	212,984.73	246,844.09	0.180
COND	21,625.08	26,182.13	29,292.74	0.137
REB	12,853.65	15,992.52	18,075.15	0.154

The module costs determined in this way can then be used to determine the investment costs of the overall system for the three cases. To determine the manufacturing costs, the OPEX must be recalculated for each case, as the quantities of required raw materials and utilities differ. These can be taken from the results of the process simulation and are already listed in Table 5.3 and Table 5.5**.** In addition to the different quantities, CO_2 costs adapted to the raw biogas flow are also assumed for each application, as these differ depending on the size of the biogas upgrading plant. The costs are listed in Table 5.15 for all four cases.

Table 5.17: Results of the conversion of CO_2 costs for the different cases.

	Unit	Case 1	Case 2	Case 3	Case 4
Price	€/t_{CO_2}	234.29	268.54	38.87	218.08
Source		OESTER (2019)	OESTER (2019)	Adapted from SCHORN et al. (2020) as explained in section above	BEYRICH et al. (2019)

The costs for case 1, 2 and 4 are calculated via conversion using equation 4.27. For case 1 and 2, the costs for the commercial "BlueFEED" system from OESTER (2019) are used, which is available in various sizes. The costs for post-combustion are added to the prices given there, which are also given in Table A 6 in appendix A, as this is necessary for the use of the CO_2 stream. In the actual plant concept of "BlueFEED", the CO_2 is released into the atmosphere and no post-combustion/after-treatment is carried out. Since the "BlueFEED" technology is not available in the size of case 4, the costs for this are taken from another source. Case 4 refers to an average BGP, so the costs of different separation processes are available. BEYRICH et al. (2019) give costs for amine scrubbing, membrane processes as well as PSA for this plant size, which all lie very close together. The costs given in Table 5.17 are the membrane process costs in order to be consistent with the other applications. Nevertheless, amine scrubbing and PSA could also be considered for this plant size and would produce similar costs. The costs for case 3 are calculated based on SCHORN et al. (2020) for the BOP and were explained in this sub-chapter in the section above.

For H_2 and the operating materials, the same costs as for the standard case are assumed in each case. This results in the costs listed in Table 5.18 for the individual cost components and the manufacturing costs. It can be seen that the specific manufacturing costs decrease as the size of the plant increases, which can be explained by the economies of scale already described in section 3.1.2. The rapid price reduction is due to the small degression coefficients, as there are only very small differences between the individual module prices.

Table 5.18: Results of the calculation of the cost components as well as the manufacturing costs for case 2 to 4.

Cost component	Unit	Case 2	Case 3	Case 4
Total module costs*	€	1,259,576.38	1,882,860.98	2,404,548.87
FCI	€	1,495,746.96	2,235,897.42	2,855,401.79
CAPEX	€	1,759,702.30	2,630,467.55	3,359,296.22
ACC	€/a	173,461.56	259,296.70	331,140.53
OPEX	€/a	482,899.22	1,225,915.24	2,715,116.76
COM	€/a	656,360.78	1,485,211.94	3,046,257.29
COM_{kg}	€/kg	**5.67**	**3.17**	**2.87**
COM_L	€/L_{GE}	**9.16**	**5.13**	**4.64**

*incl. transport costs as well as indirect and direct module cost factors

To illustrate this, the COM_{kg} for all four cases divided into six cost components are shown in Figure 5.2. It can be seen that the share of the annual capital costs in the specific COM decreases with increasing size, which can again be justified with the scale effect. This is because the module costs do not scale proportionally with the size of the plant, as can be seen from the degression coefficients. The costs for the H_2 and the operating materials remain constant across all cases, as they scale with the required quantities and are thus constant per kg of product. Only the CO_2 costs change depending on the plant, which is due to the different basic costs used in each case. This means that the larger the plant, the higher the share of raw material and operating material costs in the total costs, while the CO_2 costs decrease with increasing plant size. However, these costs seem to have hardly any impact on the total costs. The other OPEX depend on the FCI and therefore scale with them.

The H_2 costs make up a large part of the total costs with 1.67 €/kg_{MeOH}. In case 2, this corresponds to a share in COM of 29.5%, with the share of ACC slightly higher at 26.4%. In case 1, the share of ACC with 22.0% is below the share of H_2 costs with 37.9%. This trend continues in case 3 and case 4, so that in case 3 the ACC have a share of 17.5% and the H_2 costs 52.8%. This means that the H_2 costs account for more than half of the COM_{kg} in this case. In case 4, the share of H_2 costs is even higher at 58.3%. The ACC only account for a share of 10.9% in this case. It should be noted that the calculated degression coefficients between case 1 and 3 cannot be applied to an arbitrarily large capacity range, as this would lead to an underestimation of the costs for large plants and an overestimation of the costs for small plants. This must also be taken into account for the calculated costs of case 2 and 4, which are determined with the help of the degression coefficients.

Figure 5.2: Specific manufacturing costs for the four cases, indicating the capacities of the methanol synthesis plants, divided into six cost components.

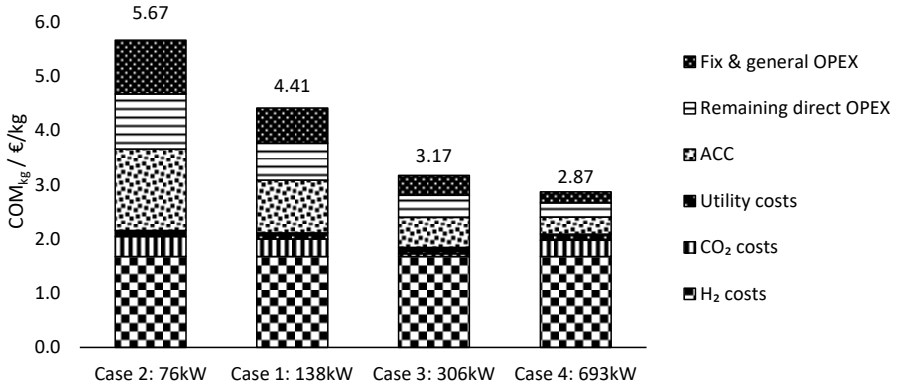

Caption: OPEX = Operational expenditures, ACC = Annual capital costs.

5.1.4 *Results of the sensitivity analysis*

Sensitivity analyses for the most important parameters are carried out for all cases, whereby the procedure was already described in section 4.2.4. The limits used for the standard case can be found in Table 5.19. For the other cases, only the values used for the FCI differ, since the costs of the corresponding case are used here. Moreover, the values for the CO_2 costs differ, as different basic values are assumed in each case. The lower limit of -50% of the CO_2 costs is assumed in all cases. For the upper limit of the CO_2 costs, a value of 491.69 €/t is assumed for case 1 and Case 2, which was converted from BEYRICH et al. (2019). For case 3 and case 4 this value is not realistic, as it is adapted to small membrane plants. Therefore, for these two cases, the standard limits of +50% to the basic value are used.

With the values used for the upper and lower limits from Table 5.19, the sensitivities for the standard case are shown in Figure 5.3 as a tornado diagram. The figure shows that out of the parameters examined, the H_2 costs and the FCI have the greatest influence on the production costs, followed by the interest rate and the CO_2 costs. By using the lower H_2 costs (4.6 €/kg), the manufacturing costs can be reduced by almost 1 €/kg. However, this value is still significantly higher than the costs for large-scale plants for renewable methanol synthesis. A reduction in H_2 costs alone is therefore not sufficient to make the small-scale plant competitive. This is due, among other things, to the larger share of ACC, which is also reflected in the increased influence of FCI on COM compared to large-scale plants.

Assuming the lower CO_2 costs, the COM can be reduced to 4.25 €/kg. If one assumes the CO_2 costs by means of amine scrubbing of 71 €/t (VIEBAHN et al., 2018) for large BGPs as a comparison, the COM result in 4.18 €/kg. This shows even more clearly that the influence of the CO_2 costs on the production costs is very small. All input costs in fact have a comparatively low impact on the COM. Reducing and increasing the costs of cooling water and steam can only change the COM_{kg} by one and two cents respectively. Electricity costs also have a very small impact of only a few cents. Thus, a significant change in COM through a change in the cost of operating materials is not possible.

Table 5.19: Values used for the variables to calculate the sensitivity for case 1.

Variable	Unit	Lower limit	Standard value	Upper limit
CO_2	€/kg	0.12	0.23	0.49
H_2	€/kg	4.60	8.93	13.40
Electricity	€/kWh	0.08	0.17	0.25
Cooling water	€/t	0.03	0.06	0.09
Steam	€/t	11.27	22.54	33.81
Interest rate	%	4	8	12
FCI	€	1,243,657.36	1,776,653.38	2,664,980.06

The results of the sensitivity analyses for the other cases can be found in Figure A 1, Figure A 2 and Figure A 3 in appendix A. When comparing the sensitivity analyses of the different cases, it can be seen that the influence of the FCI decreases with increasing plant size. In case 3, the H_2 costs have a greater influence on the manufacturing costs than the FCI. This is due to the lower share of the FCI. As a result, the influence of the H_2 costs increases with increasing plant size. For the other parameters, the sensitivities behave similarly to the standard case. The influence of the interest rate decreases with increasing plant size, as it affects the FCI, whose share decreases. The operating costs have a very small influence in all cases. Only the share of the CO_2 costs increases slightly except for case 3 where the influence is very small.

In addition to the sensitivity analyses for individual parameters, a "best subcase" and a "worst subcase" are also determined for each case, in which all varied parameters simultaneously assume the value of the upper and lower limit, respectively. The results obtained for the four cases examined can be found in Figure 5.4. The mean value at the border between the red and green areas represents the costs with the standard values. This shows the currently possible maximal potential for cost reduction as well as the most expensive case possible. For the

standard case, costs of 2.73 €/kg could be achieved in the best subcase, which is still well above the costs for similar process setups in large plants. For case 3 and case 4, costs could be achieved that come closer to the calculated costs for large-scale plants.

Figure 5.3: Results of the sensitivity analysis of case 1.

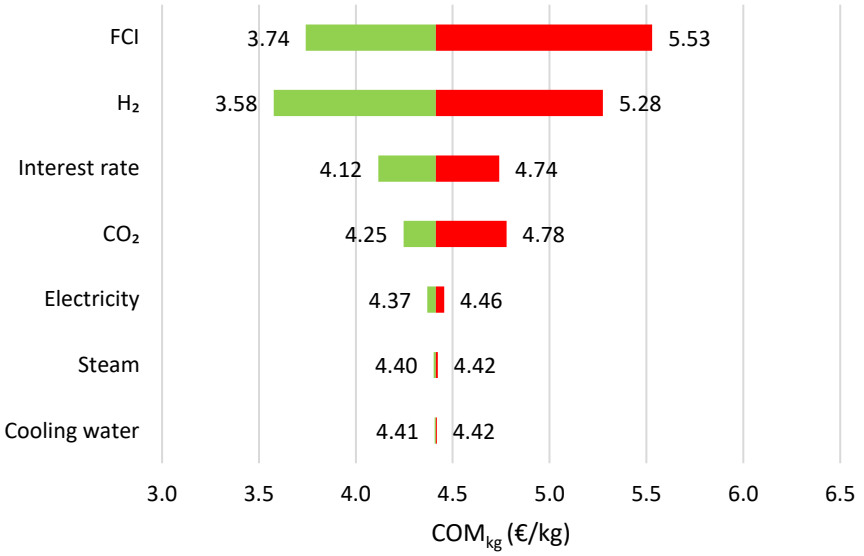

Caption: red colour means above original price, green colour means below it; FCI = fixed capital investment, COM = cost of manufacturing.

Figure 5.4: Results of the best and worst subcase scenarios of the four cases with the capacities of the methanol synthesis plant.

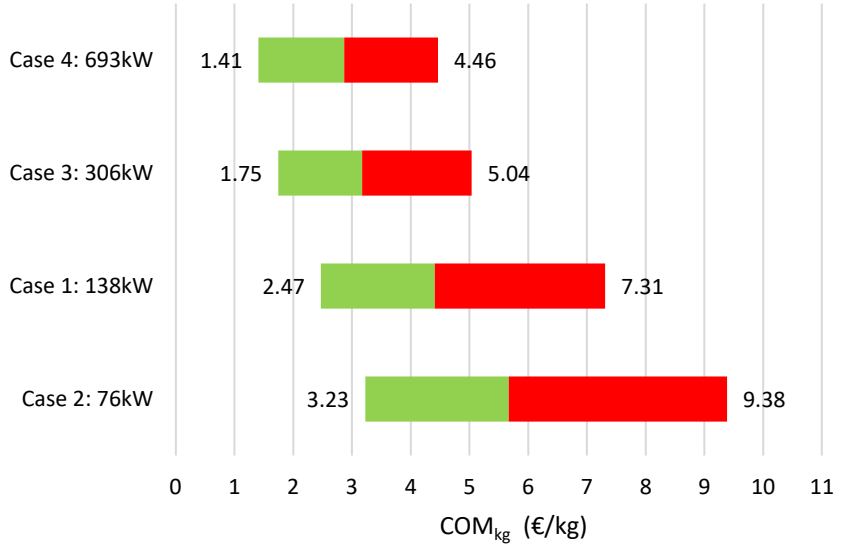

Caption: red colour means above original price, green colour means below it; COM = cost of manufacturing.

SCHEMME (2020) calculates the COM for a 50 MW plant at 1.119 €/kg and for a 300 MW plant at 1.049 €/kg. In comparison, the best subcase costs for case 3 are 1.75 €/kg and 1.41 €/kg for case 4. For better illustration, Table 5.20 shows the calculated "best subcase" costs of the four cases studied in relation to two cases studied by SCHEMME (2020). In conclusion, it can be said that the production costs of methanol from a small-manure plant and decentralised H_2 production via wind power are significantly higher than the costs of comparable technologies on a large scale. Moreover, the economic viability compared to the current methanol price is not given. Therefore, market introduction is difficult in the medium term.

Table 5.20: Classification of the plant sizes of the different cases and of SCHEMME (2020) in comparison to the respective specific manufacturing costs (COM_{kg}).

	Unit	Case 2	Case 1	Case 3	Case 4	SCHEMME (2020), 1	SCHEMME (2020), 2
Plant size	kW	76	138	306	693	50,000	300,000
COM_{kg}	kg/h	3.23	2.47	1.75	1.41	1.119	1.049

5.1.5 *Results of the cost analysis and possible revenues*

Costs and revenues of the biogas and biogas upgrading plants

A cost estimation for the biogas plant (BGP) is carried out to determine additional costs and revenues for the PtF system. The small plant from case 2 is not included as data is lacking about the plant. Moreover, no improvement in profitability is expected for an even smaller plant. The annual costs for biogas upgrading are calculated, using the price for CO_2 shown in Table 5.17 and multiplying it with the annual production of CO_2. For the BGP using the BOP, the price of 6.42 €/t is used as shown in Table 5.14. It does not include the LIR, as this is considered in the lower profits from electricity sales. The costs and revenues of the BGPs and biogas upgrading plants assumed in this study are shown in Table 5.21. Profits from the BGPs together with biogas upgrading or the BOP are equal to 140,299.90 €/a for the small-manure plant, 182,273.59 €/a for such a plant in combination with the BOP and 690,142.17 €/a for the large plant. The total costs for the small-manure plant are almost twice as high as the one with the BOP expansion, showing significant advantages for the BOP. The LIR due to lower heat and electricity sales loses about 21,200 €/a, but this is more than compensated for by lower manufacturing costs. Moreover, CO_2 sales are higher and become more relevant for an increasing CO_2 price. Under the aspect of GHG-quotas that are considered for alternative fuels, biomethane from BGPs and renewable methanol could reach even higher CO_2 sales.

Table 5.21: Costs and revenues of the biogas and biogas upgrading plants.

	75 kW	75 kW + BOP	500 kW
Biogas plant (€/a)	68,091.02	68,486.05	377,825.30
Biogas upgrading plant/Biogas oxyfuel expansion (€/a)	68,286.26	4,137.08	318,511.66
Total cost (€/a)	**136,377.27**	**72,623.13**	**696,336.96**
Electricity sales (€/a)	141,142.50	119,924.08	660,790.00
Heat sales (€/a)	43,316.00	33,542.13	286,563.90
Digestate sales (€/a)	61,092.59	61,092.59	154,695.64
Credit for discharging of manure (€/a)	23,838.14	23,838.14	247,916.67
CO_2 sales (€/a)	7,287.94	16,104.74	36,512.93
Total revenues (€/a)	**252,839.03**	**230,664.18**	**1,306,933.54**
Profits (€/a)	**140,299.90**	**181,878.55**	**690,142.17**

BOP = Biogas oxyfuel process.

The LCOE amounts to 11 €-ct/kWh for the small-manure plant, while the large plant shows specific costs of 9 €-ct/kWh. The BOP has the highest costs with 13.3 €-ct/kWh, but has the advantage to provide pure CO_2 for further usage. The plants would still be favourable under the current subsidisation scheme. Under the EEG, large plants above 150 kW have to expect future prices of 9-16.9 €-ct/kWh for inventory plants (Bestandsanlagen) and 14.9 €-ct/kWh for new plants, which underlines the problem of omitted financial support mentioned above (DANIEL-GROMKE et al., 2020). The LCOE can be found in Table 5.22. The specific costs for biogas upgrading are shown as well. The specific costs of 5.7 €-ct/kWh_{LHV} for the large plant are generally favourable, especially for a manure-based plant. Biogas upgrading is more expensive for the small plant, but with 7.2 €-ct/kWh_{LHV} prove to be competitive. Revenues from sales of biomethane are not taken into account here, but could be added if there was a possibility to feed it into the grid or sell it as a fuel. Nevertheless, the transport or a connection to the NG grid bears costs and thus must also be considered (DANIEL-GROMKE et al., 2020). As BGPs are often located in remote regions, such a concept would only work if plants are located optimally. For the PtF system, this is not of interest, thus, further analyses lie out of the scope of this work.

Table 5.22: The calculated levelised cost of electricity (LCOE) for the biogas plants investigated and the specific costs when including biogas upgrading.

	75 kW	75 kW + BOP	500 kW
LCOE (€/kWh_{el})	0.107	0.133	0.089
Specific costs for biogas upgrading (€/kWh_{LHV})	0.072	-	0.057

BOP = Biogas oxyfuel process.

Feasibility of the entire system

Economic feasibility of the entire concept is considered which includes annual manufacturing costs as well as annual revenues. The results are shown in Table 5.23. Here, the costs and revenues of the BGPs are also considered. The methanol production includes the biogas upgrading and H_2 production costs. For case 1, the COM for the methanol production are taken from Table 5.12. The COM of case 3 was adapted for excluding the LIR which is already considered in the lower electricity sales of the BGP. The COM for case 4 is taken from Table 5.18. In order to calculate the profits, methanol sales at a competitive price of 0.275 €/kg (METHANEX, 2020) are assumed. Profits are negative for the three cases investigated, amounting to -621,270.81 €/a for the small-manure

plant, -1.12 million €/a for the BOP and -1.60 million €/a for the large plant. It is evident that even without the costs of the BGP, the system is still unprofitable and revenues cannot compensate the costs.

In revenues from co-products, electricity sales are the most relevant, but would have to increase by a factor of 5 to make case 1 profitable. This requires an electricity price of 1.20 €/kWh, which is very unlikely. In the BOP case, the higher methanol sales compensate for the lower income from heat and electricity sales. If the owner of the BGP takes manure from a livestock farm, which has an excess of it, it is possible to receive a remuneration for it. In the calculation of manufacturing costs described above, this is not taken into account, as small-manure plants mostly utilise the manure they produce themselves and rarely require additional amounts. However, if one assumes a remuneration of 10 €/m³ for the purchase of manure, a revenue of 23,838.14 €/a would be achieved for the standard case. This would result

Table 5.23: Annual profits by the entire Power-to-Fuel system presented for the cases 1, 3 and 4.

	Case 1	Case 3	Case 4
Manufacturing costs			
Biogas plant (€/a)	68,091.02	68,091.02	377,825.30
Methanol production (€/a)	934,515.00	1,485,211.94	3,046,257.29
Total costs (€/a)	**1,092,561.90**	**1,624,281.02**	**3,515,262.51**
COM_{kg} (€/kg)*	4.73	3.32	3.23
Revenues			
Electricity sales (€/a)	141,142.50	119,924.08	660,790.00
Heat sales (€/a)	43,316.00	33,542.13	286,563.90
Digestate sales (€/a)	61,092.59	61,092.59	154,695.64
Credit for discharging of manure (€/a)	23,838.14	23,838.14	247,916.67
Methanol sales (€/a)	58,241.15	128,749.03	291,860.25
Oxygen sales (€/a)	46,416.88	46,416.88	149,903.40
CO_2 sales (€/a)	7,287.94	16,104.74	36,512.93
Total revenues (€/a)	381,335.20	429,667.60	1,828,242.78
Profits	-621,270.81	-1,124,030.39	-1,595,839.81

* If the system is not considered as an expansion, but including the biogas plant; BOP = Biogas oxyfuel process.

in production costs of 4.30 €/kg of methanol. Hence, the COM would only decrease by a few cents. A price for the digestate of 25.8 €/t is assumed according to

WEICHGREBE (2015), which results in annual revenues of 61,092.59 €/a for case 1. As the BGP owner usually uses the digestate as fertiliser on their own fields, the revenues from digestate could also be seen as a cost saving for not having to purchase mineral fertiliser. The O_2 from the production of H_2 could also be sold. A price of 150 €/t is assumed according to RIVAROLO et al. (2016). At a quantity of almost 310 t/a of O_2, an additional annual revenue of 46,416.88 € could be achieved for the standard case. If a CO_2 price of 25 €/t is considered, an additional revenue of 7,287.94 €/a could be achieved from not having to buy the CO_2 from the market. If the price is as high as 250 €/t, revenues of 72,879.35 €/a are reached. Revenues from CO_2 sales double for case 3 compared to case 1, which make this case more interesting in terms of that. However, only at a CO_2 cost greater than 2,160 €/t in the standard case would the profit be equal to zero. This scenario is not realistic, at least in the foreseeable future.

Further considerations of market introduction

Costs could decrease under certain conditions, e.g., if standardisation and simplifications are introduced. Especially, the investment cost of the methanol plant needs to be reduced as it is one of the main cost drivers for the standard case. The membrane upgrading technology developed by the Apex AG presents an example that has become profitable due to standardisation. Higher production quantities of modules of the methanol plant could, thus, potentially beat down the price of the entire plant. The concept of an 80% learning curve is applied to the FCI in order to see the effect of an increase in numbers of pieces. This approach follows the assumption that each duplication of the production decreases the costs by 20%. The costs that can be reached for case 1, 3 and 4 are shown in Table 5.24. The FCI would, hence, significantly decrease and only be less than a tenth of the costs today.

Table 5.24: Module costs when adjusted by a learning curve of 80%.

Module	Number of pieces	Case 1 Module cost (€)	Case 3 Module cost (€)	Case 4 Module cost (€)
CP-1	1000	38,381.50	49,142.13	63,417.46
CP-2	1000	45,295.40	58,052.17	74,991.28
CP-3	1000	9,343.11	13,370.57	19,347.47
CP-4	1000	11,211.73	16,031.77	23,206.02
R-1	1000	22,423.47	27,717.48	34,497.28
H-1	1000	1,801.35	1,988.26	2,198.83

H-2	1000	1,681.76	1,681.76	2,049.29
H-3	1000	3,228.98	3,266.35	3,305.43
H-4	1000	1,412.68	1,556.56	1,721.03
H-5	1000	1,498.63	1,659.34	1,812.19
V-1	1000	962.34	1,009.06	1,074.50
V-2	1000	295.24	328.88	379.42
V-3	1000	291.51	308.32	332.18
C	1000	19,975.57	23,044.34	26,707.82
COND	1000	2,541.33	2,832.83	3,169.39
REB	1000	1,532.27	1,730.34	1,955.68
Total	1000	161,876.87	203,720.14	260,165.27
Total today	1	2,114,217.52	2,583,108.13	3,197,559.16

The COM for the system as an expansion (system expansion) and the entire system (base scenario) with and without revenues is shown in Figure 5.5 as opposed to cost reduction opportunities. The costs for the system expansion, as investigated without any revenues, consider an expansion to an already existing BGP. Costs are calculated in sections 5.1.2 and 5.1.3. If the revenues generated by the system are also taken into account for the system expansion (incl. all possible revenues), it results in much lower COM_{kg} of 3.04 € for case 1, 2.60 € for case 3 and 1.38 € for case 4. This is due to the fact that revenues from the system can reduce the utility costs to one fourth which would cause the OPEX to almost cut in half. The costs for the entire system investigated, including the construction of the biogas plants, are also presented (Base scenario). The costs are obviously higher for the entire system, implying that an extension causes lower manufacturing costs. Nevertheless, it only saves a few cents. Here, the revenues make a relevant difference again.

A possibility for reduction in COM would be a decrease in the H_2 cost. This is likely to occur in the near future, as CAPEX for electrolysers are expected to decrease to 500 €/kW. Using the new H_2 price of 6.57 €/kg, calculated particularly for this farm-site application, would result in COM of 3.96 €/kg methanol for the standard case. The decrease is not high enough, as the storage and WTG still produce high costs. Therefore, another scenario is assumed, where costs for all H_2 generation modules, i.e. WTG, electrolyser and storage, are decreased by a factor of three to transfer the cost decrease of the CAPEX to the other modules. Hence, the storage and the WTG also decrease significantly in costs. If this is the case, a H_2 price of 3.22 €/kg is reached. For case 4, this would make a great difference, as COM_{MeOH}

would be 1.77 €/kg and get closer to the costs of large-scale plants. This is due to the fact that H_2 generation makes the highest contribution to COM in case 4.

Apart from this, a possible adaptation of the plant concept of the small-scale plant, which could lead to a reduction in costs, would be not to carry out all the steps up to the production of pure methanol at the site of the small-manure plant. Instead, the methanol-water separation in the column could be carried out at the site of a large-scale plant, so that one larger column could be used instead of many smaller columns. This would reduce investment costs and lead to a reduction in specific manufacturing costs of almost 10%. Another possibility is to use only one recirculation system, which would eliminate the need for some components, but also reduces the achievable purity. As the column is the most expensive module among the separation vessels, a scenario without the column would reach costs of 4.08 € for case 1 and 2.78 € for case 4 among others. Last but not least, the FCI from the 80% learning curve are used to calculate the COM of the base scenario. With these, COM_{MeOH} could reach 2.42 €/kg in case 1 and 2.04 €/kg in case 3.

Figure 5.5: Scenario results for costs of manufacturing for the methanol.

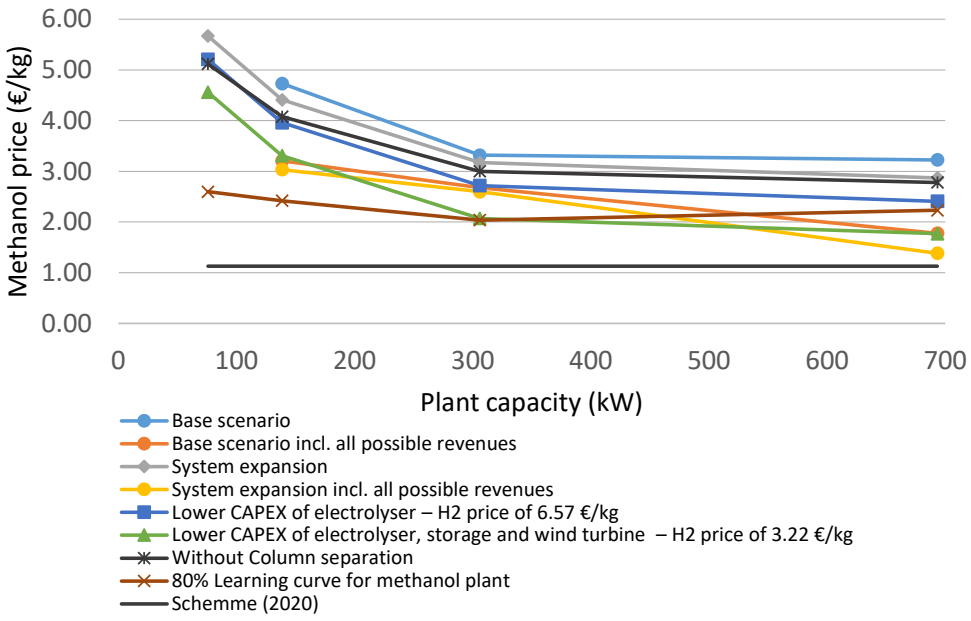

Caption: CAPEX = Capital expenditures.

The impact of the H_2 costs increases in case 4, which is why the decrease in FCI does not cause lower COM_{MeOH} compared to case 3, namely 2.23 €/kg. Hence, the decrease in FCI is especially interesting for the smaller cases, i.e. the standard case and case 3, as the FCI makes up the largest part of the COM. Especially for case 4, a combination of decreased H_2 costs as well as learning curves for the methanol plant could be interesting.

5.2 **Results of the life cycle assessment**

This sub-chapter presents and discusses the results of the LCA. The presentation follows in parts the results and discussion of the published paper by EGGEMANN et al. (2020). As some adaptations were made in the LCI, the results deviate from the ones presented before. The overall conclusion did not change, however. Only the values had to be adjusted, as the performance of the system was slightly worse. Moreover, the reference system has been expanded to consider two different possibilities for conventional methanol production in Germany. First, section 5.2.1 presents the results of the scenario analysis, second, these results are compared to the conventional methanol production system in section 5.2.2. Section 5.2.3 presents the results of the sensitivity analysis and section 5.2.4 discusses the results and LCA assumptions. Lastly, section 5.2.5 deals with the results and discussion of the additional LCA which focusses on the comparison of two biogas production concepts and adds to the debate whether or not to include manure savings of emissions through manure storage inside biogas systems.

5.2.1 *Scenario analysis*

The results of the LCIA are shown in Table 5.25. The majority of scenario formulations for the proposed PtF system yield negative values due to co-product credits, which offset net impacts from the integrated system itself. This translates into negative impact values per FU. Only the scenarios B1 to B3 that include replaced wind energy obtain positive values and thus environmental burdens for all categories but FD. The other scenarios also show positive values in POF and AP, mainly due to emissions from the CHP. In general, those scenarios that include replaced coal electricity generate the largest reductions across impact categories, the category of AP and ODP showing some exceptions. The worst scenario across all formulations is B2, which shows the greatest impacts across categories, with positive values for all categories but FD. When comparing the CC results amongst the scenarios, the lowest impact values in absolute terms, between -2.58 to -2.74 kg CO_2-eq., are achieved in scenarios C1 to C3. In both cases, CHP

electricity replaces electricity from coal as the most CO_2-intensive electricity mix. CC outcomes are quantified at values between -0.93 to -1.09 kg CO_2-eq. in scenarios A1 to A3, respectively, which consider the average electricity mix as an avoided process; by contrast, CC shows burdens of 0.84 to 1.00 kg CO_2-eq. in scenarios B1 to B3. When comparing scenario formulations that differ in terms of the fertilisers being replaced, scenario B2 generates the greatest impact for CC (1.00 kg CO2-eq.), while the lowest value is found for scenario C1 with avoided urea production (-2.74 kg CO2-eq.).

In general, the three scenarios including replacement of the MOP fertiliser (A2, B2 and C2) yield the highest values across all categories, which is due to the relatively higher content of K_2O (60%) in MOP, which translates into smaller environmental credits than those from replacing urea (46%) and SSP (20%). This means that for the same amount of valuable fertiliser, less MOP has to be produced compared to the others and, hence, less fertiliser is replaced, thus fewer credits are achieved. Fertiliser credits in all categories - except for CC - are the greatest when SSP is replaced, followed by urea and then MOP. In FD, SSP and urea replacement yield similar credits, as well as urea and MOP in freshwater EP. The lowest impact values for ODP are achieved in scenario A3 (-1.03 kg CFC-11-eq.), in which electricity from the grid is replaced, implying that the German grid mix causes more kg CFC-11 eq. emissions than coal-based electricity. The reason for this can be found in the composition of the average electricity mix in Germany, which includes a large share of NG according to Ecoinvent 3.5 (Wernet et al., 2016). As a result, electricity from the average German mix generates chlorofluorocarbon emissions (as CFC-11 eq.) in larger amounts per MJ compared to coal-based electricity.

Table 5.25: Results from the life cycle impact assessment of the different scenarios assessed for producing 1 kg of methanol by means of the Power-to-Fuel system proposed, as compared with conventional fossil-based methanol production.

	CC [kg CO_2-eq.]	FD [kg oil-eq.]	EP freshwater [kg P-eq.]	EP marine [kg N-eq.]	HT [kg 1,4-DB-eq.]	POF [kg NO_x-eq.]	ODP [kg CFC-11-eq.]	AP [kg SO_2-eq.]
A1	-1.09	-0.82	-1.99E-03	-1.33E-04	-1.69	2.32E-02	-1.02E-06	1.33E-03
A2	-0.93	-0.75	-1.97E-03	-1.24E-04	-1.60	2.35E-02	-9.66E-07	2.14E-03
A3	-1.04	-0.82	-2.25E-03	-1.35E-04	-2.18	2.27E-02	-1.03E-06	3.52E-04
B1	0.84	-0.09	8.10E-04	5.16E-05	1.26	2.71E-02	1.58E-07	1.03E-02
B2	1.00	-0.02	8.31E-04	6.02E-05	1.35	2.74E-02	2.10E-07	1.11E-02
B3	0.88	-0.09	5.53E-04	4.89E-05	0.77	2.65E-02	1.50E-07	9.32E-03
C1	-2.74	-1.13	-7.79E-03	-4.92E-04	-6.93	2.22E-02	-7.69E-07	6.65E-03
C2	-2.58	-1.06	-7.77E-03	-4.84E-04	-6.84	2.25E-02	-7.18E-07	7.45E-03
C3	-2.69	-1.13	-8.05E-03	-4.95E-04	-7.42	2.17E-02	-7.77E-07	5.67E-03
R	0.85	0.79	8.65E-05	6.16E-06	0.12	1.37E-03	1.49E-07	1.62E-03

R = Reference scenario, CC = climate change, FD = fossil depletion, EP = eutrophication potential, HT = human toxicity, POF = photochemical ozone formation, ODP = stratospheric ozone depletion, AP = acidification potential.

5.2.2 *Comparison with the conventional system and contribution analysis*

When comparing LCIA results from the proposed scenarios with those obtained from the reference scenario, all scenario formulations for the scenarios replacing grid mix (A) and coal electricity (C) perform better in all impact categories but POF and AP. The scenarios replacing wind electricity (B) perform worse in most categories. In general, the greatest savings are observed for the impact categories of EP and HT, which show values that are between 14-27 times lower in scenarios options A and 56-94 times lower in scenario options C. Savings in the CC category are still notable, associated with impact values around 2.1 (A) and 4 (C) times lower relative to the reference scenario. Generally, the worst-case scenarios as for co-product credits in the PtF system generate the greatest savings relative to conventional methanol production, and the other way round. The best-case scenarios, i.e. scenario options B, only show improvements compared to conventional methanol production in terms of CC and FD. This is due to the fact that neither electricity nor heat nor fertiliser credits are high enough to offset the impacts by the system. Impacts are between 0.01-19 times higher than the reference scenario.

The contribution of each sub-process to the overall impacts from the proposed PtF scenarios is shown in Figure 5.6 (for all values see Table A 10 in appendix A) for those categories that deliver greater savings as compared to the reference scenario, namely EP (freshwater as an example) and HT; CC and FD are also included, since these are the two impact categories to be potentially improved by a renewable fuel production system. AP is shown, as an example where the highest credits of the fertiliser replacement can be achieved and POF because of its significant contributions caused by the CHP. The remaining categories are included in Figure A 4 in appendix A. It holds for all scenarios that the share of electricity credits from the CHP is greater when the electricity from the average mix (A) and electricity from coal (C) are considered. In scenario options B, environmental credits of the heat from CHP and from digestate become more important in most categories. In terms of HT, EP and AP, the effect of the heat credit is negligible for all scenario options, being even smaller than credits from replaced fertiliser production. Electricity credits play an important role in all impact categories. Fertiliser credits, on the other hand, are small in most categories and negligible as compared to electricity credits. As most grid electricity is required for methanol production, followed by electricity for the biogas plant and CO_2 recovery, impacts are the highest for methanol production followed by the two others in all categories.

In terms of credits, electricity credits associated with CHP production account for 28-39% of the overall impacts in the CC in scenario options A and for shares of 53-54% in options C and thus make a significant contribution. The share of electricity credits is however much lower in B, i.e. 1.4%. CO_2-eq. credits from heat production account for 30-32% of the impact and are therefore the most important co-product credits in these scenario options. They also play a big part in FD with 44-48%. A relevant impact in CC is made by the combustion of biogas in the CHP (around 14% in A, 22-23% in B and 11% in C) caused by the CH_4 emissions to air. The impacts from biogas production are comparatively low but become more important in scenario options B, where credits are in general lower. In freshwater and marine EP, impacts are very small and outweighed by the electricity credits for scenario options A and C. The same applies for HT. Usually, electricity for H_2 production makes relatively small contributions comparable to those of the electricity production taking electricity from the grid mix. However, impacts to HT by wind electricity for H_2 generation become more relevant with contributions of 15-16% in scenario options A and in B even higher with 31-40%. This is due to the release of mostly zinc and some other metals to freshwater. In EP, the contribution by the wind electricity is also slightly higher with >10%, though barely mentionable (<5%) in A and C. EP and HT emissions that are caused by grid electricity

production also become more important in B. Electricity for methanol production contributes 10-13% of emissions in scenario options A and around 5% in C. In B, the production is relevant for 39-50% of kg P-eq. emissions, 20-26% of kg 1,4-DB eq. emissions to HT and 37-43% of kg N-eq. emissions. The kg NO_x-eq. and kg SO_2-eq. emissions generated by the CHP unit, i.e. through the combustion of biomethane, account for between 73% to 86% of POF and 30% and 55% of AP across scenarios. Biogas production also contributes to AP through NH_3 emissions to air, although its contribution is with <10% relatively small in all scenarios. The waste water treatment and activated carbon production do not make relevant contributions to any of the categories.

Figure 5.6: Contribution analysis of the processes included in the expanded system for the impact categories climate change (CC), fossil depletion (FD), freshwater eutrophication (EP), photochemical ozone formation (POF) acidification (AP) and human toxicity (HT).

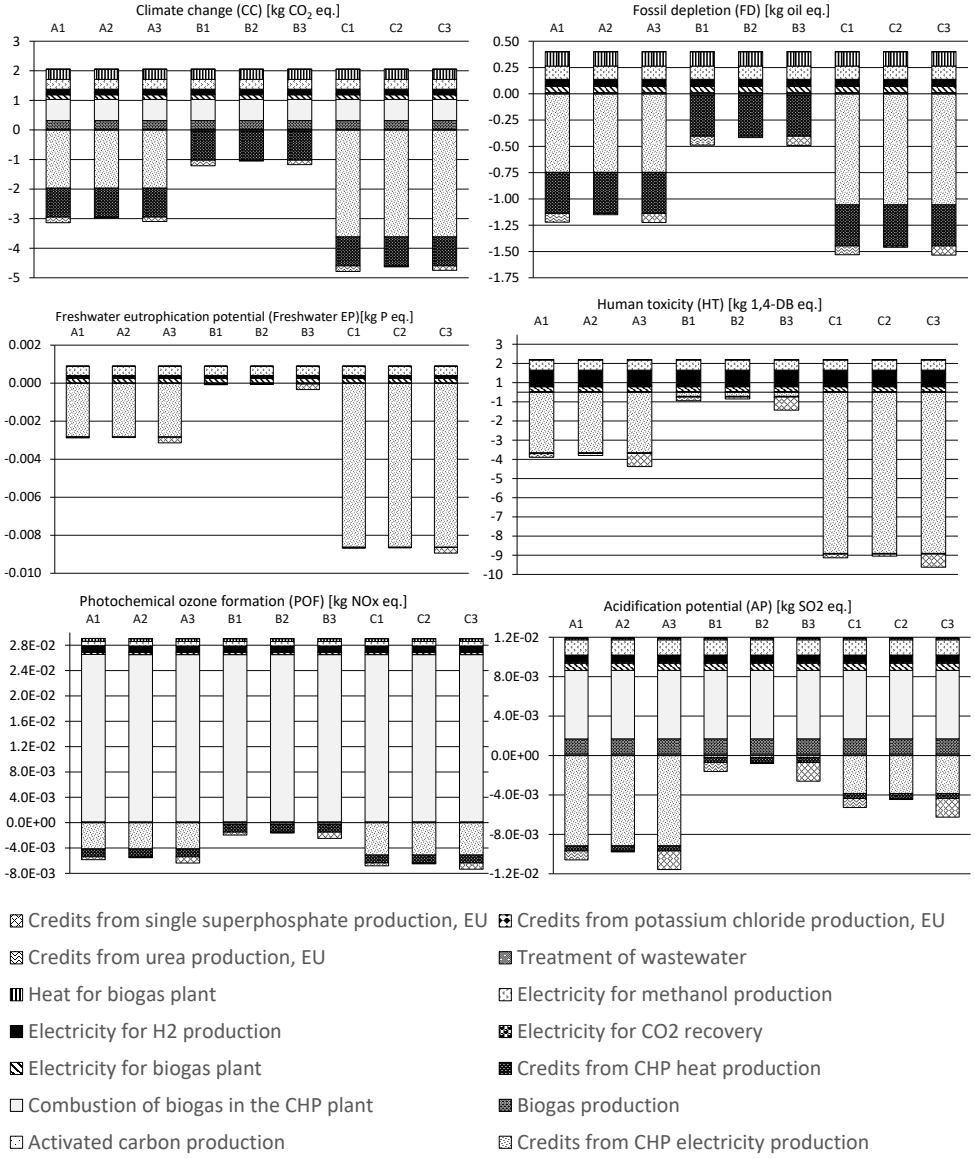

Caption: CHP = Combined heat and power plant.

In the reference system for fossil-based methanol production, electricity production accounts for the largest share of the impacts of EP and HT. While heat production makes the greatest contribution to CC and ODP, NG production accounts for the largest shares of FD, POF, and AP (see Figure 5.7). The NG production is assumed to be from Russia, as most NG is imported from there, and thus also encompasses losses from transport. Although the BMWI (2020) predicts Germany to be highly dependent on NG imports in the future, one may suggest that NG could also be produced from German NG. Therefore, NG coming from German fields is shortly considered in a complementary LCA simulation to present another potential NG source. However, the results only show small improvements. The CC category notes the highest improvements due to the avoided CH_4 losses, while other categories also perform slightly better. There appears to be a trade-off, as the German production achieves 34% less emissions of kg CO_2-eq., but causes 34% more emissions of kg SO_2-eq. and 16% more of kg NO_x-eq. Hence, it cannot be concluded that it is less polluting to take German NG for methanol production. The results for this case are shown in Table A 11 in appendix A.

Figure 5.7: Contribution analysis of the reference scenario for the impact categories climate change (CC), fossil depletion (FD), freshwater and marine eutrophication (EP), acidification (AP) and human toxicity (HT).

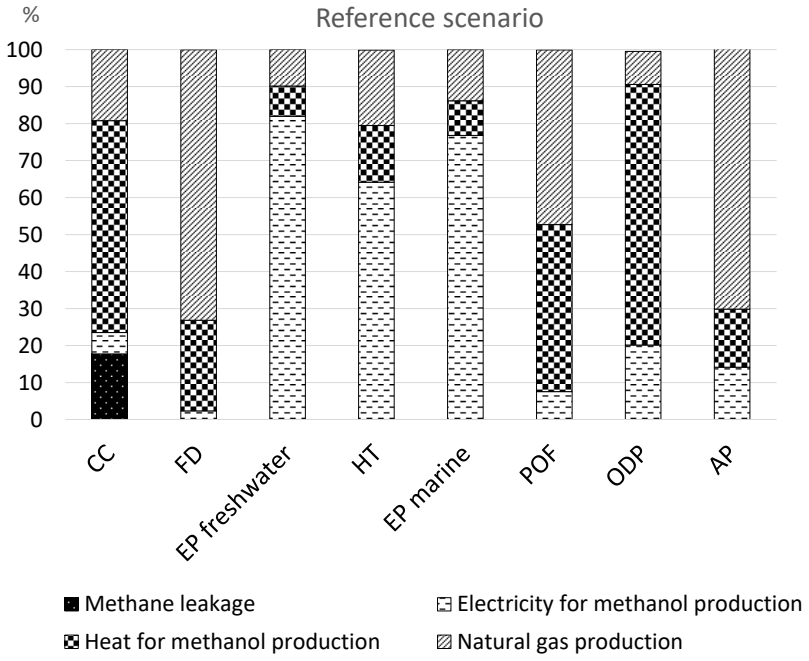

5.2.3 *Sensitivity analysis*

Results from the sensitivity analysis are shown in Table 5.26 including only those scenarios and impact categories for which the difference in the impact value relative to the reference scenarios is higher than ±10%. Note that the variability in outcomes greatly depends on the extent to which co-products credits are affected, which vary asymmetrically with the +10% and -10% change in the parameter, respectively. An inaccuracy in EGGEMANN et al. (2020) was corrected, which did not vary the change in parameters evenly, introducing a bias. Therefore, the results presented here deviate from the ones before. Especially, the impacts in CH_4 losses lost their significant impact in CC.

Variability in electricity production for methanol synthesis as well as the heat demand of the fermenter are associated with the greatest variability in FD with a maximal change of ±80 and ±86%, respectively, in scenario B2. Electricity demand for the electrolyser and for the biogas plant also account for significant changes of up to ±36% and ±38%, respectively, for the same scenario. This is due to the fact that, in scenario B2, the energy flows make relatively significant contributions after the heat credits of around 7-17%. Other critical parameters are the electricity demand in the electrolyser and the methanol synthesis as well as the heat demand for the biogas plant with further contributions in FD and ODP in scenarios B1 and B3. This is the result again of comparatively large shares of electricity demand in total oil-eq. and CFC-11-eq. emissions. On the contrary, variability in CH_4 emissions from biogas production for CC generate changes smaller than ±5% relative to the reference values. It shows that energy demand affects the impacts much more than the individual CH_4 emissions. Parameters determining the overall energy requirements across sub-processed thus greatly influence the environmental performance of the integrated PtF system and must be carefully considered in process design and upscaling.

Table 5.26: Change in results from the life cycle impact assessment relative to the reference values, when changing the parameters by ±10% through sensitivity analysis. Only changes over ±10% relative to the reference values are shown.

Para-meter	CC [CO_2 -eq.]	FD [oil -eq.]	EP fresh [P-eq.]	HT [1,4-DB-eq.]	EP marine [N-eq.]	POF [NO_x -eq.]	ODP [CFC-11-eq.]	AP [SO_2 -eq.]
Electricity demand of electrolyser								
A2								19.89 -19.89
B2		35.44 -36.08						
B3				10.70 -10.68				
Electricity demand for methanol synthesis								
A1								12.03 -11.28
A2								44.32 -44.03
B1		14.50 -14.16					12.66 -13.29	
B2		79.87 -80.38						
B3		13.95 -14.06					13.33 -13.33	
Electricity demand of the biogas plant								
B2		37.59 -37.97						
Heat demand of the biogas plant								
B1		15.64 -15.30						
B2		86.14 -86.71						
B3		15.06 -15.17						

CC = climate change, FD = fossil depletion, EP = eutrophication potential, HT = human toxicity, POF = photochemical ozone formation, ODP = stratospheric ozone depletion, AP = acidification potential.

Additionally, CH_4 emissions were varied according to assumptions from pre-storage of raw manure and manure credits in the PtF system. This change in emissions is much higher than the ±10% varied above. While all other categories remain the same for the variation in CH_4 emissions, only the category of CC adapts. Results are shown in Figure 5.8. In all scenarios, the LCA_{Credit} performs the best, accounting for the lowest values, which is due to the manure credits. They show significant improvements of 18-59% in kg CO_2-eq. emissions towards LCA_{Base}, depending on the scenario. $LCA_{Storage}$ performs worse with the same shares. However, it is doubtable whether such high emissions occur at all, as open raw-manure storage does not occur at most plants.

Figure 5.8: Results for the category of climate change for the calculated life cycle assessments (LCAs) of the Power-to-Fuel system, considering different CH_4 emissions; LCA_{Base} refers to the accounting of AD emissions, while $LCA_{Storage}$ accounts for both AD emissions and emissions from pre-storage of manure and LCA_{Credit} neglects pre-storage emissions but instead considers the avoided pre-storage emissions as manure credits.

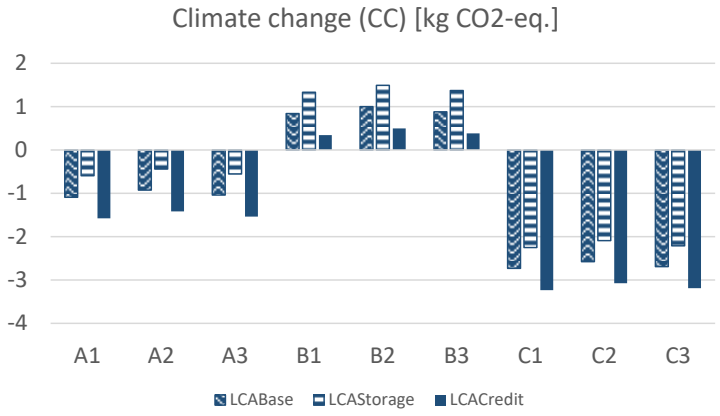

5.2.4 *Discussion of the life cycle assumptions*

The scenario analysis of the multi-functional PtF system assessed shows that environmental impacts are largely dependent on the choices regarding co-product credits when performing system expansion in attributional LCA. Specifically, credits from the electricity generated by the CHP are the main contributor to the impact savings estimated for the PtF system across impact categories, as also found by LANSCHE et al. (2012). After all, these findings support the idea that electricity produced from manure-based biogas in CHP units is generally more

environmentally-friendly than that from NG, in terms of CC, AP and ODP (ESTEVES et al., 2019). Environmental credits associated with the use of the digestate as a fertiliser account for a small share of absolute impacts, although they increase in importance in the scenarios with replaced wind-electricity, especially when SSP is assumed to be replaced. This is in line with the results from the FNR (2013, p. 219), as for CC only. It must be noted that using digestate as fertiliser can deliver further GHG benefits in agricultural production, relative to applying untreated manure (ESTEVES et al., 2019). The kg NO_x-eq. and kg SO_2-eq. emissions generated by the CHP made relevant contributions though could be reduced with exhaust gas treatment. An oxidation catalyst already exists at the large plant which is why emissions are expected to be lower for it. Moreover, its digestate storage occurs in a gas-tight tank. Thus, the main difference in case of the large and the small-manure plant, when compared with each other, would be their CH_4 emissions from the plant and their CHP emissions. It is expected that when the PtF system is up scaled that the large plant would generate fewer emissions overall. The emissions by the other processes would be expected to remain the same per FU.

Ammonia and urea modelling methodology changed in the update to the most recent Ecoinvent 3.7 version in 2020 (MORENO RUIZ et al., 2020, p. 37). In earlier versions, there was no CO_2 capture by urea production, although a production site is usually located next to ammonia production plants and directly uses the CO_2 emissions of the latter that are released into the atmosphere. In the most recent version, the process achieved an additional CO_2 input corresponding to the required carbon in urea synthesis. Therefore, the process that is replaced by digestate fertiliser misses to account for the saved CO_2 emissions in this study, using version 3.5. It presents more emissions in comparison to the urea production process in version 3.7. MORENO RUIZ et al. (2020) also point out that the urea has lower values in the GWP. With this born in mind, saved emissions are possibly slightly lower in the scenarios affected, as the overall process performs better in terms of emissions. In fact, other commercial fertilisers could have been considered instead of urea, e.g. ammonium nitrate, which is the most commonly used inorganic N fertiliser in the EU and globally (FERTILIZERS EUROPE, 2019). Since the digestate originates from organic residues, i.e. manure and straw residues, it was considered that it rather substitutes for organic fertilisers. Such an integrated PtF system also valorises manure following circular economy principles (EC, 2020) to supply renewable energy in a flexible way.

An alternative system design was taken into account, in which renewable energy is not produced in sufficient amounts for the system and electricity from the German grid is needed to generate H_2. This scenario causes even greater impacts than fossil-

based methanol (see Table A 12 in appendix A), highlighting the need to generate renewable energy for self-consumption. As a limitation, this study does not include upstream impacts associated with the production of capital goods for the PtF system production. However, these are expected to be comparatively low in contrast to impacts from operational stages. Finally, it could also be discussed whether to consider other heat replacements as well. Yet, since the replaced heat is less relevant to the current scenarios and different types of NG-fired heat sources yield similar emissions, we did not consider them. The results for all scenarios with replaced heat production by condensing, modulating boilers and atmospheric, non-modulating boiler as compared to the main LCA are shown in Table A 13 in appendix A.

This attributional LCA applies the system expansion approach to include those processes that would potentially be replaced in the German market by the several co-products generated (i.e. digestate, heat and electricity), according to the ISO (2006b). A scenario analysis was carried out by assuming environmental credits associated with both average and also marginal technologies (e.g. wind electricity), in order to assess the variability in the results due to such modelling choices. Attributional LCA is usually based on average LCI data, while consequential LCA uses marginal data to estimate impacts from a change in demand of the FU (TILLMAN, 2000). However, consequential LCA requires additional economic modelling to simulate how changes in the life cycle affect the whole economic system (EARLES et al., 2011, WEIDEMA et al., 2018). Another alternative could have been to apply partitioning to solve the multifunctionality problem and allocate environmental impacts among co-products up to the stage in which these are generated. As an accounting exercise, GHG savings brought about by the proposed system compared to conventional methanol production were estimated based on the relative energy content of co-products, as the RED II recommends. The following values were considered: 19.9 MJ/kg for methanol (MCALLISTER et al., 2011), 17.4 MJ/kg (as dry matter) for the digestate (GARDONI et al., 2016) and 22.3 MJ/m³ for biogas (FNR, 2016); together with the net energy output in MJ of electricity and heat. The RED II assumes CH_4 savings from manure management, which were included based on the EC (2018). Methanol from the PtF system delivers GHG savings of 55.0% relative to fossil-based methanol (WERNET et al., 2016), while savings increase to 101.2% if wind electricity is used across sub-processes, i.e. for biogas production, CO_2 recovery and methanol synthesis. This means that methanol production in a PtF system is energy intensive and would only meet the RED II's sustainability requirements for transport fuels after January 2026 (GHG savings >65%) if wind-based electricity is readily available in the

installation. In spite of this, the RED II provides that advanced biofuels based on non-food and waste feedstock (e.g. animal manure or sewage sludge) should account for at least 3.5% of the transport fuel market by 2030.

The way to deal with multi-functionality has been broadly discussed in the LCA literature. For instance, PELLETIER et al. (2015) suggest that system expansion should not be prioritised in attributional LCA, but the choice depends on the rationale of the analysis. MENG et al. (2019) emphasise that system expansion is a suitable method for understanding the system's overall impact when evaluating a novel technology. In this study, the system expansion approach was chosen to consider the effects of the multiple products delivered to the market by the integrated PtF system, as compared to conventional methanol production, in order to highlight benefits from 'closing loops' in fuel production towards a circular economy. Applying partitioning may constitute a simplification when analysing integrated systems in which each sub-process delivers multiple co-products, some of which are used as inputs in other units. Indeed, most LCAs of integrated or circular production processes apply system expansion to deal with the multi-functionality issue (COLLET et al., 2017, ESCOBAR et al., 2015, LANSCHE et al., 2012); although this can hinder comparative sustainability assessments between systems. The RED II identifies challenges when applying energy allocation if a CHP is used in the processing of biofuels, bioliquids and biomass fuels, as is the case here; while the system expansion approach is accepted for the purposes of policy analysis. Similarly, the International Organization for Standardization (2006a) even recommends avoiding partitioning in both closed-loop and open-looped product systems.

In LCA, impacts are not proportional to the FU but specific to the scale of production. When performing system expansion, the scale of production also determines the quantity of co-products generated and hence the products to be potentially replaced in the market. For instance, it can be expected that if digestate production increases with the biogas production capacity, not all of it could be employed as fertiliser, depending on the demand by the agricultural sector and associated market prices. This shows the importance of performing prospective analyses on co-product credits with consequential LCA approaches in order to capture the current and future socio-political conditions affecting market behaviour (ZAMAGNI et al., 2012). Furthermore, consequential LCA approaches could also be applied to consider additional waste treatment scenarios from cradle-to-grave (AHLGREN et al., 2015, LUND et al., 2010). In this sense, the Environmental Product Declaration (EPD) could contribute to the further harmonisation of the cut-off criteria (BORGHI et al., 2007). The system has been conceptualised here as a

methanol production system (with a product-based FU), but could also be assessed as a waste treatment system (with an input-based FU). In any case, the system is aligned with the EU's circular economy strategy (EC, 2020) which aims at reducing waste generation, by enhancing reuse and recycling and the establishment of a market for secondary products. However, this should not encourage the production of either straw residues or manure from industrial livestock farming, which highlights the need for adequate regulations in bio-based feedstock markets from a supply chain perspective by taking into account subsequent market responses.

5.2.5 *Results and discussion of the additional life cycle assessment*

The results for the CHP (case i), as shown in Table 5.27, present positive values for the scenario option of replaced wind electricity (wind) for EP and ODP. AP has positive values as well for wind and also coal-based electricity replacement (coal). All scenarios show positive emissions in the entire category of POF. The latter are caused by the CHP emissions. The replaced wind electricity does not generate high enough credits to compensate the emissions by the system, same as in the main LCA. Emissions, here, are between -3.82 and -6.87 kg CO_2-eq. for CC. The gas flare (case ii), on the other hand, generates reductions in this category which lie close to those of the wind scenario. This means that even though the gas flare burns biogas in a cleaner way than the CHP, the credits of case i) produce reductions in the impact categories. In particular, the replaced coal-based electricity achieves emissions that are 38 to 46 times lower for HT and EP, compared to the gas flare. Replaced grid electricity production (grid mix) yields emissions that are 13 to 14 times lower for these categories. For FD, impacts can be up to five times lower and for ODP up to seven times. The detailed results for the contribution analysis of the selected impact categories are shown in Figure A 5 in appendix A. As the difference is comparatively small for most categories, the additional expenses of the CHP appear worthwhile. Environmental burdens can mostly be compensated for by the heat and electricity produced. Although the double counting of flows needs to be avoided, BGPs clearly serve multiple purposes. If not for the emission savings by the improved manure management, the gas flare scenario would not be viable. The research community about fermentation of biomass clearly supports the approach to assign BGPs their positive characteristics of avoiding raw manure storage emission and also account for these in LCAs.

Table 5.27: Results from the life cycle impact assessment of the additional assessment for producing 1 m³ of biogas in a biogas system, comparing the impact of a combined heat and power unit with those of a gas flare.

	CC [kg CO_2 eq.]	FD [kg oil eq.]	Fresh-water EP [kg P eq.]	Marine EP [kg N eq.]	HT [kg 1,4-DB eq.]	POF [kg NO_x eq.]	ODP [kg CFC-11 eq.]	AP [kg SO_2 eq.]
				Case i)				
Grid mix	-5.46	-0.67	-2.28E-03	-1.52E-04	-2.54	1.37E-02	-9.98E-07	-1.92E-03
Wind	-3.82	-0.04	1.20E-04	5.85E-06	-0.02	1.70E-02	7.68E-09	5.75E-03
Coal	-6.87	-0.93	-7.24E-03	-4.59E-04	-7.03	1.29E-02	-7.85E-07	2.62E-03
				Case ii)				
Gas flare	-3.76	0.17	1.54E-04	1.03E-05	0.18	1.79E-02	1.32E-07	6.17E-03

CC = climate change, FD = fossil depletion, EP = eutrophication potential, HT = human toxicity, POF = photochemical ozone formation, ODP = stratospheric ozone depletion, AP = acidification potential.

5.3 Summary of key findings

The achievable amounts of methanol in a novel PtF were calculated in this study. A pilot small-manure plant combined with a PtF system can produce 138.4 kW of methanol (case 1 or standard case), while other cases adapted to BGPs of 37 kW and 500 kW as well as a small-manure plant in combination with a BOP were also investigated (case 2-4). These achieve capacities of 75.7 kW, 305.9 kW and 693.3 kW, respectively. CH_4 losses that occur from biogas upgrading can easily be adjusted for by the BGP so that the CHP does not lose efficiency. The technology considered for this system is membrane processing. Thus far, biogas upgrading is not carried out in combination with smaller German BGPs due to missing profitability. Nevertheless, the LCOE for the BGPs investigated in the system as well as the specific costs for biogas upgrading showed promising values. Even though the costs are plant-specific, this could provide small-scale upgrading as a possibility for manure plants in the near future. Furthermore, the BOP may present an interesting option for CO_2 generation at BGPs. Costs can be significantly decreased when taking manufacturer prices instead of estimating them according to the method by TURTON et al. (2009). The BOP shows a high potential for biogas systems with LCOE of 13.3 €-ct/kWh which are only slightly higher than those of the small-manure plant, while providing pure CO_2 at the same time.

Manufacturing costs were calculated for renewable methanol with an achievable purity of 99.898%. Heat demand for the production process is negative, which means that there is a surplus of heat which amounts to 5.58 MJ/kg_{MeOH}. However, as the heat is at a low temperature and the amount is too small in comparison with the heat generated by the CHP, it would not be worthwhile to make use of it in the system. The electricity demand is 1.79 MJ/kg_{MeOH} and is mainly caused by the compressors. Furthermore, the production quantity of methanol is determined, which is linked with the CO_2 provision from biogas. 1.376 kg of CO_2 are required per kg of methanol produced, which is in the same range as for large-scale plants, summing up to 24.92 kg/h in the standard case. The main modules of the process are determined by the use of manufacturer enquiries. This is necessary because the modules are below the capacity limit of Turton's method and therefore the standard values cannot be used. The unit costs for the operating materials are determined from the literature. For the raw materials, the costs are calculated or converted within the scope of this work. For CO_2, the costs are available in relation to the biomethane and are converted to the costs per kg of CO_2. Costs for activated carbon and post-combustion are also added to the upgrading costs which generates costs of 234 €/t CO_2 for the standard case. For the H_2, the costs are determined from the individual costs of the three components: WTG, electrolyser and storage. This results in system costs for the H_2 of 8.93 €/kg. After estimating the operating costs, the COM and the specific COM are determined. The specific COM result in 4.41 €/kg_{MeOH} for the standard case. This is significantly higher than the market price for methanol, which was 0.275 €/kg (METHANEX, 2020) as of September 2020. They lie also above the costs for renewable methanol in large-scale plants with a similar process design.

For the other three cases investigated in the TEA, it is not possible to determine all module costs from manufacturer enquiries. Hence, the capacity method is used. For this purpose, the module costs for case 3 are requested from manufacturers and with the help of these and the results from case 1, degression coefficients are determined for the components. These are used to then calculate the module costs of the other plant sizes. As it was not possible to enquire the module costs for all components of case 3, the degression coefficients for the remaining components are determined by comparing case 1 with WALMAN (2018)**,** which calculates a plant with a similar design at a capacity of 30 MW. The module costs determined by the capacity method have a lower accuracy than the costs determined via manufacturer enquiries. CO_2 costs are adjusted for the applications which lie at 268.54 €/t for case 2 and 218.08 €/t CO_2 for case 4. The CO_2 costs for the BOP are estimated at 5.93 €/t and 38.87 €/t, depending on whether the LIR of the less efficient CHP is

accounted for or not. In the case of the specific COM, it can be seen that these become lower with increasing plant size, which is due to the decreasing share of investment costs. This is because the module costs do not increase proportionally to the size of the plant. Since small degression coefficients in the range of 0.015 to 0.452 result for all modules, the module costs rise particularly slowly. This leads to specific COM for case 4 of 2.87 €/kg_{MeOH}. However, it also means that the costs for the smaller system of case 2 increase disproportionately compared to case 1, which results in specific COM of 5.67 €/kg_{MeOH}. The BOP proved to be a more interesting option than the standard case, as higher amounts of CO_2 are available and fewer technical alterations are required. However, this case is also not competitive under the current situation, yielding specific COM of 3.17 €/kg_{MeOH}. Sensitivity analyses show that the H_2 costs and the investment costs have the greatest influence overall. The H_2 costs have a large influence in all cases. This means that by reducing the H_2 production costs, the COM could be significantly reduced, but even then they would still be above the manufacturing costs for comparable large-scale plants. This is due, among other things, to the larger share of investment costs. Including the construction of the BGP in the system raises COM to 4.73 €/kg_{MeOH} for the standard case. The system would therefore benefit from an existing biogas production site that could be extended. Interestingly, when revenues were included, COM could decrease significantly to 3.21 €/kg for the standard case and 1.78 €/kg for case 4. If a BGP has already been constructed on-site, costs could be estimated as low as 3.04 €/kg and 1.38 €/kg, respectively. Under such conditions, they would approximate costs for methanol from large-scale PtF systems. An increasing CO_2 price could also help to make the system more competitive. In general, a combination of cost reductions and increase in revenue would benefit the system.

The analysis also quantifies the environmental impacts for the PtF system of the standard case by means of an LCA. In view of the multi-functionality of the process, nine scenarios in total are assessed for the standard case to understand the uncertainty in the modelling choices of co-product credits when applying system expansion. Scenario A1 achieves CO_2-eq. savings of -1.09 kg, compared to the reference system which emits CO_2-eq. emissions of 0.85 kg; an improvement of 1.95 kg CO_2-eq. is noted. At an annual production of 212 tonnes of methanol for the standard case, a total of 413 t/a CO_2-eq. emissions could be saved. Most of the other scenarios entail impact reductions relative to the conventional methanol production, generating negative impact values, with exceptions in POF and AP. In general, replaced electricity by the CHP unit makes a particularly relevant contribution, hence the worst-case scenarios where coal-based electricity is replaced generates the greatest savings relative to conventional production. Especially, EP and HT show emissions that are up to 94 and 81 times lower for the

coal-based scenario. However, the categories of POF and AP perform mostly worse due to the emissions from the CHP. Impacts are up to 19 and 6 times higher, respectively, than the conventional alternative. Heat did not play a significant role for most impact categories and only became more important in scenarios with replaced wind-based electricity that did not generate high enough savings. Moreover, heat did not show relevant differences in avoided processes which are varied in an additional exercise. Generally, the scenario in which the digestate from AD replaces SSP as a fertiliser delivers greater environmental benefits, regardless of the energy type to be replaced in the market by the electricity from the CHP. CC and FD are the only exceptions, as urea production generates more credits than SSP. Assumptions on co-product credits thus play an important role when assessing an integrated system, such as the one proposed here, under the system expansion approach. The choice of avoided processes should consider the market conditions in which co-production takes place, as well as the scale of production of the process itself, which determines subsequent market responses from co-product generation. LCA outcomes are also subject to parameter variability, e.g., in measurements, which is why they are assessed by means of a sensitivity analysis. Variability in parameters determining the energy needs of the system proves to be critical for the overall environmental performance.

Moreover, the manure credit or improved manure management can influence the CC performance of the PtF system, hence, the system assumptions need to be presented clearly. In this case, pre-storage emissions of raw manure are not applicable, as storage occurs below the ground. The additional LCA considers a manure credit which is done to show the multi-purpose of BGPs in general. It reveals the relative improvements for a BGP using a CHP towards one using a gas flare. However, the gas flare also presents its benefits by avoiding CH_4 emissions both from improved manure management and a cleaner flue gas. Reductions in CO_2-eq. emissions varied between -5.46 kg for the classic plant as compared to -3.76 kg for the gas flare.

Chapter 6
Conclusions

This chapter presents the conclusion for the evaluation of the PtF system. It highlights limitations and aspects for further research. Finally, it draws some conclusions, answering the research questions.

6.1 Limitations and further research

The plant investigated in the LCA is used as a representative of small-manure plants, though having certain features that others may not have. As each BGP is unique and plant-specific data is used in this study, it is important to look at various plant options individually. The analyses focussed on German conditions. Hence, it may also be interesting to see whether such a system would be applicable for other EU countries with biogas production or even on an international scale. In this context, water consumption for e-fuels is important to consider, especially in warmer countries. The system may also be interesting in a different German setting, e.g. in Bavaria where solar power could be considered for H_2 production. Furthermore, it was decided not to model the costs and emissions of livestock farming because the concept could potentially be applicable to other locations in combination with a small plant using biowaste or MSW and without the direct connection to a livestock farm. However, environmental impacts would then have to be re-evaluated, depending on the feedstock as well as its generation and storage. It would also be possible to consider larger BGPs that already utilise biogas upgrading. However, they usually feed energy crops and other plant materials, so that such plants would have to be considered carefully. It is important to bear in mind that these types of plants are not the future. Policies, such as the RED II, focus clearly on agricultural residues and waste products for future BGPs.

As the emissions are expected to be much lower for BGPs that cover their digestate storage and treat their CHP flue gas, it would be interesting to consider this within

the system. If the system was able to achieve GHG savings of 65%[1] according to the RED II, the trading of GHG quotas could also generate additional revenues. In comparison to the conventional system, CO_2-eq. emissions of approximately 413 t/a in total can be reduced for a capacity of 212 t/a of methanol, when generated in the PtF system proposed. If traded with a GHG quota of 260 €/t as of October 2020 (MOZGOVOY, 2020), an additional annual revenue of 107,380 € can be achieved. Quotas are expected to rise, as is the share of quota quantities. A share of 6% was required in 2020 and is expected to increase further to 7-16% in the near future (MOZGOVOY, 2020). Under this aspect, the PtF system shows an interesting option for further analyses. Furthermore, the option of biomethane injection into the grid and possible costs and revenues may be interesting to consider. A BGP would have the opportunity to inject the biomethane that is not needed for the CHP into the gas grid and earn an additional revenue, given that it is located in a favourable location. Then, grid connection fees would also become relevant. Yet, the NG as an intermediate storage would also be of interest. The system also offers other interesting adjustments, such as the use of the excess biomethane as a fuel on site, providing another source of income. In addition to that, the option of trading with CO_2 certificates, especially for biogas upgrading plants, has recently gained interest and will become relevant under the future RED. However, the plant must have a sufficient supply of biogas in order to produce its required energy. Therefore, it would probably be an option for larger plants. PtG routes could also be considered then, though adding to the complexity of the system and leading away from renewable methanol. Overall, these options are very site-specific and not optional for all BGPs.

It is possible to consider only the biogas upgrading and sell the CO_2, which is shown to be profitable for the BGPs investigated. Further analyses should investigate sensitivities and production opportunities for the plants in order to consider options after their loss of financial support. However, such concepts will depend on the market, and it will only be relevant for plants that lie in the trading area of a central CO_2 plant. In this case, transport costs also play a role as well as the liquefaction of the CO_2. This would require additional energy. A stand-alone system would thus be preferable, but this depends highly on the location and infrastructure. Hence, this may also be interesting to analyse in further studies.

[1] (currently 55% when replacing German grid electricity)

The LCA compares the climate change potential and, among others, the impacts on soil and water for methanol production in a local-scale biogas concept with the conventional production of methanol. A further analysis could compare the system with a different PtF path taking waste CO_2 from steel production. Moreover, applying a consequential LCA perspective could provide further insights on the price-mediated effects triggered by marginal changes in supply and demand of the main product, considering co-product substitution across sectors, although this requires further economic modelling. For this, the economic performance of the proposed PtF technology could be linked with environmental aspects in an LCC, in order to estimate trade-offs amongst sustainability dimensions, while providing technical assistance in planning and upscaling. Furthermore, a more comprehensive sensitivity analysis based on on-site measurements combined with uncertainty analysis would be necessary to better inform decision-making in other technical, geographical and socio-political contexts.

Last but not least, new technologies in agriculture usually pose many challenges to manufacturers and farmers, such as legal frameworks, financing issues and particularly social tolerance. It is therefore of interest to get a realistic assessment of the technology and to identify possible challenges and obstacles also with regard to acceptance. Against the background of a holistic evaluation of the described PtF concept, the practical implications of the technology within the existing plant infrastructure in Germany will be evaluated in a further study. For this purpose, a key question interview is planned to be conducted with responsible persons from the biogas sector. For this, possible stakeholders need to be identified. A subsequent strength-weaknesses SWOT[2] analysis can be carried out, summarising the results generated by the interviews.

6.2 **Final conclusions**

The study tried to answer the question whether a PtF system as the one proposed in combination with manure-based BGPs could be an option in a future energy system. For this, the system was evaluated by means of a TEA and LCA to determine its costs and environmental impacts. The profitability analysis comprised the calculation of investment and operational costs as well as the specific production costs and the revenues and profits of the entire system, while the LCA

[2] Strengths, weaknesses, opportunities, threats

investigated the impacts under assumption of co-product credits generated by the system.

In conclusion, it can be said that the concept investigated in this study cannot be operated competitively at present and that market introduction will also be difficult in the short term. Even assuming a "best subcase", the concept of case 1 is still more than twice as expensive as comparable large-scale plants. An increase in size decreases production costs, though not enough to compete with other current PtF products. Case 3 with the use of the BOP in combination with the small-manure plant shows a higher potential than case 1, which is due to the larger amount of available CO_2 and fewer conversion measures. The additional step of biogas upgrading, which causes much higher CO_2 costs can be avoided with this process. Overall, case 4 reached the lowest manufacturing costs, although still not competitive. Assuming revenues of different kinds, which occur inside the system, also showed possibilities to reduce production costs. In this case, case 4 achieves a convergence with the costs of large-scale plants for renewable methanol synthesis. The system would then, however, be dependent on several co-product prices. Economic feasibility appears to be a problem, at least in the near future. Even the influence of CO_2 sales on the production costs could not make a difference. With a CO_2 break-even cost of 2,160 €/t, it is very unlikely to become profitable. Nevertheless, since PEM electrolysis is still at the beginning of its industrial use, its price is expected to fall in the next few years. This would lead to a reduction in H_2 production costs. Therefore, a combination of this, together with a high CO_2 price can help to increase profitability. In order to achieve a convergence with the costs of large-scale plants for renewable methanol synthesis, it is also necessary for the plant concept to be standardised in order to reduce the investment costs. The prices received from the enquiries present prices for individual pieces. Once the material is more established and standardised processes are used for production, these costs can decrease as presented by the means of learning curves. In the end, technology adoption is, however, largely dependent on the economic performance of the system as compared to available alternatives.

The environmental analysis shows a much higher current potential of the system, as it has the great advantage that it uses bio-based carbon sources instead of fossil ones. With this, it contributes to the idea of a circular economy by promoting closed carbon cycles and, in spite of the uncertainty, it shows the potential to outperform conventional methanol production from an environmental point of view. This applies under the condition that raw materials are readily available and co-products are generated at competitive prices. In this sense, adopting the PtF technology on a

large scale could help to meet the EU's RED II goals as for consumption of advanced fuels, although actual GHG savings are conditional on the kind of electricity replaced by the system. Apart from mitigating climate change and fossil depletion by substituting for fossil fuels, the PtF system reduces the quantity of manure waste to be treated and disposes it safely. Aside from the advantages of producing a renewable energy carrier which can avoid emissions and at the same time store excess renewable energy, the system can also support the search in finding new business models for BGPs when they lose their financial support after the 20-year period. Simple biogas upgrading offers promising options for the smaller scale, also for the provision of CO_2, as well as the BOP. Finally, the phasing out of coal in Germany, will require fuels that are supplied with CO_2 from coal plants to come up with new carbon sources. If the energy system undergoes these changes, according to the merit order, other technologies may first be implemented. However, this system could be something for the later stages. At this point in time, the effective date is still difficult to foresee, but with a certain combination of decreased utility and module costs and increased potential revenues, there may be a positive outlook for the PtF system after all.

Chapter 7
References

ADLER, P., BILLIG, E., BROSOWSKI, A., DANIEL-GROMKE, J., FALKE, I., FISCHER, E. (2014a) *Leitfaden Biogasaufbereitung und -einspeisung:* Fachagentur für Nachwachsende Rohstoffe e. V. (FNR), Gülzow-Prüzen.

ADLER, P., BILLIG, E., BROSOWSKI, A., DANIEL-GROMKE, J., FALKE, I., FISCHER, E., GROPE, J., HOLZHAMMER, U., POSTEL, J., SCHNUTENHAUS, J. (2014b) Leitfaden Biogasaufbereitung und-einspeisung:

AG BERGLAND CLAUSNITZ, AGRARGENOSSENSCHAFT "BERGLAND" CLAUSNITZ E.G. (2019). "Windkraft." Retrieved, 08.12.2020, from https://www.agrar-bergland-clausnitz.de/energie/windkraft/.

AGENTUR FÜR ERNEUERBARE ENERGIEN. (2019). Retrieved 17.03.2019, from https://www.foederal-erneuerbar.de/landesinfo/bundesland/NI/kategorie/bioenergie/auswahl/270-installierte_leistun/#goto_270.

AGRARHEUTE.COM. (2016, 02.02.2016). "Abgabe von Schweinegülle so teuer wie nie." Retrieved, 27.11.2020, from https://www.agrarheute.com/tier/abgabe-schweineguelle-so-teuer-nie-519453.

AHLGREN, S., BJÖRKLUND, A., EKMAN, A., KARLSSON, H., BERLIN, J., BÖRJESSON, P., EKVALL, T., FINNVEDEN, G., JANSSEN, M., STRID, I. (2015) Review of methodological choices in LCA of biorefinery systems-key issues and recommendations: *Biofuels, Bioproducts and Biorefining* 9: 606-619.

AL-BREIKI, M., BICER, Y. (2020) Comparative life cycle assessment of sustainable energy carriers including production, storage, overseas transport and utilization: *Journal of Cleaner Production* 279: 123481.

ALKHAYAT, W. A., GERRARD, A. M. (1984) Estimating manning levels for process plants: *AACE Transactions*: I.2.1–I.2.4.

ALLIED MARKET RESEARCH. (2020, Zugriff am 25. September 2020). "Renewable Methanol Market Overview." Retrieved, 17.11.2020, from https://www.alliedmarketresearch.com/renewable-methanol-market.

APEX AG. (n.a.). "Referenzliste - Biomethan." Retrieved, 10.08.2020, from https://biomethan.acrona-group.com/fileadmin/user_upload/downloads/biomethan/referenzliste_biomethan_190624.pdf.

ASPEN TECHNOLOGY, I. (2017) Aspen Plus V10.

AUGELLETTI, R., CONTI, M., ANNESINI, M. C. (2017) Pressure swing adsorption for biogas upgrading. A new process configuration for the separation of biomethane and carbon dioxide: *Journal of Cleaner Production* 140: 1390-1398.

AWE, O. W., ZHAO, Y., NZIHOU, A., MINH, D. P., LYCZKO, N. (2017) A review of biogas utilisation, purification and upgrading technologies: *Waste and Biomass Valorization* 8: 267-283.

BAENA-MORENO, F. M., LE SACHÉ, E., PASTOR-PÉREZ, L., REINA, T. (2020) Membrane-based technologies for biogas upgrading: a review: *Environmental Chemistry Letters*: 1-10.

BANDI, A., SPECHT, M. (2004) Gewinnung von Methanol aus Biomasse: In Zentrum für Sonnenenergie- und Wasserstoff-Forschung Baden-Württemberg.

BAYERISCHES LANDWIRTSCHAFTLICHES WOCHENBLATT. (2019). "75 kW-Biogasanlagen bewähren sich." Regenerative Energie Retrieved, 10.07.2020, from https://www.wochenblatt-dlv.de/regionen/schwaben/75-kw-biogasanlagen-bewaehren-554694.

BAYLFU, BAYERISCHE LANDESAMT FÜR UMWELT, (2007) Biogashandbuch Bayern.

BDEW, BUNDESVERBAND DER ENERGIE UND WASSERWIRTSCHAFT E.V., (2020) *BDEW-Strompreisanalyse Januar 2020: Haushalte und Industrie:* Berlin.

BECK, T., ALBRECHT, S., LINDNER, J. P., BOS, U., KNÜPFFER, E. (2019). "Handlungsempfehlungen für Ökobilanzen biobasierter Produkte." Retrieved, from

https://www.researchgate.net/publication/330540899_Handlungsempfehlungen_fur_Okobilanzen_biobasierter_Produkte_Recommendations_for_life_cycle_assessments_of_biobased_products.

BEGER, B. BEGER GMBH BEHÄLTER- UND APPARATEBAU, SCHWEIßFACHBETRIEB,. (Zugriff am 25. September 2020). Retrieved, 25.09.2020, from http://www.beger-druckbehaelter.de/.

BEYRICH, W., KASTEN, J., KRAUTKREMER, B., DENYSENKO , V., RENSBERG, N., SCHMALFUß, T., ERDMANN, G., JACOBS, B., HÜTTENRAUCH, J., SCHUMANN, E., KÖNIG, J., EDEL, M. (2019) Schlussbericht zum Vorhaben In Verbundvorhaben: Effiziente Mikro-Biogasaufbereitungsanlagen (eMikroBGAA), Fraunhofer IEE, DBFZ, Deutsches Biomasseforschungszentrum, DBI, Gas- und Umwelttechnik GmbH, Dena, Deutsche Energie-Agentur (eds).

BFE, BUNDESMINISTERIUM FÜR ENERGIE,. 2019. Biogas-Veredelung im kleinen Massstab. Umweltperspektiven (August 2019), 11.01.2021.

BHANDARI, R., TRUDEWIND, C. A., ZAPP, P. (2014) Life cycle assessment of hydrogen production via electrolysis – a review: *Journal of Cleaner Production* 85: 151-163.

BIEGLER, L. T., GROSSMANN, I. E., WESTERBERG, A. W. (1997) *Systematic Methods of Chemical Process Design:* Prentice-Hall, Upper Saddle River, NJ.

BIENERT, K., SCHUMACHER, B., ROJAS ARBOLEDA, M., BILLIG, E., SHAKYA, S., ROGSTRAND, G., ZIELIŃSKI, M., DĘBOWSKI, M. (2019) Multi-indicator assessment of innovative small-scale biomethane technologies in Europe: *Energies* 12: 1321.

BILLIG, E., DECKER, M., BENZINGER, W., KETELSEN, F., PFEIFER, P., PETERS, R., STOLTEN, D., THRÄN, D. (2019) Non-fossil CO2 recycling—The technical potential for the present and future utilization for fuels in Germany: *Journal of CO2 Utilization* 30: 130-141.

BIOBG (2012) Betriebsanleitung 3-Kammer Aktivkohlefilter. Retrieved, 15.09.2020, from https://www.opendata.uni-halle.de/bitstream/1981185920/13265/3/Betriebsanleitung%203Kammer-AKF-BioBG-2012.pdf.

BIOGAS-ADDITIVE.DE, BIOGAS-ADDITIVE.DE GMBH & CO. KG. (n.a.). "Die beliebtesten Fehler in Biogasanlagen, die Sie anderen überlassen sollten."

Retrieved 14.11.2020, from https://www.google.com/url?sa=t&rct=j&q=&esrc=s&source=web&cd=&cad=rja&uact=8&ved=2ahUKEwi-o4uF24HtAhUOJhoKHX98DakQFjAEegQIBxAC&url=https%3A%2F%2Fsilo.tips%2Fdownload%2Fdie-beliebtesten-fehler-in-biogasanlagen-die-sie-anderen-berlassen-sollten&usg=AOvVaw1H_AYaW9bTkjkvCyBZwT9e.

BIOGAS INFO. (2020). "Feedstocks." Retrieved, 15.09.2020, from http://www.biogas-info.co.uk/about/feedstocks/.

BIOSLING (2012) A new plant system for biogas upgrading on a small scale, farm size level. Retrieved, 16.08.2020, from http://biosling.se/en/products/biosling/.

BMWI, FEDERAL MINISTRY FOR ECONOMIC AFFAIRS AND ENERGY (2019) Renewable energy sources in figures, National and International Development, 2018, Berlin.

BMWI, FEDERAL MINISTRY OF ECONOMIC AFFAIRS AND ENERGY,. (2020). "Natural gas supply in Germany." Retrieved, 29.12.2020, from https://www.bmwi.de/Redaktion/EN/Artikel/Energy/gas-natural-gas-supply-in-germany.html.

BORGHI, A. D., BINAGHI, L., BORGHI, M. D., GALLO, M. (2007) The application of the environmental product declaration to waste disposal in a sanitary landfill: four case studies: *International Journal of Life Cycle Assessment* 12: 40-49.

BÖRJESSON, P., TUFVESSON, L., LANTZ, M. (2010) Life cycle assessment of biofuels in Sweden: *Lund: Department of Technology and Society, Lund University.*

BOZZANO, G., MANENTI, F. (2016) Efficient methanol synthesis: Perspectives, technologies and optimization strategies: *Prog Energy Combust Sci* 56: 71–105.

BOZZANO, G., PIROLA, C., ITALIANO, C., PELOSATO, R., VITA, A., MANENTI, F. 2017. Biogas: a Possible New Pathway to Methanol? , 2017, 523–528.

BRÄNDLE, G., SCHÖNFISCH, M., SCHULTE, S. (2020) Estimating long-term global supply costs for low-carbon hydrogen: In EWI Working Paper.

BRAUTSCH, M., LECHNER, R. (2013) Effizienzsteigerung durch Modellkonfiguration in BHKW-Anlagen: In Fraunhofer IRB Verlag (ed).

BRYNOLF, S., TALJEGARD, M., GRAHN, M., HANSSON, J. (2018) Electrofuels for the transport sector: A review of production costs: *Renewable and Sustainable Energy Reviews* 81: 1887-1905.

BSE ENGINEERING. (2020, Zugriff am 25. September 2020). "Flex Methanol." Retrieved, 17.11.2020, from http://www.bse-engineering.eu/small-scale-methanol-plant-flexmethanol.html.

BUNDESNETZAGENTUR. (2020). "Informationen zu Strom- und Gaspreisen für Haushaltskunden." Retrieved, 15.12.2020, from https://www.bundesnetzagentur.de/DE/Sachgebiete/ElektrizitaetundGas/Verbraucher/PreiseRechnTarife/preiseundRechnungen-node.html#FAQ402188.

BUNDESNETZAGENTUR AND BUNDESKARTELLAMT (2020) Monitoringbericht 2020.

BURATTI, C., BARBANERA, M., FANTOZZI, F. (2013) Assessment of GHG emissions of biomethane from energy cereal crops in Umbria, Italy: *Applied Energy* 108: 128-136.

BUTTLER, A., SPLIETHOFF, H. (2018) Current status of water electrolysis for energy storage, grid balancing and sector coupling via power-to-gas and power-to-liquids: A review: *Renewable and Sustainable Energy Reviews* 82: 2440-2454.

CANEVESI, R. L., BORBA, C. E., DA SILVA, E. A., GRANDE, C. A. (2019) Towards a design of a pressure swing adsorption unit for small scale biogas upgrading at: *Energy Procedia* 158: 848-853.

CARBON RECYCLING INTERNATIONAL. (2020, Zugriff am 25. September 2020). "Projects." Retrieved, 17.11.2020, from https://www.carbonrecycling.is/projects#project-goplant.

CASTELLANI, B., RINALDI, S., BONAMENTE, E., NICOLINI, A., ROSSI, F., COTANA, F. (2018) Carbon and energy footprint of the hydrate-based biogas upgrading process integrated with CO2 valorization: *Science of The Total Environment* 615: 404-411.

CAVALETT, O., CHAGAS, M. F., SEABRA, J. E., BONOMI, A. (2013) Comparative LCA of ethanol versus gasoline in Brazil using different LCIA methods: *The International Journal of Life Cycle Assessment* 18: 647-658.

CHAVES, I. D. G., LÓPEZ, J. R. G., ZAPATA, J. L. G., ROBAYO, A. L., NIÑO, G. R. (2016) *Process Analysis and Simulation in Chemical Engineering:* Springer International Publishing, Cham.

CHERUBINI, F., BARGIGLI, S., ULGIATI, S. (2009) Life cycle assessment (LCA) of waste management strategies: Landfilling, sorting plant and incineration: *Energy* 34: 2116-2123.

CHOI, E., SONG, K., AN, S., LEE, K., YOUN, M., PARK, K., JEONG, S., KIM, H. (2018) Cu/ZnO/AlOOH catalyst for methanol synthesis through CO2 hydrogenation: *Korean J Chem Eng* 35: 73–81.

CHRISTENSEN, P., DYSERT, L. R. (2011) *Cost Estimate Classification System - As Applied in Engineering, Procurement, and Construction for the Process Industries.*

CLAUSEN, L. R., HOUBAK, N., ELMEGAARD, B. (2010) Technoeconomic analysis of a methanol plant based on gasification of biomass and electrolysis of water: *Energy* 35: 2338-2347.

COLLET, P., FLOTTES, E., FAVRE, A., RAYNAL, L., PIERRE, H., CAPELA, S., PEREGRINA, C. (2017) Techno-economic and Life Cycle Assessment of methane production via biogas upgrading and power to gas technology: *Applied Energy* 192: 282-295.

CREMIATO, R., MASTELLONE, M. L., TAGLIAFERRI, C., ZACCARIELLO, L., LETTIERI, P. (2017) Environmental impact of municipal solid waste management using Life Cycle Assessment: The effect of anaerobic digestion, materials recovery and secondary fuels production: *Renewable Energy*.

DANIEL-GROMKE, J., RENSBERG, N., DENYSENKO, V., BARCHMANN, T., OEHMICHEN, K., BEIL, M., BEYRICH, W., KRAUTKREMER, B., TROMMLER, M., REINHOLZ, T. (2020) Optionen für Biogas-Bestandsanlagen bis 2030 aus ökonomischer und energiewirtschaftlicher Sicht: In Dessau-Roßlau: UBA-FB.

DANIEL-GROMKE, J., RENSBERG, N., DENYSENKO , V. D., TROMMLER, M., REINHOLZ, T., VÖLLER, K. D., BEIL, M., BEYRICH, W. I. (2017) Anlagenbestand Biogas und Biomethan - Biogaserzeugung und -nutzung in Deutschland: In DBFZ Report.

DE JONG, M. L. (2018) *Small Scale Methanol Production: Process modelling and design of an autonomous, renewable container sized methanol plant:* Delft.

DECKER, M., SCHORN, F., SAMSUN, R. C., PETERS, R., STOLTEN, D. (2018) Techno-economic analysis of a stand-alone power-to-liquid concept: In UFZ EnergyDays – Energy landscapes of today and tomorrow Leipzig.

DECKER, M., SCHORN, F., SAMSUN, R. C., PETERS, R., STOLTEN, D. (2019) Off-grid power-to-fuel systems for a market launch scenario–A techno-economic assessment: *Applied Energy* 250: 1099-1109.

DEN HEIJER, N. (2019). Data Biogas upgrading Pentair Haffmans. 22.01.2019.

DENA, DEUTSCHE ENERGIE-AGENTUR (2017) biogaspartner - gemeinsam einspeisen; Biogaseinspeisung und -nutzung in Deutschland und Europa Markt, Technik und Akteure.

DENA, DEUTSCHE ENERGIE-AGENTUR. (2019a, March 2019). "Einspeiseatlas." Retrieved, 05.08.2020, from https://www.biogaspartner.de/einspeiseatlas/.

DENA, DEUTSCHE ENERGIE-AGENTUR. (2019b, March 2019). "Einspeiseatlas." Retrieved 20.04.2020, from https://www.biogaspartner.de/einspeiseatlas/.

DENA, DEUTSCHE ENERGIE-AGENTUR GMBH, (2019c) Branchenbarometer Biomethan 2019, Berlin.

DENA, DEUTSCHE ENERGIE-AGENTUR GMBH, (2020) Branchenbarometer Biomethan 2020, Berlin.

DEUTZ, S., BONGARTZ, D., HEUSER, B., KÄTELHÖN, A., LANGENHORST, L. S., OMARI, A., WALTERS, M., KLANKERMAYER, J., LEITNER, W., MITSOS, A. (2018) Cleaner production of cleaner fuels: wind-to-wheel–environmental assessment of CO 2-based oxymethylene ether as a drop-in fuel: *Energy & Environmental Science*.

DIETRICH, R. U., ALBRECHT, F., PREGGER, T. (2018) Production of Alternative Liquid Fuels in the Future Energy System: *Chemie Ingenieur Technik* 90: 179-192.

DIMITRIOU, I., GARCÍA-GUTIÉRREZ, P., ELDER, R. H., CUÉLLAR-FRANCA, R. M., AZAPAGIC, A., ALLEN, R. W. (2015) Carbon dioxide utilisation for production of transport fuels: process and economic analysis: *Energy & Environmental Science* 8: 1775-1789.

DOTZAUER, M., PFEIFFER, D., THRÄN, D., LENZ, V., POHL, M., MÜLLER-LANGER, F. (2018) Technologiebericht 1.1 Bioenergie: In Wuppertal, Karlsruhe, Saarbrücken: Wuppertal Institut, ISI, IZES (Publ.).

EARLES, J. M., HALOG, A. (2011) Consequential life cycle assessment: a review: *The International Journal of Life Cycle Assessment* 16: 445-453.

EBA, EUROPEAN BIOGAS ASSOCIATION, GIE, GAS INFRASTRUCTURE EUROPE (2020) European Biomethane Map 2020, Brussels, Belgium.

EBA, EUROPEAN BIOGAS ASSOCIATION,. (2020). "EBA Statistical report 2019: European Overview." Retrieved, 10.11.2020, from https://www.europeanbiogas.eu/eba-statistical-report-2019-european-overview/.

EC, EUROPEAN COMMISSION (2018) Directive (EU) 2018/2001 of the European Parliament and of the Council of 11 December 2018 on the promotion of the use of energy from renewable source.

EC, EUROPEAN COMMISSION. (2020). "Circular Economy Action Plan." Retrieved, 25.05.2020, from https://ec.europa.eu/environment/circular-economy/.

EC, EUROPEAN COMMISSION, JRC, JOINT RESEARCH CENTRE, IES, INSTITUTE FOR ENVIRONMENT AND SUSTAINABILITY (2010) International Reference Life Cycle Data System (ILCD) Handbook - General guide for Life Cycle Assessment -Detailed guidance: In Luxembourg: Publications Office of the European Union.

EC, EUROPEAN COMMISSION (2019) Fertilisers in the EU - Prices, trade and use: In EU Agricultural Markets Briefs.

ECONOMIC INDICATORS. (2019, Zugriff am 25. September 2020). "Chemical Engineering." Retrieved, from www.chemengonline.com.

EDWARDS, R., LARIVÉ, J.-F., RICKEARD, D., WEINDORF, W. (2014) Well-to-Tank Report Version 4. a: *JEC Well-to-Wheels Analysis Well-to-Wheels Analysis of Future Automotive Fuels and Powertrains in the European Context Joint Research Centre (JRC).*

EGGEMANN, L., ESCOBAR, N., PETERS, R., BURAUEL, P., STOLTEN, D. (2020) Life cycle assessment of a small-scale methanol production system: A power-to-fuel strategy for biogas plants: *J Cleaner Prod* 271: 122476.

EKVALL, T., WEIDEMA, B. P. (2004) System boundaries and input data in consequential life cycle inventory analysis: *The international journal of life cycle assessment* 9: 161-171.

EMEP/EEA (2016) Biological treatment of waste - Anaerobic digestion at biogas facilities: In *EEA air pollutant emission inventory guidebook 2016 (EEA Report No 21/2016)*, Luxembourg.

EMR. (2020). "Global Methanol Market." Retrieved, 15.11.2020, from https://www.expertmarketresearch.com/reports/methanol-market.

ENERGIEAGENTUR.NRW. (2020). "Power-to-X." Retrieved, 28.09.2020, from https://www.energieagentur.nrw/tool/sektorenkopplung/information/power-to-x.php.

ENVIMAC, ENVIMAC ENGINEERING GMBH. Retrieved, 25.09.2020, from http://www.envimac.de/.

ERNEUERBARE ENERGIEN. (2011, 02.09.2011). " Landwirt eröffnet eigene Bio-Tankstelle." Retrieved, 05.08.2020, from https://www.erneuerbareenergien.de/archiv/landwirt-eroeffnet-eigene-bio-tankstelle-150-482-31805.html.

ESCOBAR, N., RIBAL, J., CLEMENTE, G., SANJUÁN, N. (2014) Consequential LCA of two alternative systems for biodiesel consumption in Spain, considering uncertainty: *Journal of cleaner production* 79: 61-73.

ESCOBAR, N., SANCHÍS, F. J. R., SEÑER, A. R., POLO, G. C., VIDAL, A. P., PELLICER, N. S. (2015) Uncertainty analysis in the environmental assessment of an integrated management system for restaurant and catering waste in Spain: *The International Journal of Life Cycle Assessment* 20: 244-262.

ESTEVES, E. M. M., HERRERA, A. M. N., ESTEVES, V. P. P., MORGADO, C. D. R. V. (2019) Life cycle assessment of manure biogas production: A review: *Journal of Cleaner Production* 219.

EUROSTAT. (2018, 26.09.2018). "Statistik der erneuerbaren Energien." Eurostat Statistics Explained Retrieved 07.09.2018, from https://ec.europa.eu/eurostat/statistics-explained/index.php?title=Renewable_energy_statistics/de.

FACHVERBAND BIOGAS. (2020). "Branchenzahlen 2019." Retrieved, 16.09.2020, from https://www.biogas.org/edcom/webfvb.nsf/id/de_branchenzahlen.

FACHVERBAND BIOGAS E.V. (2018) Düngen mit Gärprodukten: In Freising:

FERRARI, M., VARONE, A., STÜCKRAD, S., WHITE, R. J. (2014) Sustainable synthetic fuels: In Potsdam: IASS.

FERTILIZERS EUROPE (2019) Industry facts and figures 2019.

FINNVEDEN, G., HAUSCHILD, M. Z., EKVALL, T., GUINÉE, J., HEIJUNGS, R., HELLWEG, S., KOEHLER, A., PENNINGTON, D., SUH, S. (2009) Recent developments in life cycle assessment: *Journal of environmental management* 91: 1-21.

FIRMANSYAH, H., TAN, Y., YAN, J. (2018) Power and methanol production from biomass combined with solar and wind energy: analysis and comparison: *Energy Procedia* 145: 576-581.

FLUITEC, FLUITEC MIXING + REACTION SOLUTIONS AG,. (Zugriff am 25. September 2020). Retrieved, 25.09.2020, from https://www.fluitec.ch/statische-mischer-waermetauscher.html.

FNR, FACHAGENTUR NACHWACHSENDE ROHSTOFFE (2012) Biomethan: In Bioenergie, FNR (ed), Gülzow.

FNR, FACHAGENTUR NACHWACHSENDE ROHSTOFFE (2013) Leitfaden Biogas–Von der Gewinnung zur Nutzung. Fachagentur Nachwachsende Rohstoffe eV(Ed), Gülzow.

FNR, FACHAGENTUR NACHWACHSENDE ROHSTOFFE (2014) *Leitfaden Biogasaufbereitung und -einspeisung*, Gülzow.

FNR, FACHAGENTUR NACHWACHSENDE ROHSTOFFE (2016) *Leitfaden Biogas - Von der Gewinnung zur Nutzung*, Gülzow.

FNR, FACHAGENTUR NACHWACHSENDE ROHSTOFFE. (2018). "Verfahren zur Biogasaufbereitung." Abb 129 Retrieved, 17.08.2020, from https://mediathek.fnr.de/grafiken/daten-und-fakten/bioenergie/biogas/verfahren-zur-biogasaufbereitung.html.

FNR, FACHAGENTUR NACHWACHSENDE ROHSTOFFE. (2020a, 16.09.2020). "Forscherverbund will wirtschaftliche Güllevergärungsanlage im kleinen Leistungsbereich entwickeln." Retrieved, 14.04.2021, from https://www.fnr.de/presse/pressemitteilungen/aktuelle-mitteilungen/aktuelle-nachricht/forscherverbund-will-wirtschaftliche-guellevergaerungsanlage-im-kleinen-leistungsbereich-entwickeln.

FNR, FACHAGENTUR NACHWACHSENDE ROHSTOFFE E. V. (2019a) Bioenergy in Germany - Facts and Figures 2019. FNR (ed), Gülzow.

FNR, FACHAGENTUR NACHWACHSENDE ROHSTOFFE E. V. (2020b). "Biogasaufbereitung." Retrieved 22.10.2020, 22.10.2020, from https://biogas.fnr.de/biogas-gewinnung/anlagentechnik/biogasaufbereitung.

FUCHSZ, M., KOHLHEB, N. (2015) Comparison of the environmental effects of manure- and crop-based agricultural biogas plants using life cycle analysis: *Journal of Cleaner Production* 86: 60-66.

GARDONI, D., GUARINO, M. (2016) Drying and combustion of an anaerobic digestate: Results and economical evaluation of a demonstrative-scale plant: *Int J Eng Res Sci* 2: 148-155.

GÖKGÖZ, F., LIEBETRAU, J., NELLES, M. 2020. Kombinierte Bereitstellung von Strom und Kraftstoff an Biogasanlagen - Wirtschaftlichkeit von Anschlussszenarien. Landtechnik, 141-160.

GONZÁLEZ-GARCÍA, S., IRIBARREN, D., SUSMOZAS, A., DUFOUR, J., MURPHY, R. J. (2012) Life cycle assessment of two alternative bioenergy systems involving Salix spp. biomass: Bioethanol production and power generation: *Applied Energy* 95: 111-122.

GRAF, F., BAJOHR, S. (2013) *Biogas : Erzeugung, Aufbereitung, Einspeisung:* DIV, München.

GROSSO, M., NAVA, C., TESTORI, R., RIGAMONTI, L., VIGANÒ, F. (2012) The implementation of anaerobic digestion of food waste in a highly populated urban area: an LCA evaluation: *Waste Management & Research* 30: 78-87.

GUTHRIE, K. M. (1969) Data and techniques for preliminary capital cost estimating: *Chem Eng* 76: 114.

HAENEL, H.-D., RÖSEMANN, C., DÄMMGEN, U., DÖRING, U., WULF, S., EURICH-MENDEN, B., FREIBAUER, A., DÖHLER, H., SCHREINER, C., OSTERBURG, B. (2020) Calculations of gaseous and particulate emissions from German agriculture 1990-2018: Report on methods and data (RMD) Submission 2020: In Thünen Report.

HANSEN, J. B., NIELSEN, P. E. H. (2008) *"Methanol Synthesis" in: Handbook of Heterogeneous Catalysis online:* Wiley-VCH Verlag GbmH & Co. KGaA.

HAUG, HAUG SAUER KOMPRESSOREN AG,. (Zugriff am 25. September 2020). Retrieved, 25.09.2020, from https://www.haug.ch/de.

HEMMERLING, U., PASCHER, P., NAß, S. (2018) Situationsbericht 2017/18: Trends und Fakten zur Landwirtschaft, Deutscher Bauernverband.

HERBERT SMITH FREEHILLS. (2020). "Hydrogen in Germany " Retrieved, 08.12.2020, from https://www.lexology.com/library/detail.aspx?g=6182a7ff-ddc2-453b-9b6c-ca27f5b27b95.

HEUSER, P.-M., GRUBE, T., HEINRICHS, H., ROBINIUS, M., STOLTEN, D. (2020) Worldwide Hydrogen Provision Scheme Based on Renewable Energy: *Preprints 2020* 2020020100.

HIJAZI, O., MUNRO, S., ZERHUSEN, B., EFFENBERGER, M. (2016) Review of life cycle assessment for biogas production in Europe: *Renewable and Sustainable Energy Reviews* 54: 1291-1300.

HIRANO, M., AKANO, T., IMAI, T., KURODA, K. (1995) Methanol synthesis from carbon dioxide on CuO-ZnO-Al2O3 catalysts: *Energy Convers Manage* 36: 585–588.

HOFER, ANDREAS HOFER HOCHDRUCKTECHNIK GMBH,. (Zugriff am 25. September 2020). Retrieved, 25.09.2020, from https://www.hofer-hochdrucktechnik.de/home/.

HOWDEN, HOWDEN THOMASSEN COMPRESSORS B.V.,. (Zugriff am 25. September 2020). Retrieved, 25.09.2020, from https://www.howden.com/en-gb.

HOYER, K., HULTEBERG, C., SVENSSON, M., JERNEBERG, J., NØRREGÅRD, Ø. (2016) Biogas Upgrading - Technical Review, Energiforsk (ed).

HUIJBREGTS, M. A., NORRIS, G., BRETZ, R., CIROTH, A., MAURICE, B., VON BAHR, B., WEIDEMA, B., DE BEAUFORT, A. S. (2001) Framework for modelling data uncertainty in life cycle inventories: *The International Journal of Life Cycle Assessment* 6: 127.

HUIJBREGTS, M. A. J., STEINMANN, Z. J. N., ELSHOUT, P. M. F., STAM, G., VERONES, F., VIEIRA, M. D. M., HOLLANDER, A., ZIJP, M., VAN ZELM, R. (2016) ReCiPe 2016: A harmonized life cycle impact assessment method at midpoint and endpoint level Report I: Characterization.

HUISMAN, G., VAN RENS, G., DE LATHOUDER, H., CORNELISSEN, R. (2011) Cost estimation of biomass-to-fuel plants producing methanol, dimethylether or hydrogen: *Biomass and Bioenergy* 35: S155-S166.

IEA, INTERNATIONAL ENERGY AGENCY. (2020). "The Future of Hydrogen - Seizing today’s opportunities." Retrieved, 08.12.2020, from https://www.iea.org/reports/the-future-of-hydrogen.

IMPCA. (2015). "Methanol Reference Specification." International Methanol Producers & Consumers Association, Brussels.

INERATEC. (2017, Zugriff am 25. September 2020). "Modulare chemische Anlagen." Retrieved, 17.11.2020, from https://ineratec.de/technologien/.

IPCC (2006a) Emissions from Livestock and Manure Management: In *Guidelines for National Greenhouse Gas Inventories*.

IPCC (2006b) Biological Treatment of Solid Waste: In *Guidelines for National Greenhouse Gas Inventories*.

IPNI, INTERNATIONAL PLANT NUTRITION INSTITUTE (2019) Single Superphosphate: In Norcross, Georgia: same as author.

ISO, INTERNATIONAL ORGANIZATION FOR STANDARDIZATION, (2006a) *ISO 14040 - Environmental Management: Life Cycle Assessment; Principles and Framework:* ISO.

ISO, INTERNATIONAL ORGANIZATION FOR STANDARDIZATION, (2006b) *ISO 14044 - Environmental Management: Life Cycle Assessment; Requirements and guidelines:* ISO.

JOKORA. (2020). "Eisen-II-Chloridlösung 30%." Retrieved, 30.12.2020, from https://www.jokora.de/biogasanlagen/eisen-ii-chloridloesung/eisen-ii-chloridloesung-30-1200-kg-ibc-container.

KAPOOR, R., GHOSH, P., TYAGI, B., VIJAY, V. K., VIJAY, V., THAKUR, I. S., KAMYAB, H., NGUYEN, D. D., KUMAR, A. (2020) Advances in biogas valorization and utilization systems: A comprehensive review: *Journal of Cleaner Production* 273: 123052.

KEHLER, T., AZUMA-DICKE, N., FRIEDL, V., KIRCHSTRAßE, N., MÜLLER-SYRING, G., GROßE, C., GLANDIEN, J., EYßER, M. (2016) Critical evaluation of default values for the GHG emissions of the natural gas supply chain.

KHAN, I. U., OTHMAN, M. H. D., HASHIM, H., MATSUURA, T., ISMAIL, A., REZAEI-DASHTARZHANDI, M., AZELEE, I. W. (2017) Biogas as a renewable energy fuel–A review of biogas upgrading, utilisation and storage: *Energy Conversion and Management* 150: 277-294.

KIND, M., MARTIN, H. (2013) *VDI–Wärmeatlas: Mit 320 Tabellen:* Springer Vieweg, Berlin.

KOHLHEB, N., WLUKA, M., BEZAMA, A., THRÄN, D., AURICH, A., MÜLLER, R. A. (2020) Environmental-Economic Assessment of the Pressure Swing Adsorption Biogas Upgrading Technology: *BioEnergy Research*: 1-9.

KREIDELMEYER, S., DAMBECK, H., KIRCHNER, A., WÜNSCH, M. (2020) Kosten und Transformationspfade für strombasierte Energieträger, AG, P. (ed).

KUCKSHINRICHS, W., HAKE, J.-F. (2012) *CO2-Abscheidung,-Speicherung und-Nutzung: Technische, wirtschaftliche, umweltseitige und gesellschaftliche Perspektive-Advances in Systems Analysis 2:* Forschungszentrum Jülich.

KUPFER, T., BAITZ, M., COLODEL, C. M., KOKBORG, M., SCHÖLL, S., RUDOLF, M., THELLIER, L., BOS, U., BOSCH, F., GONZALEZ, M., SCHULLER, O., HENGSTLER, J., STOFFREGEN, A., THYLMANN, D. (2019) GaBi Database & Modelling Principles: In thinkstep AG.

L&C SCIENCE TECHNOLOGY. (2020). "Low Capacity PSA Testing Instrument." Retrieved, 15.08.2020, from http://www.landcscience.com/psa-300-lc/.

LANSCHE, J., MÜLLER, J. (2012) Life cycle assessment of energy generation of biogas fed combined heat and power plants: environmental impact of different agricultural substrates: *Engineering in Life Sciences* 12: 313-320.

LEE, U., HAN, J., WANG, M., WARD, J., HICKS, E., GOODWIN, D., BOUDREAUX, R., HANARP, P., SALSING, H., DESAI, P. (2016) Well-to-wheels emissions of Greenhouse gases and air pollutants of dimethyl ether from natural gas and renewable feedstocks in comparison with petroleum gasoline and diesel in the United States and Europe: *SAE International Journal of Fuels and Lubricants* 9: 546-557.

LEMS, R., DIRKSE, E. H. M. (2010) Small scale biogas upgrading: Green gas with the DMT Carborex-MS® system: In 15th European Biosolids and Organic Resources Conference, Leeds, UK.

LENTON, T. M., ROCKSTRÖM, J., GAFFNEY, O., RAHMSTORF, S., RICHARDSON, K., STEFFEN, W., SCHELLNHUBER, H. J. (2019) Climate tipping points—too risky to bet against: In Nature Publishing Group.

LI, H., MEHMOOD, D., THORIN, E., YU, Z. (2017) Biomethane production via anaerobic digestion and biomass gasification: *Energy Procedia* 105: 1172-1177.

LIEBETRAU, J., REINELT, T., AGOSTINI, A., LINKE, B. (2017) *Methane emissions from biogas plants:* IEA bioenergy.

LOHSE, D. (2019) Kohlenstoffdioxid-Gewinnung aus Biogasanlagen für die weitere Verwendung im Power-to-Fuel Konzept – Technoökonomische Bewertungen und Anlagensimulationen: In Rheinisch-Westfälische Technische Hochschule Aachen.

LOMBARDI, L., FRANCINI, G. (2020) Techno-economic and environmental assessment of the main biogas upgrading technologies: *Renewable Energy*.

LUND, H., MATHIESEN, B. V., CHRISTENSEN, P., SCHMIDT, J. H. (2010) Energy system analysis of marginal electricity supply in consequential LCA: *The International Journal of Life Cycle Assessment* 15: 260-271.

MAN. (2020). "Gasmotoren zur Energieerzeugung." Retrieved, 15.04.2021, from https://www.engines.man.eu/man/media/content_medien/doc/global_engines/power/Power_Gas_DE_190919_web.pdf.

MARŠÁLEK, J., BROŽ, P., BOBÁK, M. Complex biogas membrane upgrading to BioCNG at agriculture biogas plant: *Chemical Papers*: 1-13.

MATSCHOSS, P., HAUSER, E., MÜLLER-LANGER, F., SCHRÖDER, J., BRAND, U., DIETRICH, R.-U., EGGEMANN, L., PETERS, R., THEISS, L., DITTMEYER, R., RÖSCH, C., HAASE, M., MILLINGER, M., TERRAPON-PFAFF, J., FUCHS, A.-L., SCHMIDT, M. (2020) Synthetische Kraftstoffe – Ökonomie, Gesellschaft, Nachhaltigkeit: *Forschung für den European Green Deal, Beiträge zur FVEE-Jahrestagung 2020*: 37-42.

MATZEN, M., DEMIREL, Y. (2016) Methanol and dimethyl ether from renewable hydrogen and carbon dioxide: Alternative fuels production and life-cycle assessment: *Journal of cleaner production* 139: 1068-1077.

MAXIMATOR, MAXIMATOR GMBH,. (Zugriff am 25. September 2020). Retrieved, 25.09.2020, from https://www.maximator.de/flycms/de/web/1/-/Startseite.html.

MCALLISTER, S., CHEN, J.-Y., FERNANDEZ-PELLO, A. C. (2011) *Fundamentals of combustion processes:* Springer.

MCMANUS, M. C. (2012) Environmental consequences of the use of batteries in low carbon systems: The impact of battery production: *Applied Energy* 93: 288-295.

MEFCO$_2$. (2016, Zugriff am 25. September 2020). Retrieved, 17.11.2020, from http://www.mefco2.eu/.

MENG, F., MCKECHNIE, J. (2019) Challenges in Quantifying Greenhouse Gas Impacts of Waste-Based Biofuels in EU and US Biofuel Policies: Case Study of

Butanol and Ethanol Production from Municipal Solid Waste: *Environmental science & technology* 53: 12141-12149.

MERGEL, J., EMONTS, B., FIECHTER, S., HEBLING, C., JENTSCH, M., MERTEN, F., PITSCHAK, B. (2012) *Wasserelektrolyse und regenerative Gase als Schlüsselfaktoren für die Energiesystemtransformation.*

METHANEX. (2020). "Monthly Average Regional Posted Contract Price History." Retrieved, 25.09.2020, from www.methanex.com.

METHANOL INSTITUTE. (2020). "MMSA Global Methanol Supply and Demand Balance." Retrieved, 25.22.2020, from https://www.methanol.org/methanol-price-supply-demand/.

MEZZULLO, W. G., MCMANUS, M. C., HAMMOND, G. P. (2013) Life cycle assessment of a small-scale anaerobic digestion plant from cattle waste: *Applied Energy* 102: 657-664.

MIGNARD, D., SAHIBZADA, M., DUTHIE, J., WHITTINGTON, H. (2003) Methanol synthesis from flue-gas CO2 and renewable electricity: a feasibility study: *International Journal of Hydrogen Energy* 28: 455-464.

MILANI, D., KHALILPOUR, R., ZAHEDI, G., ABBAS, A. (2015) A model-based analysis of CO2 utilization in methanol synthesis plant: *Journal of CO2 Utilization* 10: 12-22.

MILLINGER, M., TAFARTE, P., JORDAN, M., HAHN, A., MEISEL, K., THRÄN, D. (2020) Electrofuels from Excess Renewable Electricity at High Variable Renewable Shares: Cost, Greenhouse Gas Abatement, Carbon Use and Competition.

MITSUI CHEMICALS INC. (2008, Zugriff am 25. September 2020). "Mitsui Chemicals to Establish a Pilot Facilityto Study a Methanol Synthesis Process from CO2." Retrieved, from https://jp.mitsuichemicals.com/en/release/2008/pdf/080825e.pdf.

MODISHA, P. M., OUMA, C. N. M., GARIDZIRAI, R., WASSERSCHEID, P., BESSARABOV, D. (2019) The Prospect of Hydrogen Storage Using Liquid Organic Hydrogen Carriers: *Energy Fuels* 33: 2778–2796.

MOGHADDAM, E. A., AHLGREN, S., HULTEBERG, C., NORDBERG, Å. (2015) Energy balance and global warming potential of biogas-based fuels from a life cycle perspective: *Fuel Processing Technology* 132: 74-82.

MOGHADDAM, E. A., AHLGREN, S., NORDBERG, Å. (2016) Assessment of novel routes of Biomethane Utilization in a life cycle Perspective: *Frontiers in bioengineering and biotechnology* 4: 89.

MORALES, M., QUINTERO, J., CONEJEROS, R., AROCA, G. (2015) Life cycle assessment of lignocellulosic bioethanol: environmental impacts and energy balance: *Renewable and Sustainable Energy Reviews* 42: 1349-1361.

MORENO RUIZ, E., VALSASINA, L., FITZGERALD, D., SYMEONIDIS, A., TURNER, D., MÜLLER, J., MINAS, N., BOURGAULT, G., VADENBO, C., IOANNIDOU, D. (2020) Documentation of changes implemented in ecoinvent database v3. 7. ecoinvent Association, Zürich, Switzerland.

MOZGOVOY, A. (2020) Biomethan als Kraftstoff im ländlichen Raum: In Biokraftstofftagung, 26.11.2020.

NYÁRI, J., MAGDELDIN, M., LARMI, M., JÄRVINEN, M., SANTASALO-AARNIO, A. (2020) Techno-economic barriers of an industrial-scale methanol CCU-plant: *Journal of CO2 Utilization* 39: 101166.

O'KEEFFE, S., FRANKO, U., OEHMICHEN, K., DANIEL-GROMKE, J., THRÄN, D. (2019) Give them credit-the greenhouse gas performance of regional biogas systems: *GCB Bioenergy* 11: 791-808.

OEHMICHEN, K. (2020). Phone call. 04.05.2020.

OEHMICHEN, K., THRÄN, D. (2017) Fostering renewable energy provision from manure in Germany–Where to implement GHG emission reduction incentives: *Energy Policy* 110: 471-477.

OESTER, U. (2019) Small biogas upgrading systems for gas grid injection or vehicle refuelling: In IBBK Biogas, Schwäbisch Hall.

OESTER, U., DUTTWILER, S. (2018) Blue BONSAI - Klein-Biogasaufbereitungsanlage mit Biogas Tankstelle: In BFE, Bundesamt für Energie, (ed) Bern.

OSTERBURG, B. (2019) Klimaschutz und Wirtschaftsdüngermanagement: In Biogas-Fachgespräch „Nutzungsoptionen und Handlungsempfehlungen für den Erhalt und den Ausbau der Güllenutzung in Biogasanlagen“, Deutsche Biomasse Forschungszentrum, DBFZ (ed) Leipzig, Germany.

OTT, J., GRONEMANN, V., PONTZEN, F., FIEDLER, E., GROSSMANN, G., KERSEBOHM, D. B., WEISS, G., WITTE, C. (2012) *"Methanol" in: Ullmann's encyclopedia of industrial chemistry.*

OTTO, A. (2015). Chemische, verfahrenstechnische und ökonomische Bewertung von Kohlendioxid als Rohstoff in der chemischen Industrie. 268, Forschungszentrum, Zentralbibliothek.

PAOLINI, V., PETRACCHINI, F., SEGRETO, M., TOMASSETTI, L., NAJA, N., CECINATO, A. (2018) Environmental impact of biogas: A short review of current knowledge: *Journal of Environmental Science and Health, Part A* 53: 899-906.

PEARSON, R. J., TURNER, J. W. G. (2014) 2 - The role of alternative and renewable liquid fuels in environmentally sustainable transport: In *Alternative Fuels and Advanced Vehicle Technologies for Improved Environmental Performance*, Folkson, R. (ed) pp 19-51. Woodhead Publishing.

PEDERSEN, T. H., SCHULTZ, R. H., KÆR, S. K., HOFFMANN, P. (2014) *Technical and economic assessment of methanol production from biogas:* LAP LAMBERT Academic Publishing Aalborg.

PELLETIER, N., ARDENTE, F., BRANDÃO, M., DE CAMILLIS, C., PENNINGTON, D. (2015) Rationales for and limitations of preferred solutions for multi-functionality problems in LCA: is increased consistency possible?: *The International Journal of Life Cycle Assessment* 20: 74-86.

PÉREZ-CAMACHO, M. N., CURRY, R., CROMIE, T. (2019) Life cycle environmental impacts of biogas production and utilisation substituting for grid electricity, natural gas grid and transport fuels: *Waste Management* 95: 90-101.

PÉREZ-FORTES, M., SCHÖNEBERGER, J. C., BOULAMANTI, A., TZIMAS, E. (2016) Methanol synthesis using captured CO 2 as raw material: Techno-economic and environmental assessment: *Applied Energy* 161: 718-732.

PETERS, M. S., TIMMERHAUS, K. D., WEST, R. E. (2003) *Plant design and economics for chemical engineers:* McGraw-Hill, Boston.

PETERS, R., BALTRUWEIT, M., GRUBE, T., SAMSUN, R. C., STOLTEN, D. (2019) A techno economic analysis of the power to gas route: *Journal of CO2 Utilization* 34: 616-634.

PETERS, R., DECKER, M., EGGEMANN, L., SCHEMME, S., SCHORN, F., BREUER, J. L., WEISKE, S., PASEL, J., SAMSUN, R. C., STOLTEN, D. (2020) Thermodynamic and ecological preselection of synthetic fuel intermediates from biogas at farm sites: *Energy, Sustainability and Society* 10: 4.

POESCHL, M., WARD, S., OWENDE, P. (2010) Evaluation of energy efficiency of various biogas production and utilization pathways: *Applied Energy* 87: 3305-3321.

POESCHL, M., WARD, S., OWENDE, P. (2012a) Environmental impacts of biogas deployment–Part II: life cycle assessment of multiple production and utilization pathways: *Journal of Cleaner Production* 24: 184-201.

POESCHL, M., WARD, S., OWENDE, P. (2012b) Environmental impacts of biogas deployment – Part I: life cycle inventory for evaluation of production process emissions to air: *Journal of Cleaner Production* 24: 168-183.

PONTZEN, F., LIEBNER, W., GRONEMANN, V., ROTHAEMEL, M., AHLERS, B. (2011) CO2-based methanol and DME – Efficient technologies for industrial scale production: *Catalysis Today* 171: 242–250.

PREVITALI, D., VITA, A., BASSANI, A., ITALIANO, C., AMARAL, A. F., PIROLA, C., PINO, L., PALELLA, A., MANENTI, F. (2018) Methanol synthesis: a distributed production concept based on biogas plants: *Chemical Engineering Transactions* 65: 409-414.

PRIEUR-VERNAT, A., PACITTO, P., HEC, D., BICHLER, V. (2011). LCA of the European gas chain: challenges and results. International Gas Union Research Conference, Seoul, South Korea.

PROGNOS (2018) *Status und Perspektiven flüssiger Energieträger in der Energiewende (Endbericht).*

PST PURENERGY. (2020). "Erdgas Fakten - So kommt das Erdgas nach Deutschland." Retrieved, 29.10.2020, from https://www.pst-energie.de/magazin/erdgas-fakten/so-kommt-das-erdgas-nach-deutschland/.

RAU, F. (2019). Personal Communication. 25.03.2019.

RAU, F. (in press). Einsatz biogener Kraftstoffe zur Senkung der Emissionen von stationären Verbrennungsmotoren. Technische Universität Bergakademie Freiberg.

RENÓ, M. L. G., LORA, E. E. S., PALACIO, J. C. E., VENTURINI, O. J., BUCHGEISTER, J., ALMAZAN, O. (2011) A LCA (life cycle assessment) of the methanol production from sugarcane bagasse: *Energy* 36: 3716-3726.

RENON, H., PRAUSNITZ, J. M. (1968) Local compositions in thermodynamic excess functions for liquid mixtures: *AIChE J* 14: 135–144.

RIVAROLO, M., BELLOTTI, D., MAGISTRI, L., MASSARDO, A. F. (2016) Feasibility study of methanol production from different renewable sources and thermo-economic analysis: *Int J Hydrogen Energy* 41: 2105–2116.

ROBINIUS, M., LINßEN, J., GRUBE, T., REUß, M., STENZEL, P., SYRANIDIS, K., KUCKERTZ, P., STOLTEN, D. (2018a) Comparative Analysis of Infrastructures: Hydrogen Fueling and Electric Charging of Vehicles.

ROBINIUS, M., LINßEN, J., GRUBE, T., REUß, M., STENZEL, P., SYRANIDIS, K., KUCKERTZ, P., STOLTEN, D. (2018b) Comparative Analysis of Infrastructures: Hydrogen Fueling and Electric Charging of Vehicles: *Forschungszentrum Jülich Jülich (Schriften des Forschungszentrums Jülich, Reihe Energie und Umwelt, 408).*

ROCHA, M. H., CAPAZ, R. S., LORA, E. E. S., NOGUEIRA, L. A. H., LEME, M. M. V., RENÓ, M. L. G., DEL OLMO, O. A. (2014) Life cycle assessment (LCA) for biofuels in Brazilian conditions: a meta-analysis: *Renewable and Sustainable Energy Reviews* 37: 435-459.

RUSSOW, F. (2013). "Gasfackeln - technische Grundlagen und Anwendung auf landwirtschaftlichen Biogasanlagen." Biogas Forum Bayern Retrieved, 25.08.2020, from http://www.biogas-forum-bayern.de/publikationen/Gasfackeln_-_technische_Grundlagen_und_Anwendung_auf_landwirtschaftlichen_Biogasanlagen.pdf.

RUTZMOSER, K., HORLACHER, D., SCHULTHEIß, U. (2014). "Festmist- und Jaucheanfall, Mengen und Nährstoffgehalte aus Bilanzierungsmodelle." Schrift 502 Retrieved, from http://www.landwirtschaftskammern.de/pdf/guelledaten-rinder.pdf.

SABA, S. M., MÜLLER, M., ROBINIUS, M., STOLTEN, D. (2018) The investment costs of electrolysis–A comparison of cost studies from the past 30 years: *International journal of hydrogen energy* 43: 1209-1223.

SÄCHSISCHES NETZWERK BIOMASSE E.V. (2020a). "Biogasanlage Clausnitz Anlage 1: Nassfermentationsanlage " Retrieved, 20.08.2020, from https://www.biomasse-freiberg.de/anlagen/biogasanlagen/clausnitz-6.html.

SÄCHSISCHES NETZWERK BIOMASSE E.V. (2020b). "Biogasanlage Clausnitz Anlage 2: 75 kW-Anlage." Retrieved, 20.08.2020, from https://www.biomasse-freiberg.de/anlagen/biogasanlagen/clausnitz-4.html.

SALA, S., CERUTTI, A. K., PANT, R. (2018) Development of a weighting approach for the Environmental Footprint: *Publications Office of the European Union: Luxembourg*.

SCHEMME, S. (2020) *Techno-ökonomische Bewertung von Verfahren zur Herstellung von Kraftstoffen aus H2 und CO2:* RWTH, Aachen.

SCHEMME, S., BREUER, J., KÖLLER, M., MESCHEDE, S., WALMAN, F., SAMSUN, R. C., PETERS, R., STOLTEN, D. (2019) H2 based synthetic fuels: A techno-economic comparison of alcohol, ether and hydrocarbon production: *Hydrogen Energy*.

SCHEUTZ, C., FREDENSLUND, A. M. (2019) Total methane emission rates and losses from 23 biogas plants: *Waste Management* 97: 38-46.

SCHIEBAHN, S., GRUBE, T., ROBINIUS, M., TIETZE, V., KUMAR, B., STOLTEN, D. (2015) Power to gas: Technological overview, systems analysis and economic assessment for a case study in Germany: *International journal of hydrogen energy* 40: 4285-4294.

SCHNEIDER-GÖTZ, N., MASTEL, K. (2007) Gärreste aus Biogasanlagen - Nähr- und Schadstoffe, Einsatzmöglichkeiten im Ackerbau: In Landwirtschaftliches Technologiezentrum Augustenberg (LTZ) (ed), Karlsruhe.

SCHOLWIN, F., GROPE, J., CLINKSCALES, A., DANIEL-GROMKE, J., RENSBERG, N., DENYSENKO, V., STINNER, W., RICHTER, F., RAUSSEN, T., KERN, M., TURK, T., REINHOLD, G. (2019) Aktuelle Entwicklung und Perspektiven der Biogasproduktion aus Bioabfall und Gülle: In Umweltbundesamt (ed) Dessau-Roßlau.

SCHOLWIN, F., GROPE, J., SCHÜCH, A., DANIEL-GROMKE, J., BEIL, M., HOLZHAMMER, U. (2014) Ist-Stand der Biomethannutzung: *Kosten–Klimawirkungen–Verwertungswege KWK aus Biogas, Biomethan und Erdgas im Vergleich, Dossier Weimar: Institut für Biogas, Kreislaufwirtschaft & Energie*

SCHORN, F. (2018) *Dynamische Simulation und Auslegung eines Power-to-Liquid-Konzeptes mit integrierter Wasserstoffproduktion:* Aachen.

SCHORN, F., LOHSE, D., SAMSUN, R. C., PETERS, R., STOLTEN, D. (2020) The Biogas-Oxyfuel Process as a Carbon Source for Power-to-Fuel Synthesis: Enhancing Availability while Reducing Separation Effort: *Journal of CO2 Utilization 45.*

SCHWARTZENTRUBER, J., RENON, H. (1989) Extension of UNIFAC to high pressures and temperatures by the use of a cubic equation of state: *Ind Eng Chem Res* 28: 1049–1055.

SIMLA, T., STANEK, W. (2019) Thermo-ecological assessment of import of natural gas to Poland: *CONTEMPORARY PROBLEMS OF POWER ENGINEERING AND ENVIRONMENTAL PROTECTION 2019*: 49.

SMOLINKA, T., WIEBE, N., STERCHELE, P., PALZER, A., LEHNER, F., JANSEN, M., KIEMEL, S., MIEHE, R., WAHREN, S., ZIMMERMANN, F. (2018) *Studie IndWEDe Industrialisierung der Wasser-elektrolyse in -Deutschland: -Chancen und -Herausforderungen für nachhaltigen Wasserstoff für Verkehr, Strom und -Wärme:* Berlin.

SONNEMANN, G., VIGON, B. (2011) Global guidance principles for Life Cycle Assessment (LCA) databases: a basis for greener processes and products.

SOTERIADES, A. D., GONZALEZ-MEJIA, A. M., STYLES, D., FOSKOLOS, A., MOORBY, J. M., GIBBONS, J. M. (2018) Effects of high-sugar grasses and improved manure management on the environmental footprint of milk production at the farm level: *Journal of cleaner production* 202: 1241-1252.

STATISTA. (2019). "Jährliche Entwicklung des Wechselkurses des Euro gegenüber dem US-Dollar von 1999 bis 2019." Retrieved, from https://de.statista.com/statistik/daten/studie/200194/umfrage/wechselkurs-des-euro-gegenueber-dem-us-dollar-seit-2001/.

STINNER, W. (2018). Email Communication.

STINNER, W., STUR, M., PAUL, N., RIESEL, D. (2015) Gülle-Kleinanlagen: In Fachagentur Nachwachsende Rohstoffe e. V. (FNR) (ed).

SUN, Q., LI, H., YAN, J., LIU, L., YU, Z., YU, X. (2015) Selection of appropriate biogas upgrading technology-a review of biogas cleaning, upgrading and utilisation: *Renewable and Sustainable Energy Reviews* 51: 521-532.

SWANSON, R. M., PLATON, A., SATRIO, J. A., BROWN, R. C. (2010) Techno-economic analysis of biomass-to-liquids production based on gasification: *Fuel* 89: S11-S19.

SYSADVANCE. (2019). "Biogas Upgrading - Energy Catalogue." Retrieved, 16.08.2020, from https://www.sysadvance.com/#!/categoria/?id=biogas-upgrading.

ÞORBJÖRNSSON, Þ. (2016). Small-scale biogas upgrading: feasibility study of small-scale biogas upgrading in Iceland and possible methods. Reykjavik University.

THRÄN, D., BUNZEL, K., SEYFERT, U., ZELLER, V., BUCHHORN, M., MÜLLER, K., MATZDORF, B., GAASCH, N., KLÖCKNER, K., MÖLLER, I., STARICK, A., BRANDES, J., GÜNTHER, K., THUM, M., ZEDDIES, J., SCHÖNLEBER, N., GAMER, W., SCHWEINLE, J., WEIMAR, H. (2011) Final Report: Global and Regional Spatial Distribution of Biomass Potentials – Status quo and options for specification –: In DBFZ, D. B. (ed) Leipzig.

THYSSENKRUPP INDUSTRIAL SOLUTIONS AG. (2020, Zugriff am 25. September 2020). "Methanol plants." Retrieved, 17.11.2020, from https://www.thyssenkrupp-industrial-solutions.com/de/produkte-und-services/chemische-anlagen-und-prozesse/methanol-plants.

TILLMAN, A.-M. (2000) Significance of decision-making for LCA methodology: *Environmental Impact Assessment Review* 20: 113-123.

TOWLER, G. P., SINNOTT, R. K. (2008) *Chemical engineering design: Principles, practice and economics of plant and process design:* Elsevier/Butterworth-Heinemann, Amsterdam; Boston.

TREYER, K., BAUER, C., SIMONS, A. (2014) Human health impacts in the life cycle of future European electricity generation: *Energy Policy* 74: S31-S44.

TURTON, R., BAILIE, R. C., WHITING, W. B., SHAEIWITZ, J. A. (2009) *Analysis, synthesis and design of chemical processes:* Pearson Education.

USHIKOSHI, K., MORI, K., WATANABE, T., MASAMI, T., SAITO, M. (1998) A 50 kg/day class test plant for methanol synthesis from CO_2 and H_2: *Stud Surf Sci Catal*: 357–362.

UUSITALO, V., VÄISÄNEN, S., INKERI, E., SOUKKA, R. (2017) Potential for greenhouse gas emission reductions using surplus electricity in hydrogen, methane and methanol production via electrolysis: *Energy Conversion and Management* 134: 125-134.

VAN STAPPEN, F., MATHOT, M., DECRUYENAERE, V., LORIERS, A., DELCOUR, A., PLANCHON, V., GOFFART, J.-P., STILMANT, D. (2016) Consequential environmental life cycle assessment of a farm-scale biogas plant: *Journal of environmental management* 175: 20-32.

VARONE, A., FERRARI, M. (2015) Power to liquid and power to gas: An option for the German Energiewende: *Renewable and Sustainable Energy Reviews* 45: 207-218.

VCI, VERBAND DER CHEMISCHEN INDUSTRIE E.V. (2018) Chemiewirtschaft in Zahlen 2018, Frankfurt am Main.

VERHELST, S., TURNER, J. W. G., SILEGHEM, L., VANCOILLIE, J. (2019) Methanol as a fuel for internal combustion engines: *Progress in Energy and Combustion Science* 70: 43-88.

VIEBAHN, P., HORST, J., SCHOLZ, A., ZELT, O. (2018) Technologiebericht 4.4 Verfahren der CO2-Abtrennung aus Faulgasen und Umgebungsluft innerhalb des Forschungsprojekts TF_Energiewende.

WACHSMUTH, J., OBERLE, S., ZUBAIR, A., KÖPPEL, W. (2019) Wie klimafreundlich ist LNG?

Kurzstudie zur Bewertung der Vorkettenemissionen bei Nutzung von verflüssigtem Erdgas (LNG): In Climate Change, Umweltbundesamt, UBA (ed), Dessau-Roßlau.

WALLASCH, A.-K., LÜERS, S., HEYKEN, M., REHFELD, K., JACHMANN, H. (2019) *Vorbereitung und Begleitung bei der Erstellung eines Erfahrungsberichts gemäß § 97 Erneuerbare-Energien-Gesetz: Teilvorhaben II e): Wind an Land.*

WALMAN, F. (2018) *Entwicklung einer Methode zur ökonomischen Bewertung von alternativen Kraftstoffen basierend auf erneuerbarem Strom:* Aachen.

WEICHGREBE, D. (2015) *Kompendium Biogas:* Institut für Siedlungswasserwirtschaft und Abfalltechnik der Leibniz.

WEIDEMA, B. P., PIZZOL, M., SCHMIDT, J., THOMA, G. (2018) Attributional or consequential Life Cycle Assessment: A matter of social responsibility: *Journal of cleaner production* 174: 305-314.

WEINFURTNER, K. (2011) Matrix parameters and storage conditions of manure: In Umweltbundesamt, Dessau-Roßlau, 1–54.

WEINRICH, S., PATERSON, M., ROTH, U. (2020) Leitfaden zur Substrat-und Effizienz-bewertung an Biogasanlagen.

WEISKE, S. (2020/unpublished). Evaluation of Reactor Concepts for Fuel Synthesis from Hydrogen and Carbondioxide by CFD-Simulations.

WENDLAND, M., LICHTI, F. (2012) Biogasgärreste - Einsatz von Gärresten aus der Biogasproduktion als Düngemittel: In Bayern, B. F. (ed).

WERN, B., DOTZAUER, M., GAWEL, E. (2019) Analyse der gesamtökonomischen Effekte von Biogasanlagen - MakroBiogas: In IZES gGmbH, DBFZ gGmbH, UFZ GmbH.

WERNET, G., BAUER, C., STEUBING, B., REINHARD, J., MORENO-RUIZ, E., WEIDEMA, B. (2016) The ecoinvent database version 3 (part I): overview and methodology: *The International Journal of Life Cycle Assessment* 21: 1218-1230.

WETTENGEL, J. (2019). "Germany’s dependence on imported fossil fuels." Retrieved 16.12.2019, from https://www.cleanenergywire.org/factsheets/germanys-dependence-imported-fossil-fuels.

WIEGLEB, G. (2016) Physikalische Eigenschaften von Gasen: In *Gasmesstechnik in Theorie und Praxis*, pp 7-118. Springer.

WOODS, D. R. (2007) *Rules of Thumb in Engineering Practice:* Wiley-VCH, Weinheim.

WULF, S., HAENEL, H.-D., RÖSEMANN, C., GREBE, S. (2019) Berücksichtigung der Biogaserzeugung im landwirtschaftlichen Emissionsinventar: In KTBL, K. f. T. u. B. i. d. L. (ed) Darmstadt.

ZÄH, M. 2006. Biogas-Zündstrahlaggregat ES 2656 von Schnell - Intelligentes Herz. Profi Veredelungstechnik, 52-55.

ZAMAGNI, A., GUINÉE, J., HEIJUNGS, R., MASONI, P., RAGGI, A. (2012) Lights and shadows in consequential LCA: *The International Journal of Life Cycle Assessment* 17: 904-918.

ZHANG, Y., WHITE, M. A., COLOSI, L. M. (2013) Environmental and economic assessment of integrated systems for dairy manure treatment coupled with algae bioenergy production: *Bioresource technology* 130: 486-494.

ZIELBAUER, J., GAIDA, R., KNOTT, G. (2007) Wärmenutzung bei Biogasanlagen: In Schriftenreihe der Sächsischen Landesanstalt für Landwirtschaft, Sächsische Landesanstalt für Landwirtschaft (ed).

ZORN, S., REBBE, F., FREITAG, T., DOBMAIER, A., ILG, B., EULENSTEIN, F. (2014) Treibhausgas-Emissionen der sächsischen Landwirtschaft und ihre Minderungspotenziale: In Schriftenreihe des LfULG, Landesamt für Umwelt, Landwirtschaft und Geologie (ed).

Chapter 8
Appendices

8.1 Appendix A: Tables and figures

Table A 1: Composition of the feedstock input into the fermenter and digestate output for the two plants according to RAU (2019).

Feedstock input (fermenter)			Unit
Plant size	75	500	kW
Dairy cow manure	292 (90%)	3033 (82%)	kg/h
Straw residues from dairy cow breeding	33 (10%)	-	kg/h
Wheat grain/shreds	-	125	kg/h
Wheat residues (Abgang, d.h. Spelze und Halme)	-	42	kg/h
Residues from silo (grass and triticale)	-	417	kg/h
Sugar beet pulp (Rübenschnitzel; bought as fodder, hence residue from livestock farming)	-	83	kg/h
Iron (II) chloride	-	8	kg/h
Enzymes			
Zymaxx		0.5	kg/d
Sensopower		0.2	kg/d
Total feedstock input	325	3708	kg/h
Digestate output	274	3385	kg/h

Table A 2: Detailed composition of the digestate taken from the digestate storage facility at the large plant in Clausnitz; own measurements.

Molecule	wt%
H	5.34
C	43
N	3.36
O	26.6
Na_2O	1.28
MgO	1.47
Al_2O_3	0.33
SiO_2	3.87
P_2O_5	2.37
SO_3	2.07
Cl	1.6
K_2O	5.34
CaO	3.13
TiO_2	0.03
Cr	0.0013
Mn	0.052
Fe_2O_3	0.75
Cu	0.0017
Zn	0.04
Sr	0.0138
BaO	0.0088
Pb	0.001

Table A 3: Mass flows at different process points for case 2 and 4.

	Mass flow (kg/h)		
Flow	Case 2	Case 3	Case 4
S-1	2.55	10.32	23.41
S-2	18.76	75.79	171.83
S-3	65.08	263.07	596.41
S-4	65.08	263.07	596.41
S-5	65.08	263.07	596.41
S-6	65.08	263.07	596.41
S-7	65.08	263.07	596.41
S-8	43.03	173.93	394.33
S-9	22.05	89.14	202.09
S-10	22.05	89.14	202.09
S-11	1.2	4.86	11.02
S-12	0.47	1.91	4.34
S-13	0.73	2.95	6.68
S-14	22.68	91.67	207.83
S-15	22.68	91.67	207.83
S-16	7.67	31	70.27
S-17	15	60.62	137.42
S-18	1.36	5.48	12.43
S-19	13.63	55.08	124.86

Table A 4: Process data for component design for cases 1 to 4.

Process factor	Unit	Cases			
		Case 1	Case 2	Case 3	Case 4
Q_{H-1}	W	14132	7729	31241	70825
Q_{H-2}		4829	2639	10667	24187
Q_{H-3}		11707	6403	25881	58674
Q_{H-4}		698	382	1544	3500
Q_{H-5}		1198	656	2629	6003
Q_{R-1}		11426	6248	25258	57261
Q_{KK}		23621	12917	52213	118377
Q_{KR}		11203	6126	24760	56139
$m_{L,CP-1}$	kg/h	40.32	22.05	89.14	202.09
$m_{L,CP-2}$		41.47	22.68	91.67	207.83
$m_{L,CP-3}$		24.94	13.64	55.13	124.99
$\rho_{L,CP-1}$	kg/m^3	621.08	621.08	621.08	621.08
$\rho_{L,CP-2}$		812.52	812.52	812.52	812.52
$\rho_{L,CP-3}$		749.41	747.41	749.41	747.41
n_{R-1}	mol/sec	3.03	1.66	6.69	15.17
ρ_{R-1}	Nm^3/h	43.25	43.25	43.25	43.25

Table A 5: Calculated size parameters of the main components for cases 1 to 4.

Component	Unit	Size parameters			
		Case 1	Case 2	Case 3	Case 4
CP-1	kW	6.24	3.41	13.80	31.28
CP-2		5.32	2.91	11.76	26.65
CP-3		0.62	0.34	1.37	3.10
CP-4		0.26	0.14	0.57	1.30
R-1	m³	0.085	0.046	0.187	0.424
H-1	m²	10.99	6.07	24.52	55.58
H-2		0.74	0.41	1.63	3.69
H-3		5.44	2.98	12.01	27.23
H-4		0.45	0.25	0.99	2.24
H-5		0.04	0.02	0.08	0.18
CP-1	m³	0.011	0.006	0.024	0.054
CP-2		0.009	0.005	0.019	0.043
CP-3		0.006	0.003	0.012	0.028
C-1	m²	1.40	-	-	-
COND		1.26	0.69	2.78	6.30
REB		0.15	0.08	0.33	0.73

Table A 6: CO_2 upgrading costs for the different cases and costs of the post-combustion of the flue gas as well as the activated carbon.

Type	Volume flow of raw biogas (m³/h)	Case	Costs (€/kWh)	Source
Membrane	40	Case 1	0.032	OESTER (2019)
Membrane	20	Case 2	0.038	OESTER (2019)
Membrane	250	Case 4	0.0212	BEYRICH et al. (2019)
PSA	250	–	0.023	BEYRICH et al. (2019)
Amine scrubbing	250	–	0.0218	BEYRICH et al. (2019)
Membrane	40	Max. Value	0.0763	BEYRICH et al. (2019)
Post-combustion treatment	40	Case 1 & case 2	0.0071	BEYRICH et al. (2019)
Activated carbon	40	Case 1	0.0012	BIOBG (2012)
Activated carbon	20	Case 2	0.0011	BIOBG (2012)
Activated carbon	250	Case 4	0.0132	BIOBG (2012)

Table A 7: Size parameters and module costs from WALMAN (2018).

Module	Name in source	Size parameter	Cost (€)
CP-1	C-101	538 kW	1315585
CP-2	C-102	139 kW	1074866
CP-3	non-existent	-	-
CP-4	C-103	52 kW	1048814
R-1	CP-103 & E-104	unknown	807505
H-1	E-108	1750 m²	1343877
H-2	E-102	7 m²	110457
H-3	E-109	1140 m²	829903
H-4	E-106	178 m²	341863
H-5	E-105	71 m²	152070
CP-1	CP-101	1.86 m³	317108
CP-2	CP-102	2.46 m³	46800
CP-3	non-existent	-	-
C-1	T-101	67.32 m³	450317
COND	E-103	2950 m²	146761
REB	E-107	30 m²	123778

Figure A 1: Results of the sensitivity analysis of case 2.

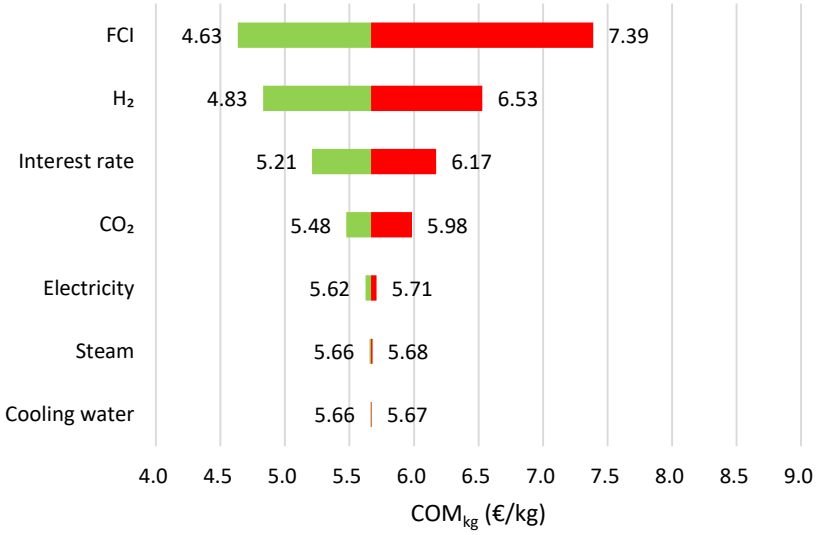

Caption: red colour means above original price, green colour means below it; FCI = fixed capital investment, COM = cost of manufacturing.

Figure A 2: Results of the sensitivity analysis of case 3.

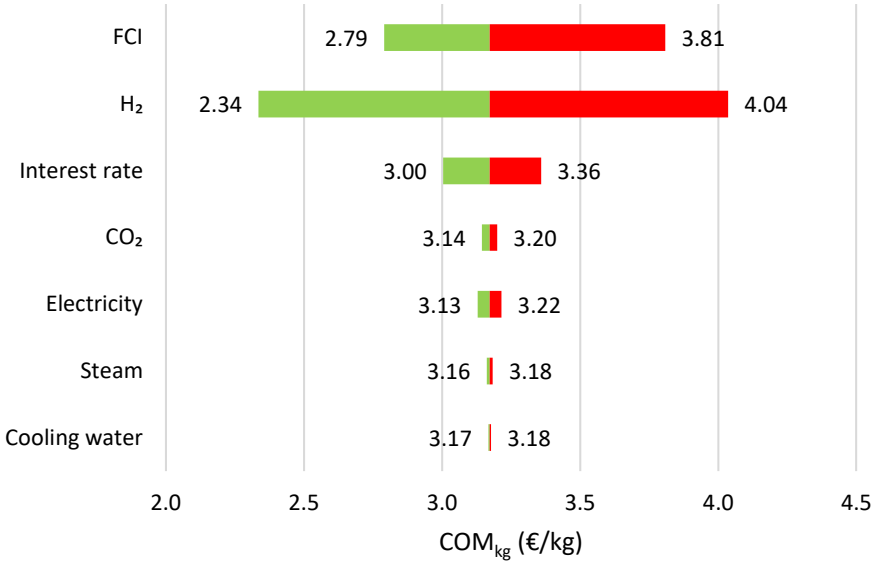

Caption: red colour means above original price, green colour means below it; FCI = fixed capital investment, COM = cost of manufacturing.

Figure A 3: Results of the sensitivity analysis of case 4.

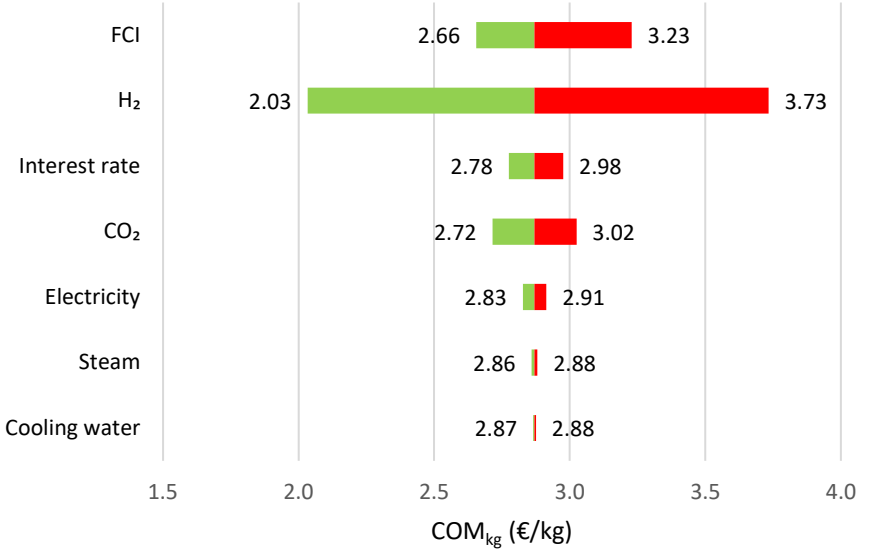

Caption: red colour means above original price, green colour means below it; FCI = fixed capital investment, COM = cost of manufacturing.

Table A 8: Assumptions for the operating expenditures for the 75 kW plant.

Parameter	Price	Unit	Quantity	Unit	Comment
Electricity	0.169	€/kWh	212500	kW/h	BDEW (2020, p. 23) for industry (without electricity tax)
EEG levy	0.064	€/kWh	51000	kWh_{el}/a	BUNDESNETZAGENTUR (2020)
Heat	0	€/kWh	34.4	kW/h	From own supply
Labour	20	€/h	182.5	h/a	½ hour per day (RAU, 2019)
Manure	0	€/t	2555	t/a	Residue from livestock farming
Straw residues	0	€/t	292	t/a	Residue from livestock farming
Activated carbon	3	€/kg	720	kg/a	RAU (2019), change every ½ year; BIOBG (2012, p. 2) Amount Junior: 3*120 kg for maximal volume stream of 200 Nm€/h
Lubricants, consumables	4364	€/a			STINNER et al. (2015, p. 32), adjusted for the CEPCI
Services and repairs	9102	€/a			1-3% of investment cost according to (BAYERISCHES LANDWIRTSCHAFTLICHES WOCHENBLATT, 2019)
Insurance	2276	€/a			BAYERISCHES LANDWIRTSCHAFTLICHES WOCHENBLATT (2019): 0.5% of FCI
Other costs	2000	€/a			BAYERISCHES LANDWIRTSCHAFTLICHES WOCHENBLATT (2019)

Table A 9: Assumptions for the operating costs for the 500 kW plant.

Parameter	Price	Unit	Quantity	Unit	Comment
Electricity	0.169	€/kWh	340000	kW/h	BDEW (2020, p. 23) for industry (without electricity tax)
EEG levy	0.064	€/kWh	340000	kWh_{el}/a	BUNDESNETZAGENTUR (2020)
Heat	0	€/kWh	294.4	kW/h	From own supply
Labour	20	€/h	182.5	h/a	½ hour per day by the farmer
Manure	0	€/t	26572	t/a	Residue from livestock farming
Straw residues	0	€/t	1095	t/a	Residue from livestock farming
Feed residues	0	€/t	365	t/a	Residue from livestock farming
Beet pulp/ slices	0	€/t	730	t/a	Residue from livestock farming
Silo (grass + triticale)	0	€/t	3650	t/a	Own production for livestock farm, therefore residue
Zymaxx enzyme	32	€/d			BIOGAS-ADDITIVE.DE (n.a., p. 6)
Senso-power enzyme	32	€/d			No price found, assumption: similar to Zymaxx
Iron (II) chloride	0.38	€/kg	73	t/a	JOKORA (2020)
Activated carbon	3	€/kg	1440	kg/a	RAU (2019), change every ½ year; BIOBG (2012, p. 2) Amount Eco: 3*240 kg for maximal volume stream of 400 Nm€/h
Lubricants, con-sumables	4364	€/a			STINNER et al. (2015, p. 32), default value due to lack of data
Services and repairs	5539	€/a			1-2% of total costs according to RAU (2019)
Insurance	12873	€/a			FNR (2016, p. 163): 500 kW plant with input of 80% renewable raw materials and 20% manure
Other costs	4982	€/a			FNR (2016, p. 163): 500 kW plant with input of 80%

	renewable raw materials and 20% manure

Table A 10: Values of the contribution analysis for each scenario and impact category.

	Elec-credit	Act-Carb	Bio-Prod	CHP	Heat-Credit	Elec-Bio	Elec-CO_2	Elec-H_2	Elec-MeOH	Heat-Bio	WTT	Urea-Credit	MOP-Credit	SSP-Credit	Heat-MeOH	NG-Prod	CH_4-Leak
Climate Change (CC)																	
A1	-1.97	0.03	0.29	0.72	-0.98	0.16	0.03	0.16	0.33	0.34	2.81E-04	-0.19	0.00	0.00	0.00	0.00	0.00
A2	-1.97	0.03	0.29	0.71	-0.98	0.16	0.03	0.16	0.33	0.34	2.81E-04	0.00	-0.03	0.00	0.00	0.00	0.00
A3	-1.97	0.03	0.29	0.71	-0.98	0.16	0.03	0.16	0.33	0.34	2.81E-04	0.00	0.00	-0.15	0.00	0.00	0.00
B1	-0.04	0.03	0.29	0.71	-0.98	0.16	0.03	0.16	0.33	0.34	2.81E-04	-0.19	0.00	0.00	0.00	0.00	0.00
B2	-0.04	0.03	0.29	0.71	-0.98	0.16	0.03	0.16	0.33	0.34	2.81E-04	0.00	-0.03	0.00	0.00	0.00	0.00
B3	-0.04	0.03	0.29	0.71	-0.98	0.16	0.03	0.16	0.33	0.34	2.81E-04	0.00	0.00	-0.15	0.00	0.00	0.00
C1	-3.62	0.03	0.29	0.71	-0.98	0.16	0.03	0.16	0.33	0.34	2.81E-04	-0.19	0.00	0.00	0.00	0.00	0.00
C2	-3.62	0.03	0.29	0.71	-0.98	0.16	0.03	0.16	0.33	0.34	2.81E-04	0.00	-0.03	0.00	0.00	0.00	0.00
C3	-3.62	0.03	0.29	0.71	-0.98	0.16	0.03	0.16	0.33	0.34	2.81E-04	0.00	0.00	-0.15	0.00	0.00	0.00
Ref	0.00	0.00	0.00	0.00	0.00	0.00	0.00	0.00	0.05	0.00	0.00	0.00	0.00	0.00	0.49	0.16	0.15

	Elec-credit	Act-Carb	Bio-Prod	CHP	Heat-Credit	Elec-Bio	Elec-CO_2	Elec-H_2	Elec-MeOH	Heat-Bio	WTT	Urea-Credit	MOP-Credit	SSP-Credit	Heat-MeOH	NG-Prod	CH_4-Leak
Fossil depletion (FD)																	
A1	-0.75	0.01	0.00	0.00	-0.39	0.06	0.01	0.06	0.13	0.14	0.00	-0.08	0.00	0.00	0.00	0.00	0.00
A2	-0.75	0.01	0.00	0.00	-0.39	0.06	0.01	0.06	0.13	0.14	0.00	0.00	-0.01	0.00	0.00	0.00	0.00
A3	-0.75	0.01	0.00	0.00	-0.39	0.06	0.01	0.06	0.13	0.14	0.00	0.00	0.00	-0.09	0.00	0.00	0.00
B1	-0.01	0.01	0.00	0.00	-0.39	0.06	0.01	0.06	0.13	0.14	0.00	-0.08	0.00	0.00	0.00	0.00	0.00
B2	-0.01	0.01	0.00	0.00	-0.39	0.06	0.01	0.06	0.13	0.14	0.00	0.00	-0.01	0.00	0.00	0.00	0.00
B3	-0.01	0.01	0.00	0.00	-0.39	0.06	0.01	0.06	0.13	0.14	0.00	0.00	0.00	-0.09	0.00	0.00	0.00
C1	-1.06	0.01	0.00	0.00	-0.39	0.06	0.01	0.06	0.13	0.14	0.00	-0.08	0.00	0.00	0.00	0.00	0.00
C2	-1.06	0.01	0.00	0.00	-0.39	0.06	0.01	0.06	0.13	0.14	0.00	0.00	-0.01	0.00	0.00	0.00	0.00
C3	-1.06	0.01	0.00	0.00	-0.39	0.06	0.01	0.06	0.13	0.14	0.00	0.00	0.00	-0.09	0.00	0.00	0.00
Ref	0.00	0.00	0.00	0.00	0.00	0.00	0.00	0.00	0.02	0.00	0.00	0.00	0.00	0.00	0.19	0.58	0.00
Acidification potential (AP)																	
A1	-9.17E-03	1.49E-04	1.54E-03	6.94E-03	-5.11E-04	7.33E-04	1.30E-04	7.00E-04	1.54E-03	1.79E-04	2.16E-06	-9.08E-04	0.00	0.00	0.00	0.00	0.00
A2	-9.17E-03	1.49E-04	1.54E-03	6.94E-03	-5.11E-04	7.33E-04	1.30E-04	7.00E-04	1.54E-03	1.79E-04	2.16E-06	0.00	-9.95E-05	0.00	0.00	0.00	0.00

	Elec-credit	Act-Carb	Bio-Prod	CHP	Heat-Credit	Elec-Bio	Elec-CO_2	Elec-H_2	Elec-MeOH	Heat-Bio	WTT	Urea-Credit	MOP-Credit	SSP-Credit	Heat-MeOH	NG-Prod	CH_4-Leak
A3	-9.17E-03	1.49E-04	1.54E-03	6.94E-03	-5.11E-04	7.33E-04	1.30E-04	7.00E-04	1.54E-03	1.79E-04	2.16E-06	0.00	0.00	-1.89E-03	0.00	0.00	0.00
B1	-2.00E-04	1.49E-04	1.54E-03	6.94E-03	-5.11E-04	7.33E-04	1.30E-04	7.00E-04	1.54E-03	1.79E-04	2.16E-06	-9.08E-04	0.00E+00	0.00	0.00	0.00	0.00
B2	-2.00E-04	1.49E-04	1.54E-03	6.94E-03	-5.11E-04	7.33E-04	1.30E-04	7.00E-04	1.54E-03	1.79E-04	2.16E-06	0.00	-9.95E-05	0.00	0.00	0.00	0.00
B3	-2.00E-04	1.49E-04	1.54E-03	6.94E-03	-5.11E-04	7.33E-04	1.30E-04	7.00E-04	1.54E-03	1.79E-04	2.16E-06	0.00	0.00	-1.89E-03	0.00	0.00	0.00
C1	-3.85E-03	1.49E-04	1.54E-03	6.94E-03	-5.11E-04	7.33E-04	1.30E-04	7.00E-04	1.54E-03	1.79E-04	2.16E-06	-9.08E-04	0.00	0.00	0.00	0.00	0.00
C2	-3.85E-03	1.49E-04	1.54E-03	6.94E-03	-5.11E-04	7.33E-04	1.30E-04	7.00E-04	1.54E-03	1.79E-04	2.16E-06	0.00	-9.95E-05	0.00	0.00	0.00	0.00
C3	-3.85E-03	1.49E-04	1.54E-03	6.94E-03	-5.11E-04	7.33E-04	1.30E-04	7.00E-04	1.54E-03	1.79E-04	2.16E-06	0.00	0.00	-1.89E-03	0.00	0.00	0.00
Ref	0.00	0.00	0.00	0.00	0.00	0.00	0.00	0.00	2.29E-04	0.00	0.00	0.00	0.00	0.00	2.55E-04	1.14E-03	0.00

	Elec-credit	Act-Carb	Bio-Prod	CHP	Heat-Credit	Elec-Bio	Elec-CO_2	Elec-H_2	Elec-MeOH	Heat-Bio	WTT	Urea-Credit	MOP-Credit	SSP-Credit	Heat-MeOH	NG-Prod	CH_4-Leak
Freshwater eutrophication potential (EP)																	
A1	-2.83E-03	1.60E-05	0.00	0.00	-1.42E-05	2.27E-04	4.02E-05	1.25E-04	4.77E-04	4.97E-06	6.45E-07	-3.57E-05	0.00	0.00	0.00	0.00	0.00
A2	-2.83E-03	1.60E-05	0.00	0.00	-1.42E-05	2.27E-04	4.02E-05	1.25E-04	4.77E-04	4.97E-06	6.45E-07	0.00	-1.46E-05	0.00	0.00	0.00	0.00
A3	-2.83E-03	1.60E-05	0.00	0.00	-1.42E-05	2.27E-04	4.02E-05	1.25E-04	4.77E-04	4.97E-06	6.45E-07	0.00	0.00	-2.93E-04	0.00	0.00	0.00
B1	-3.09E-05	1.60E-05	0.00	0.00	-1.42E-05	2.27E-04	4.02E-05	1.25E-04	4.77E-04	4.97E-06	6.45E-07	-3.57E-05	0.00	0.00	0.00	0.00	0.00
B2	-3.09E-05	1.60E-05	0.00	0.00	-1.42E-05	2.27E-04	4.02E-05	1.25E-04	4.77E-04	4.97E-06	6.45E-07	0.00	-1.46E-05	0.00	0.00	0.00	0.00
B3	-3.09E-05	1.60E-05	0.00	0.00	-1.42E-05	2.27E-04	4.02E-05	1.25E-04	4.77E-04	4.97E-06	6.45E-07	0.00	0.00	-2.93E-04	0.00	0.00	0.00

	Elec-credit	Act-Carb	Bio-Prod	CHP	Heat-Credit	Elec-Bio	Elec-CO_2	Elec-H_2	Elec-MeOH	Heat-Bio	WTT	Urea-Credit	MOP-Credit	SSP-Credit	Heat-MeOH	NG-Prod	CH_4-Leak
C1	-8.63E-03	1.60E-05	0.00	0.00	-1.42E-05	2.27E-04	4.02E-05	1.25E-04	4.77E-04	4.97E-06	6.45E-07	-3.57E-05	0.00	0.00	0.00	0.00	0.00
C2	-8.63E-03	1.60E-05	0.00	0.00	-1.42E-05	2.27E-04	4.02E-05	1.25E-04	4.77E-04	4.97E-06	6.45E-07	0.00	-1.46E-05	0.00	0.00	0.00	0.00
C3	-8.63E-03	1.60E-05	0.00	0.00	-1.42E-05	2.27E-04	4.02E-05	1.25E-04	4.77E-04	4.97E-06	6.45E-07	0.00	0.00	-2.93E-04	0.00	0.00	0.00
Ref	0.00	0.00	0.00	0.00	0.00	0.00	0.00	0.00	7.09E-05	0.00	0.00	0.00	0.00	0.00	7.09E-06	8.53E-06	0.00
Marine eutrophication potential (EP marine)																	
A1	-1.89E-04	1.06E-06	0.00	0.00	-1.16E-06	1.51E-05	2.68E-06	1.24E-05	3.18E-05	4.05E-07	3.45E-06	-9.59E-06	0.00	0.00	0.00	0.00	0.00
A2	-1.89E-04	1.06E-06	0.00	0.00	-1.16E-06	1.51E-05	2.68E-06	1.24E-05	3.18E-05	4.05E-07	3.45E-06	0.00	-9.92E-07	0.00	0.00	0.00	0.00
A3	-1.89E-04	1.06E-06	0.00	0.00	-1.16E-06	1.51E-05	2.68E-06	1.24E-05	3.18E-05	4.05E-07	3.45E-06	0.00	0.00	-1.22E-05	0.00	0.00	0.00

	Elec-credit	Act-Carb	Bio-Prod	CHP	Heat-Credit	Elec-Bio	Elec-CO_2	Elec-H_2	Elec-MeOH	Heat-Bio	WTT	Urea-Credit	MOP-Credit	SSP-Credit	Heat-MeOH	NG-Prod	CH_4-Leak
B1	-4.56E-06	1.06E-06	0.00	0.00	-1.16E-06	1.51E-05	2.68E-06	1.24E-05	3.18E-05	4.05E-07	3.45E-06	-9.59E-06	0.00	0.00	0.00	0.00	0.00
B2	-4.56E-06	1.06E-06	0.00	0.00	-1.16E-06	1.51E-05	2.68E-06	1.24E-05	3.18E-05	4.05E-07	3.45E-06	0.00	-9.92E-07	0.00	0.00	0.00	0.00
B3	-4.56E-06	1.06E-06	0.00	0.00	-1.16E-06	1.51E-05	2.68E-06	1.24E-05	3.18E-05	4.05E-07	3.45E-06	0.00	0.00	-1.22E-05	0.00	0.00	0.00
C1	-5.48E-04	1.06E-06	0.00	0.00	-1.16E-06	1.51E-05	2.68E-06	1.24E-05	3.18E-05	4.05E-07	3.45E-06	-9.59E-06	0.00	0.00	0.00	0.00	0.00
C2	-5.48E-04	1.06E-06	0.00	0.00	-1.16E-06	1.51E-05	2.68E-06	1.24E-05	3.18E-05	4.05E-07	3.45E-06	0.00	-9.92E-07	0.00	0.00	0.00	0.00
C3	-5.48E-04	1.06E-06	0.00	0.00	-1.16E-06	1.51E-05	2.68E-06	1.24E-05	3.18E-05	4.05E-07	3.45E-06	0.00	0.00	-1.22E-05	0.00	0.00	0.00
Ref	0.00	0.00	0.00	0.00	0.00	0.00	0.00	0.00	4.73E-06	0.00	0.00	0.00	0.00	0.00	5.77E-07	8.53E-07	0.00

Human toxicity (HT)

	Elec-credit	Act-Carb	Bio-Prod	CHP	Heat-Credit	Elec-Bio	Elec-CO_2	Elec-H_2	Elec-MeOH	Heat-Bio	WTT	Urea-Credit	MOP-Credit	SSP-Credit	Heat-MeOH	NG-Prod	CH_4-Leak
A1	-3.16	0.03	0.00	0.00	-0.04	0.25	0.04	0.82	0.53	0.01	1.83E-03	-0.19	0.00	0.00	0.00	0.00	0.00
A2	-3.16	0.03	0.00	0.00	-0.04	0.25	0.04	0.82	0.53	0.01	1.83E-03	0.00	-0.10	0.00	0.00	0.00	0.00
A3	-3.16	0.03	0.00	0.00	-0.04	0.25	0.04	0.82	0.53	0.01	1.83E-03	0.00	0.00	-0.68	0.00	0.00	0.00
B1	-0.21	0.03	0.00	0.00	-0.04	0.25	0.04	0.82	0.53	0.01	1.83E-03	-0.19	0.00	0.00	0.00	0.00	0.00
B2	-0.21	0.03	0.00	0.00	-0.04	0.25	0.04	0.82	0.53	0.01	1.83E-03	0.00	-0.10	0.00	0.00	0.00	0.00
B3	-0.21	0.03	0.00	0.00	-0.04	0.25	0.04	0.82	0.53	0.01	1.83E-03	0.00	0.00	-0.68	0.00	0.00	0.00
C1	-8.40	0.03	0.00	0.00	-0.04	0.25	0.04	0.82	0.53	0.01	1.83E-03	-0.19	0.00	0.00	0.00	0.00	0.00
C2	-8.40	0.03	0.00	0.00	-0.04	0.25	0.04	0.82	0.53	0.01	1.83E-03	0.00	-0.10	0.00	0.00	0.00	0.00
C3	-8.40	0.03	0.00	0.00	-0.04	0.25	0.04	0.82	0.53	0.01	1.83E-03	0.00	0.00	-0.68	0.00	0.00	0.00
Ref	0.00	0.00	0.00	0.00	0.00	0.00	0.00	0.00	0.08	0.00	0.00	0.00	0.00	0.00	0.02	0.03	0.00
Photochemical ozone formation (POF)																	
A1	-4.14E-03	1.40E-04	0.00	2.64E-02	-1.24E-03	3.31E-04	5.87E-05	9.95E-04	6.96E-04	4.35E-04	2.07E-06	-4.55E-04	0.00	0.00	0.00	0.00	0.00

	Elec-credit	Act-Carb	Bio-Prod	CHP	Heat-Credit	Elec-Bio	Elec-CO_2	Elec-H_2	Elec-MeOH	Heat-Bio	WTT	Urea-Credit	MOP-Credit	SSP-Credit	Heat-MeOH	NG-Prod	CH_4-Leak
A2	-4.14E-03	1.40E-04	0.00	2.64E-02	-1.24E-03	3.31E-04	5.87E-05	9.95E-04	6.96E-04	4.35E-04	2.07E-06	0.00	-1.42E-04	0.00	0.00	0.00	0.00
A3	-4.14E-03	1.40E-04	0.00	2.64E-02	-1.24E-03	3.31E-04	5.87E-05	9.95E-04	6.96E-04	4.35E-04	2.07E-06	0.00	0.00	-9.85E-04	0.00	0.00	0.00
B1	-2.50E-04	1.40E-04	0.00	2.64E-02	-1.24E-03	3.31E-04	5.87E-05	9.95E-04	6.96E-04	4.35E-04	2.07E-06	-4.56E-04	0.00	0.00	0.00	0.00	0.00
B2	-2.50E-04	1.40E-04	0.00	2.64E-02	-1.24E-03	3.31E-04	5.87E-05	9.95E-04	6.96E-04	4.35E-04	2.07E-06	0.00	-1.42E-04	0.00	0.00	0.00	0.00
B3	-2.50E-04	1.40E-04	0.00	2.64E-02	-1.24E-03	3.31E-04	5.87E-05	9.95E-04	6.96E-04	4.35E-04	2.07E-06	0.00	0.00	-9.85E-04	0.00	0.00	0.00
C1	-5.11E-03	1.40E-04	0.00	2.64E-02	-1.24E-03	3.31E-04	5.87E-05	9.95E-04	6.96E-04	4.35E-04	2.07E-06	-4.56E-04	0.00	0.00	0.00	0.00	0.00
C2	-5.11E-03	1.40E-04	0.00	2.64E-02	-1.24E-03	3.31E-04	5.87E-05	9.95E-04	6.96E-04	4.35E-04	2.07E-06	0.00	-1.42E-04	0.00	0.00	0.00	0.00

	Elec-credit	Act-Carb	Bio-Prod	CHP	Heat-Credit	Elec-Bio	Elec-CO_2	Elec-H_2	Elec-MeOH	Heat-Bio	WTT	Urea-Credit	MOP-Credit	SSP-Credit	Heat-MeOH	NG-Prod	CH_4-Leak
C3	-5.11E-03	1.40E-04	0.00	2.64E-02	-1.24E-03	3.31E-04	5.87E-05	9.95E-04	6.96E-04	4.35E-04	2.07E-06	0.00	0.00	-9.85E-04	0.00	0.00	0.00
Ref	0.00	0.00	0.00	0.00	0.00	0.00	0.00	0.00	1.04E-04	0.00	0.00	0.00	0.00	0.00	6.20E-04	6.48E-04	0.00
Stratospheric ozone depletion (ODP)																	
A1	-1.20E-06	6.55E-09	0.00	0.00	-2.11E-07	9.58E-08	1.70E-08	6.93E-08	2.02E-07	7.39E-08	7.96E-10	-7.44E-08	0.00	0.00	0.00	0.00	0.00
A2	-1.20E-06	6.55E-09	0.00	0.00	-2.11E-07	9.58E-08	1.70E-08	6.93E-08	2.02E-07	7.39E-08	7.96E-10	0.00	-2.24E-08	0.00	0.00	0.00	0.00
A3	-1.20E-06	6.55E-09	0.00	0.00	-2.11E-07	9.58E-08	1.70E-08	6.93E-08	2.02E-07	7.39E-08	7.96E-10	0.00	0.00	-8.19E-08	0.00	0.00	0.00
B1	-2.20E-08	6.55E-09	0.00	0.00	-2.11E-07	9.58E-08	1.70E-08	6.93E-08	2.02E-07	7.39E-08	7.96E-10	-7.44E-08	0.00	0.00	0.00	0.00	0.00
B2	-2.20E-08	6.55E-09	0.00	0.00	-2.11E-07	9.58E-08	1.70E-08	6.93E-08	2.02E-07	7.39E-08	7.96E-10	0.00	-2.24E-08	0.00	0.00	0.00	0.00

	Elec-credit	Act-Carb	Bio-Prod	CHP	Heat-Credit	Elec-Bio	Elec-CO_2	Elec-H_2	Elec-MeOH	Heat-Bio	WTT	Urea-Credit	MOP-Credit	SSP-Credit	Heat-MeOH	NG-Prod	CH_4-Leak
B3	-2.20E-08	6.55E-09	0.00	0.00	-2.11E-07	9.58E-08	1.70E-08	6.93E-08	2.02E-07	7.39E-08	7.96E-10	0.00	0.00	-8.19E-08	0.00	0.00	0.00
C1	-9.49E-07	6.55E-09	0.00	0.00	-2.11E-07	9.58E-08	1.70E-08	6.93E-08	2.02E-07	7.39E-08	7.96E-10	-7.44E-08	0.00	0.00	0.00	0.00	0.00
C2	-9.49E-07	6.55E-09	0.00	0.00	-2.11E-07	9.58E-08	1.70E-08	6.93E-08	2.02E-07	7.39E-08	7.96E-10	0.00	-2.24E-08	0.00	0.00	0.00	0.00
C3	-9.49E-07	6.55E-09	0.00	0.00	-2.11E-07	9.58E-08	1.70E-08	6.93E-08	2.02E-07	7.39E-08	7.96E-10	0.00	0.00	-8.19E-08	0.00	0.00	0.00
Ref	0.00	0.00	0.00	0.00	0.00	0.00	0.00	0.00	3.00E-08	0.00	0.00	0.00	0.00	0.00	1.05E-07	1.33E-08	0.00

Elec-credit = Credits from CHP electricity production, Act-Carb = Activated carbon production, Bio-Prod = Biogas production, CHP = Combustion of biogas in the CHP plant, Heat-Credit = Credits from CHP heat production, Elec-Bio = Electricity for biogas plant, Elec-CO_2 = Electricity for CO_2 recovery, Elec-H_2 = Electricity for H_2 generation from on-shore wind, Germany, Elec-MeOH = Electricity for methanol production, Heat-Bio = Heat for biogas plant, WTT = Treatment of wastewater, Urea-Credit = Credits from urea production, EU, MOP-Credit = Credits from potassium chloride production, EU, SSP-Credit = Credits from single superphosphate production, EU, Heat-MeOH = Heat for methanol production, NG-Prod = Natural gas production, Russian, CH_4-Leak = Methane leakages.

Figure A 4: Contribution analysis of marine eutrophication (marine EP) and stratospheric ozone depletion (ODP).

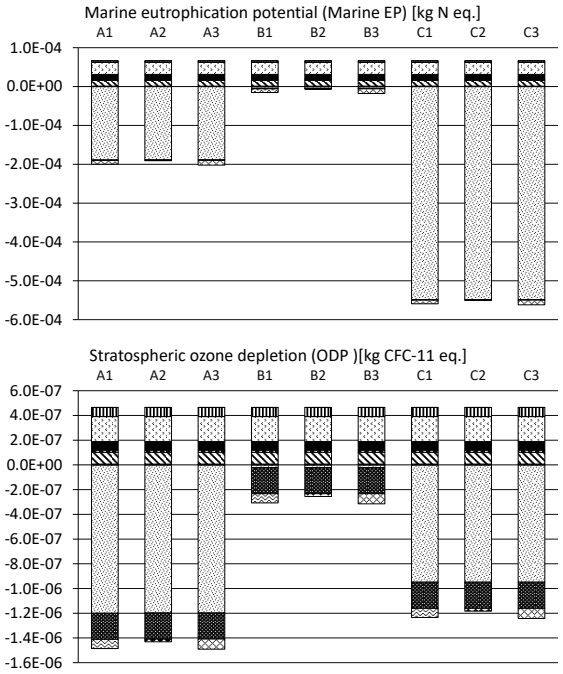

Table A 11: LCA results of conventional methanol production with German natural gas (NG) as compared to Russian NG and the percentage improvement in emissions.

	Russian NG	German NG	Improvement for German NG
CC [kg CO_2 eq.]	0.852	0.635	34%
FD [kg oil eq.]	0.793	0.759	4%
EP freshwater [kg P eq.]	8.65E-05	8.62E-05	0%
HT [kg 1,4-DB eq.]	0.123	0.116	6%
EP marine [kg N eq.]	6.16E-06	5.82E-06	6%
POF [kg NO_x eq.]	1.37E-03	1.63E-03	-16%
ODP [kg CFC-11 eq.]	1.49E-07	1.49E-07	0%
AP [kg SO_2 eq.]	0.0016	0.0025	-34%

Table A 12: Results for a system, which utilises German grid-mix electricity for hydrogen production instead of wind-based electricity (Scenario A1).

	CC [kg CO_2 eq.]	FD [kg oil eq.]	EP fresh-water [kg P eq.]	HT [kg 1,4-DB eq.]	EP marine [kg N eq.]	POF [kg NO_x eq.]	ODP [kg CFC-11 eq.]	AP [kg SO_2 eq.]
Total	4.730	1.390	6.48E-03	7.079	4.28E-04	3.48E-02	2.55E-06	2.85E-02
Credits from CHP electricity production	-1.970	-0.747	-2.83E-03	-3.161	-1.89E-04	-4.14E-03	-1.20E-06	-9.17E-03
Activated carbon production	0.027	0.011	1.60E-05	0.035	1.06E-06	1.40E-04	6.55E-09	1.49E-04
Biogas production	0.291	0	0	0	0	0.00E+00	0.00E+00	1.54E-03
Combustion of biogas in the CHP plant	0.715	0	0	0	0	2.64E-02	0.00E+00	6.94E-03
Credits from CHP heat production	-0.977	-0.390	-1.42E-05	-0.038	-1.16E-06	-1.24E-03	-2.11E-07	-5.11E-04
Electricity for biogas plant	0.157	0.060	2.27E-04	0.252	1.51E-05	3.31E-04	9.58E-08	7.33E-04
Electricity for CO_2 recovery	0.028	0.011	4.02E-05	0.045	2.68E-06	5.87E-05	1.70E-08	1.30E-04
Electricity for H_2 production	5.980	2.270	8.60E-03	9.588	5.73E-04	1.26E-02	3.64E-06	2.78E-02
Electricity for methanol production	0.332	0.126	4.77E-04	0.532	3.18E-05	6.96E-04	2.02E-07	1.54E-03
Heat for biogas plant	0.342	0.136	4.97E-06	0.013	4.05E-07	4.35E-04	7.39E-08	1.79E-04
Treatment of wastewater	0	0	6.45E-07	0.002	3.45E-06	2.06E-06	7.96E-10	2.16E-06
Credits from urea production, EU	-0.191	-0.084	-3.57E-05	-0.193	-9.59E-06	-4.55E-04	-7.44E-08	-9.08E-04

Table A 13: Results of replaced heat variations.

	CC [kg CO_2 eq.]	FD [kg oil eq.]	EP fresh-water [kg P eq.]	HT [kg 1,4-DB eq.]	EP marine [kg N eq.]	POF [kg NO_x eq.]	ODP [kg CFC-11 eq.]	AP [kg SO_2 eq.]
Main LCA								
A1	-1.09	-0.821	-1.99E-03	-1.689	-1.33E-04	2.32E-02	-1.02E-06	1.33E-03
A2	-0.927	-0.749	-1.97E-03	-1.597	-1.24E-04	2.35E-02	-9.66E-07	2.14E-03
A3	-1.04	-0.823	-2.25E-03	-2.178	-1.35E-04	2.26E-02	-1.03E-06	3.52E-04
B1	0.839	-0.088	8.10E-04	1.258	5.16E-05	2.70E-02	1.58E-07	1.03E-02
B2	0.998	-0.016	8.31E-04	1.350	6.02E-05	2.74E-02	2.10E-07	1.11E-02
B3	0.880	-0.090	5.53E-04	0.767	4.89E-05	2.66E-02	1.50E-07	9.32E-03
C1	-2.736	-1.130	-7.79E-03	-6.934	-4.92E-04	2.22E-02	-7.69E-07	6.65E-03
C2	-2.577	-1.059	-7.77E-03	-6.843	-4.84E-04	2.25E-02	-7.18E-07	7.45E-03
C3	-2.694	-1.133	-8.05E-03	-7.423	-4.95E-04	2.17E-02	-7.77E-07	5.67E-03
Atmospheric, non-modulating boiler (<100 kW)								
A1	-1.190	-0.811	-2.01E-03	-1.793	-1.35E-04	2.32E-02	-1.03E-06	1.08E-03
A2	-1.028	-0.739	-1.99E-03	-1.700	-1.27E-04	2.36E-02	-9.78E-07	1.89E-03
A3	-1.145	-0.813	-2.27E-03	-2.279	-1.38E-04	2.27E-02	-1.04E-06	1.00E-04
B1	0.738	-0.078	7.92E-04	1.154	4.91E-05	2.71E-02	1.46E-07	1.00E-02
B2	0.897	-0.006	8.13E-04	1.245	5.77E-05	2.74E-02	1.98E-07	1.09E-02
B3	0.779	-0.080	5.35E-04	0.665	4.64E-05	2.66E-02	1.38E-07	9.07E-03
C1	-2.837	-1.120	-7.81E-03	-7.036	-4.95E-04	2.23E-02	-7.81E-07	6.39E-03
C2	-2.678	-1.049	-7.79E-03	-6.944	-4.86E-04	2.26E-02	-7.29E-07	7.20E-03
C3	-2.795	-1.123	-8.06E-03	-7.524	-4.97E-04	2.17E-02	-7.89E-07	5.41E-03

Condensing, modulating boiler (<100 kW)								
A1	-1.110	-0.785	-2.01E-03	-1.792	-1.35E-04	2.34E-02	-1.02E-06	1.14E-03
A2	-0.952	-0.713	-1.99E-03	-1.700	-1.27E-04	2.38E-02	-9.64E-07	1.94E-03
A3	-1.070	-0.787	-2.27E-03	-2.281	-1.38E-04	2.30E-02	-1.02E-06	1.55E-04
B1	0.814	-0.052	7.89E-04	1.155	4.88E-05	2.74E-02	1.60E-07	1.01E-02
B2	0.973	0.020	8.10E-04	1.247	5.74E-05	2.76E-02	2.12E-07	1.09E-02
B3	0.855	-0.054	5.32E-04	0.668	4.62E-05	2.68E-02	1.52E-07	9.12E-03
C1	-2.760	-1.090	-7.81E-03	-7.034	-4.95E-04	2.24E-02	-7.67E-07	6.45E-03
C2	-2.600	-1.020	-7.79E-03	-6.942	-4.86E-04	2.28E-02	-7.15E-07	7.26E-03
C3	-2.720	-1.100	-8.07E-03	-7.523	-4.98E-04	2.20E-02	-7.75E-07	5.47E-03

Figure A 5: Contribution analysis for the additional LCA showing the different scenarios of replaced electricity generation compared to the gas flare.

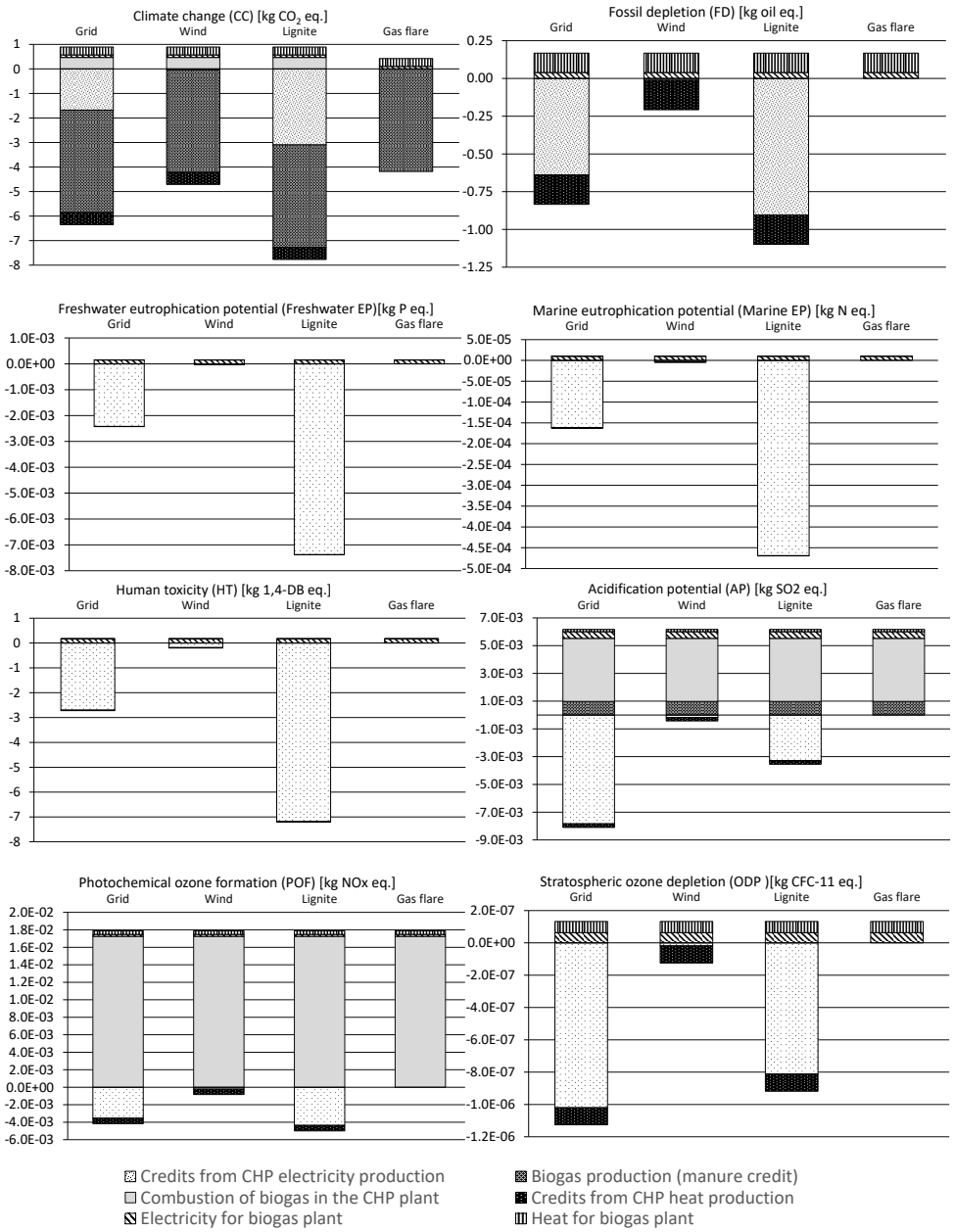

8.2 Appendix B: Enquiry texts for manufacturers

8.2.1 *Verdichter*

Sehr geehrte Damen und Herren,

ich bin auf der Suche nach vier verschiedenen Verdichtern:

1. Verdichter für Wasserstoff von 10 bar auf 80 bar mit einem Volumenstrom von 55 Nm^3/h.
2. Verdichter für CO_2 von Umgebungsdruck auf 80 bar mit einem Volumenstrom von 20 Nm^3/h.
3. Verdichter für ein Gemisch aus CO_2 (60 Gew.-%), Methanol (36 Gew.-%) und Wasser (4 Gew.-%) von 75 bar auf 80 bar mit einem Volumenstrom von 180 Nm^3/h.
4. Verdichter für ein Gemisch aus CO_2 (74 Gew.-%),Wasserstoff (16 Gew.-%), Methanol (6 Gew.-%) und Kohlenstoffmonoxid (4 Gew.-%) von Umgebungsdruck auf 80 bar mit einem Volumenstrom von 2 Nm^3/h.

Fertigen Sie Verdichter in dieser Größenordnung?

Mit freundlichen Grüßen

8.2.2 *Reaktor*

Sehr geehrte Damen und Herren,

Ich bin auf der Suche nach einem Reaktor zur Methanolsynthese. Dieser soll als stehender Rohrbündelreaktor ausgeführt werden, in welchem sich die Katalysatorpellets in den Rohren befinden. Unten an den Rohren müssen Siebe oder ähnliches angebracht sein, damit die Pellets nicht herausfallen können. Die Rohre sollen dann von unten nach oben durchströmt werden. Durch das Gehäuse soll zur Kühlung des Reaktors Wasserdampf geleitet werden. Das benötigte Gesamtvolumen für den Behälter beträgt 85 L. Der Massenstrom liegt bei 120 kg/h. Die Reaktion läuft bei 80 bar und 250°C ab.

Können Sie Reaktoren in dieser Art fertigen und mir ein Preisangebot machen?

Mit freundlichen Grüßen

8.2.3 *Wärmeübertrager*

Sehr geehrte Damen und Herren,

ich bin auf der Suche nach sieben verschiedenen Wärmeübertragern:

Wärmeübertrager 1: Leistung von 14 kW

Rohre:

Medium: Gemisch aus CO2 (50 Gew.-%), Methanol (25 Gew.-%), Wasser (12 Gew.-%), Wasserstoff (10 Gew.-%) und Kohlenstoffmonoxid (3 Gew.-%) [gasförmig]

Massenstrom: 120 kg/h

Eintrittstemperatur: 250°C

Austrittstemperatur: 150°C

Druck: 80 bar

Dichte: 27,83 kg/m³

Viskosität: 0;0136 mPas

Spez. Wärmekapazität: 3009 J/kgK

Wärmeleitfähigkeit: 0,081 W/mK

Mantel:

Medium: Gemisch aus CO_2 (83 Gew.-%) und Wasserstoff (17 Gew.-%) [gasförmig]

Massenstrom: 120 kg/h

Eintrittstemperatur: 90°C

Austrittstemperatur: 230°C

Druck: 80 bar

Dichte: 23,07 kg/m³

Viskosität: 0,0206 mPas

Spez. Wärmekapazität: 2897 J/kgK

Wärmeleitfähigkeit: 0,087 W/mK

Wärmeübertrager 2: Leistung von 5 kW

Rohre:

Medium: Gemisch aus CO_2 (50 Gew.-%), Methanol (25 Gew.-%), Wasser (12 Gew.-%), Wasserstoff (10 Gew.-%) und Kohlenstoffmonoxid (3 Gew.-%) [gasförmig]

Massenstrom: 120 kg/h

Eintrittstemperatur: 150°C

Austrittstemperatur: 135°C

Druck: 80 bar

Dichte: 30,18 kg/m³

Viskosität: 0,0175 mPas

Spez. Wärmekapazität: 3044 J/kgK

Wärmeleitfähigkeit: 0,077 W/mK

Mantel:

Medium: Methanol [flüssig]

Massenstrom: 28 kg/h

Eintrittstemperatur: 37°C

Austrittstemperatur: 67°C

Druck: 1,01325 bar

Dichte: 786,19 kg/m³

Viskosität: 0,4804 mPas

Spez. Wärmekapazität: 2910 J/kgK

Wärmeleitfähigkeit: 0,19 W/mK

Wärmeübertrager 3: Leistung von 12 kW

Rohre:

Medium: Gemisch aus CO_2 (50 Gew.-%), Methanol (25 Gew.-%), Wasser (12 Gew.-%), Wasserstoff (10 Gew.-%) und Kohlenstoffmonoxid (3 Gew.-%) [gasförmig]

Massenstrom: 120 kg/h

Eintrittstemperatur: 135°C

Austrittstemperatur: 80°C

Druck: 80 bar

Dichte: 32,26 kg/m³

Viskosität: 0,0165 mPas

Spez. Wärmekapazität: 3165 J/kgK

Wärmeleitfähigkeit: 0,08 W/mK

Mantel:

Medium: Methanol (66 Gew.-%) und Wasser (34 Gew.-%) [flüssig]

Massenstrom: 42 kg/h

Eintrittstemperatur: 70°C

Austrittstemperatur: 80°C

Druck: 1,01325 bar

Dichte: 23,94 kg/m³

Viskosität: 0,3637 mPas

Spez. Wärmekapazität: 3913 J/kgK

Wärmeleitfähigkeit: 0,226 W/mK

Wärmeübertrager 4: Leistung von 0,7 kW

Rohre:

Medium: Gemisch aus Methanol (62 Gew.-%), Wasser (35 Gew.-%) und CO2 (3 Gew.-%) [flüssig]

Massenstrom: 41 kg/h

Eintrittstemperatur: 64°C

Austrittstemperatur: 55°C
Druck: 1,01325 bar
Dichte: 14,85 kg/m³
Viskosität: 0,3584 mPas
Spez. Wärmekapazität: 3443 J/kgK
Wärmeleitfähigkeit: 1,741 W/mK

Mantel:
Medium: Kühlluft [gasförmig]
Massenstrom: unbekannt
Eintrittstemperatur: 30°C
Austrittstemperatur: 44°C
Druck: 1,01325 bar

Wärmeübertrager 5: Leistung von 1,2 kW

Rohre:
Medium: Wasser [flüssig]
Massenstrom: 14 kg/h
Eintrittstemperatur: 100°C
Austrittstemperatur: 22°C
Druck: 1,01325 bar

Mantel:
Medium: Gemisch aus Methanol (66 Gew.-%) und Wasser (34 Gew.-%) [flüssig]
Massenstrom: 42 kg/h
Eintrittstemperatur: 55°C
Austrittstemperatur: 70°C
Druck: 1,01325 bar
Dichte: 812,52 kg/m³
Viskosität: 0,4331 mPas
Spez. Wärmekapazität: 3700 J/kgK
Wärmeleitfähigkeit: 0,222 W/mK

Wärmeübertrager 6 (Kondensator): Leistung von 24 kW

Rohre:

Medium: Gemisch aus Methanol (99 Gew.-%) und CO2 (1 Gew.-%) [kondensierend]

Massenstrom: 72 kg/h

Eintrittstemperatur: 64°C

Austrittstemperatur: 32°C

Druck: 1,01325 bar

Mantel:

Medium: Kühlwasser [flüssig]

Massenstrom: unbekannt

Eintrittstemperatur: 20°C

Austrittstemperatur: 44°C

Druck: 1,01325 bar

Wärmeübertrager 7 (Reboiler): Leistung von 12 kW

Rohre:

Medium: Wasserdampf

Massenstrom: unbekannt

Eintrittstemperatur: 210°C

Austrittstemperatur: 145°C

Druck: 40 bar

Mantel:

Medium: Gemisch aus Methanol (1 Gew.-%) und CO2 (99 Gew.-%) [verdampfend]

Massenstrom: 32 kg/h

Eintrittstemperatur: 100°C

Austrittstemperatur: 100°C

Druck: 1,01325 bar

Alle Wärmeübertrager sollen aus Edelstahl gefertigt werden.

Fertigen Sie Wärmeübertrager in dieser Größenordnung und können mir ein Preisangebot für diese machen?

Mit freundlichen Grüßen

8.2.4 *Trennbehälter*

Sehr geehrte Damen und Herren,

ich bin auf der Suche nach drei verschiedenen Druckbehältern:

Behälter 1: Volumen von 11 L, max. Betriebsüberdruck 85 bar

Behälter 2: Volumen von 9 L, max. Betriebsüberdruck 2 bar

Behälter 3: Volumen von 6 L, max. Betriebsüberdruck 2 bar

Alle drei Behälter sollen aus Edelstahl (z.B. 1.4571) gefertigt werden und drei Anschlüsse (oben, unten sowie einen seitlichen) besitzen. Beim Fluid handelt es sich um ein Gemisch aus Methanol, Wasser, Wasserstoff, CO_2 und Kohlenstoffmonoxid.

Fertigen Sie Druckbehälter für diesen Anwendungsbereich und können mir ein Preisangebot machen?

Mit freundlichen Grüßen

8.2.5 *Kolonne*

Sehr geehrte Damen und Herren,

ich bin auf der Suche nach einer Destillationskolonne zur Trennung eines Methanol-Wasser-Gemischs. Das Gemisch tritt mit einem Massenstrom von 42 kg in die Kolonne ein mit einem Anteil von 65 Gew.-% Methanol, 34 Gew.-% Wasser

und 1 Gew.-% CO_2. Am Eintritt hat das Gemisch eine Temperatur von 80°C. Am Austritt soll das Methanol eine Reinheit von etwa 98,7 Gew.-% aufweisen.

Fertigen Sie Kolonnen in diesem Bereich und können mir ein Angebot dazu machen?

Mit freundlichen Grüßen